# Differentiation of embryonic stem cells through controlled release of growth factors from microspheres

**Eghosa Omoregie Andrew Olaye, MPharm**

Thesis submitted to the University of Nottingham
for the degree of Doctor of Philosophy

**February 2009**

# Abstract

The development of microspheres for the sustained delivery of protein and small drug delivery has been utilised in tissue engineering and drug delivery applications. However problems exist in obtaining a controlled and predictable release pattern of the encapsulated molecules from these materials. In this study, microspheres with a zero order release kinetic profile and no lag phase were developed from a novel PLGA based polymer blend.

The novel PLGA based polymer blend was made from blending PLGA with varying compositions of the triblock co-polymer PLGA-PEG-PLGA. These blends were subsequently used in the fabrication of lysozyme and dexamethasone loaded microspheres.

Blending of the triblock copolymer with PLGA resulted in a reduction of the glass transition temperature (36.1ºC against 59.7ºC) and an increased mechanical strength (25.25 ± 1.26MPa against 0.26 ± 0.05MPa) for PLGA and 30% triblock *w/w* microspheres respectively. An incremental increase in the triblock composition within the Triblock/PLGA blends resulted in a corresponding reduction in glass transition temperature of the microspheres.

Varying the triblock composition within the microspheres showed no significant effect on entrapment efficiency (EE) of lysozyme (protein) and dexamethasone (drug) within fabricated microspheres (EE ~ 60% for and 75% for loading weight 5% w/w for lysozyme and dexamethasone microspheres respectively). Controlled release experiments showed incorporation of the triblock increased the burst release of the protein and drug molecules from the microspheres and improved their release kinetics, with zero-order release profile (post burst phase) observed at a triblock composition of 30% *w/w*. A positive correlation between the amount of triblock within the triblock / PLGA blend and the rate of protein and drug release was also observed.

The induction of osteogenesis and chondrogenesis within stem cells seeded on dexamethasone and ascorbate phosphate, and TGF-β3 loaded scaffolds was successfully demonstrated. Zonal release of TGF-β3 and BMP4 proteins from a bilayered scaffold was also demonstrated. However experiments conducted to demonstrate the tissue zonation within a bone cartilage bilayered construct developed from embryonic stem cell seeded TGF-β3 and BMP4 loaded bilayered scaffolds yielded inconclusive data.

These results suggests that protein and drug loaded injectable microspheres for tissue engineering applications can be formed from triblock/PLGA blends, and that by varying the triblock composition, the temperature at which the microspheres form scaffolds, the release kinetics and the mechanical strength of the resulting scaffolds can be controlled.

# Presentations and Publications

The work presented in this thesis has been reported in the following presentations, publications and patent applications.

## Presentations

**Olaye A E,** Buttery L D K, Rose FRAJ, Shakesheff K M. (2008) Spatial control of mES cell differentiation within microsphere based scaffolds. Oral and Poster Presentation at Society For Biomaterials (SFB), Atlanta, USA. September 2008.

**Olaye A E,** Buttery L D K, Rose FRAJ, Shakesheff K M. (2008) Modulation of drug release from microspheres. Poster Presentation at RSC Faraday Discussion (139), York, UK. March 2008.

## Publication

**Olaye A E,** Buttery L D K, Rose FRAJ, Shakesheff K M. (2008) Determining the differentiation of embryonic stem cells through localised growth factor delivery. European Cells and Materials 16:86

## Patent application

UK Patent Application No:0823483.3. Filing date 24/12/2008. Controlled Release Particles. Inventors: KM Shakesheff, FRAJ Rose, Chau DYS, **Olaye A. E**

# Acknowledgements

I would like to take this opportunity to express my gratitude to my supervisors Prof. Kevin Shakesheff, Dr Felicity Rose and Dr Lee Buttery, for their guidance support and providing me with the opportunity to undertake this exciting project. I would also like to acknowledge the financial support and funding obtained from BBSRC, and RegenTech.

I would also like to acknowledge the assistance provided by Dr Qingpu Hou, Dr Wenxin Wang, and Dr George Pasparaskis for their advice and support on the synthesis and characterization of the triblock co-polymer PLGA – PEG – PLGA. My gratitude is also extended to Dr Dave Barrett, Dr Catherine Otori, and Mr Paul Cooling for assistance and training provided in operating the Agilent HPLC machine, Mrs Christine Granger-Boultby for SEM training, and Mr Lee Hibbert for NMR training. I would also love to extend special thanks to Dr Lloyd Hamilton, and Dr Lisa White for providing training on use of the rheometers and texture analyser, and microCT machines.

My special acknowledgements to Mr David Gothard and Mr David Carter for their continuous supply of embryonic stem cells and general cell culture advice whilst undertaking this project. My thanks also extends to the post-docs in our lab Dr Daniel Howard, Dr David Chau, and Dr Glen Kirkham, all of whom provided invaluable

guidance, direction, training and scientific expertise during my PhD studies, I would also like to acknowledge the general support obtained from all the tissue engineering group members.

My deep gratitude to my family members for all their love, encouragement, support, and words of wisdom provided during the course of this PhD programme and in life in general. Your kindness and support has enabled me get this far and will hopefully take me further.

Finally I will like to say a special thank you to the most important person in my life – my wife Bisi, whose support, motivation, inspiration and love has provided the energy necessary for me to undertake and complete this PhD programme. Above all my acknowledgements goes to God, for providing me with the wisdom, will power and vigour to undertake such a momentous project.

# Table of Contents

# List of Figures

**Chapter 1**



**Chapter 2**



**Chapter 3**

**Chapter 4**

# List of Tables

# Abbreviations

| | |
|---|---|
| % | per cent |
| Π | pi (3.14217) |
| ± | plus or minus |
| ºC | degrees Celcius |
| δ | phase angle |
| < | less than |
| µm | micrometer |
| µl | microlitre |
| µg | microgram |
| 3D | three dimensional |
| AB/AM | antibiotic/antimycotic |
| Asc | ascorbate-2-phosphate |
| BMP | bone morphogenetic protein |
| BMP4 | bone morphogenetic protein 4 |
| BCA | bicinchoninic acid |
| BSA | bovine serum albumin |
| $CO_2$ | carbon dioxide |
| $dH_2O$ | distilled water |
| DCM | dicholoromethane |
| Dex | dexamethasone |
| DMEM | dulbecco's modified eagle's medium |
| DMSO | dimethylsulfoxide |
| DNA | deoxyribonucleic acid |
| EDTA | ethylenediaminetetracetic acid |
| ES | embryonic stem |
| ESC | embryonic stem cells |
| FCS | fetal calf serum |

| | |
|---|---|
| GAG | glycosaminoglycans |
| GPC | gel permeation chromatography |
| HPLC | high performance liquid chromatography |
| HPLC-UV | high performance liquid chromatography-ultra violet |
| HRP | horse radish peroxidise |
| kDa | kilo Dalton |
| MPa | mega Pascal ($10^6$ Pa) |
| MSC | mesenchymal stem cells |
| M*n* | number average molecular weight |
| M*w* | weight average molecular weight |
| NMR | nuclear magnetic resonance |
| PBS | phosphate buffered saline |
| PEG | poly (ethylene glycol) |
| PCL | poly(ε - caprolactone) |
| $P_{DL}LA$ | poly(DL-lactic acid) |
| PLGA | poly(lactide –*co*-glycolude) |
| PVA | poly (vinyl alcohol) |
| RGD | argininine-glycin-aspartine |
| rhBMP-2 | recombinant human BMP-2 |
| S/O/W | solid – in – oil – in - water |
| SEM | scanning electron microscopy |
| Stdev | standard deviation |
| Tg | glass transition temperature |
| TGF-β | transforming growth factor-β |
| TGF-β3 | transforming growth factor-β3 |
| VEGF | vascular endothelial growth factor |
| W/O/W | water– in – oil – in – water |
| w/w | weight per weight (weight / weight) |
| w/v | weight per volume (weight / volume) |

# CHAPTER 1

# Introduction

## 1.1. Tissue Engineering Overview.

Tissue engineering is an interdisciplinary field centred on developing materials, scaffolds, or devices that provide biochemical and biophysical cues to facilitate cell survival, proliferation, differentiation, and organization into functional biological substitutes for the study, repair, and maintenance of tissue function (Langer & Vacanti, 1993; Griffith and Naughton, 2002). Tissue engineering emerged in the early 90's with a focus on the development of tissues as a solution to the increasing problems associated with sourcing functional organs and tissues for transplants. Early developments were driven by skin repair in venuous and diabetic ulcers. The drivers for clinical and commercial research into the use of tissue engineering as alternative treatment options are the recent advancements in proteomics, genomics and molecular biology techniques and an increase in the understanding of mechanisms underpinning tissue morphogenesis and repair (Knothe et al., 2008).

Recently the focus of tissue engineering has progressed to include a substantial emphasis on the greater impact of providing more effective experimental systems for the *in vitro* studying of complex human tissue physiology and pathophysiology (Griffith and Swartz, 2006). This change in direction emerged in part due to the limitation of animal models in illuminating many crucial facets of human physiology

and pathophysiology, especially in areas of tissue-specific transcriptional regulation (Odom et al., 2007), diseased states (Vargo-Gogola and Rosen, 2007; Rangarajan et al., 2004) and drug-induced liver toxicity (Sivaraman et al., 2005).

In addition even though traditional two dimensional techniques utilized in the *in vitro* culture of animal cells can be automated and adapted to high-throughput assays, most scalable cell cultures lack physiologically relevant microenvironmental stimuli comparable to that of native tissues. Engineered tissue constructs consisting of human or animal cells are being developed for a broad range of application areas. These areas include hepatic drug metabolism and toxicity testing (Khetani and Bhatia, 2008; Lee at al., 2008; Sivaraman et al., 2005), lymphoid tissue neogenesis (Stachiowak, 2007; James et al., 2005) stem cell differentiation (Engler et al., 2006; Inanc et al., 2008; Koay et al., 2007); and co-culture systems for elucidating information on cellular interactions during normal and diseased physiology states (Hendriks and van Blitterswijk, 2007). The potential information elucidated from these application areas offers promise for meeting the data collection demands of high-throughput screening and systems biology (Cosgrove et al., 2008)..

In tissue neogenesis and repair within the body, the extracellular matrix (ECM) is able to stimulate individual cells through a diverse set of microenvironment cues such as bound or stored molecular signals (i.e. growth factors and cytokines); soluble cell signalling factors released from adjacent and distant cells; cell surface receptor mediated interactions (Lutolf and Hubbell 2005) and mechanical forces (Griffith and Swartz, 2006). These cues together activate a network of complex cell signalling pathways that regulates cell behavioural phenotypes. The ECM regulates the resultant

cell behaviour by not only providing these cues, but by also regulating their quantitative amounts, activity, spatial arrangements, and temporal sequences (Miyata et al. 2002).

Thus the central challenge of tissue engineering is to elicit and maintain desired cell behaviours through externally-applied and -induced chemical signals and mechanical forces in a predictable fashion (Cosgrove et al., 2008). To achieve this challenge tissue engineering combines aspects of different sciences including cell biology, genomics, proteomics, developmental biology, material science, polymer chemistry, and mathematic modelling for the design, modification and proliferation of living tissues using biomaterials, cells and growth factors either alone or in combination.

Based on the varied clinical and commercial applications of tissue engineered constructs a wide range of strategies involving *in vivo* and *in vitro* techniques have been developed in the design of these constructs to meet their intended use. Current strategies utilised generally involve a combination of any of the following components:

A) Identification, isolation, expansion and differentiation of a suitable cell source.
B) Choice and design of a suitable scaffold material to provide structural support and / or biological for facilitating tissue proliferation and ingrowth.
C) Seeding or encapsulation of cells into scaffolds.
D) *In vitro* culture of scaffolds (seeded or unseeded) under appropriate media conditions to form mature tissues for use in various clinical and industrial applications.

E) Transplantation of mature tissue / tissue constructs into animal and human host subjects to promote repair and regeneration of tissue defects.

## 1.2. Scaffolds.

A key focus of tissue engineering is the organisation of cells into functional tissues or organs through the use of biological substrates to control the growth, differentiation and behaviour of these cells (Hubbell, 1995). These biological substrates are termed scaffolds and can provide not only the mechano-architectural framework for the tissue development, but also the proximity for cell to cell interactions, matrix deposition and cell signalling. Current research is rapidly evolving towards designing, developing and manufacturing specialised scaffolds that (i) degrades into naturally occurring by-products when placed in the body, (ii) be incorporated with growth factors to direct ltissue repair (iii) promote cellular attachment and colonization (iv) alters their mechanical properties in response to particular stimuli (smart materials) (Pachence and Khon, 1997; Hubbell, 1995; Chau *et al*. 2008).

### 1.2.1. The Role of Scaffolds in Tissue Engineering.

Scaffolds have been used in the successful regeneration of different tissue types in both *in vivo* and *in vitro* experiments and within varying clinical settings. Examples of *in vivo* and *in vitro* experiments involving the use of scaffolds include for nerve regeneration (Cao & Soichet, 1999; Friedman et al., 2002), bone (Yang et al., 2004; Schneider et al., 2003), liver (Risbud et al., 2002; Thomas et al., 2006), pancreas (Cheng et al., 2006), cartilage (Horobin et al., 2006), and eye (Pratoomsoot et al., 2008). Current clinical applications utilising scaffold includes use for repairing of osteochondral defects, eye trauma, heart valve repair and as sutures for wound repair.

A significant challenge of tissue engineering is to develop a system allowing the localisation of a sufficient number of cells within the defect site in order to enhance neo tissue formation. Poor retention of cells and signalling molecules has been implicated as a major factor for reduced efficacy of cell suspensions and growth factors transferred directly to tissue defects, in regenerating new tissue *in vivo* when compared to *in vitro* 2d models (Seeherman and Wozney, 2005). The use of scaffolds as a cell support and delivery device for growth factor release has been shown to massively improve *in vivo* tissue engineering. In addition the difficulties of most cells being able to form fully viable 3D tissue with a homogenous cell phenotype mix (Landers et al., 2002, Pérez-Pomares et al., 2006) again necessitates the use of scaffolds for maintaining the specific phenotypic characteristics of the cells. For example, chondrocytes have been shown to lose their phenotypic characteristics becoming fibroblast-like (Buckwalter et al., 1997a) and a decrease of cartilage specific markers such as collagen type II and aggrecan (Hauselmann et al., 1994). In contrast chondrocytes grown on 3D culture systems such as PLGA (Chung et al., 2008), agarose gel (Connelly et al., 2008), and collagen (Muller-Rath et al., 2007), have been shown to maintain their phenotype, proliferate and synthesize cartilage specific markers.

There are several criteria that need to be fulfilled for a scaffold to be used successfully in tissue regeneration. First, the scaffold must have a highly porous structure, which would aid tissue growth in three dimensions. The porous structure is required for the efficient migration of cells through the scaffold; high surface area for seeding of cells; and efficient diffusion of nutrition and gases to all the cells. Secondly, the scaffold material has to be bioactive to ensure that it is able to connect to the surrounding

tissue without scar tissue formation. Thirdly, the scaffold should have a controllable rate of degradation, which can be tailored to give way to the tissue as it forms (Tabata 2004). The mechanical properties of the scaffolds should be similar to those of the host tissue, and be maintained long enough for the sufficient regeneration of the tissue. When degraded, the scaffolds should lead to non-toxic products, which can be metabolised.

### 1.2.2. Scaffold Materials

Through the development of a scaffold that is bioactive and biodegradable and to which cells can attach, proliferate into and migrate throughout, new tissue is regenerated slowly replacing the scaffold. The success in achieving tissue regeneration is mainly dependent on the scaffold design and the choice of material used in formulating the scaffold. Depending on the specific intended application of the matrix, whether for structural support, drug-delivery capability, or both, certain material categories may be more or less well suited to the final structure.

In choosing a material for scaffold formation, the following design criteria should be considered (Thomson et l., 1997, Kim & Mooney, 1998, Temenof & Mikos, 2000, Freyman et al., 2001, Zhu et al., 2004, Kretlow et al., 2007)

(i) The materials used for scaffold fabrication and its degradation products must be biocompatible and non-immunogenic.

(ii) Biodegradable, enzymatically degradable or resorbable and their products must be easily metabolised or excreted by the body.

(iii) A controllable degradation rate, which can be tuned to match the rate of *in vivo* / *vitro* tissue formation or release of encapsulated bioactive factors within the scaffold.

(iv) Easily fabricated into three dimensional scaffolds into a variety of shapes and sizes.

The scaffolds that are utilised within tissue engineering can be divided into two broad divisions of solid based scaffolds and hydrogels. Solid based scaffolds generally have a defined shape at room temperature and are utilised primarily as structural supports in the development of tissue constructs. These constructs can be used in aiding tissue regeneration either through temporal filling of a defect, or as a temporal tissue replacement. Hydrogels are swollen matrices that consists of highly hydrated polymeric chains (water content ≥30% of content) formed by cross-linking networks of polymer chains (Drury and Mooney 2003).

Solid based and hydrogel scaffolds are made out of natural polymers such as collagen, and fibrin; synthetic polymers such as poly(α-hydroxyacid)s and poly fumarate; and inorganic materials such as hydroxypaptite and tricalcium phosphate have all been used in tissue engineering. Summarised in table 1.1 are examples of some of the scaffold materials that have been used for tissue engineering applications

#### 1.2.2.1. Natural Polymers.

Natural polymers used to fabricate scaffolds for tissue engineering applications include collagen (Kakudo et al., 2007; Ibusuki et al., 2007; Dawson et al., 2008), hyaluronan (Borzacchiello et al., 2007; Cui et al., 2006), fibrin (Osathanon et al.,

| Materials | Types | Benefits | Potential Issues | References |
|---|---|---|---|---|
| Natural Polymers | Chitosan, Chitin, Collagen, Gelatin, Hyaluronic acid, alginate, Agarose | Biocompatible, bioresorbable. tailored mechanical strength and degradability | Sterilisation issues Immunogenic, difficulties in processing and sourcing, possible disease transmission and generally poor mechanical strengths | Simmons et al., 2004; Kim & Valentini 2001; Karageorgiou et al., 2006; Bax et al., 1999; Den Boer et al., 2002; Mao et al., 1998; Gao et al., 1997; Baier et al., 2003; Kimura et al., 2003; Stevens et al., 2009. |
| Inorganic Materials | Calcium orthophosphate cements; porous coralline; ceramics; Hydroxypaptite; titanium; bioactive glass, β-tricalcium phosphate; ceramics | Excellent biocompatibility, good affinity for growth factors and generally good mechanical strength; | Some materials are brittle; difficult to mould into different shapes and forms; localised heat dissipation (which could be detrimental to cells). | Ijiri et al., 1007; Pajamäki et al., 1993; Yuan et al., 1998; Laffargue et al., 1999; Urabe et al., 2002; Edwards et al., 2004; Den Boer et al., 2003; Puleo et al., 2002; Bessho et al., 1999; |

| Materials | Types | Benefits | Potential Issues | References |
|---|---|---|---|---|
| Synthetic Polymers | Poly (lactic acid); Poly (glycolide); Poly (lactide –co- glycolide); Poly(lactic acid-co-ethylene glycol); Poly (propylene fumarate); Poly(ethylene therephtalate); Polycaprolactone; Polyhydroxyalkanoates; Poly(glycerol sebacate); Pluronic F127; Polyphosphazenes, Polyanhydrides. | Tailored biodegradability, Design flexibility (can be processed into different shapes and forms) | Acidic Breakdown products might cause inflammatory response; some types might have poor cell adhesion; poor affinity for growth factors. Encapsulation methods involve solvents that might denature proteins. Poor mechanical strength. | Behravesh et al., 1999; Saitoa et al., 2003; Bessho et al., 2002; Lucas et al., 1990; Lakshmi et al., 2003; Clokie & Urist, 2000; Yang et al., 2004; Brunet-Maheu et al., 2008; Ma et al., 2005; Savarino et al., 2007; Chen & Wu 2005; Wang et al., 2002. |

**Table 1.1** Example of materials used in various tissue engineering applications

2008), chitosan (Zhang eta l., 2006; Risbud et al., 2002), silk (Wang et al., 2005; Hofmann et al., 2006), alginate (Elkayam et al., 2006), and Agarose (Stevens et al., 2005; Stokols et al., 2006). Many of the naturally occurring animal-derived polymers are components of extracellular matrix. They are biocompatible, bioresorbable and can be formulated into many configurations with variable residence time through the enzymatic treatment and chemical cross-linking of the polymer. Collagen formulations used as scaffolds include gelatin, and fibrillar collagen. Hyaluronans, chitosan, alginate and agarose can be formulated into hydrogels, sponges. Fibrin, can be formulated as an adhesive glue-type delivery vehicle for growth factors such as BMPs (Schmokel et al., 2004). .However, several issues limit the use of natural polymers in tissue engineering. Poor mechanical strength, rapid degradation, and batch to batch variation with materials are examples of issues limiting the use of these materials as scaffolds. Other disadvantages of natural polymers include sourcing, processing, possible disease transmission and immunogenicity of the polymers (Seeherman and Wozney, 2005).

#### 1.2.2.2. Synthetic Polymers

Synthetic polymers have been widely used for tissue engineering (Kannan et al., 2005; Liu et al., 2004). The poly (α-hydroxy acid) polymers such as polylactide, polyglycolide and their copolymers (poly(D,L-lactide-co-glycolide) (PLGA) are the most commonly used synthetic polymers. The biocompatibility and resorbability of these polymers underlies its extensive use in tissue engineering either as a temporary scaffold or as carriers for the delivery of bioactive molecules. Another contributory factor influencing its extensive use is related to the fact that these polymers have been approved by certain governmental agencies such as US Food and Drug

Administration (FDA) and the European Medicines Agency (EMEA) for use as medical sutures, drug delivery devices and orthopaedic implants.

Additional synthetic polymers used include poly(ε – caprolactone) (PCL) (Hutmacher, 2000), polyanhydrides (Lucas et al., 1990), polyphosphazenes (Lakshmi et al., 2003) polypropylene fumarate (Behvrevesh et al., 1999), polyethylene glycol- PLA (Miyamoto et al., 1993), poloxamers (Clokie et al., 2000), and polyphosphate polymers (Renier and Kohn 1997) Their design flexibility, elimination of disease transmission and batch to batch variability represent major advantages for the use of synthetic polymers in tissue engineering. Synthetic polymers can be easily processed into porous three-dimensional scaffolds, linearly oriented scaffolds, microspheres, polymer fibres and sheets (Seeherman and Wozney, 2005).

Degradation of these polymers occurs by hydrolysis, cellular mediated degradation and enzymatic pathways. The decrease in local pH resulting from acid breakdown products of the polymer during bulk degradation; excessive inflammatory responses, and poor clearance associated with high molecular weight polymers are some of the disadvantages associated with synthetic polymers. The design of newer surface eroding polymers has been used to improve the release profiles of growth factors from scaffolds and reduce the problems associated with bulk degradation (Wang et al., 2003). In addition, scaffolds produced from synthetic polymers have a low capacity for facilitation of cellular responses due to the lack of adhesion groups such as proteins for receptor mediated cell surface binding (Suciati, 2006). Adsorbing proteins such as collagen unto the scaffold surfaces (Kaufmann et al., 1997; Chen et al., 2003), deposition of hydrophilic polymers unto the scaffold surface using plasma

polymerisation techniques (Barry et al., 2006; Park et al., 2007); and the attachment of functional domains such as Arg-Gly-Asp (RGD) (Quirk et al., 2001; Yang et al., 2001) have all been used successfully for improving cell attachment, and proliferation within scaffolds from these polymers.

### 1.2.2.3. Inorganic Materials.

This class includes ceramics, such as various compositions of calcium phosphate (e.g. hydroxyapatite (HAP), and tricalcium phosphate (TCP)), and non-ceramics, such as calcium phosphate-based cements (CPCs). Other inorganic carriers include calcium sulphates, metals and bioglass. HAP is widely used because it is the major component of bone and has been used clinically since the 1980s in prosthetics (Jarcho, 1981). In addition, HAP has the ability to bond directly with bone because its chemical nature is identical to that of bone. HAPs are typically presented in a granular or block form; however, unless combined with other materials, HAP is brittle and HAP blocks are difficult to shape to bone defects. Injectable CPCs harden *in vivo* and have also been tested as carriers of bone morphogenic proteins for the promotion of bone formation (Edwards et al., 2000; Seeherman et al., 2001. Typical CPCs are comprised of two components, which react and harden when mixed, and because the crystals are not fused they are slowly resorbable (Schmitz et al., 1999). A potential disadvantage of some CPCs is that they undergo an exothermic reaction that might denature labile proteins. The low temperature calcium orthophosphate cements (CPC) have proven to be extremely versatile materials that can be formulated as injectable cements, implantable cements and solid implants. The most commonly used CPCs precipitate out in aqueous solutions of calcium phosphates as crystals, which become entangled to form the cement structure. The low temperature precipitation allows for the

addition of growth factors such as BMP as a lyophilized powder to the cement components or in the aqueous phase prior to the cementing reaction without risking damage to the protein. In addition to being biocompatible, calcium orthophosphates, and bioglass (as well as hydroxyapatites) are generally very osteoconductive materials that promote have been shown to promote bone formation directly on their surfaces (Seeherman and Wozney, 2005). The major disadvantages of CPCs include phase separation during injection, a lack of intrinsic macroporosity to allowcell infiltration and decreased mechanical tensile and shear properties compared to bone and other materials. Modifications to CPC formulations can be made to increase the injectability (Bohner et al., 2005) and macroporosity *in vivo*. Increased macroporosity can be achieved by the addition of gas evolving excipients to CPC formulations to induce granulation or to form pores (del Real et al., 2002; Seeherman et al., 2002). The lack of biomechanical strength can circumvented by using the appropriate external or internal fixation in combination with CPC. High temperature calcium orthophosphates can be fabricated into preformed granules or blocks. Porous ceramic blocks can also be fabricated to mimic the threedimensional structure of trabecular bone (Dutta Roy et al., 2003; Tada et al., 2002). Due to the high temperature sintering process, BMPs can generally only be surface coated onto these materials after fabrication. In addition, the residence time of high temperature calcium orthophosphates is prolonged and mechanical strength is generally adequate only in compression. Calcium orthophosphates with prolonged residence time also tend to form bone the outer surface encasing the residual carrier and slowing resorption further.

### 1.2.3. Scaffold Fabrication Methods.

Numerous techniques have been utilised in preparing the scaffolds for tissue engineering or drug delivery applications. Determining which method to be used is dependent on several factors including the function, constituent material of the fabricated scaffold. Discussed below are some of the different techniques that have been employed for the fabrication of scaffolds. A more extensive overview of these and other techniques utilised can be found in the review by Weigel et al., 2006.

#### 1.2.3.1.Solvent Casting / Particular leaching

Solvent-casting particulate leaching method involves the mixing of a polymer solution (i.e. PLA in chloroform) with water soluble particles of defined size (Lee and Feldman 1998). The mixture is then cast into a mould of desired shape and the solvent then removed by evaporation under vacuum. This leads to polymer solidifying around the salt particles. The entrapped salt can then be leached out of the scaffold by rinsing in distilled water, leaving a highly porous polymer scaffold with a defined pore structure (Mikos et al. 1994; Lee and Feldman 1998; Liu and Ma 2004). A variation to this approach involving the use of spheres rather than salt crystals as pore forming materials has also been used in forming porous scaffolds (Marra et al. 1999). The solvent casting / particulate leaching technique has been used in the fabrication of scaffolds for the delivery of angiogenic factors for promotion of angiogenesis (Hile et al., 2000).

#### 1.2.3.2. Heat Sintering

An increasingly popular method of 3D scaffold fabrication is the heat fusion (sintering) of polymer microparticles. The microstructure of the particles is generally

well preserved with bonding of the adjacent microparticles occurring through the thermal fusion of the polymers through heating of the polymers above their glass transition temperature (Borden et al., 2002 & 2003).

#### 1.2.3.3. Super-critical Fluid

Denaturation of growth factors during scaffold fabrication has been indicated as the main cause of activity loss of protein released from scaffold. Super critical fluid technique has been developed recently to form scaffolds to improve on the current fabrication methods. Scaffold fabrication using SCF technology (RESS technique) normally involves the dissolution of the polymer/growth factor complex in supercritical CO2 (scCO2). This is followed by a rapid expansion of the mixture into a low temperature and pressure environment which leads to scaffold formation (Vasita et al., 2006). Another technique utilizing the scCO2 is the PGSS technique, which involves using the scCO2 to plasticize the polymer by lowering the glass transition temperatures (Tg) of the polymer. This technique involves the application of the SCF under pressure into the polymer and growth factor mixture until the mixture is saturated. This is followed by depressurizaton through a nozzle, leading to the formation of highly porous scaffolds as the gas comes out of liquefied polymer. Porous BMP-2-encapsulated poly(DL-lactic acid) (PLA) scaffolds generated by the supercritical fluid process was shown to promote adhesion, migration, proliferation, and differentiation of human osteoprogenitor cells on three-dimensional scaffolds (Yang et al., 2004).

#### 1.2.3.4. Rapid Prototyping/Solid Free-Form Fabrication

Rapid prototyping and solid free-form fabrication methods are common terms for techniques that creates a scaffold directly from a computer aided design (CAD) data set. Scaffold construction using these techniques involves the addition of the material,

layer by layer through the guidance of the computer program (Weigel et al., 2006). Once the layer is complete, the build platform is indexed downward by one layer thickness and the process is repeated. The layer by layer approach utilized for construction of the scaffolds facilitates improved reproducibility and enables the design of complex scaffolds with an exact pre-defined shape and an internal architecture that is predefined and perfectly suited to mimic that of the tissue that is to be regenerated (Houtmacher, Sittinger et al. 2004; Yeong, Chua et al. 2004). Cells can be incorporated into the pre-fabricated layer prior to final assembly of the scaffold (Chua et al., 2003), and parameters such as the pore size, interconnectivity, and porosity can be controlled more precisely using these techniques (Zhang et al., 2005).

#### 1.2.3.5. 3-D Printing

3-Dimensional printing, is used to create complex three-dimensional scaffolds by building up printed layers of polymer using an inkjet printer to deposit a binder solution unto the polymer bed (Tsang and Bhatia 2004). It involves the spreading of a layer of powder over a building platform, followed by the precise deposition of a binder solution by an inkjet printer on the powder layer to facilitate the joining of the single particle powders to form a 2D layer of the scaffold (Leukers et al., 2005). This process is further repeated to completely generate the scaffold. The binder is then allowed to dry, after which the non-joined polymer is removed by an air jet flow, and the finished scaffold can then be retrieved (Pfister et al., 2004).

#### 1.2.3.6. Selective laser sintering

This technique involves the use of deflected laser beams such as infra-red and $CO_2$ laser beams to sinter layers of powdered materials such as wax or polymers to form

scaffolds (Giordano et al, 1996). The laser beam selectively scans over the polymer surface, leading to deformation and fusion of the surface polymer. New layers of the polymer are then deposited by a roller, and the laser sintering repeated thereby building a new sintered layer on top of the previous layer The fusion of the polymer chains at the surface is as a result of the laser beam leading to an increase in the glass transition temperature of the polymer (Weigel et al., 2006).

#### 1.2.3.7. Stelithography

The stelithography method is based on the initiation of a photopolymerization or crosslinking chemical reaction by the electromagnetic radiation of a polymer liquid (Dhariwala et al., 2004). The process involves the direction of a light source of electromagnetic radiation onto selected regions of the liquid polymer. This radiation leads to the formation of scaffolds through the solidification of the polymer liquid due to either a polymerization or cross-linking reactions (Cooke, Fisher et al. 2002). Further layers of the polymer liquid can be solidified through the direction of the light source to another layer of the polymer liquid.

#### 1.2.3.8. Electrospinning method

Electrospinning method has been used in fabricating 3D fibre scaffolds in the micrometer or nanometer scale by electrically charging a droplet of polymer solution or melt. A surface charge greater than the surface tension of the droplet of polymer solution is generated by a high voltage electrostatic field operated between the nozzle of a syringe and a metallic collector plate. Fibre scaffolds are generated due to the narrowing of the ejected jet stream of polymer solution that occurs as it undergoes increasing surface energy due to the evaporation of the solvent.

Electrospinning technique can be used in fabricating scaffolds from both natural and synthetic polymers. Li and co-workers produced silk fibroin fibre scaffolds containing bone morphogenetic protein 2 (BMP-2) and/or nanoparticles of hydroxyapatite (nHAP) using electrospinning, and showed its ability in inducing *in vitro* bone formation from human bone marrow-derived mesenchymal stem cells (hMSCs). The electrospun scaffolds containing BMP-2 supported higher calcium deposition and enhanced transcript levels of bonespecific markers than the electrospun scaffolds without BMP-2, indicating that the scaffolds were an efficient delivery system for BMP-2. X-ray diffraction (XRD) analysis revealed that the apatite formed on the silk fibroin/BMP-2 scaffolds had higher crystallinity than on the silk fibroin scaffold controls (Li et al., 2006).

### 1.3. Growth Factors.

Growth factors are proteins that possess profound influence on the proliferation and differentiation of cells. Together with hormones, neuropeptides and cytokines, they form a wide family of protein signalling molecules, which play important roles in controlling tissue morphogenesis, repair and immune modulation (Cooper, 1997). They are able to stimulate the differentiation of stem cells. The growth factors include many subgroups such as insulin growth factors (IGFs), transforming growth factor super family (TGF α and β families), and platelet derived growth factors. Growth factors are secreted by many cells in the body, and their effects could be induced in the same cell secreting the growth factor (autocrine), on nearby cells (paracrine), or on distant target cells (endocrine). In addition they could also be expressed on the cell surface of one cell and bind the receptors expressed on other cells (juxtacrine).

Growth factors are proteins that modulate cellular activities by binding to receptors on the cell surface. The binding of growth factors to the cell receptors leads to the activation of various internal cellular processes such as cellular proliferation and differentiation. Growth factors are produced by a variety of cell types, many of which show great versatility in their ability to initiate and regulate several cellular processes in a whole host of different cell types. However, some growth factors show specificity only to a particular cell-type (Babensee, McIntire et al. 2000).

Several growth factors have been characterised and their function elucidated, examples of which include Platelet derived growth factor (PDGF) which has been shown to promote proliferation of connective tissue, glial and smooth muscle cells and EGF, which promotes proliferation of mesenchymal, glial and epithelial cells. TGF-α is important for normal wound healing while TGF-β has been shown to possess anti-inflammatory properties (suppresses cytokine production and class II MHC expression), promotes wound healing, inhibits macrophage and lymphocyte proliferation.

Growth factors are produced either as inactive or partially active precursors which are subsequently bound to proteins on the extracellular matrix (ECM) to aid the maintenance of their stability and function. These precursors require proteolytic cleavage followed by activation to form the active growth factors. An example of this is the TGF-β growth factor responsible for attraction and proliferation of osteoblasts in sites of bone resorption. The inactive form of TGF-β is released by primary osteoblasts, which is then incorporated into the ECM by binding to the latent TGF-β

binding protein-1 (LTBP1). It is then proteolytically cleaved by osteoclasts in areas of bone resorption and then activated to the active TGF-β. (Dallas, Rosser et al. 2002)

### 1.3.1. The Role of Growth Factors in Tissue Engineering.

Tissue engineering applications often requires the provision of large number of cells with good regenerative and differentiation potential. However, difficulties in sourcing this amount of cells with similar phenotype, genotype, and from the same batch in a short period of time exists. In the past, direct cell expansion of the required cells has been postulated as a solution, however problems such as poor number of cells isolated from tissues, a slower *in vitro* rate of proliferation during cell expansion, changes in specific phenotypic expression and limited life span of the cells indicated the need for a more robust method. Growth factor supplementation in culture media during cell expansion has been used successfully in overcoming these problems. Hence the artificial regeneration of tissues using tissue-engineering techniques often involves the need for the application for growth factors alongside transferred cells, especially cells with low regenerative potential. Several growth factors have been used in tissue engineering and clinical applications and are summarised in Table 1.2.

The use of growth factors alongside cells has also been shown to successfully improve phenotypic expression (Forte et al., 2005), minimize de-differentiation (Tsai et al., 2007; Park et al., 2008), induce migration of stem cells (Urbich et al., 2005; Martin et al., 2008) promote cell proliferation (Suzuki et al., 2008; Gao et al., 2008), and improve survival of cells (Kortesidis et al., 2005; Fan et al., 2007) in culture conditions. TGF-β1 (Zaleskas et al., 2001; and Pei et al., 2002) and BMP-2 (Vitale-Brovarone et al., 2006) have been used successfully in maintaining the phenotypic

expression, improve survival and proliferation of chondrocytes and osteoblasts when grown on scaffolds respectively.

In tissue engineering applications, growth factors have gained widespread use in differentiation of stem cells and progenitor cells into different cell lineage for both *in vivo* tissue regeneration and *in vitro* culture techniques. *In vitro* tissue techniques have been utilised in developing tissue models for better understanding of diseased mechanism of tissue, tissue morphogenesis and regeneration, and further investigate the potential applications of stem cells in repair of tissues. For example, the effects of members of the TGF-β superfamily on stem cells isolated from adipose tissue (Estes et al., 2006; Awad et al., 2004; Afizah et al., 2007; Lin et al., 2007) and umbilical cord blood (Kumar et al., 2007; Wagner et al., 2005) for the engineering of articular cartilage and bone has been investigated extensively

### 1.3.2. Growth Factor Delivery.

Advances in growth factor mechanisms have implicated it in tissue morphogenesis and repair. A number of sources exist in the obtainment growth factors, which include production of recombinant growth factors, purification from cell extracts and the utilisation of gene therapy to induce growth factor production. However, several barriers exit in administering growth factors using the normal pharmaceutical forms or routes. These include the short half-life, enzymatic and proteolytic degradability, rapid diffusion from sites of application and slow tissue penetration. In addition, there

| Growth Factor | Signalling Functions | Delivery Methods | Tissue Engineering Application | References |
|---|---|---|---|---|
| VEGF | Endothelial cell proliferation | Alginate Hydrogels<br>PLGA-PEG microspheres<br>PLGA Sponge | Angiogenesis, and adjunct for bone regeneration | Kaigler et al., 2006; Grossman et al., 2005; Kanczler et al., 2007 |
| IGF-1 | Extracellular matrix production; cell growth; and apoptosis inhibitor | Collagen scaffold<br>Porous calcium phosphate implant.<br>PLGA microspheres | Cartilage and bone regeneration<br>Adipose tissue regeneration | Jacklenec et al., 2008; Capicto & Specto, 2007.<br>Holland et al., 2005<br>Yuksel et al., 2005 |
| BMP-2 | MSCs migration, proliferation and differentiation along osteogenic pathway. Ossification and osteoblast proliferation and differentiation. | PLGA and PLA microspheres, Gelatin hydrogels, ceramics, metals | Bone regeneration | Suciati et al., 2006; Yang et al., 2004; Kempen et al., 2008; Yoshikawa & Myoui, 2005; Walboomers & Jansen, 2005. |
| TGf-β1 | MSCs migration, proliferation and differentiation along chondrogenic pathway. Chondrocytes proliferation and differentiation, Cartilage matrix synthesis. | Fibrin gels, gelatine microspheres, PEG-based hydrogels,<br>Chitosan microspheres | Cartilage regeneration | Catelas et al., 2008; Holland et al., 2003; Lee et al., 2004; |

| Growth Factor | Signalling Functions | Delivery Methods | Tissue Engineering Application | References |
|---|---|---|---|---|
| TGF-β2 | Chondrocyte proliferation and cartilage matrix synthesis | Collagen gel heparin | Cartilage regeneration | Schroeder-Tefft et al., 1997 |
| TGF-α | Osteoblasts proliferation and differentiation | Ceramics | Bone regeneration | El-Ghannam, 2005 |
| bFGF | Endothelial cell proliferation. Fibroblast proliferation Schwann cell proliferation. | Gelatin/hyaluron/chitosan ternary scaffold. Gelatin microspheres PLA/Gelatin scaffold | Cartilage regeneration Wound healing, angiogenesis, Nerve cell survival | Tan et al., 2007; Kimura et al., 2008. Wang et al., 2003 |
| PDGF-BB | Endothelial cell proliferation. Osteoblast adhesion. Smooth muscle cell proliferation. | PLGA microspheres. PLGA Scaffold | Angiogenesis and wound healing. Bone regeneration | Jin et al., 2008; Chen et al., 2007; Wei et al., 2006 |
| EGF | Hepatocyte proliferation. Epidermal keratinocyte proliferation | PLA Fibres PLGA / Collagen scaffold | Liver regeneration. Wound healing | Ma et al., 2007; Smith et al., 2006 |
| NGF | Axonal and cholinergic proliferation | PLGA microspheres Chitosan and ceramics | Neuronal regeneration | Bloch et al., 2001; Wang et al., 2005; Chen et al., 2006 |

**Table 1.2** Growth factors used in tissue engineering applications

is the requirement for targeted and controlled release of growth factors at a suitable concentration to the responsive cells to contend with.(Babensee, McIntire et al. 2000)

Hence, major challenges lie in the requirement for growth factor delivery mechanisms to mimic the in-vivo release profiles during natural tissue regeneration or morphogenesis. A way of resolving the challenge involves the utilisation of a sort of depot delivery system (mimicking the natural ECM), which releases a programmed concentration of the growth factor at a controlled rate (Tabata 2004). In addition to controlling the rate of growth factor delivery to the desired cells, the delivery system should also provide a structural support for the growth factors and the cells that might be co-delivered. It should also be able to maintain the growth factor stability and activity, alongside possessing biocompatible and biodegradable properties.

### 1.3.3. Scaffolds as Growth Factor Delivery Devices.

In choosing a scaffold for the delivery of growth factors, the following issues need to be considered.

a) Scaffold should be able to protect the growth factors from denaturing factors such as circulating proteases and an oxidative environment (Miell et al 1992; Uludag et al., 1999; and Zakrzewska et al., 2005).

b) As most cells require the continuous exposure to growth factors, for the growth factor mediated effects to be mediated, scaffolds should be able to present the growth factors in an active form and in an the required concentration. This is an important necessity as several studies has shown that withdrawal of the growth factors may reduce or abolish the growth factor effects (Park et al., 2000; Lum et al., 2005).

c) Scaffolds should be able to localise the growth factor released to the target site, so as to minimise possible toxic effects on non-target tissues.

Several advantages of using biologically derived materials as growth factor delivery systems exist due to their similarity to natural ECM. These advantages include, possession of inherent properties of biological recognition; presentation of receptor-binding ligands; and susceptibility to cell-triggered proteolytic degradation & remodelling. However, factors such as complexities associated with purification, illicit immunogenic response, pathogen transmission and inability to modulate the degradation rate have limited its clinical relevance.

One way of enhancing the *in-vivo* delivery of growth factors involves incorporating into a polymer carrier, thereby facilitating its sustained release over a period (Babensee, McIntire et al. 2000). This polymer carrier is termed a scaffold and forms the basis of several delivery devices used within tissue engineering. Through incorporation within scaffolds, it is possible to stabilise the biological activity of the growth factor, its structure and provide sustained delivery over an extended period.

These polymeric scaffolds have been utilised in the design of tissue-engineered constructs in delivering several growth factors for the correction of a wide range of medical conditions. They have been shown to present the growth factors in a controlled manner, leading to the chemo-attraction of self-derived cells residing along the delivery devices, leading to the infiltration and subsequent proliferation of the implants with the necessary cells that will aid tissue regeneration.

### 1.3.4. Methods of Growth Factor Incorporation.

Growth factor delivery strategies involving scaffolds include the direct incorporation of growth factor or the encapsulation of growth factor secreting cells into scaffold. Alternatively another approach involves the encapsulation of plasmid DNA encoding for the growth factors within the scaffolds, leading to the production of growth factors within cells (Chen and Mooney, 2003). A variety of polymeric scaffolds have been used to deliver growth factors, including natural or synthetic polymers that generally form either hydrogel or solid polymer scaffolds. The various techniques currently employed in the incorporation of growth factors within polymeric scaffolds can be broadly divided into two methods — attachment of the growth factors unto the scaffold and the physical entrapment of growth factor within the scaffold.

#### 1.3.4.1. Attachment of growth factors to polymeric scaffold

This method involves the attachment of growth factors onto preformed scaffolds. The techniques could vary from the immobilization of the growth factor onto the surface of the polymer through chemical crosslinking (DeLong et al., 2005; Mann et al., 2001), to the adsorption of the growth factor unto the scaffold (Lee et al., 2007) The adsorption of growth factors onto scaffolds harnesses possible physicochemical interactions such as the formation of ionic complexes, that occur between the polymer material and the growth factors. Park and co-workers were able to load TGF-β1 into gelatine microspheres through the formation of ionic complex during incubation of gelatine microspheres in aqueous TGF-β1 solution at pH 7.4. The ionic complex formation was attributed to the association of negative charged moieties on the gelatine microspheres and positive charged moieties within the TGF-β1 molecule (Park et al., 2005).

### 1.3.4.2. Entrapment of growth factors within scaffold.

In addition to the attachment of growth factors to polymeric scaffolds, growth factors can be directly incorporated within scaffolds using the scaffold fabrication techniques described above (section 1.2.3). These methods involve the mixing of the growth factor with the polymers prior to scaffold fabrication. The main challenge of this set of methods is to ensure that the processing conditions do not significantly denature the incorporated growth factors while still able to secrete the growth factor in a sustained manner (Sokolsky-Papkov et al., 2007). A variety of polymeric scaffolds have been used to deliver growth factors, including natural or synthetic polymers that generally form either hydrogel or solid based polymer scaffolds.

Hydrogel scaffolds can be made from synthetic polymers such as poly(ethylene glycolide), poly vinyl alcohol, or naturally occurring polymers such as collagen, chitosan and gelatin. Release of growth factors from hydrogels is believed to be either through diffusion of the growth factor through the highly hydrophilic scaffold, mechanical stimulation, or hydrolytic degradation of the scaffold (Drury and Mooney, 2003). They are formed by the crosslinking of polymer chains to form a scaffold made up of connected polymer chains. Crosslinking can be done either through physical (UV irradiation, freeze drying and heating) and chemical means such as ionic crosslinking in presence of divalent ions or utilization of chemical crosslinkers such as glutaraldehyde and carbodiimide.

### 1.3.5. Microsphere as Growth Factor Delivery Devices.

Growth factor loaded scaffolds can also be manufactured from growth factor loaded microspheres. Microspheres can be made either through the polymerization of

solutions of monomers and proteins to form microspheres, or directly from solutions of preformed polymers and proteins. Growth factor loaded microspheres can be used for tissue engineering applications either by direct fusing of microspheres directly to form scaffolds, or combination with other scaffold forming materials to form composite scaffolds. In work undertaken by Wei and co-workers, PDGF-BB loaded microspheres were incorporated in poly(lactic acid) PLLA nano fibrous scaffold. Sustained release for days to months of bioactive PDGF-BB was achieved by the microspheres in scaffold. Kempen et al (2003) and Hedberg et al., (2002) showed the application of PLGA and poly(propylene fumarate) (PPF) microspheres in microsphere/scaffold composite for controlled release of growth factors for bone tissue engineering.. Discussed below are methods currently employed in the fabrication of empty and protein loaded microspheres.

#### 1.3.5.1. Microspheres prepared by polymerization of monomers.

Microsphere fabricated by polymerization of monomers generally involves the polymerization of colloidal monomers dispersed in a liquid, which is a non-solvent of the monomer. Spherical droplets are formed by oil-soluble organic monomers dispersed in an aqueous based medium, or by water-soluble monomers dissolved in water dispersed in an organic phase. The polymerization of the dispersed monomers is achieved through three main techniques; emulsion, suspension, and dispersion methods (Freiberg and Zhu, 2004).

The emulsion method takes place in two stages. The first stage is the formation of micelles by the dispersion of a monomer in an aqueous medium containing a surfactant and water-soluble initiator. This is followed by the second stage, which is

the polymerization of the monomers, by the water-soluble initiator to form the microspheres. Suspension method involves the dispersion of monomer droplets into a water phase containing a stabilizer. An initiator soluble in the monomer phase is used in initiating polymerization within the dispersed monomer droplets (Piirma, 1985). The dispersion method is similar to the suspension method but generally involves the dissolving of the monomer, initiator and stabilizer in an organic medium. Due to the solubility of the initiator within the monomer, polymerization takes place within the monomer droplets. Precipitation of the microspheres formed from the polymerization of the monomers occurs due to its insolubility within the organic solvent (Strover and Li, 1996).

#### 1.3.5.2. Microspheres prepared from polymers.

Microspheres can be prepared using any of the following techniques.

##### 1.3.5.2.1. Solvent evaporation

This method was first described by Ogawa, et al. (1988), and has become the most extensively used method of microsphere fabrication. It is based on the principle that microsphere formation can occur by the evaporation of an organic solvent such as dichloromethane (chloroform and ethyl acetate have also been used), from dispersed oil droplets containing both the polymer and the molecule of interest (MOI) (drug or protein) (Freiberg and Zhu, 2004). Two popular variations of this technique are currently used and are schematically represented in Fig.1.1 A & B.

The double emulsion method involves dissolving the MOI into water, followed by the dispersion of this in an organic solution containing the polymer – leading to the

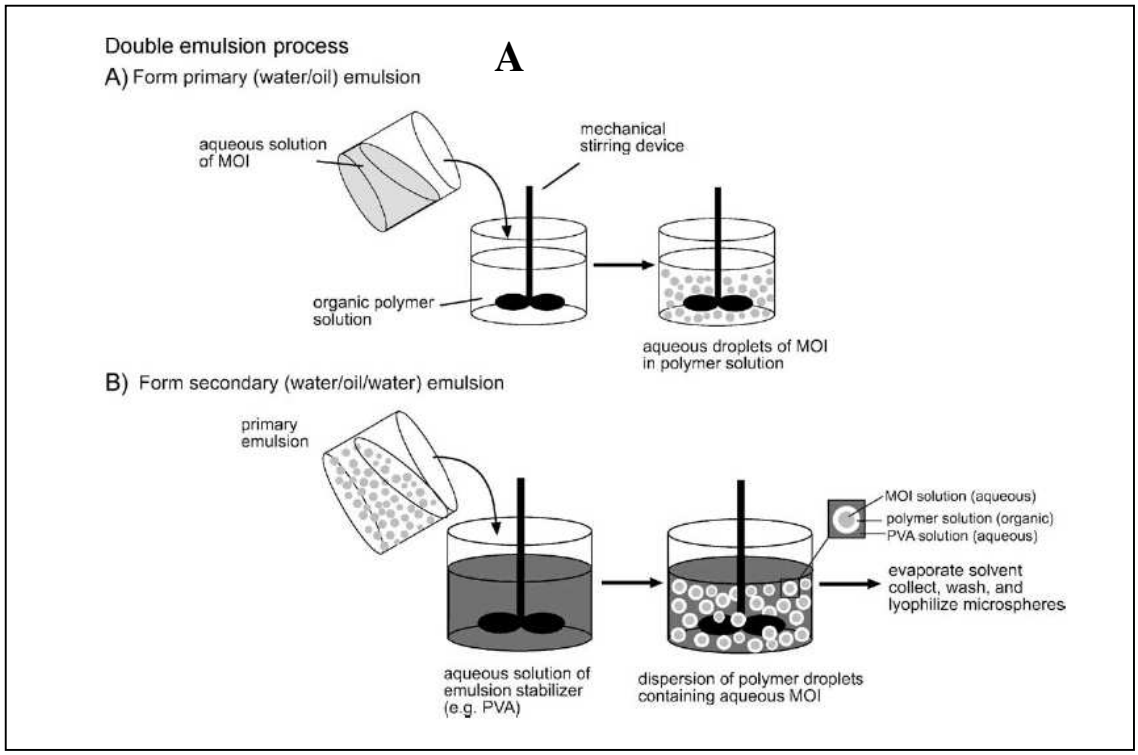


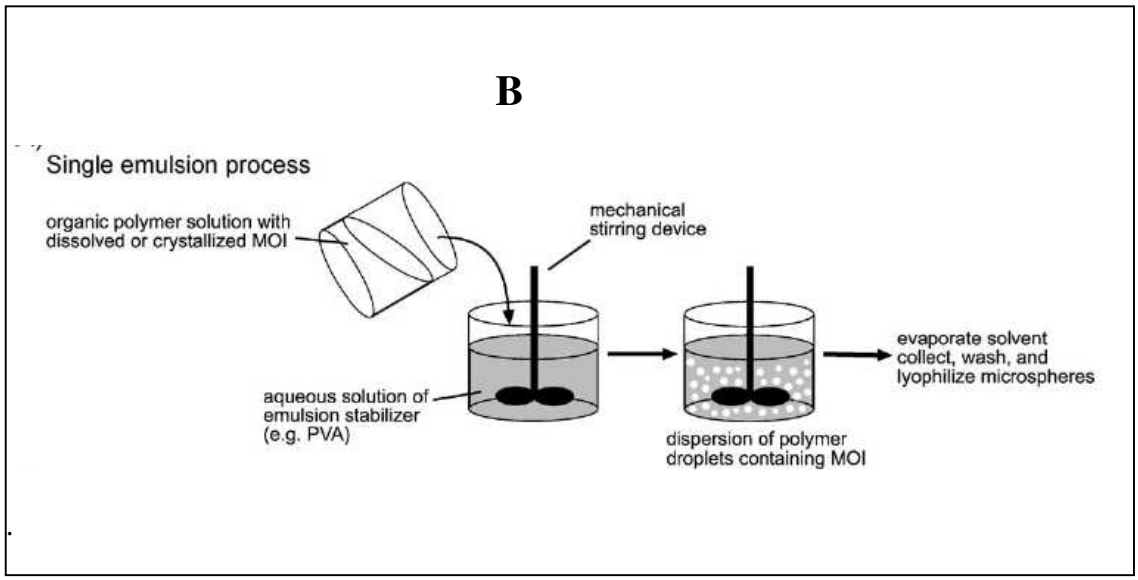


Figure 1.1: Schematic representation of the (A) Double and (B) Single emulsion process (Whittlesey and Shea, 2004).

formation of the primary W/O emulsion. The final O/W emulsion is formed by dispersion of the primary emulsion in an aqueous medium containing stabilizers such as poly (vinyl alcohol) (PVA) or poly (ethylene glycol) (PEG), under continuous mechanical agitation The single emulsion method involves the dispersion or dissolving of MOI directly into the organic solution of the polymer. The mixture is then transferred into the aqueous solution containing the stabilizer. The MOI could be micronized by lyophilisation with PEG, CDs etc before dispersing it into the organic polymer solution to improve entrapment efficiency of the protein (Morita, et al., 2001). Microsphere formation occurs due to the evaporation of the organic solvent from the emulsion droplets, and the phase separation of the polymer due to an interaction with a non-solvent. The microspheres are then collected either by centrifuging or filtration, washed and lyophilised to obtain the free flowing and dried microspheres.

#### 1.3.5.2.2 Hot melt microencapsulation

This method involves the mixing of pre-sieved drug particles with melted polymer. The mixture is then suspended in a continuously stirred non-miscible solvent (like silicone oil), which is heated to 5ºC above the melting point of the polymer. On stabilization of the emulsion, polymer particle solidification occurs on cooling. The resulting microspheres can be obtained by decantation with petroleum ether (Mathiowitz and Langer, 1987).

#### 1.3.5.2.3 Solvent removal

Solvent removal is another non-aqueous method for microsphere formation, particularly suitable for water labile polymers. This method involves the dispersion or

dissolving of the molecule of interest (drug or protein) in a solution of the polymer in a volatile organic solvent like methylene chloride. This mixture is then suspended in silicone oil containing Span 85 and methylene chloride (Carino et al., 1999). On pouring of the polymer solution into silicone oil, petroleum ether is added and mixture is stirred continuously until solvent is extracted into the oil solution. The resulting microspheres can then be dried in vacuum (Vasir et al., 2003).

#### 1.3.5.2.4 Spray drying

The spray drying process involves the dissolving or dispersion of the MOI into the polymer solution, which is then followed by spray drying. The protein/ polymer dispersion is sprayed through a heated nozzle, followed by the rapid evaporation of the organic solvent by a hot gas flow. A variation of the conventional spray-drying method is the cryogenic method. This method involves the spraying under ultrasonic conditions of protein/PLGA dispersion into liquid nitrogen over solid ethanol. Evaporation of the liquid nitrogen results in the melting of the ethanol, leading to the extraction of the organic solvent from the microparticles formed by the spraying process (Weert et al., 2000). This method has been used to prepare PLGA microspheres that release bioactive recombinant human growth hormone (rhGH) over a one-month period (Johnson et al., 1997; Weert et al., 2000) and has resulted in the formation of a protein-containing PLGA microparticle formulation currently on the market (Nutropin Depot) (Weert et al., 2000).

A novel method for the preparation of PLGA microparticles involves the use of a supercritical fluid, such as carbon dioxide to induce microparticle formation (Young et al., 1999). “A mixture of protein suspended or dissolved in an organic PLGA

solution is sprayed in supercritical carbon dioxide, which results in dissolution of the organic solvent in the supercritical phase and precipitation of protein-loaded PLGA microparticles" (Weert et al., 2000).

#### 1.3.5.3.5 Phase inversion

The process involves mixing of the MOI into a dilute organic solution of the polymer. This mixture is subsequently poured into an unstirred bath of a strong non-solvent (petroleum ether), in a solvent to non-solvent ratio of 1:100. This leads to the spontaneous production of microspheres through phase inversion. The microspheres produced can then be filtered, washed with petroleum ether and dried with air (Chickering et al.1996).

### 1.3.5.3. Microsphere Release Kinetics.

Protein and growth factor release from biodegradable polymers is a function of the rate of hydrolysis of ester linkages that makes up the polymer chains. It is also dependent on the diffusion and flow of the protein through the pores present in the microspheres. These pores can be formed during the microsphere process fabrication or from the gradual hydrolysis of the polymer the microspheres are fabricated from (Herrero-Vanrell and Refojo, 2001). The mechanism of protein release from microspheres has been well characterized and shown to occur in five various ways. A) The initial release from the drugs that are entrapped on or close to the surface of the material – known as the initial burst phase. B) Release through pores that might be present on the micropheres. C) Diffusion of protein through the intact polymer barrier. D) Diffusion of protein through the water-swollen barrier. This water-swollen barrier is formed on incubation of the microspheres in the release media and is dependent on

the polymer hydrophilicity. E) Polymer erosion and bulk degradation, release affected by the rate of erosion and hydrolysis of polymer chains, leading to pore formation within the matrix (Sinha and Trehan; 2003).

The main factors affecting protein release rate revolves around the structure of the microphere matrix and the chemical properties that are associated with both the polymer and the encapsulated protein. The most desirable release profile is a zero order kinetic profile which shows a constant release rate of protein with time. However in many cases release rates are more complicated and often involve a tri-phasic release pattern consisting of two main release phases of protein separated by a lag phase where there is little or no release. The first release is normally the initial burst release and occurs within the first 24 hours where the protein at the surface of the microsphere is released. The second main release is normally a more constant release with release rate dependent on diffusion and degradation of the polymer.

Factors affecting protein release from microspheres such as polymer molecular weight, protein-polymer interactions, porosity and size distributions of the microspheres, can be exploited as means of controlling the release from microspheres, in order to achieve zero order release profiles.

#### 1.3.5.3.1. Molecular weight

Makino et al. (2000) showed that by varying the MW of PLGA, they were able to improve the linearity of the release profile. They observed that the lowest MW (19,000) produced close to linear release profile. While the higher MWs (23,000; 44,000 and 74,000), which showed an increasing shift towards the more characteristic

tri-phasic pattern. Park and co-workers (1994, 1995) showed in a series of experiments that the protein release from high MW polymer microspheres was characterised by a slow drug release (after the initial burst phase) due to diffusion, followed by the main drug release due to degradation. While that of the lower MW microspheres showed a steady controlled release after initial burst phase. Thus indicating that after the initial burst stage, degradation is the main release mechanism for low MW polymers, while diffusion and degradation are the dominant release mechanisms for higher MW polymers.

#### 1.3.5.3.2. Blends of structurally different polymers

The physical blending of two polymers can affect the release profiles of polymer spheres. Edlund and Albertsson (2000) observed that by employing varying mixtures of blend composition of poly(l-lactic acid) (PLLA) and poly(1,5-dioxepan-2-one) (PDXO), the degradation rate of the matrix can be increased with increasing amount of PDXO. The lower degradation rate of PLLA over PDXO was attributed to the increased crystallinity in PLLA with crystalline regions degrading more slowly than the amorphous regions (Edlund and Albertsson, 2000).

#### 1.3.5.3.3. Microsphere Matrix Modification.

Another approach of regulating the abnormal release behaviour of proteins from PLGA micropheres involves the chemical modification of PLGA by compounds such as polyethylene glycol (PEG) to form multiblock polymers. The PEG/PLGA di- or tri-block copolymers, facilitates the diffusion of the hydrophilic proteins out of the microspheres and also accelerates the erosion rate of the matrix (Mallarde et al., 2003; Lee et al., 2006).

#### 1.3.5.3.4. Porosity

The porosity in a system of spheres is determined by microsphere hardening as the organic solvent evaporates during preparation. Differences in porosity of microspheres have been shown to affect the release kinetics. This is noticeable in a study by Yang, et al. (2000) where a highly porous matrix released a drug at a considerably higher rate than its non-porous counterpart. Another factor related to sphere porosity is the initial burst effect, which is dependent on the leaching which occurs at the outer wall of the sphere as it becomes hydrated (LeCorre et al., 1994; Okada et al., 1994; Ghaderi et al., 1996). This can be reduced by the formation of a non-porous outer sphere skin (Yang et al., 2000).

#### 1.3.5.3.5. Size distribution

The release profiles can also be influenced by size of the microspheres, with the rate of protein release decreasing with increasing microsphere size (Bezemer et al., 2000). Mixing microspheres of different sizes it is possible to obtain another degree of controlling release. More importantly, linear, zero-order kinetics is obtainable by combining the proper formulation of microsphere sizes. In a detailed study carried out by Berkland et al. (2001, 2002), they were able to obtain a zero-order release by mixing microspheres of different sizes.

#### 1.3.5.3.6. Co-encapsulation of additives within the microspheres.

In addition to improving the release kinetics of proteins, the co-encapsulation of additives is important in circumventing the problem of protein inactivation and incomplete release. In activation and incomplete release of proteins from PLGA microspheres can be attributed to non-covalent aggregation of the encapsulated

protein and hydrophobic interactions between the polymer and protein. Additives generally co-encapsulated within the microspheres include diluent proteins such as human or bovine serum albumin (Meinel et al., 2000); urea (Nam et al., 2000); non-ionic surfactants (Lee et al., 2006); basic additives such as $Mg(OH)_2$ (Aubert-Pouëssel et al., 2002) and $Ca(OH)_2$ (Zhu and Schwendeman 2000); and small hydrophilic compounds such as sucrose (Lee et al., 2006) and PEG 400 (Péan et al., 1999).

### 1.3.5.4. Methods of assessing *in vitro* release from microspheres.

The extended release profile of microsphere-based formulations necessitates the performance of long term release studies. These long term release studies could be obtained by performing *in vivo* experiments in animals or *in vitro* release experiments at body temperatures using buffers that are physiologically similar to the body fluids. Due to the regulatory hurdles that need to be cleared, the labour and expense involved with assessing *in vivo* drug release, *in vitro* drug release studies at 37˚C (physiological temperature) have gained increasing importance and relevance (Okada and Toguchi, 1995; D'Souza and DeLuca, 2006). Hence the focus of the remaining part of this section will be on the methods currently utilised in assessing *in vitro* release.

*In vitro* release studies are performed mainly to determine the quantity of drug or protein that is released at a given time; as a method of quality control to support batch release and to comply with specifications of batches proven to be clinically and biologically effective; assess formulation factors and manufacturing methods that are likely to influence bioavailability; and to fulfil various requirements by regulatory authorities (Burgess et al., 2002; D'Souza and DeLuca, 2006). An *in vitro* release profile provides fundamental information on the structure and behaviour of the formulation on a molecular level and possible interactions between protein and

polymer that might affect the rate and mechanism of protein release. Thereby, provides a scientific approach to the design and development of microspheres with desired release properties.

Currently there are three main methods of undertaking *in-vitro* release studies; these are the incubation, flow and dialysis methods.

#### 1.3.5.4.1 Incubation Methods.

This is the most commonly used technique and involves the incubation of microspheres in a physiological medium such as phosphate buffer saline over an extended period of time under static or agitated conditions. The incubated microspheres could be suspended in the physiological medium by the use of detergents such as Tween 80 as suspending agents, and sodium azide as bactericidal agents to maintain aseptic conditions. At intermittent intervals, protein release can be monitored by separating the supernatant from the microspheres through filtration or centrifugation,. The supernatant can then be assayed for the protein content. For protein molecules that are not stable in the release media employed, the remaining protein content within the microspheres at intermittent intervals can be used as a determinant of the *in vitro* release profile of the microsphere (Blanco-Prieto et al., 2004; and Woo et al., 2002). The advantage of this technique involves the ease and relative low cost of setting up the experiments. However, the main disadvantage involves the sampling method, i.e. centrifugation could result in the denaturing of proteins, while filtration is not advisable for proteins that bind to the filters (D'Souza and DeLuca, 2006). Other disadvantages include loss in volume of the microspheres through filtration that could lead in inaccurate estimation of protein release,

microsphere aggregation (when incubated under static conditions), and the need for total buffer replacement to maintain sink conditions (D'Souza and DeLuca, 2006).

#### 1.3.5.4.2. Flow Method.

This method involves placing microspheres in a column, through which media is continuously pumped at a constant flow rate with the use of a peristaltic pump, syringe driver or high-performance liquid chromatography pumps. The buffer could be re-circulated through the column containing the microspheres (when using a peristaltic pump) (Fig 1.2), or fresh buffer could be pumped in continuously through the system, with a collecting vessel used to collect the eluent. The microspheres could be immobilised within the column with the buffer circulated over it or the columns could have built in filters to ensure that the microspheres are not collected along with the eluent. The main factor for consideration in the use of this method is the selection of flow of the flow rate through the microsphere contining column. This is due to the positive correlation between the flow rate and the cumulative release that has been discovered (D'Souza and DeLuca, 2006). However in choosing the flow rate the sensitivity of the assay being utilised in the analysis of protein released has to be factored in.

The main attractions of the flow method is that it simulates *in vivo* environment (through the circulation of media to the microspheres), and that the samples can be easily assayed for protein content without need for separation of the microspheres from the eluent. Drawbacks to this method involves the incomplete release of proteins from the microspheres when low flow rates are used; the potential for pressure build

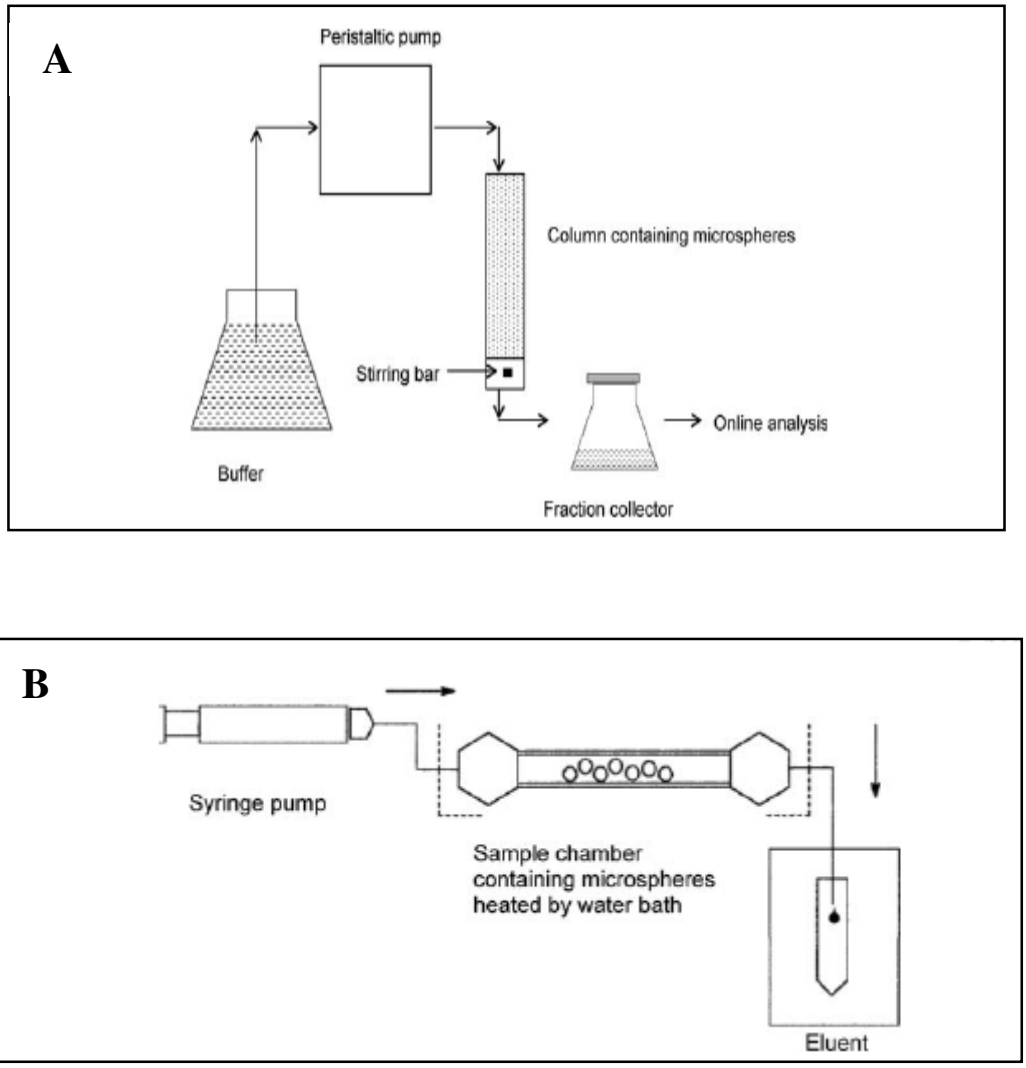


Figure 1.2: Flow through method utilising (A) peristaltic pump. (Cortesi et al, 1994; D'Souza and DeLuca 2006) and (B) syringe driver (Aubert-Pouëssel et al, 2002; D'Souza and DeLuca 2006)

up and variation in actual flow rate due to filter clogging by polymer degradation products (D'Souza and DeLuca, 2006).

#### 1.3.5.4.3. Dialysis Method.

This method involves the physical separation of the microspheres from the bulk media by the use of a dialysis membrane. The techniques could involve the utilisation of a dialysis bag containing a suspension of the microspheres placed in a vessel containing buffer (Wang et al., 2004; Siepman et al., 2004, or the use of a tube (containing a suspension of microspheres with a dialysis membrane at one end, placed in a vessel filled with buffer (Kostanki et al., 2000; D'Souza and DeLuca, 2006). Another technique involves the use of a two chamber (consisting of a smaller chamber made of the dialysis membrane and holding the suspension of the microspheres, placed in the buffer filled outer chamber (Gido et al., 1993). The protein released from the microspheres flows from the inner chamber containing the microspheres through the dialysis membrane into the buffer of the outer chamber. The attractions of this method is that the dialysis method allows for the maintenance of a constant pH, as water soluble oligomers are able to diffuse through the dialysis membrane, the relative ease of sampling and media replacement. It is also believed to mimic the *in vivo* conditions, in which a stagnant layer surrounds the microspheres. Disadvantage of this method is that the method cannot be employed for proteins that bind to the polymer or the dialysis membrane (D'Souza and DeLuca, 2006).

## 1.4. Cells.

A consideration of the cells to be used is the starting point for any tissue engineering applications. In addition to having a sufficient quantity of cells free of pathogens and

contamination, a need for determining the cell source is required. The greatest challenge in utilization of cells within tissue engineering is to optimize the isolation, proliferation and differentiation of cells and to design scaffolds or delivery systems that yield tissue growth in three dimensions. Ideally, cells are harvested from a patient expanded *in vitro* and then seeded on a scaffold and then implantation of the resultant tissue. Many cell sources have been identified for use in tissue engineering applications and they can be broadly divided into primary cells and stem cells.

### 1.4.1. Primary Cells

Primary cells are tissue specific cells that can be isolated directly from various tissue samples. Sources of tissue samples could be from the patient (autologous), from other human sources (allogenic) or from other species (xenogenic). However problems with disease transmission, immune acceptance, off the shelf availability and ability to source large quantities of cells currently limits their use in tissue engineering applications (Lanza et al., 2007).

### 1.4.2. Stem Cells

Stem cells can be defined as undifferentiated cells that have the capacity for both self-renewal and differentiation into one or more types of specialized cells. However a broader definition might be required in view of the observation of dedifferentiation and trans-differentiation of certain mature cells (Mezey et al., 2000; Toma et al., 2001). Current sources of stem cells for tissue engineering include embryos and adult donors. Stem cells obtained from embryos can be classified into embryonic stem cells, embryonic germ cells, and embryonic carcinoma cells. Adult stem (AS) cells can be obtained from various organs and their related tissues, with each type of AS cell

carrying a prefix which refers to its origin tissue, such as mesenchymal stem (MS) cells, hematopoietic stem (HS) cells and olfactory mucosa stem (OMS) cells (Murrell W. 2005; Lee K. D. 2008; Park J. 2008).

Although stem cells can provide a virtually inexhaustible cell source for tissue engineering applications, embryonic carcinoma cells are not currently utilised clinically due to their potential malignancy (Andrews, P. W et al., 2000). While embryonic germ cells has not been as widely characterised as embryonic stem cells. The range of cell types to which stem cells can differentiate varies, with embryonic stem cells the most pluripotent. AS cells (or progenitor cells) are undifferentiated cells found amongst differentiated cells within many tissues of the body (Langer and Vacanti, 1999). They are multipotent, occur in the body of children and adults and arise after embryonic development. They are also responsible for dividing to replace dying cells and regenerate damaged tissues. Examples of adult stem cells include mesenchymal stem cells, hematopoietic stem cells, and adipose derived stem cells. Given the multi-lineage potential and high proliferation capacity of these cells, they represent a high source of cells for tissue engineering, however their limited plasticity and ability to trans-differentiate to form cells outside the lineage of their origin tissue, i.e. pancreatic stem cells forming epithelial cells has limited their clinical use (Summer R. 2008; Meier K. 2008; Chim H. 2008).

### 1.4.3. Embryonic Stem Cells

Embryonic stem cells (ES cells) are stem cells derived from the inner cell mass of an early stage embryo known as a blastocyst. They possess the capability to differentiate into all derivatives of the three primary germ layers: ectoderm, endoderm, and mesoderm. These include each of the more than 220 cell types in the adult body. ES

cells can be identified by the existence of pluripotency markers present on the cell membrane. These cell markers include stage specific embryonic antigen (SSEA) 3 and SSEA-4 (expressed only on human ES cells), Oct3/4, Sox-2, Rex-1 and Nanog (Bielby R. C. 2004; Hatano S. Y. 2005).

### 1.4.3.1. Embryonic stem cell sources.

There are two primary sources of ES cells which include current ES cell lines (can be obtained from the stem cell bank), and embryos. The embryos used are either cloned embryos, aborted embryos and unused *in vitro* fertilisation (IVF) embryos (Thomson J. A. 1998). To date, ES or ES-like cells have been isolated by culture of blastocyst stage embryos from mice, (Evans and Kaufman 1981; Martin 1981), pigs (Notarianni et al. 1990; Chen et al. 1999), sheep (Dattena et al. 2006), cattle (Saito et al. 1992; Iwasaki et al. 2000; Mitalipova et al. 2001), minks (Sukoyan et al. 1992), rats (Iannaccone et al. 1994; Vassilieva et al. 2000), hamsters (Doetschman et al. 1988), and more recently, from humans (Thomson et al. 1998) and rabbits (Graves and Moreadith 1993; Schoonjans et al. 1996). However despite the successful isolation of ES cells from these species, an understanding of their ES cell biology are still in their infancy when compared with that in mice and humans (Chiang, S. K et al., 2008).

### 1.4.3.2. ES cell culture and differentiation

*In vitro* culture of ES cells involves the co-culture with a feeder layer consisting of mouse embryonic fibroblasts (MEFs) (Nichols J. 1990; Cheng L. 1994). MEFs support ES cell growth and maintain their pluripotency, through the action of secreted leukemia inhibiting factor (LIF) (Piquet . 1994; Keller G. M. 1995; Furue M. 2005), which acts to suppress differentiation (Zandstra P. W. 2000). The functions of LIF are

carried out *via* heterodimerization of the low-affinity LIF receptor (LIFR) and the membrane bound signaling complex gp130 (Smith A. G. 2001; Viswanathan S. 2002), resulting in the transcription of self-renewal genes within the nuclei of the ES cells.

Current differentiation methodologies involve the withdrawal of LIF from culture medium, and supplementation of culture medium with growth factors. However, despite a plethora of studies showing successful differentiation of ES cells using this approach, the differentiation process has been observed to be highly inefficient (Wiles M. V. 1999; Schuldiner M. 2000), with induction of ES cells differentiation across multiple lineages reported. Despite these limitations, utilisation of ES cells for clinical applications using tissue engineering applications is currently being widely explored (Polak, J M, 2008).

#### 1.4.3.3. Mouse vs. Human ES cells

Currently, although sixty-four different derivations of human ES cell lines are currently listed by the NIH stem cell registry, limited data on the fundamental properties of these lines are currently available with less than 10 cell lines available in sufficient numbers for analysis. As a result most studies involving ES cells are currently carried out on the more ubiquitous mouse and human ES cell lines (Ginis, I et al., 2004). Mouse and human ES cells are similar in their expression of similar markers such as *oct-4, nanog, sox-2,* and *utf*-1, normally characteristic of undifferentiated stem cells, their ability to grow as colonies of tightly packed cells on inactivated murine embryonic fibroblast (MEF) feeders or in conditioned medium

(CM) derived from such MEFs (Xu, C. et al., 2001), and their ability to form teratoma (Wei, C.L et al., 2005).

Recent studies however suggest that differences exist between mouse and human ES cell lines in morphology, patterns of embryonic antigen immunostaining, expression of differentiation markers, as well as expression profiles of cytokines, cell cycle, and cell death-regulating genes (Ginis et al., 2004). Human ES cells, unlike mouse ES cells, have been observed not to require LIF for their propagation or for maintenance of pluripotency (Reubinoff et al., 2000; Thomson et al., 1998a), are able to differentiate into trophoblast-like cells (Odorico et al., 2001; Thomson et al., 1998a), and show differences in their telomerase activity and regulation (Forsyth et al., 2002). These differences suggest that caution must be exercised in extrapolation of the data obtained from studies involving mouse ES cells unto human ES cells.

### 1.4.4. Methods of Cell Delivery.

Incorporating cells into scaffolds provides a means of aiding regeneration of tissues, especially those that have a low regenerative potential. Cell seeding into scaffolds at high density has been associated with enhancement of tissue formation in cartilage, bone and cardiac tissues when compared to scaffolds without seeded cells. The current methods of incorporating cells into scaffolds can be performed using a variety of techniques. These techniques involve static seeding, perfusion, spinner flask and the use of centrifuge (Sodian, Lemke et al. 2002).

The static method is the simplest and most commonly used technique, it involves the incubation of prefabricated scaffold in culture medium containing the desired cells for

a given time (based normally on the duration it takes for the cells to be attached and migrate successfully into the internal walls of the scaffold) (Xiao, Riesle et al. 1999).

The perfusion method involves passing the cultured cells medium under a constant perfusion velocity through the pores of the scaffolds in a bioreactor (Zhao and Ma 2005). The spinner flask method is another well established and utilised method and involves the incubation of a scaffold in a spinner flask containing a cultured cell medium and continuously stirred (Vunjak-Novakovic, Obradovic et al. 1998; Kitagawa, Yamaoka et al. 2005). While the centrifuge method involves the use of centrifugal force in seeding the cells into the scaffold and is a slight modification of the spinner flask method (Godbey, Hindy et al. 2004). Another recently used technique involves using magnetic force in stabilizing magnetically labelled cells (magnetic cationic liposomes) on scaffolds (Shimizu, Ito et al. 2005) .

### 1.4.5. Cell Adhesion

In tissue engineering, interactions between scaffold materials and cells are important determinants on the rate of formation and quality of regenerated tissue. This is partly due to the role the nature of the surface plays in directing cellular response. Surface chemistry and topography plays important roles in determining the adsorption of protein molecules, attachment and alignment of cells to the materials used in the production of the scaffolds (Liu and Ma 2004; Liu, Won et al. 2005). Designing scaffolds to be bioactive is a prerequisite in aiding compatibility with the biological environment it will be transplanted into. This is also important in aiding the coordination of cellular responses such as cell attachment, migration, proliferation, differentiation and ultimately tissue regeneration, through biological interaction between the scaffold and the cell.

In spite of the beneficial properties that characterizes biodegradable polymers such as poly(α-hydroxy acids) (i.e. poly(glycolic acid), poly(lactic acid), and their ubiquitous use as scaffold materials in tissue regeneration, their lack of functional groups on the polymeric chains prevents it in being able to interact with the cells through conjugation of specific cell-recognisable signal molecules. (Liu, Won et al. 2005)

Hence, in order to increase the bioactivity of the scaffolds, there is a need to modify the surface properties so that they present with functional groups that are able to interact with the receptors of cells and coordinate the desired cellular responses. Current approaches in modifying the surface properties include the surface coating of polymer with the desired proteins, the attachment of functional groups to the polymer chains, or plasma modification of the surface. Surface coating of polymer with the desired proteins is a simple and efficient way of improving the surface bioactive properties of the polymers. It involves the adsorbing the required molecules unto the surface of the polymers, and is achieved by direct physical adsorption through the placing of polymer in a solution of the surface modifying species until effective coating of the surface of the polymer has occurred (Ito et al. 2003; Liu et al. 2005). Another technique of improving the surface properties of the scaffold substrate includes functionalizing the substrate through chemical modification leading to either the attachment or exposition of functional groups which has been observed in improving the cell-seeding on its own or after coupling to the desired protein that is used to improve the surface properties of the substrate. Examples of studies that has utilised this approach include those undertaken by Gao et al which involves the hydrolysis of ester bonds present on the surface of PGA under strong alkaline conditions and was shown to improve the cell seeding density and cell spreading

across the surface indicating improved cell adhesion (Gao, Niklason et al. 1998). Another approach by Cai et al involved partially hydrolysing the surface of Poly(D-L-lactic acid) under alkaline conditions and grafting chitosan onto the surface via the attachment to the exposed carboxylic acid group. This new surface was shown to improve the adhesion and proliferation of osteoblasts when compared to unmodified surfaces (Cai, Liu et al. 2002).

An important new technique that is gaining prominence is the attachment of peptide fragments (which are recognisable motifs of ECM proteins) that interacts with the integrins on the receptors of the cell surface. Most popular of these peptide fragments include Arginine- Glycine- Aspartatic acid(RGD) from fibronectin, others utilised include Arginine-glutamic acid- asapartic acid- valine (REDV) also from fibronectin, tyrosine- isoleucine- glycine- serine- arginine (YIGSR) and isoleucine– lysine- valine-alanine- valine (IKVAV) both from the ECM protein laminin. Further modification of these surfaces could also include attachment with a variety of biologically active molecules that are specific to the tissue engineering applications (Drury and Mooney 2003).

Another technique recently elucidated is called the plasma exposure, which utilised low pressure gas treatment (i.e. ammonia) in inducing a transmutation from of the surface of the substrate from a hydrophobic to a hydrophilic surface without altering the morphology. The desired group (such as RGD) is subsequently introduced to the modified surface (Hu, Winn et al. 2003; Liu and Ma 2004). This technique however has limitations in terms of the plasma penetration leading to it being limited to 2D films (Liu and Ma 2004).

### 1.5. Multiple Tissue Engineering.

Natural tissue regeneration is a much more complex process than the delivery of a single growth factor to the responsive cells. Rather it often involves the interplay between several environmental signals including the attraction of cells to the site of tissue repair and coordinated presentation of a multitude of growth factors to these responsive cells. Discussed below are techniques applied which have taken into cognisance this complexity.

#### 1.5.1. Multiple Growth Factor Delivery.

Some recently carried studies have shown that combining signals that modulate tissue regeneration into a single scaffold, shows better tissue regeneration profiles than when only one signal is used. In studies carried out by Holland and co-workers the release kinetics of a dual delivery hydrogel system of IGF-1 and TGF-β1 and the effects the presence of each growth factor will have on the release kinetics of the other was investigated. The IGF-1 and TGF-β1 was separately incorporated into microparticles and then formulated into a hydrogel scaffold. The presence of TGF-β1 slightly altered the release rate of IGF-1 (Holland et al. 2005). In another study investigating the effect dual delivery of BMP2 and TGF-β3 within a scaffold had on bone formation, Simmons and co-workers observed a significant increase and acceleration of bone formation in scaffolds implanted into the backs of SCID mice when compared with scaffolds delivering a single growth factor (Simmons et al. 2004). These studies clearly indicate the feasibility of delivering multiple signals utilising a single scaffold and it resulting in an increased efficiency of tissue regeneration. However, there is the possibility the incorporation of one growth factor might influence the release kinetics of the other growth factor. Further exploration of this phenomenon is required for

utilisation of single scaffolds for multiple growth factor delivery – and will be the subject of a study later in this report.

### 1.5.2. Biphasic Scaffold.

Due to the multiphasic nature and presence of multiple cell lines of most tissues and organs, tissue engineered constructs need to be able to present a sectioned environment for the support and development of cell types along different lineages. This multi-layered approach allows the co-culturing of distinct cell types within 3D systems without the risk of growth factors or other ECM molecules produced by the encapsulated cells to influence the proliferation or differentiation of the other cells. Currently, few attempts have been undertaken in engineering tissues consisting of multiple cell types. An example of such attempt is the osteochondral construct composed of bone and cartilage tissues. This approach involves the integration of separately pre-fabricated chondral construct and the osteoconstruct. (Holland et al. 2005).

#### 1.5.2.1. Biphasic Scaffold – Osteochondral Defect Treatment Option. .

Osteochondral defects are the most prevalent musculoskeletal disorders, affecting about 10% of the western world population older than 30, and most of the people over the age of 65, with total costs estimated at over $28.6 billion/year within the US alone (Felson and Zhang, 1998). The main pathological features of osteochondral defects involves the degeneration of the cartilage, synovium, joint capsule and subchondral bone tissues, and develops as a result of the destruction of cartilage matrix. This leads to a progressive loss in joint function, together with the destabilization of supramolecular structures, including the collagen network, and changes in the

expression profile of matrix molecules (Aigner and McKenna, 2002; Mano and Reis, 2007)

Clinical treatment options for osteochondral defects, mostly involve surgical techniques such as resection, and mosaicplasty. Resection involves the excision of cartilage from one location within the body, and grafting it to the joint. Mosaicplasty involves the transfer of osteochondral cylindrical plugs from a joint area of minor load, such as the femoral trochlear groove, into pre-drilled holes at the defect site (van der Kooy and Weiss, 2000). Other surgical techniques currently utilised include arthroscopic lavage and debridement in order to eliminate debris from the joints (Jackson *et al*., 2003; Shannon *et al*., 2001), and full periosteal and perichondrial transplantation to full-thickness cartilage defects which is aimed at introducing undifferentiated stem cells into the environments (Mano and Reis, 2007). Currently replacement of skeletal joints with a synthetic prosthesis represents the optimal treatment for end-stage disease (Kandel et al., 2006).

However, all these surgical treatment options have limitations with the exhibition of undesirable side effects such as endochondral ossification and fibrocartilage formation which deteriorates with time, and the treatment limitation to small lesions, making the overall outcome generally inadequate (Frenkel and Cesare, 2004; Hunziker, 2000, 2002; Newman, 1998; Redman *et al*., 2005). Even the successful replacement of defective cartilage with prosthesis has shown failure rates of up to 20% after 10 years (Soderman et al., 2001; Barrack, 2000).

Biological treatment options that have been explored include the *ex vivo* expansion and implantation of chondrocytes isolated from the patient's cartilage, into the cartilage defect under a flap (to confine cells within the defect) (Peterson et al., 2000; Browne et al., 2005). However histological evaluation of cartilage regenerated using this approach has indicated the presence of fibrocartilage instead of articular hyaline cartilage (Peterson et al., 2000).

Biphasic scaffolds which could incorporate different growth factors and different cells have shown immense applications as a treatment option for the management of osteochondral defects. Biphasic scaffolds could also be used to satisfy the mechanical and biological requirements of both the cartilage and bone tissues (Mano and Reis, 2007). Elisseeff and co workers demonstrated in their study the ability to develop adjacent to each other cartilage and bone tissue through the incorporation of mesenchymal stem cells and chondrocytes in the different layers of the bilayered hydrogel scaffolds (Elisseeff et al. 2005).

In another study carried out by Holland et al, the rate of osteochondral repair in a rabbit was carried out utilising a bilayered degradable hydrogel scaffold. The bilayered scaffold design was employed to spatially control the development of cartilage and bone tissues in the joints of the rabbits with the defects. A total of three scaffolds were made, two of which had a top layer with TGF-β1 loaded microparticles, while the third scaffold had PBS loaded microparticles. The bottom layers were made up of either PBS loaded microparticles or no microparticles. These scaffolds were then implanted into the joints of the rabbits and harvested after 4 and 14 weeks. Histological evaluation of the implants showed that after 14 weeks, infiltration of the implant with healthy tissue occurred, with the top layer of the

scaffolds filled with hyaline cartilage tissue. While the bottom layer of the scaffold was filled with a mixture of trabecular and compact bone. No bone up-growth in the top layer of the scaffolds was observed (Holland et al. 2005).

## 1.6. Thesis Aims.

### 1.6.1. General Aims.

The advances in various scaffold fabrication and growth factor delivery methods have achieved some success in the engineering of many single tissues. However clinical conditions such as osteoarthritis involve damage transcending several tissues and as such necessitate the simultaneous regeneration of multiple tissues. Current tissue engineering approaches to simultaneously regenerate multiple tissues have shown poor tissue integration.

The work within this thesis aims to address this clinical need by developing a biphasic tissue construct for treatment of osteochondral defects. The biphasic tissue construct will consist of two different tissue types within a single scaffold matrix. The development of the biphasic tissue construct is based on the fabrication of an embryonic stem cell seeded bilayered scaffold showing zonal growth factor release.

Tissue formation is based on the control of patterning of differentiation in the seeded embryonic stem cells afforded by the spatial and localised delivery of the growth factors. The rationale for this approach is based on the fact that growth factors have specific effects on the differentiation of stem cells depending on concentration and duration of exposure. TGF-β3 and BMP-4 growth factors have been shown to direct the formation of articular cartilage and bone from mesenchymal stem cells

respectively (Moioli, E. K. et al., 2007; Yang et al., 2004). Therefore, for osteochondral engineering, zonal release of these growth factors in a scaffold could be exploited for the regeneration of articular cartilage and bone in distinct zones, thereby mimicking the natural compartmentalization of these tissues.

In this report, the actions of TGF-β3 and BMP-4 in cartilage and bone tissue formation were exploited for the development of biphasic constructs for osteochondral tissue engineering. Microspheres were employed to localise and control the release of TGF-β3 and BMP-4 to specific zones of a bilayered scaffold. It was hypothesized that by organizing growth factor loaded microspheres into a bilayered scaffold, a model for tissue zonation could be developed. Therefore two layers of different growth factor loaded microspheres will be built into a bilayered scaffold by heat fusion. The concept is represented schematically in Fig 1.3.

### 1.6.2. Experimental objectives

The general aims of this thesis are three fold: (i) To develop a PLGA composite formulation showing improved viscoelastic properties and reduced glass transition temperatures. (ii) To develop microspheres from the PLGA composite formulation showing reduced glass transition temperatures and zero-order release kinetic profiles. (iii) To demonstrate the concept of localised growth factor release and tissue zonation within bilayered scaffolds.

The experimental objectives for this thesis are as follows:

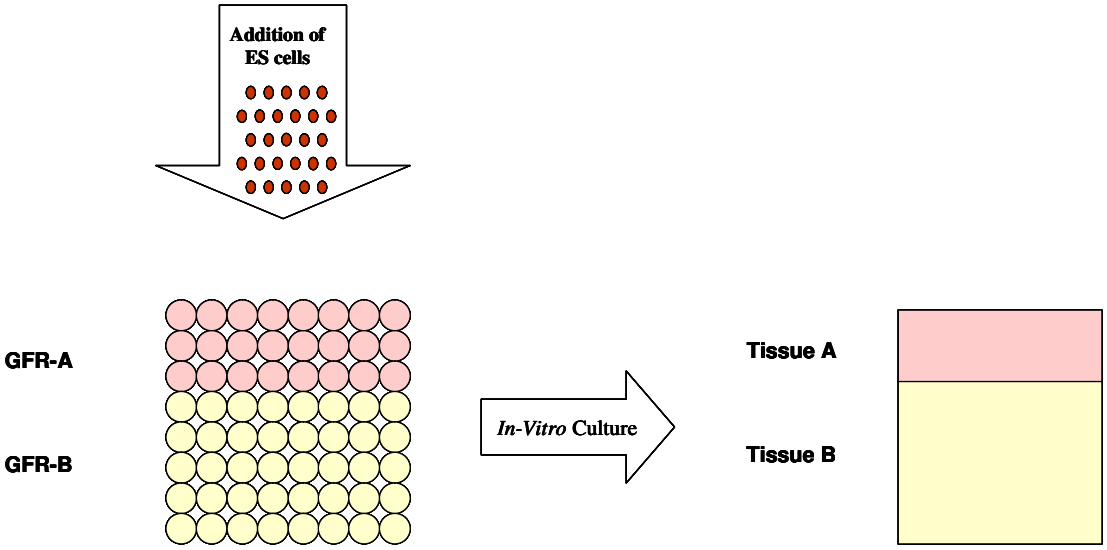


Note: GF-A = Microspheres loaded with growth factor signalling for Tissue A
GF-B = Microspheres loaded with growth factor signalling for Tissue B

**Figure 1.4. Schematic representation showing multiple tissue development using the bilayered scaffold approach.**

**1. Synthesis and Characterisation of a novel PLGA composite formulation (Chapter 3)**

Modulation of the viscoelastic properties of PLGA polymer will be achieved by blending the polymer with a thermoresponsive polymer – PLGA-PEG-PLGA, to produce polymer blends with reduced glass transition temperature (Tg). This polymer blend formulation was used for the following:

(i) Fabrication of microspheres with reduced Tg. By producing microspheres with reduced Tg, the microspheres can be sintered at low temperatures to form scaffolds. This reduced sintering temperature will be advantageous in preventing the encapsulated proteins from losing their activity due to the deleterious effects of high temperatures.

(ii) Formation of scaffolds with increased mechanical strength. Microspheres with increased viscoelastic response and reduced glass transition temperature produced from PLGA / PLGA-PEG-PLGA blends were used to fabricate scaffolds with increased mechanical strength.

**2. Modulation of protein and drug release from microspheres (Chapter 4)**

The effects of parameters influencing encapsulation and release of proteins and drugs from microspheres will be investigated in order to provide the following:

(i) Microspheres with high entrapment efficiencies. The effect of changing various parameters such as loading weight, and protein micronisation in order to increase the amount of protein retained within the microspheres (entrapment efficiency) was investigated.

(ii) Microspheres with zero-order kinetic profile. The effect of the thermoresponsive, but also hydrophilic polymer PLGA-PEG-PLGA on

accelerating the rate of release and reducing the lag phase of a model protein and a model drug from microspheres was assessed.

**3. Fabrication of bilayered scaffold demonstrating localised protein release and tissue zonation (Chapter 5).**

This chapter will consist of two experimental objectives:

(i) The use of a bilayered scaffold to demonstrate localised protein release. A bilayered scaffold consisting of two individual layers of TGF-β1 and BMP-4 growth factor loaded microspheres will be fabricated by heat sintering. Controlled release experiments were designed to investigate the localization of the growth factor release to the area surrounding the respective growth factor loaded microsphere zone.

(ii) Formation of a biphasic tissue construct through the patterning of differentiation of embryonic stem cells on a bilayered scaffold. The effect of bilayered scaffold loaded with TGF-β1 and BMP-4 growth factors on the differentiation of embryonic stem cells along the chondrogenic and osteogenic pathways in order to produce cartilage rich and bone rich zones on the scaffold was investigated.

# CHAPTER 2

# Materials and Methods

## 2.1 Polymer and Protein Sources

PEG 1500, partially hydrolysed poly vinyl alcohol (Mw 25,000) and stannous 2-ethylhexanoate (stannous octoate) were purchased from Sigma (Dorset, UK). D,L-lactide was purchased from Alfa Aesar (Avocado, Lancaster, UK) and glycolide was obtained from Purac (Netherlands). These materials were utilised for the fabrication of the triblock co-polymer PLGA-PEG-PLGA as detailed in Chapter 3. PLGA 118kDa (85:15) was obtained from Lakeshore Biomaterials (Birmingham, USA). The synthesized triblock was blended with PLGA to form blends of PLGA / triblock, which was investigated for reduced glass transition temperature (Chapter 3) and for the increased rate of release of proteins and drug molecules from microspheres (Chapter 4).

For protein encapsulation and release studies, several model proteins were utilised without purification. Chicken egg lysozyme, ribonuclease A, horse myoglobin, trypsin, and horse radish peroxide were purchased from Sigma (UK). PEG 6000 was obtained from BDH Chemicals Ltd. (UK) and utilised for protein micronisation during microsphere encapsulation. For drug encapsulation and release studies the model drug – dexamethasone purchased from Sigma (UK) was used.

Recombinant human bone morphogenic proterin -2 (BMP-4) and transforming growth factor beta-3 (TGF-β3) were purchased from R & D Systems (UK). These growth factors were utilised for the development of bilayered scaffolds as detailed in Chapter 5.

STO Neo Leukemic (SNL) mouse fibroblasts, and mouse ES cells were a kind gift from Mr David Gothard, of Wolfson Centre for Stem Cells, Tissue Engineering and Modelling (STEM), Division of Drug Delivery and Tissue Engineering, Centre for Biomolecular Sciences, University of Nottingham, UK. The ES cell line was originally derived from mouse columnar epiblast epithelium (CEE). It is unknown when the ES cells were first isolated and therefore, the passage number is also unknown.

## 2.2. PLGA-PEG-PLGA synthesis and characterization.

The triblock PLGA-PEG-PLGA was synthesized via ring-opening polymerisation of $_{D,\ L}$-lactide and glycolide onto PEG 1500 using the catalyst stannous octonoate, by following the method described by Zentner et al with slight modifications. In brief, 5.5g of poly (ethylene glycol) (M*w* 1500) was weighed out into a single neck round bottomed flask and heated under vacuum using a schlenk line at 120ºC for three hours to drive out all the moisture. The resulting molten PEG was removed from vacuum and under an argon atmosphere 3.5g, 8.0g of glycolide and $_{D,L}$ lactide respectively were added to the molten PEG, then heated further at 150ºC for 30mins. After which 0.0375g of the catalyst stannous (II) octonoate was added and the reaction was allowed to proceed at 155ºC for 8 hours under a dry argon atmosphere provided using a Schlenk line (Fig 2.1). The synthesised polymer was then purified by dissolving in cold distilled water (5ºC) followed by precipitation of the polymer at 80ºC. This

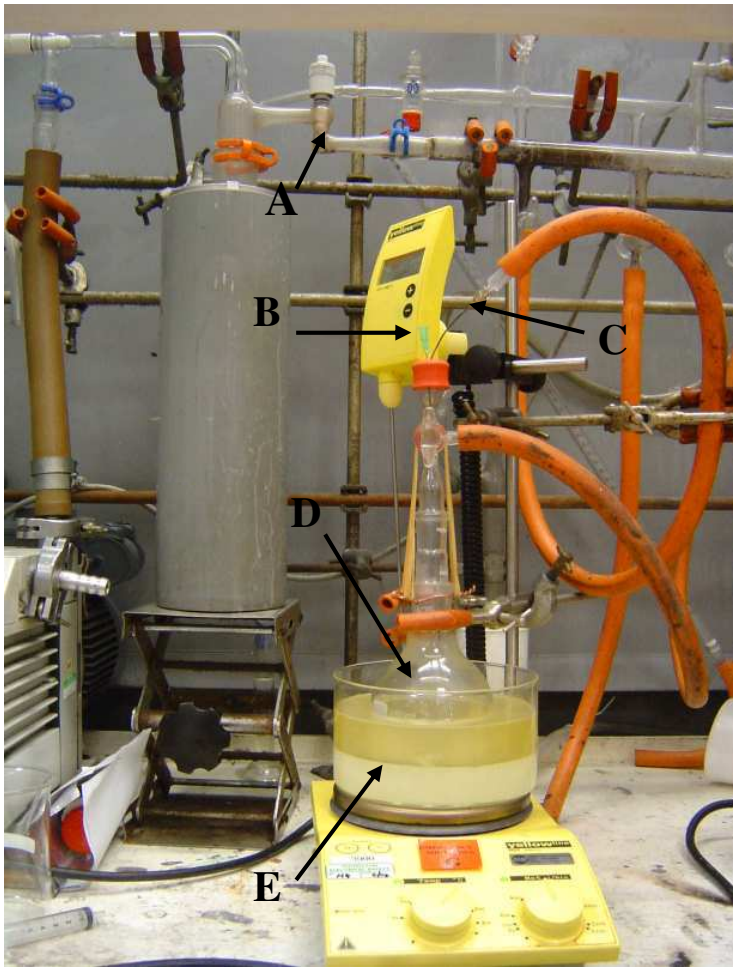


Figure 2.1: Photograph showing the set-up for synthesis of the triblock – PLGA-PEG-PLGA. A – Schlenk line; B – Injector used for the delivery of $N_2$ or argon gas into reaction chamber; C – Needle for pressure and gas outlet; D – round bottom flask; and E – liquid paraffin used for uniform heating of round bottom flask.

purification step was repeated twice. The purified polymer was then transferred into glass jars and water extracted by snap freezing the polymer in liquid nitrogen followed by storing in a Modulyo freeze dryer system (Edwards, Crawley UK) for three days.

The synthesized triblock co-polymer was characterized using gel permeation chromatography (GPC) and nuclear magnetic resonance (NMR). The molecular weights and polydispersity indices of the synthesized triblock were determined by GPC performed using a K-501 HPLC pump with a linear calibration range of *M*w 200–2,000,000 g/mol. For analysis, 10mg of the polymer was dissolved in 3ml of tetrahydrofuran (THF) in toluene. On complete dissolution of the polymer, the solution was filtered using a 0.2µm Minisart-RC syringe filter unit (Sartorius, Epsom UK) into small GPC vials. The filtered samples was then run using THF at a flow rate of 1ml/min. Molecular weight values were calculated using the inbuilt Varian Cirrus GPC/SEC Online software package which had been calibrated against polystyrene standards. A total of four samples were used for the GPC analysis.

The molecular weight and the lactide: glycolide ratio of the synthesized PLGA-PEG-PLGA polymer was determined using NMR ($^1$H NMR). $^1$H NMR analysis was performed by dissolving 10mg of the Polymer in 1ml of deuterated chloroform ($dCDCl_3$) and filtered using a 0.2µm Minisart-RC syringe unit. $^1$H NMR spectra of the dissolved samples was obtained using a Bruker AMX-400 Ultrashield spectrometer (Bruker BioSpin MRI Ltd., Coventry, UK) at a frequency of 400MHZ at 25ºC. Integration of the signals specific to each of the monomers (peaks corresponding to CH and $CH_3$ of $_{D, L}$ –lactide, $CH_2CH_2$ of ethylene glycol and $CH_2$ of

glycolide) along with a tetramethylsilane (TMS) signal as the zero chemical shift were obtained using the inbuilt TopSpin$^{TM}$ NMR software package. The integrated signals were then normalized to the number of H in each monomer (corresponding to each peak) to determine the number molecular weight ($M_n$) of each monomer. The lactide: glycolide ratio was determined by obtaining the ratio of the normalized integrated signal values of $CH_3$ and $CH_2$ respectively. Further details on calculations in obtaining the polymer $M_n$ can be found in Chapter 3.

## 2.3. Triblock blend formation

A 30% (*w/w*) of triblock in PLGA polymer blend was produced using a simple in-house derived hot-blending protocol. Briefly, 7.0g of PLGA 8515 (Mw 118 Kda) (Lakeshore Biomaterials, Birmingham USA) was weighed out onto a ceramic tile and gradually heated to 75°C using a Yellow Line MST Basic C hot plate and TC1 thermostat set-up (Scientific Laboratory Supplies Ltd., Nottingham, UK) until molten. 3.0g of triblock was then added to the PLGA melt and allowed to melt before the mixture was stirred several times using a metal spatula to enhance good distribution of the triblock with the PLGA. The polymer blend was allowed to cool by removal of the heat source. On cooling of the polymer blend (to about 50ºC), it was removed from the ceramic tile using a scalpel before being milled down to form a powder, by snap-freezing in liquid nitrogen and blended using a Krups 75 household coffee grinder (Argos, Nottingham, UK). Long term storage of the triblock-polymer blend was achieved by vacuum sealing using an Orved VM12 vacuum sealer and bag (Orved, Saint Quentin, France) and stored at a -20ºC freezer. Triblock – PLGA blends containing different compositions of the triblock PLGA – PEG – PLGA (10%, 20%, 30%, 50% and 75%) were manufactured using the aforementioned method.

## 2.4. Microsphere fabrication and characterisation.

Microspheres were fabricated using single oil in water emulsion method. In brief, 1.0g of the triblock – PLGA blend was weighed out into a glass scintillation vial, and dissolved in 4.0ml of dichloromethane (DCM) (Fisher, Loughborough UK). 4.0ml of 0.3% w/v poly vinyl alcohol (PVA) solution was then added to the polymer solution and then homogenised using a vortex VM20 mixer (Chiltern Scientific, Bucks UK) at scale 3 for 1min. The resulting emulsion was then transferred into a beaker with 100ml of 0.3% PVA solution stirring at 300rpm with a magnetic flea. This was allowed to stir on a IKA magnetic stirrer (Sigma, Dorset UK) in a fume hood till the microspheres hardened (approximately three hours), after which the microspheres were harvested through vacuum filtration using a grade 1, 11µm cellulose filter paper (Whatman, Maidstone UK). Microspheres were then dried in a Modulyo freeze dryer system. Dried microspheres were then fractionated using a AS200 sieve shaker (Retsch UK Ltd., Leeds, UK) at amplitude of 1.60mm/g, a 40s interval time and total running time of 20 minutes. Long term storage was achieved by vacuum packaging and storage at -20ºC. The 100 - 300µm (except as otherwise stated) size factions was used in all subsequent experiments and analysis involving the microspheres.

### 2.4.2 Microsphere characterization

Particle size analysis and SEM characterization were undertaken to investigate the size distribution and surface morphology of the fabricated microspheres.

#### 2.4.2.1 Particle size distribution

10mg of pre-fractionated microspheres was dispersed in 3ml of distilled water containing 0.2% Tween 20 (Sigma, UK), and left overnight on a roller to enhance

wetting and dispersion of the microspheres. The mean diameter and particle size distribution of the microspheres were then measured using a laser light scattering particle size analyser (Coulter, UK).

#### 2.4.2.2 Scanning electron microscopy (SEM)

Microspheres made from PLGA and 30% Triblock/ PLGA blend were loaded unto aluminium stubs with pre-fixed carbon tabs. The microspheres were then sputter coated with gold for 3 min using a Balzer Union SCD 030 sputter coater. The surface morphology of the coated microspheres was examined and images obtained by SEM using a JSM-6060 imaging system (JEOL ltd. Herts, UK) with an ionising radiation of 10kV.

## 2.5. Dynamic mechanical Analysis.

The effect of triblock on the viscoelastic properties of PLGA was investigated using a Physica MCR 301 oscillatory Rheometer (Anton Parr, Hertford UK) fitted with a 25mm parallel plate measuring systems and RheoPlus application software. The parallel plate was equilibrated to a starting temperature of 4ºC and temperature oscillation sweep tests was performed at a frequency of 1 rad on the blends of PLGA with a temperature range of 4 - 90 ºC. 260mg of pre-sieved PLGA/triblock blend with the 100 - 300µm size fraction was weighed out unto the flat surface of the parallel plate rheometer and a temperature sweep from 4ºC – 90ºC at 1ºC per min rate change was performed. Temperature oscillation sweeps was performed on PLGA and all the blends of triblock – PLGA fabricated in section 2.3. A plot showing the rate of change of the storage and loss modulus and the phase angle with increase in temperature was obtained as an output from the rheometer.

## 2.6. Protein and drug loading of microspheres

Proteins and drugs were encapsulated into microspheres as depicted in the figure below (Fig 2.2). Protein loaded microspheres were made using the S/O/W method outlined by Morita et al., 2001 with slight modifications. In brief, the protein to be encapsulated was micronised by dissolving in 1ml of distilled water ($dH_2O$) containing 60mg of PEG 6000 (BDH Chemicals, Poole UK) followed by freeze-drying for 48 hours – this constitutes the micronisation step. The protein/PEG lyophilisate was then dispersed in 1ml of dichloromethane (DCM) (Fisher Scientific, Loughborough UK) by vortexing at scale 4 for 30seconds using a VM20 vortex mixer (Chiltern Scientific, Bucks UK). The resulting protein suspension was then added to 3ml of DCM solution containing 1g polymer using VM20 vortex mixer for 1min, at scale 3. 4ml of 0.3% polyvinyl alcohol (PVA) solution (Sigma Aldrich, Dorset UK) was added to protein / polymer mixture and emulsified using the vortex mixer for one minute at scale 5. The resulting emulsion was then poured into 100ml 0.3% PVA stirring at 300rpm with a magnetic stirrer. This was allowed to stir till the microspheres hardened (approximately three hours), after which the microspheres were harvested through vacuum filtration and allowed to dry in a freeze dryer.

For ascorbate-2-phosphate (Asc) and dexamethasone (Dex) encapsulation (see chapters 4 and 5), slight variations from the above mentioned method. The micronisation step was avoided in Asc and Dex encapsulation. Asc was encapsulated using a w/o/w double emulsion method by first dissolving the drug in 400µl of distilled water before homogenisation into the DCM polymer solution. Dex was encapsulated by its direct dispersion into the DCM polymer solution prior to emulsification.

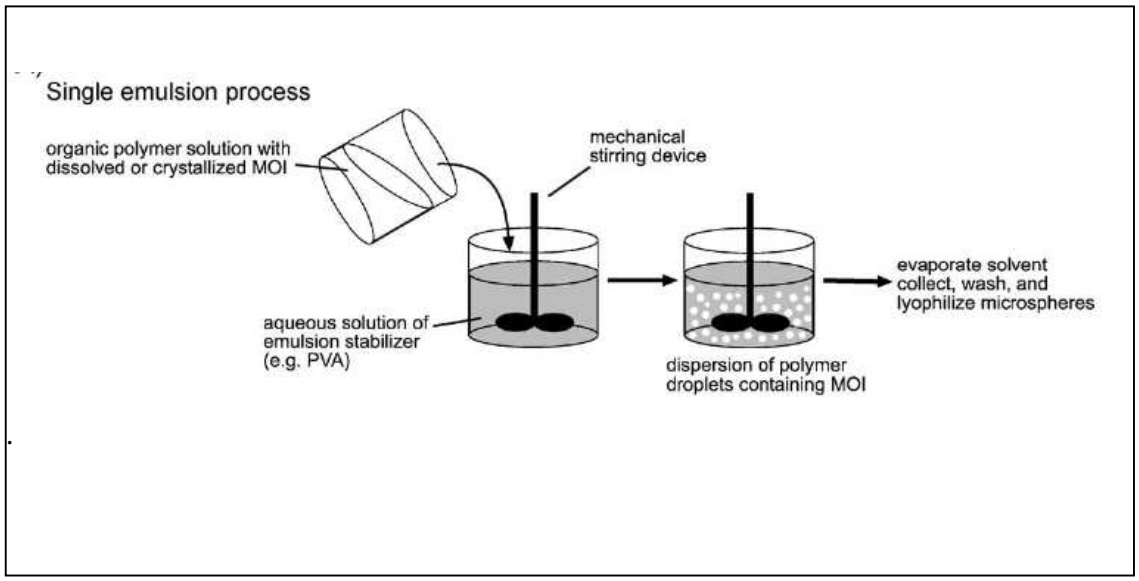


Figure 2.2: Schematic representation of the single emulsion process used in encapsulating protein and drug molecules into polymer microspheres. The dissolved or crystallized MOI (molecule of interest) represents the drug or protein to be encapsulated (Whittlesey and Shea, 2004).

### 2.6 2. Encapsulation efficiency of protein loaded microspheres

The protein content of the microspheres was determined using the method described by Kim et al (2005) with slight modifications. In brief, 20mg of microspheres was dissolved in 1.0ml of ethyl acetate (Fisher Scientific, Loughborough UK.). This was allowed to stand at room temperature for about 1 hour allowing the complete dissolution of the microspheres. 2.0ml of PBS was added to the above solution, vortexed for 1min and centrifuged at 5,000rpm at 5°C for 5 min. The oily top layer (containing the dissolved microspheres in ethyl acetate) was removed and washed with 2.0ml and 1.0ml of PBS following the same process described above. The aqueous portions from the three washes were pooled together and then the amount of protein determined using the micro BCA method (section 2.6.4.1). The entrapment efficiency of the protein within the microspheres was calculated using the formula below.

$$\frac{\text{Actual Loading Weight}}{\text{Theoretical Loaded Weight}} \times \frac{100}{1} = \text{Entrapment efficiency.}$$

The activity of the entrapped protein was determined using the method described below.

### 2.6.3. Controlled Release

Controlled release of proteins form microspheres was determined using the set up described by Aubert Poussell 2002 with slight modifications (Fig 2.3). In brief, 50mg of lysozyme microspheres was placed into an Omega Column tube (Presearch Ltd, UK) made of protein resistant PEEK material. At each end of the column tubes were 0.5μm PEEK frits (Presearch Ltd, UK). Connected at one end using a 1/16" OD

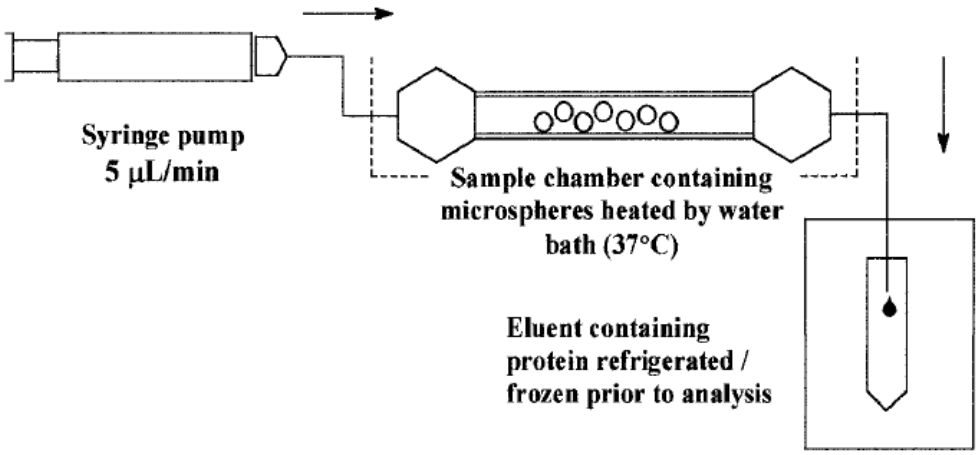


Figure 2.3: Schematic representation of the set-up used for the release of lysozyme from microspheres. 20mg of protein loaded microspheres was incubated in 2ml of PBS at 37ºC. The syringe pump was powered using a PhD 2000 syringe driver to deliver PBS at rate of 2µl/min to the microspheres contained in a sample chamber. The eluent was harvested in falcon tubes at various time intervals and stored in the fridge. (Reference Abbou-Poussel)

(0.040" ID) HPLC PEEK tube to a 20ml plastipak syringe fixed to a Harvard PHD 2000 pump. The other end of the column tube was connected to an eluent vessel

On completion of the set up (See Fig 2.4), the PHD 2000 pump (Harvard, Kent UK) was set to give a continuous infusion at a rate of 2.0µml/min. The eluent buffer used was phosphate buffer saline (PBS) at pH 7.4. This buffer was loaded into the plastipak syringe connected to the PHD 2000 pump. The set-up was allowed to run and the eluent was collected at fixed periods to assay for protein content. The protein content in the eluent was determined by assaying for the protein using the method described in section 2.6.4.1 (microBCA Assay).

## 2.6.4. Protein release assays

The following assays were utilised to determine the quantity and activity of the proteins in the analysis of samples from entrapment efficiency and retention activity of the proteins within microspheres, and samples from release studies from protein loaded microspheres and scaffolds.

### 2.6.4.1. Micro-BCA Assay

The microBCA assay is based on the formation of a purple-blue complex of the bicinchoninic acid (BCA) with Cu+ due to the reduction of Cu 2+ to Cu+ when a peptide bond is present in an alkaline environment (Wiechelman et al., 1988). The assay was undertaken using a quantipro microBCA kit (Sigma Aldrich, Dorset UK) following the manufacturer's protocol. In brief, 100µl of aqueous protein solutions (in distilled water or in PBS) was incubated with 100 µl of freshly prepared BCA working solution (which was prepared following the manufacturers instructions) in a

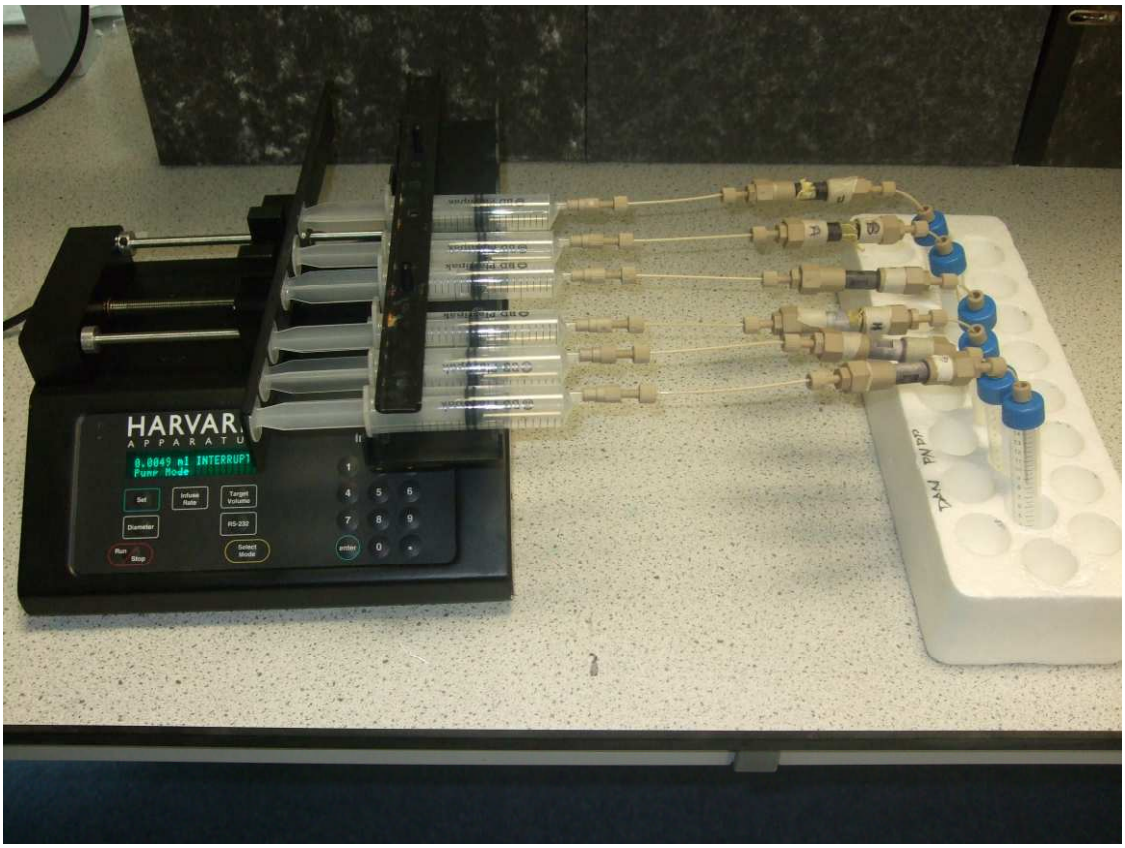


Figure 2.4: Photograph showing the set-up for release of lysozyme from microspheres. 20mg of protein loaded microspheres was loaded into protein resistant PEEK coated chambers with 0.5µm filters attached to both ends. PBS was drawn into 20ml syringes and a PhD 2000 syringe driver was used to deliver PBS from the syringes into the PEEK chambers via PEEK coated silicon tubes. A collecting vessel was used to collect the PBS with eluted protein at the other end. The eluent was harvested at various time intervals and stored in the fridge.

96 well plate at 60ºC for 1 hour. The plate was allowed to cool to room temperature before absorbance reading was recorded using a Lucy 1.0 plate reader (Anthos Labtec, Cambridge, UK). The protein concentrations of the samples were determined by comparing against a standard curve of known concentrations of protein (0, 1, 2, 5, 10, 20, 50, 100µg/ml). Where required, samples with high concentrations of proteins were diluted to obtain an absorbance values within the linear part of the standard curve.

#### 2.6.4.2. Lysozyme Activity Assay

Assaying for active lysozyme involved following the method described by Sohier et al. (2006) with slight modifications. It involves following the change in turbidity of a solution of *Micrococcus lysodeitikus* that occurs as lysozyme lyses the β1,4 glycosidic bond within the cell wall of the bacteria. In brief, 150µl of the lysozyme solution was placed in a 96 well plate, to which 100µl of a 2.3mg/ml solution of *Micrococcus lysodeitikus* was added. The change in turbidity over a 1min period was determined, by following the decrease in absorbance values obtained at 450nm using KC4 plate reader (Labtech, Ringmer UK). The change in absorbance values was then correlated to values obtained from the standard concentration curve (0.5 - 20µg/ml) to determine the amount of active protein.

## 2.7. Scaffold Fabrication

Microspheres fabricated from PLGA, and triblock - PLGA blends containing 10% & 30% PLGA-PEG-PLGA were sintered from scaffolds at temperatures just above the glass transition temperature of the polymer blend at 60ºC. In brief, 120mg of microspheres was weighed and poured into a 5mm by 10mm Teflon mould

(Chemistry Workshop, University of Nottingham UK) and heated at 60 ºC for three hours. Following heating the scaffolds were cooled to room temperature to terminate microsphere fusion, and removed from the mould. The sintered scaffolds were packed by vacuum sealing and stored in the freezer at -20 ºC until required for further use.

## 2.8. Mammalian Cell Culture

### 2.8.1. SNL Fibroblast Media

SNL fibroblasts were cultured in a standard culture media (SCM) containing Dulbecco's Modified Eagles Medium (DMEM) (Invitrogen, Paisley U.K.), 10% (*v/v*) Fetal Calves Serum (FCS), 1% (*w/v*) antibiotic solution (consisting of 10,000 units/ml of penicillin and 100mg/ml of streptomycin sulphate) (Invitrogen), 2mM L-glutamine and 500μM β-mercaptoethanol (β-Mercap). SCM was made fresh every 1 to 2 months. SNL fibroblasts cultures were incubated at 37°C, 5% $CO_2$ in a humidified atmosphere in T75$cm^2$ flasks. Flasks were incubated under stationary conditions until approximately 80-90% confluent. Confluency was judged by viewing under an Olympus CKX-31compact inverted microscope (Olympus, Hertfordshire UK). Once confluent, media was carefully aspirated and cultures were washed twice with PBS. The cells were then treated with 3ml trypsin/EDTA for 5mins at room temperature to minimize cell damage. Once the cells had fully detached from the flask surface, the suspension was transferred to a 15ml Falcon tube. The suspension was repeatedly pipetted to disperse cell clumps before the addition of 6ml SCM to inactivate the trypsin/EDTA. Suspensions were centrifuged for 5mins at 1000rpm in a Mistral 1000 centrifuge (MSE, London U.K.). Media was then aspirated, and the pellets suspended in 4ml SCM and passaged in a typical ratio of 1:4. 9ml SCM was added to each of the

4 x T75cm$^2$ flasks before 1ml of cell suspension was added. SNLs were cultured for approximately 3 to 4 days until confluent, with media changed every 2 to 3 days.

### 2.8.2. Embryonic Stem Cell Culture

ES cells were proliferated in embryonic stem cell culture media (ECM). ECM consisted of SCM supplemented with 500units/ml leukemia inhibiting factor (Chemicon, Hampshire U.K.) (LIF). LIF is added to the culture media as a maintenance factor of ES cell pluripotency. ES cells were cultured in T25cm$^2$ flasks on a feeder layer of mitotically inactivated SNL fibroblasts (mSNLs) under stationary conditions at 37°C, 5% $CO_2$ and a humidified atmosphere until approximately 80% confluency. Media was carefully aspirated once confluent and cultures washed twice with 5ml PBS. Cells were then passaged in a typical ratio of 1:5 using the passaging of SNL method described in 2.9.1. Media was changed when the phenol red indicator began to turn yellow; approximately 1-2 days, dependent on confluency.

### 2.8.3. Scaffold cell seeding

Prior to cell seeding scaffolds were sterilised by soaking under gentle rotation in a solution of 70% (*v/v*) ethanol in distilled water for 10 minutes, This was followed by soaking in 10% (*v/v*) antibiotic / antimycotic solution in PBS (consisting of 10,000 units/ml of penicillin, 100mg/ml of streptomycin sulphate, and 25µg/ml amphotericin B) for 1 hour, and then scaffolds were washed in distilled water for 1 hour. Following sterilisation, scaffolds were pre-soaked in sterilised FCS solution for a 1 hour at 37ºC, 5% $CO_2$. Suspensions of cells to be seeded on scaffolds were cultured and prepared as described in section 2.8.2. Cell counts of viable cells were then assessed by mixing cell suspension with an equal volume of Trypan blue, loaded unto a haemocytometer

and counting of cells that didn't uptake the trypan blue die. These viable cell numbers were used to determine the final cell concentration for scaffold cell seeding. 4 x $10^6$ cells suspended in 50 µl of ES media (excluding LIF and β Mercap) was pipetted repeatedly through the scaffold in a non-tissue culture treated 24 well plate. The new cell / scaffold constructs were incubated in a sterile incubator at 37ºC and 5% $CO_2$ for 3 hours. Cell / scaffold constructs were then removed from incubator and either evaluated for cell viability (Alamar blue™ assay, section 2.9.1), or cultured further in a differentiation media (Cell differentiation, section 2.8.4). Cells / scaffold constructs were fabricated in triplicates for biochemical analysis and duplicates for image analysis.

### 2.8.4. Cell Differentiation.

Differentiation of cells on scaffold constructs was carried out to evaluate the possibility of using scaffolds as devices for the localised delivery of growth factors. These growth factors can be used for the differentiation of stem cells. Following seeding of mES embryoid body cells on scaffolds (Scaffold cell seeding, 2.8.3), the scaffolds were transferred into 20ml universal tubes containing the differentiation media, and incubated for 28 days with complete media replacement every two to three days. In general, differentiation media consisted of DMEM supplemented with 15% (*v/v*) of fetal calf serum (FCS), 2mM L-glutamine, 1% (v/*v*) antibiotic solution (consisting of 10,000 units/ml of penicillin and 100mg/ml of streptomycin sulphate), and 10mM β-glycerophosphate. Additional supplements were added, depending on the experimental investigation (Scaffold induced differentiation, Chapter 5).

## 2.9. Biochemical Assays

The following assays were undertaken to determine the quantity of various cell matrix proteins located on embryonic stem cell seeded scaffolds prior to and after cell differentiation studies. The quantification of the matrix proteins were used to determine the degree of proliferation and differentiation of the murine embryonic stem cells seeded on the scaffolds.

### 2.9.1. Alamar Blue Colorimetric Assay

Alamar blue colorimetric assay was used to determine the viability of cells on scaffolds. The presence of viable cells results in the colorimetric change of alamar blue working solution from a non-fluorescent blue to a fluorescent red due to the cells metabolic activity leading to a chemical reduction of the immediate surrounding environment. In brief the assay was carried out as follows; cell scaffold constructs were washed in PBS for 5 mins to totally remove all traces of culture media. After which the scaffold constructs were incubated in 2ml of alamar blue working solution (containing 1 part of Alamar Blue solution (AbD Serotec, Kidlington, UK) and 9 parts of Hanks Balanced Salts Solution (HBSS) without Phenol Red (Sigma Aldrich, Dorset UK)) under mild agitation at 37$^{o}$C, 5% $CO_2$ for 60 mins. 100 µl of the solution (post-incubation with scaffolds) was transferred to a 96 microtitre well plate, and the absorbance values measured at 570nm using a KC4 plate reader (Labtech, Ringmer UK).

### 2.9.2. DNA Hoescht Assay.

The amount of DNA in cells was quantified following the method described by Kim et al., 1988 with slight modifications. This method is a fluorescence assay based on

the intercalation of Hoescht 33258 dye with DNA. In brief, cells from monolayer or on scaffolds were digested in 1mL of 0.1% papain solution (Sigma Aldrich, Dorset UK) at 60°C for 16 h. 100µl of the sample digests were mixed in a 24 well plate with 2mL of a 0.1µg/ml Hoescht dye solution (pH 7.4) containing 10mM Tris, 1mM EDTA disodium salt, and 0.1mM NaCl. The fluorescent values were obtained using a labtech plate reader (Labtech, Ringmer UK), at an excitation wavelength of 360nm and 450nm. Amount of DNA was determined by comparing the respective fluorescent values obtained with those obtained from preparing a standard curve of DNA standards from salmon at a concentration of 0.5 - 10µg/ml.

### 2.9.3. Alkaline Phosphatase Assay (ALP).

For quantification of ALP activity, a para-nitro phenol substrate (pNPP) was used. In brief, cell scaffold constructs were washed thoroughly in distilled water for 5 minutes. Then the scaffolds were incubated each with 2ml of pNPP substrate under alkaline conditions (Sigma Aldrich, Dorset UK) for 20 minutes under gentle agitation. The absorbance readings of the resulting solution at 450nm were determined using a plate reader (Labtech, Ringmer, UK). The alkaline phosphatase values were normalised to the amount of DNA in the sample detected by hoescht assay (section 2.9.2), by dividing the readings by the total amount of DNA (in ng) present in the sample.

### 2.9.4. Osteocalcin Assay

The levels of osteocalcin present in the media used to culture cells on scaffolds were determined using a mouse osteocalcin ELISA kit (Biomedical Technologies Inc. MA, USA). In brief 25ul of the media was added to the designated individual wells within the kit, 100ul of the osteocalcin antiserum was then added to each well, covered. The

wells were then covered tightly with the plastic seal supplied with the kit, and incubated at 4ºC for 24 hours. After incubation, the wells were then aspirated gently and washed five times with 0.3ml PBS wash buffer (supplied with the kit). After third wash, the wells were inverted and placed on a blotting paper for five minutes to allow for complete removal of wash buffer. 100µl of the streptavidin-horseradish peroxidase reagent was then added to the wells, swirled gently for 1 minute using a plate shaker and then incubated at room temperature for 30 minutes. 100µl of a solution containing equal volumes of 3,3,5,5 - tetramethyl benzidine (TMB) substrate solution and hydrogen peroxidise solution was added to the wells and incubated at room temperature, in the dark for 15 minutes. 100µl of the stop solution (provided in the kit) was added to the wells, swirled gently on the plate shaker for 20 seconds and absorbance measured at 450nm. To quantify the amount a standard curve of osteocalcin ranging from 1.56 – 50ng/ml was used.

### 2.9.5. GAG Assay

The glycosaminoglycan content of the tissue deposited on the sc affolds was determined using a dimethylmethylene blue spectrophotometric (DMMB) assay. In brief, the DMMB solution was prepared by dissolving 16 mg of DMMB (Sigma Aldrich, Dorset, UK) in 5 mL of 95% ethanol. The dissolved dye was diluted in 3 mL formic acid (Sigma Aldrich, Dorset, UK) and 25.6 mL 1M NaOH (Sigma Aldrich, Dorset, UK), and the volume made up to 1 L with distilled water, which provided a formate buffer of pH 3.5. After 4 weeks of cultivation, the dry weight of each control sample or cell–scaffold hybrid was obtained after 24 hours of freeze drying. These scaffolds were digested in 1mL of 0.1% papain solution (Sigma Aldrich, Dorset, UK) at 60°C for 16 h. 40µl of sample digests were mixed with 250µL DMMB reagent in a

96-well microplate at room temperature. The absorbance values at 595nm was measured in a KC4 plate reader (Labtech, Rigmer, UK) and was compared with a linear standard curve obtained from GAG standards (0 to 100 µg/mL of chondroitin-4-sulfate; (SigmaAldrich, Dorset, United Kingdom) to estimate the GAG content in each sample (per mg of scaffold).

### 2.9.6. Hydroxyproline and Collagen Assay

Total collagen was determined by measuring the amount of hydroxyproline present in each cell / scaffold construct. Papain digests of the constructs were undertaken as detailed in section 2.9.2. The papain digests were hydrolyzed by incubating 250 µl of the papain digest with 250 µl of 6N HCl at 120ºC for 16 h. The hydrolysate was then transferred into open glass scintillation vials and incubated at 90°C until a dry brown residue at the bottom of vial was obtained. The residue was then allowed to cool down to room temperature and re-dissolved in 1 ml of 0.25M PBS pH 6.5 50 µl of the resulting solution was then transferred into 96 well plate and absorbance values at 570nm using a Lucy 1.0 plate reader (Anthos Labtec, UK). The protein concentrations of the samples were determined by comparing against a standard curve of known hydroxyproline concentrations of protein (0, 1, 2, 5, 10, 20, 30µg/ml). The total collagen expressed as a % of the scaffold was calculated using the formula below

$$\frac{\text{[hydroxyproline] (µg/ml) x dilution factor x proportion hydrolysed}}{\text{Dry weight scaffold (g) x 0.143 x } 10^6} \times 100\%$$

Where required, samples with high concentrations of collagen were diluted to obtain an absorbance values within the linear part of the standard curve.

## 2.10. Bilayered Scaffold Fabrication.

Bilayered scaffold consisting of two separate regions of different protein loaded microspheres fused together (Fig 2.5). In brief approximately 50mg of microspheres A was loaded into a 5" x 10" teflon mould and tapped gently to allow the particles settle to into the mould. Then 50mg of microspheres B was added to the teflon mould containing microspheres A, and again gently tapped. The mould containing the microspheres A and B were then incubated in a fan assisted oven at the required sintering temperature and duration (see section 5.3.4 for details). Microspheres A and B could represent any of the following depending on the intended applications:

(i) Two different protein loaded microspheres;

(ii) A protein loaded microsphere and a non loaded microsphere

(iii) A protein loaded microsphere and a drug loaded microsphere

(iv) A drug loaded microspheres and non loaded microspheres respectively.

### 2.10.1. Protein Zonal Release

A scaffold with a specific zone of entrapped protein within microspheres has been shown to induce patterned differentiation of cells localised to the zones containing the entrapped proteins (Suciati et al., 2006). The release of proteins from a bilayered scaffold was investigated. In brief bilayered scaffolds containing TGF-β3 and BMP4, was incubated in a 20ml universal tube containing 4ml of PBS. A 1mm plastic washer was used to separate the PBS solution in contact with the region of TGF-β3 loaded from the BMP4 loaded region of the scaffold (Fig 2.5). It was hypothesized that the presence of the washer will localise the proteins released to the area immediately surrounding the region of scaffold the protein was released from, and limiting the transit diffusion of the released proteins away from the region. At various time

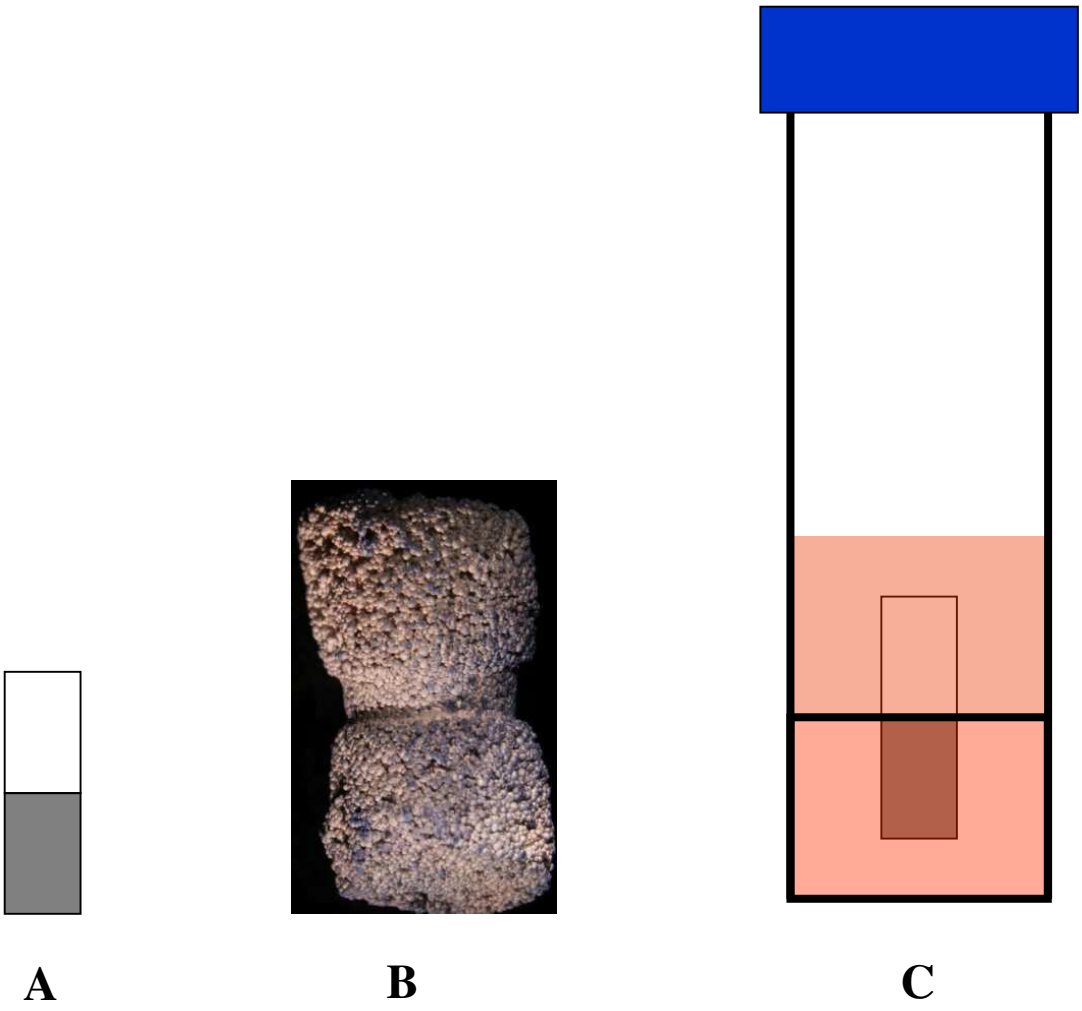


Figure 2.5: Schematic representation of A & B) Bilayered Scaffold and C) Bilayered scaffold zonal release set up. A & B) are diagrammatic and photograph representations of a bilayered scaffold consisting of two separate microsphere layers. Top layer consists of TGF$\beta_3$ loaded microspheres and bottom layer consists of BMP4 loaded microspheres. C) Representation of the set-up used to investigate the release of TGF$\beta_3$ and BMP4 from the bilayered scaffold. A plastic washer was used to limit the diffusion and mixing of proteins across the sections.

intervals the PBS solutions from each section (A & B) was harvested and the amount of TGF- β3 and BMP4 in each section was determined using ELISA (section 5.3.4.3).

## 2.11. Histochemical and Immunocytochemical Staining

### 2.11.1. Alizarin Red Staining

A 2% w/v Alizarin red solution was formed by suspending 2g of Alizarin Red S powder (Sigma Aldrich, Dorset UK) in 100ml of distilled water. The resulting suspension was filtered using a grade 1 filter paper to form the alizarin red solution. The pH of the solution was then adjusted to a final pH of 4.2 using 1M NaOH solution. The final solution was then stored at room temperature until required for further use.

The samples to be stained were fixed in 10% neutral buffered formalin solution and the fixed samples were stored in PBS (pH 7.2) at 4ºC until required for further use.

Post-fixed stained scaffolds were stained for calcium deposits using the alizarin red solution by incubating the scaffolds in the solution for 10mins. The excess background staining was removed from the scaffold by washing the excess dye in distilled water followed by blotting the scaffold on blotting paper. The scaffold was then allowed to dry overnight in the fume hood before viewing for red stained calcium deposits

### 2.11.2. Masson's Trichrome Staining.

Masson's trichrome staining was used to differentiate between collagenous tissue and other tissue types such as smooth muscle tissue. The scaffolds to be stained were fixed in Bouin's solution (Sigma Aldrich, Dorset UK) for 1 hour at in an oven preset to

56ºC. The scaffolds were then removed from the oven, allowed to cool down to room temperature and then washed gently under running water until the yellow color disappears. The scaffold was then rinsed in distilled water and then stained in Weigert's hematoxylin (Accustain Trichrome stain kit (Sigma Aldrich, Dorset UK)) for 10 minutes. The scaffolds were then gently washed in running water for 10 minutes, followed by gentle rinsing in distilled water. The scaffolds were then stained in Biebrich scarlet-acid fuchsin solution (Accustain Trichrome stain kit (Sigma Aldrich, Dorset UK)) for 2 minutes. The scaffolds was then rinsed in distilled water, and then stained in phosphomolybdic-phosphotungstic acid solution (Accustain Trichrome stain kit (Sigma Aldrich, Dorset UK)) for 10 minutes. The scaffolds were then blotted dry on white tissue and then stained in aniline blue solution for 5 minutes. The scaffolds were then rinsed in distilled water, blot dried and then placed in 1% acetic acid solution for 5 minutes. The scaffold was then allowed to dry overnight in the fume hood before viewing for stained region.

### 2.11.3. Alcian Blue / Sirius Red Staining.

Prior to histochemical staining, scaffolds were fixed with 4% paraformaldehyde. The scaffolds were then stained with Weigert's haematoxylin for 8 minutes, and then washed under running tap water for 10 minutes. Scaffolds were then blot dried with blotting paper and then stained for 10 minutes in 0.5% (*w/v*) alcian blue solution for 20 minutes. After which scaffolds were again washed under running tap water and in distilled water, blot dried and then treated with 1% phosphomolybdic-phosphotungstic acid solution for 10 minutes. After which the scaffolds were stained by treating with 0.1% picrous -sirius red solution for 1 hour. The scaffolds were then rinsed in distilled water, blot dried and then washed twice with 1% acetic acid solution for 5 minutes.

The scaffold was then allowed to dry overnight in the fume hood before viewing for stained region.

### 2.11.4. Single and Double Immunostaining.

Single antigen immunostaining of cell seeded scaffolds for osteocalcin were performed to determine the presence and localisation of bone nodules. While double antigen staining of cell seeded bilayered scaffolds for collagen II and osteocalcin were performed to determine the localisation of cartilage and bone nodules respectively. Prior to Immunostaining scaffolds were fixed in 4% parafaormaldehyde and stored in PBS pH 7.4 at 4ºC until when required. For single and double antigen immunostaining, the scaffolds were incubated for 10 minutes in PBS containing 0.25% Triton X-100 (Sigma Aldrich, Dorset UK). After which the scaffolds were washed three times in PBS for 5 minutes each. Scaffolds were incubated in 1% BSA in PBS pH 7.4 containing 0.1% Tween 20 (Sigma Aldrich, Dorset UK) solution for 30 min to block unspecific binding of the antibodies. Scaffolds were then incubated in a solution of the primary antibody (or mixture of the primary antibodies for double antigen staining) at a concentration of 1µg/ml in 1% BSA in PBS pH 7.4 containing 0.1% Tween overnight at 4ºC for each primary antibody. The solution was then decanted and the scaffolds washed three times in PBS, with 5 minutes per wash. The scaffolds were then incubated in the secondary antibody (or mixture of the secondary antibodies for double antigen staining) with the attached fluorochrome in 1% BSA for 1 hr at room temperature in dark. The secondary antibody solution was then decanted and the scaffold was washed three times with PBS for 5 min each in dark. The scaffold was then blotted dried and then viewed for stained region using a SMZ1500 stereoscopic fluorescent microscope (Nikkon, Alton UK). Primary antibodies used for

osteocalcin and collagen II immunostaining were goat polyclonal osteocalcin antibody (Santa Cruz Biotechnology Inc, Heidelberg, Germany), and rabbit polyclonal antibody (Abcam Plc, Cambridge, UK) respectively. The secondary antibodies used were northern lights-493 anti-goat and northern lights-557 anti-rabbit antibodies (both obtained from R&D Systems, Abingdon, UK) respectively.

## 2.12. Statistical analysis.

All experiments were performed in triplicates (except where indicated) with the results expressed as means ± standard deviations. Unpaired, two-tailed *t*-tests were performed at each time point for the controlled release and protein / drug encapsulation efficiency. The threshold for statistical significance was set at $p<0.05$.

# CHAPTER 3

# PLGA microsphere based composites.

## 3.1 Introduction

Scaffolds have been successfully used in promoting the regeneration of different tissue types in both *in vivo* and *in vitro* experiments. Examples of *in vivo* and *in vitro* experiments involving the use of scaffolds include for nerve regeneration (Hausner et al., 2007), bone (Filipczak et al., 2004), liver (Jiankang et al., 2007), skin (Sang-Soo et al., 2005), cartilage (Jung et al., 2008), and blood vessels (Kaigler et al., 2007). The success in achieving tissue regeneration is mainly dependent on the scaffold design and the choice of material used in formulating the scaffold. Depending on the specific intended application of the matrix, whether for structural support, drug-delivery capability, or both, certain material categories may be more or less well suited to the final structure.

Different materials have been used for scaffold fabrication. for tissue engineering applications (Hench and Polak, 2002, Langer 2000, Livingstone et al., 2002, Thomson et al., 1995, Liu & Ma, 2004). These materials include metals, ceramics, natural and synthetic polymers. Whilst these materials have several characteristics that make them attractive options for tissue engineering in their own right, they also have some inherent disadvantages that limit its use in tissue engineering. For example, metals and ceramics have two major disadvantages for tissue engineering applications: Their inability to degrade within the physiological environment and their limited

processability (Macquet and Jerome, 1997). These disadvantages have impacted on their use within tissue engineering applications. In contrast, the ability to modify the composition and structure of polymers to match the specific needs of the scaffold imparts on it great design flexibility and makes them great candidates for tissue engineering applications. For these reasons, polymeric materials have received considerable attention and are widely studied for bone tissue engineering applications (Liu & Ma, 2004). However the mechanical strength of scaffolds achieved utilising polymers are inadequate for several tissue engineering applications. In addition the inertness of the polymeric scaffolds often limits the successful in growth of tissue within the scaffold.

Composite materials of two or more different materials are often required to offset the limitations of the individual materials whilst combining their benefits. Several composites have been used to improve the bioactivity, degradation and mechanical properties of scaffolds in various tissue engineering applications.

For example in work carried out by Yoo et al (2005), composites scaffolds made of hyaluronic acid immobilised unto the surface of PLGA scaffolds showed improved cellular attachment, GAG and total collagen attachment compared to unmodified PLGA scaffolds. Composites of synthetic polymers and inorganic materials such as hydroxyapatite and calcium phosphate have also been investigated for use in bone tissue engineering in order to overcome the limitations of brittleness, and difficulty in shaping associated with conventional ceramic substitutes while improving on the mechanical strength achieveable with scaffolds. Ren et al showed the improvement in

the compressive mechanical strengths of PLGA scaffolds and biocompatibility when fabricated with increasing amount of the hydroxyapatite (Ren et al 2008).

In addition to optimising scaffold properties in order to promote successful tissue regeneration, the development of scaffolds that can be delivered to the site of tissue regeneration in a minimally invasive and uncomplicated manner for clinical applications is a main challenge facing clinicians (Kretlow et al., 2007). As a result interest in injectable biomaterials for tissue engineering and drug delivery has grown immensely and shows great promise for clinical applications. This growth is largely due to the minimally invasive manner in which these materials can be delivered to remote sites without the need for surgical procedures and the additional host of complications such as cost, trauma, pain and infection that might be involved (Kretlow et al., 2007; Elisseeff et al., 2004).

Current methods explored for fabricating *in situ* polymer based scaffolds include the *in situ* polymerisation or crosslinking of polymers through the use of a thermal or photo initiator (Temenoff et al., 2003; Davis et al., 2003), chemical based polymerisation (Ohya et al., 2005), and the use of aqueous solutions of thermogelling polymers (that can be optimised to undergo a sol gel transition at certain temperatures) (Pratoomsoot et al., 2008; Suggs et al., 1999). However limitations such as difficulty in controlling the solidification time exist for *in situ* scaffold fabrication. Other limitations in using these materials as controlled delivery devices include the polymerisation process (photo, thermal, or chemical based) can lead to denaturing of the growth factor. Also the release of toxic by-products, increased heat and presence

of residual compounds such as the catalyst from polymerisation reaction can result in localised tissue injury (Suggs et al., 1999).

In the work detailed in this chapter, PLGA based microspheres that can be used for formation of *in situ* scaffold was developed. It was hypothesized that blending PLGA with the thermosensitive triblock co-polymer PLGA-PEG-PLGA, will result in a reduction of the glass transition temperature of the resulting composite blend. The composite polymer blend can be exploited for development of microspheres which can sinter to form a porous scaffold at the body temperature. Successfully development of microspheres that are free flowing at room temperature, but sinter to form scaffolds at the body temperature, can be harnessed by clinicians to form *in situ* scaffolds for promoting the repair of remotely located tissues that would otherwise require highly invasive surgical techniques to insert a pre-fabricated scaffolds.

## 3.2 Chapter Aims.

The aim of this chapter was to reduce the glass transition temperature of PLGA, by blending with the thermosensitive triblock co-polymer PLGA-PEG-PLGA. The resulting blend was used to produce microspheres with reduced scaffold sintering temperature. The properties of PLGA microspheres were optimized to accelerate the rate of degradation and produce scaffolds with improved mechanical strength, thereby fulfilling the requirements for tissue engineering matrices. The experimental objectives set out to achieve this aim can be summarised as follows:

(iii) Investigate the effects of the triblock co-polymer on the glass transition temperature and viscoelastic properties of PLGA.

**(iv)** Fabrication of microspheres that can be sintered at low temperatures to form scaffolds with improved mechanical strength.

## 3.3 Materials and Methods

### 3.3.1 PLGA-PEG-PLGA Synthesis.

The triblock PLGA-PEG-PLGA was synthesized via ring-opening polymerisation of D, L-lactide and glycolide onto PEG 1500 using the catalyst stannous octoate following the method detailed in section 2.2.

### 3.3.2 Gel Permeation Chromatography (GPC).

The molecular weights and polydispersity indices of the synthesized triblock were determined by GPC following the methods detailed in section 2.2.

### 3.3.3 Nuclear Magnetic Resonance (NMR).

The molecular weight and the lactide: glycolide ratio of the synthesized PLGA-PEG-PLGA polymer was determined using NMR ($^1$H NMR). $^1$H NMR analysis was performed following the methods detailed in section 2.2.

### 3.3.4 PLGA / Triblock blend manufacture.

PLGA/Triblock blends with a triblock composition of 10%, 20%, 30%, 50% and 75% w/w were manufactured following the methods detailed in section 2.3.

### 3.3.5 PLGA / Triblock blend characterisation.

$^1$H NMR spectroscopy was used to quantify the proportions of triblock present within the different PLGA / triblock blends manufactured in section 3.3.4. In brief, 10mg of

the polymer blend was dissolved in deuterated $CDCl_3$ and analysis performed following the method for NMR analysis as described in section 2.2. The mole ratio of the PEG to LA was used as a scale of comparison and indication of the amount of triblock present within each blend.

### 3.3.6 Dynamic mechanical analysis of PLGA / Triblock

The effect of triblock on the glass transition temperature and the viscoelastic properties of PLGA was investigated following the methods described in section 2.5.

### 3.3.7 Microsphere fabrication.

Microspheres were fabricated following the methods detailed in section 2.4. Long term storage of microspheres prior to use was achieved by vacuum packaging and storage at -20ºC. The 100 - 300µm (excepted as otherwise stated) size factions was used in all subsequent experiments and analysis involving the microspheres.

### 3.3.8 Characterisation of Microspheres.

Microspheres produced from section 3.3.7 were used for analysis in section 3.3.8.i – 3.3.8 iii.

### 3.3.8.i Particle size distribution of microspheres.

The mean diameter and particle size distribution of pre-fractionated PLGA microspheres were measured using a laser light scattering particle size analyser as described in section 2.4.2.1.

### 3.3.8.ii Scanning electron microscopy (SEM)

The surface morphology of microspheres produced from PLGA and PLGA + 30% w/w triblock blends was characterized using scanning electron microscopy as described in section 2.4.2.2.

### 3.3.8.iii NMR Characterisation.

$^{1}H$ NMR spectroscopy was used to quantify the amount of triblock retained within the microspheres fabricated from the different PLGA / triblock blends manufactured in section 3.3.4. In brief, 10mg of the microspheres was dissolved in deuterated $CDCl_3$ and analysis performed following the method for NMR analysis as described in section 2.2. The mole ratio of the PEG to LA was used as a scale of comparison and indication of the amount of PLGA-PEG-PLGA within the microspheres.

### 3.3.9 Scaffold fabrication using heat sintering

Microspheres fabricated from PLGA, and PLGA / triblock blends containing 10% & 30% w/w triblock were sintered from scaffolds at temperatures just above the glass transition temperature of the polymer blend at 60ºC. In brief, 120mg of microspheres was weighed and poured into a 5mm by 10mm Teflon mould (Chemistry Workshop, University of Nottingham UK) and heated at 60 ºC for three hours. Following heating the scaffolds were cooled to room temperature to terminate microsphere fusion, and removed from the mould. The sintered scaffolds were packed by vacuum sealing and stored in the freezer at -20 ºC until required for further use. Microspheres from PLGA + 10% triblock and PLGA + 30% w/w triblock blends was also heat sintered to form scaffolds at 45 ºC to investigate the effects of triblock on scaffold mechanical strength.

### 3.3.10. Mechanical Testing of scaffolds

Compression test were carried out on scaffolds using a TA.HDplus texture analyser (Stable Micro Systems Ltd., Surrey, UK). The height and width of scaffolds fabricated in section 3.3.9 was measured and the cross sectional area determined. A compression test was carried out using a uniaxial load of 50kg applied perpendicular to the diameter of the scaffold with an approach speed of 0.1mm/sec. The compression was carried to a maximum of 70% strain. Four specimens was tested for each formulation.

## 3.4 Results

### 3.4.1 Triblock synthesis and characterisation.

PLGA-PEG-PLGA hereto known as triblock was characterized using $^1$H NMR spectrometry was undertaken to provide an insight into the chemical structure and composition of the synthesized triblock copolymer. A typical spectrum of triblock copolymer with its chemical structure is presented in Fig. 3.1. The signals pertaining to the triblock are found in $\delta$ = 5.20 ppm (CH of LA, a), 1.55 ppm ($CH_3$ of LA, b), 4.80 ppm ($CH_2$ of GA, c), and 3.65 ppm ($CH_2$ - $CH_2$ of ethylene glycol, d). $^1$H NMR yielded a number average molecular weight ($M_n$) of 5070 and was obtained by integrating the aforementioned peaks. The LA: GA ratio was determined to be 75:25 and was calculated by integrating the $CH_3$ and $CH_2$ peaks respectively and normalised to the number of $^1$H. The molecular weight of the PEG was set at 1500 (as detailed by the manufacturer), and the ratios of the integrated peaks of LA and GA after normalisation to the number of $^1$H was used to determine the number of moles of each of the monomer. The number of moles of each monomer was multiplied by the formula weight of the monomer and the sum of these values was then added to obtain

the number average molecular weight of the polymer. Details of these calculations are summarised below.

| Integrated signal values obtained are | | Normalised values of integrated signals are | |
|---|---|---|---|
| $CH_2$ - $CH_2$ of ethylene glycol – | x | $CH_2$ - $CH_2$ of ethylene glycol – | x/4 |
| $CH_3$ of Lactide - | y | $CH_3$ of Lactide - | y/3 |
| $CH_2$ of glycolide - | z | $CH_2$ of glycolide - | z/2 |

There are 4, 3 and 2 H in the signals integrated for the ethylene glycol; lactide and glycolide monomers respectively.

Molecular weight of PEG – 1500

Formula weight (FW) of ethylene glycol – 44

Therefore no. of moles of ethylene glycol = 1500/44 = 34.09.

34.09 moles of ethylene glycol gives a signal intensity – x

1 mole of ethylene glycol corresponds to 4 moles of H.

Therefore 34.09 moles of H will provide a signal intensity of – X/4.

1 mole of H will provide a signal intensity of – (X/4 ÷ 34.09) = x/136.36)

No of moles of lactide and glycolide = (y/3 ÷ x/136.36) and (z/2 ÷ x/136.36).

Assume no of moles of lactide and glycolide obtained from above is W and S respectively.

FW of lactide and glycolide = 72.06 and 58.04 respectively.

M*n* of PLGA-PEG-PLGA = (W x 72.06) + (S x 58.04) + 1500.

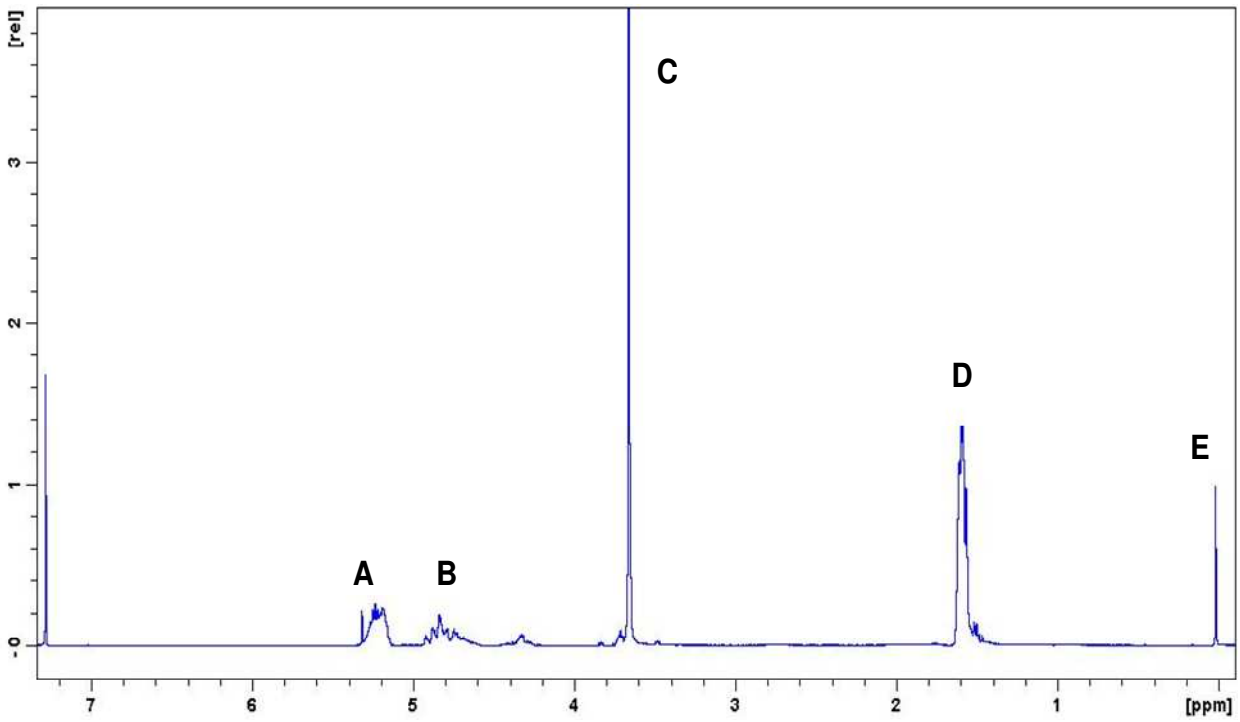


Figure 3.1: $^{1}H$ NMR spectra of PLGA–PEG–PLGA (triblock) copolymer. 1H NMR analysis of the triblock copolymer using a Bruker AMX-400 Ultrashield spectrometer was used to determine the composition of the copolymer. Peaks (A) CH of lactide moiety; (B) $CH_2$ of glycolide; (C) $CH_2CH_2$ of PEG; and (D) $CH_3$ of lactide are characteristic peaks PLGA – PEG – PLGA. and (E) Tetra methyl silane (TMS) corresponding to a zero chemical shift at zero was used as the reference peak.

GPC was used to obtain the molecular weight and molecular weight distribution Fig. 3.2 shows a typical GPC chromatograms. The weight average molecular weight (Mw) and number average molecular weight (Mn) as determined by GPC was 6676 and 5900 respectively. The retention time of the triblock copolymer was about 16 min, the other peaks and troughs in the chromatogram are from the solvent. The polydispersity of the triblock copolymers was found to be about 1.15. Unimodal GPC trace with a low polydispersity value confirms the formation of triblock copolymers with relative narrow molecular weight distributions.

### 3.4.2 PLGA / Triblock characterisation.

$^1$H NMR was used to confirm the presence of the triblock within the PLGA / PLGA-PEG-PLGA blends. $^1$H NMR spectra of the PLGA / triblock blends are shown in Fig 3.3. In Fig 3.3, it was observed that an increase in the proportion of the triblock within the PLGA / triblock blend resulted in an increase in the intensity of the $CH_2$ – $CH_2$ signal peak. The $CH_2$ – $CH_2$ signal peak was absent in the $^1$H NMR spectra corresponding to pure PLGA blend. The $CH_3$, $CH_2$ and $CH_2$ – $CH_2$ peaks representing LA, GA and PEG respectively were integrated, normalised to the number of hydrogen ions (3, 2 & 4 respectively).

Based on the assumption that the contribution of the lactide monomer from the triblock to the intensity of the $CH_3$ signal peak was insignificant when compared to the contribution of the lactide moiety from the PLGA, it was hypothesized that PEG: LA would increase incrementally with increasing concentration of the triblock within the blend. The assumption that the contribution of the lactide monomer from the triblock to the intensity of the $CH_3$ signal peak was insignificant when compared to

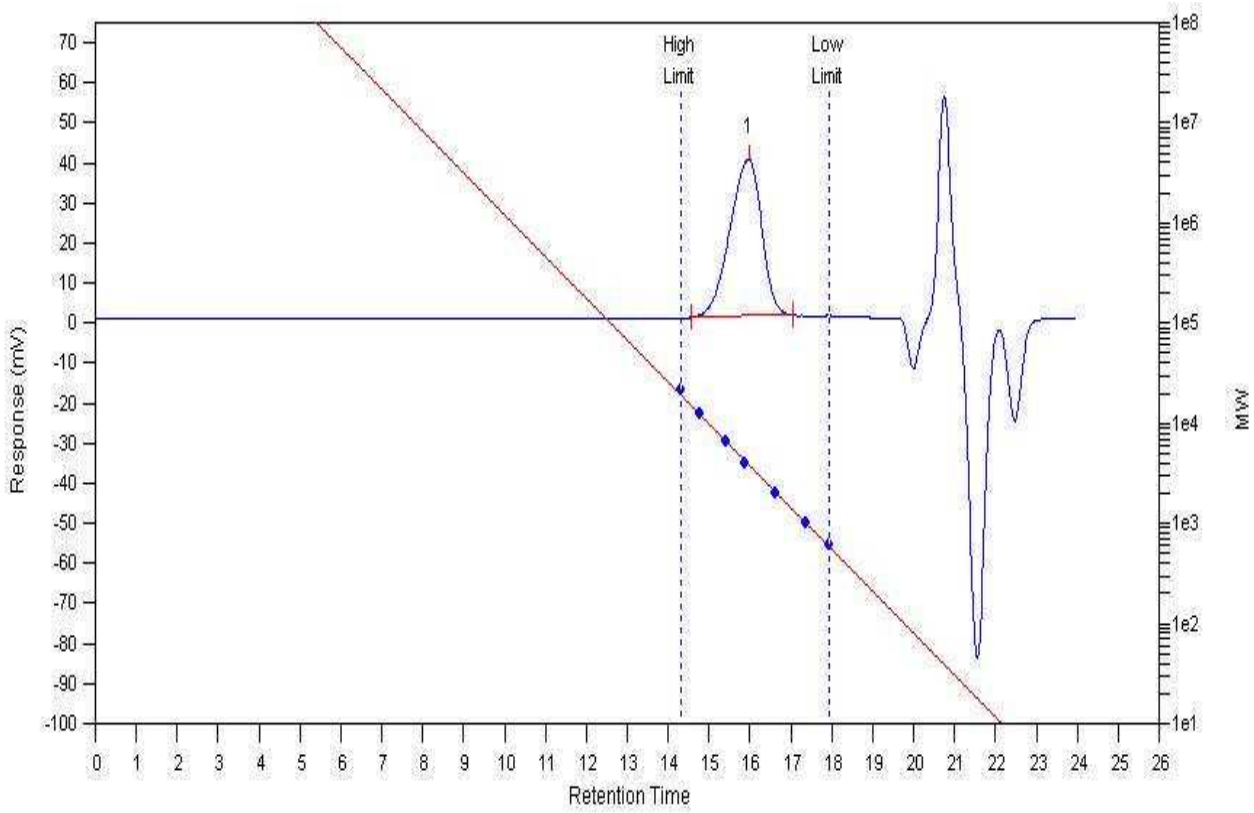


Figure 3.2: The molecular weights and polydispersity indices of the synthesized triblock were determined by GPC performed using a K-501 HPLC pump with a linear calibration range of *M*w 200–2,000,000 g/mol. For analysis, 10mg of the polymer was dissolved in 3ml of tetrahydrofuran (THF) in toluene and sample run using THF at a flow rate of 1ml/min. Molecular weight was determined against polystyrene standards.

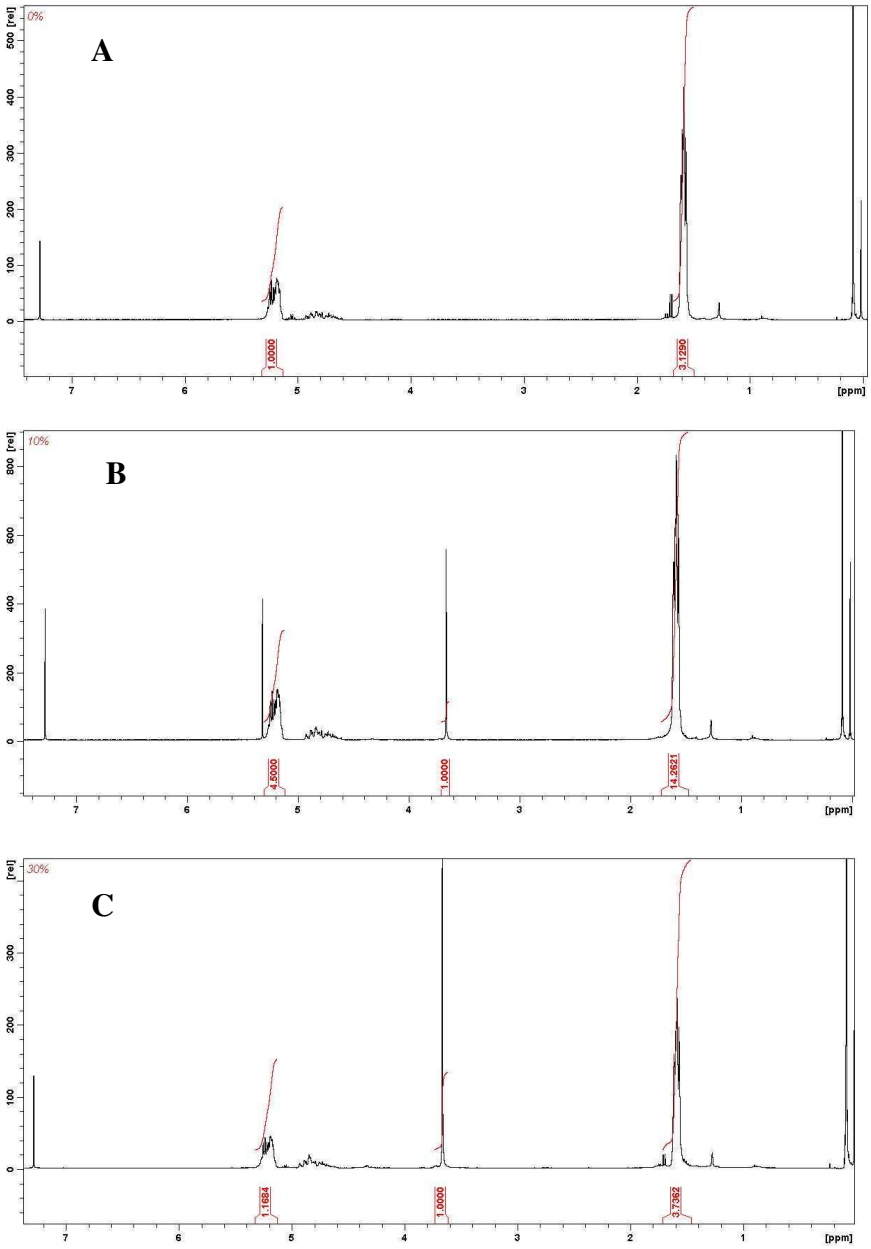


Figure 3.3: NMR Spectra for PLGA / triblock blends (A) PLGA blend; (B) PLGA + 10% triblock blend (C) PLGA + 30% triblock blend. $^{1}H$ NMR analysis was used to confirm the blending of triblock copolymer with PLGA. The presence of the $CH_2CH_2$ PEG peak at 3.65ppm in (B, C) was used as an indication of presence of the triblock within the blends.

the contribution of the lactide moiety from the PLGA was based on the rationale that since the molecular weight and the LA: GA ratio of the PLGA and triblock was approximately 109kDa and 5kDa (3.5kDa excluding the PEG portion) and 85:15 and 75:25 respectively, the additional number of moles of the lactide monomer provided by the triblock portion would be insignificant. Since the $CH_2 - CH_2$ peak is absent in pure PLGA and characteristic of the triblock

The PEG: LA ratio which is equivalent to the mole ratio of PEG: LA was calculated using the equation detailed below.

PEG: LA = (3Y / 4X : 1), where Y and X are the integrated signal of $CH_2$-$CH_2$ and $CH_3$ respectively.

The equation was obtained as follows;

| | Intensity Values | | Normalised Intensity Values |
|---|---|---|---|
| $CH_2$-$CH_2$ | Y | | Y / 4 |
| $CH_3$ | X | | X / 3 |
| No. of Moles | ≡ | Normalised Intensity Values | |
| PEG: LA mole ratio | ≡ | Y / 4**:** X / 3 = 3Y/4X**:** 1 | |

Based on the calculations above and the $^1H$ NMR spectrum, triblock copolymer was observed to have a PEG: LA ratio of 0.812:1 with an incremental reduction as the concentration of triblock within the blend decreases (Table 3.1). The pure triblock was also observed to have a lower LA: GA ratio than PLGA (2.67 vs. 5.91). This value increased incrementally with reducing concentration of triblock within the blend. Plotting these values in a graph (Fig. 3.4) shows the existence of a positive

| Blend | PEG Peak | LA Peak | GA Peak | PEG Peak (N) | LA Peak (N) | GA Peak (N) | LA:GA | PEG:LA |
|---|---|---|---|---|---|---|---|---|
| **PLGA** | 0 | 1 | 0.1125 ± 0.0024 | 0 | 0.333 | 0.0563 ± 0.0012 | 5.91± 0.12 | 0.000 |
| **10% Triblock** | 0.0845 ± 0.0036 | 1 | 0.1224 ± 0.0022 | 0.0211 ± 0.0009 | 0.333 | 0.0612 ± 0.0011 | 5.44 ± 0.09 | 0.063 ± 0.003 |
| **20% Triblock** | 0.1439 ± 0.0092 | 1 | 0.1324 ± 0.0030 | 0.036 ± 0.0023 | 0.333 | 0.0662 ± 0.0015 | 5.03 ± 0.11 | 0.108 ± 0.007 |
| **30% Triblock** | 0.2421 ± 0.0120 | 1 | 0.1504 ± 0.0028 | 0.0603 ± 0.0030 | 0.333 | 0.0752 ± 0.0014 | 4.43 ± 0.08 | 0.181 ± 0.009 |
| **50% Triblock** | 0.4195 ± 0.0280 | 1 | 0.1912 ± 0.0052 | 0.1049 ± 0.0070 | 0.333 | 0.0956 ± 0.0026 | 3.48 ± 0.09 | 0.315 ± 0.021 |
| **75% Triblock** | 0.7210 ± 0.0168 | 1 | 0.2122 ± 0.0042 | 0.1803 ± 0.0042 | 0.333 | 0.1061 ± 0.0021 | 3.14 ± 0.06 | 0.541 ± 0.013 |
| **Triblock** | 1.0812 ± 0.0424 | 1 | 0.2491 ± 0.0046 | 0.2703 ± 0.0106 | 0.333 | 0.1246 ± 0.0023 | 2.67 ± 0.05 | 0.812 ± 0.032 |

Table 3.1: As a measure of the hydrophilicity of PLGA / triblock blends and quantification of triblock dispersion within the blends, the quantification of PEG, LA and GA peak values of various triblock / PLGA blends was undertaken by integrating the peaks at 3.65ppm, 4.80ppm and 1.60ppm respectively obtained from $^{1}$H NMR analysis of PLGA / Triblock blends. The LA peak was normalised to 1.0000. PEG: LA and LA: GA mole ratios were obtained through the normalisation of integrated peak values to their respective H content. The values indicate the mean of two independent experiments and are representative.

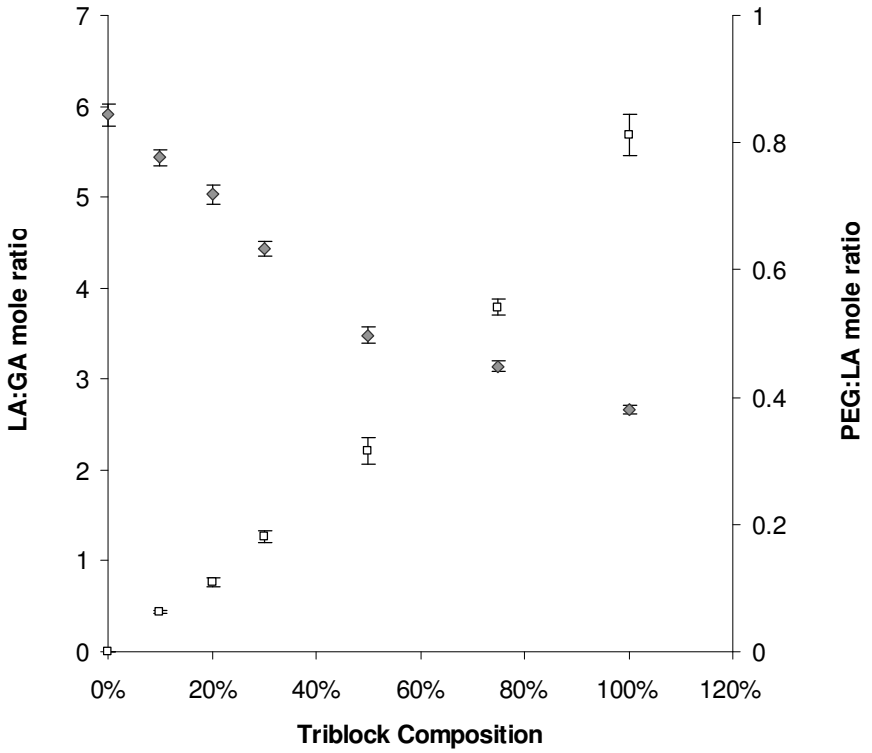


Figure 3.4: Graph showing variation of triblock composition within blend results with the PEG: LA (unbroken trend line $R^2 = 0.9773$) and LA: GA (Dotted trend line $R^2 = 0.944$) mole ratios (closed diamonds and closed squares are PEG: LA and LA: GA data series respectively). N = 3.

linear correlation between the concentration of triblock and the PEG: LA ratio, while a negative linear correlation was observed between the concentration of triblock and the LA: GA mole ratio.

### 3.4.3 Dynamic mechanical analysis of PLGA / triblock.

The effect of increasing triblock composition on the viscoelastic properties of PLGA / triblock blend was investigated. Fig 3.5 illustrates the effect of increase in temperature on the change in phase angle for the different blend compositions ranging from 0% (PLGA) to 75% w/w triblock compositions. Fig 3.6 illustrates the effect of change in temperature on the storage and loss moduli of the blend with 0 to 30% triblock composition. Results in Fig 3.5 shows that as the proportion of the triblock increases from 0 to 75% the temperature at which glass transition begins reduces. The onset of glass transition is taken as the rapid linear increase in the phase angle of the material. The glass transition temperature is taken as the temperature at which the phase angle peaks (prior to descent). It represents the transition of the material from a glassy solid state (in which the elastic properties predominates and know flow is observed) to a more rubbery state (in which the material starts to flow). In Fig 3.6 the initial storage modulus (a measure of the elastic properties of the material) at the start of the experiment of the PLGA blends containing from 0 to 30% triblock blends ranged from 2MPa to 5MPa with no particular trend. However an increase in temperature was observed to result in a gradual increase in the storage modulus for both PLGA and PLGA + 10% triblock blends (2.09 ± 0.17MPa to 19.1 ± 0.79MPa and 4.48 ± 0.36MPa to 12.4 ± 0.38MPa respectively). Whilst the storage modulus for PLGA / triblock blends containing 20% and 30%

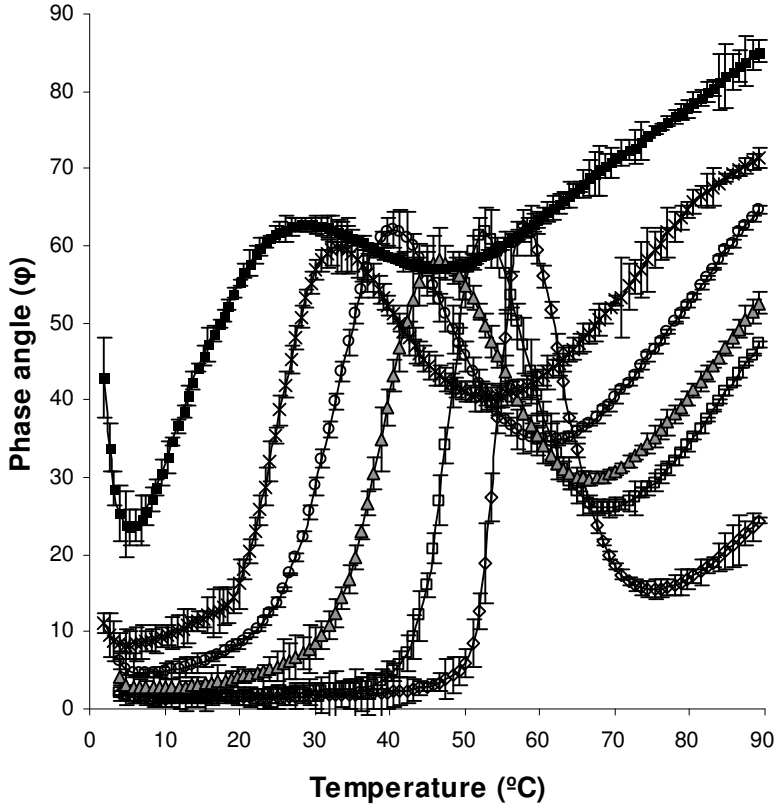


Figure 3.5: Rheological Profile of PLGA / Triblock Blends. The variation in phase angle (by which strain lags the applied stress) with temperature of PLGA + triblock blends was investigated by dynamic mechanical analysis using a Physica MCR 301 parallel plate rheometer. The glass transition temperature was set as the temperature corresponding to the peak phase angle value attained prior to descent. The glass transition temperature was significantly reduced with increasing triblock composition. PLGA (◊ - open diamonds), PLGA + 10% Triblock (□ - open squares), PLGA +20% Triblock (▲ grey triangle), PLGA + 30% Triblock (* asterisk), PLGA + 50% triblock (0 open circle), and PLGA + 75% Triblock (■ closed square). Values plotted on the charts are representative of four different independent experiments (i.e. N = 4).

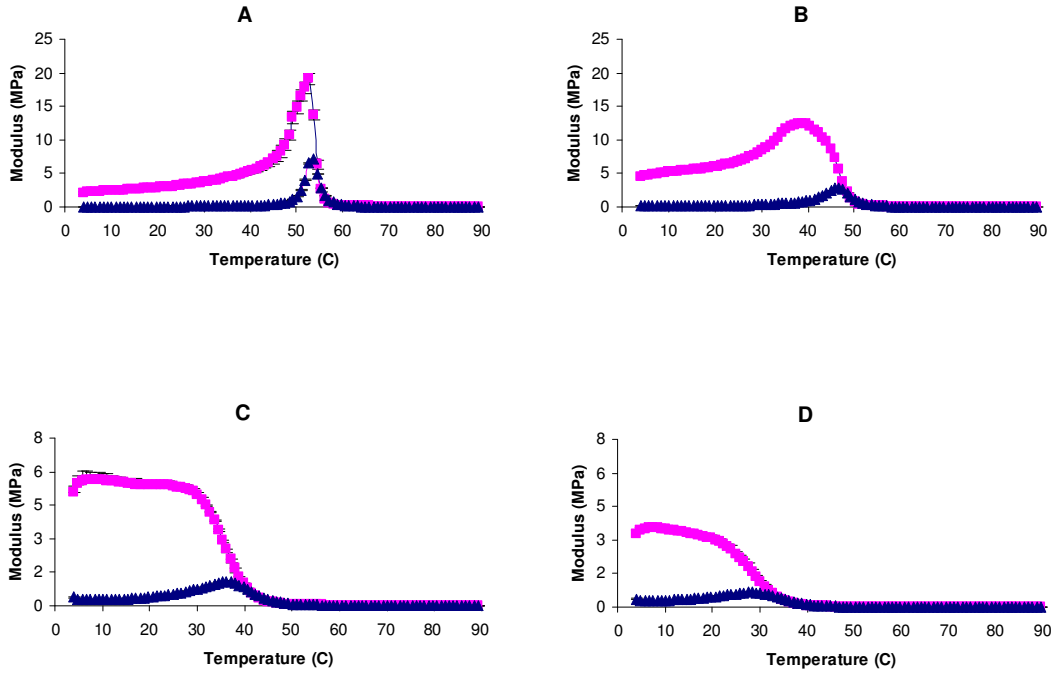


Figure 3.6: Viscoelastic profile of PLGA / Triblock blends. The variation in loss (▲ blue triangle) and storage moduli (■ pink square) with temperature of PLGA + triblock blends was investigated by dynamic mechanical analysis using a Physica MCR 301 parallel plate rheometer. The onset of glass transition was determined to be the temperature corresponding to the loss and storage moduli having equivalent values. The temperature of onset of glass transition was significantly reduced with increasing triblock composition. (A) PLGA (B) PLGA + 10% Triblock Blend (C) PLGA + 20% Triblock Blend (D) PLGA + 30% Triblock Blend. Values plotted on the charts are representative of four different independent experiments (i.e. N = 4).

triblock reduced with an increase in temperature. The loss modulus (a measure of the mobile parts of the polymer chains) increased for all blends with increase in temperature.

### 3.4.4 Microsphere fabrication and characterisation

Scanning electron microscopy (SEM) images of microspheres fabricated from PLGA and PLGA + 30% triblock blends showed microspheres were spherical in nature with no pores on the surface of the microspheres (Fig 3.7). No difference was observed in the morphology of the microspheres made from PLGA or PLGA / triblock polymer blends. Particle size analysis using the Laser Accusizer showed a microspheres particles size distribution within the range of 50 - 450µm (Fig 3.8). The average particle size of the PLGA microspheres was observed to be 225 ± 19µm.

$^{1}$H NMR characterisation of the microspheres made from PLGA, and various blends of PLGA / triblock; containing 10%, 20%, 30% and 50% triblock was undertaken to quantify the amount of triblock retained within the microspheres after the microsphere fabrication process. Fig 3.9 and Fig 3.10 shows that the triblock polymer was retained within microspheres after the microsphere fabrication process. The % triblock retention of microspheres made from the aforementioned PLGA /triblock blends was calculated using the equation detailed below.

$$\% \text{ Triblock Retained within Microspheres} = \frac{\text{PEG: LA of Microspheres}}{\text{PEG: LA of Polymer Blend}} \times \frac{100}{1}$$

The PEG: LA ratio of microspheres was confirmed as detailed above in the equation in section 3.4.2.

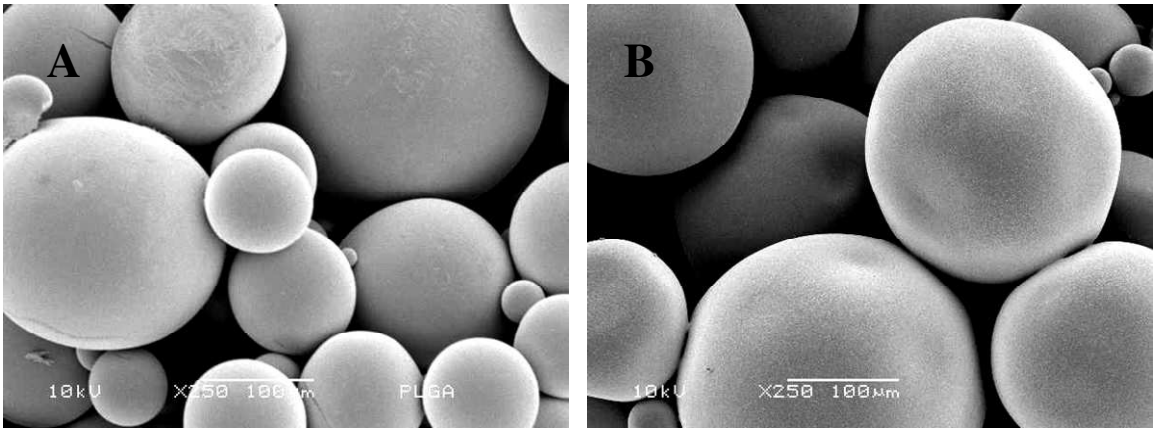


Figure 3.7: SEM images of microspheres made from (A) PLGA (B) PLGA + 30% Triblock blend. SEM images were obtained using a JSM 6060 microscope, 10kV ionising radiation and at a 250X magnification.

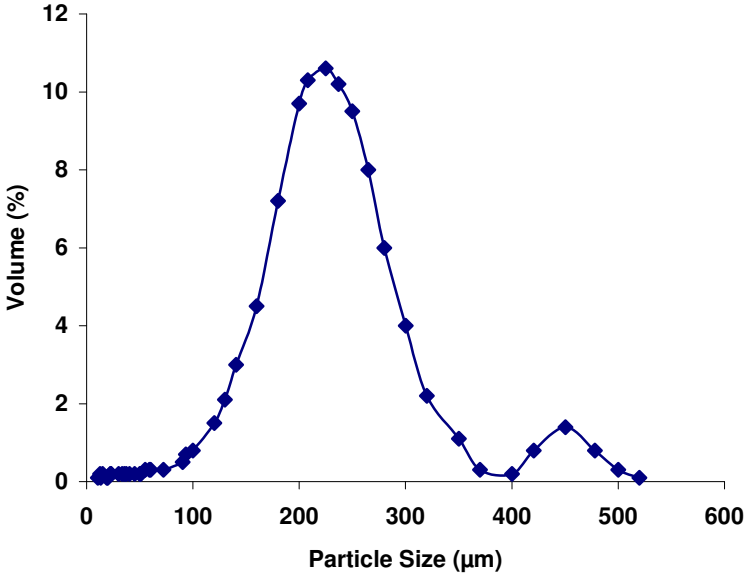


Figure 3.8: Representative particle size distribution of microspheres as measured by laser light scattering particle size analyser.

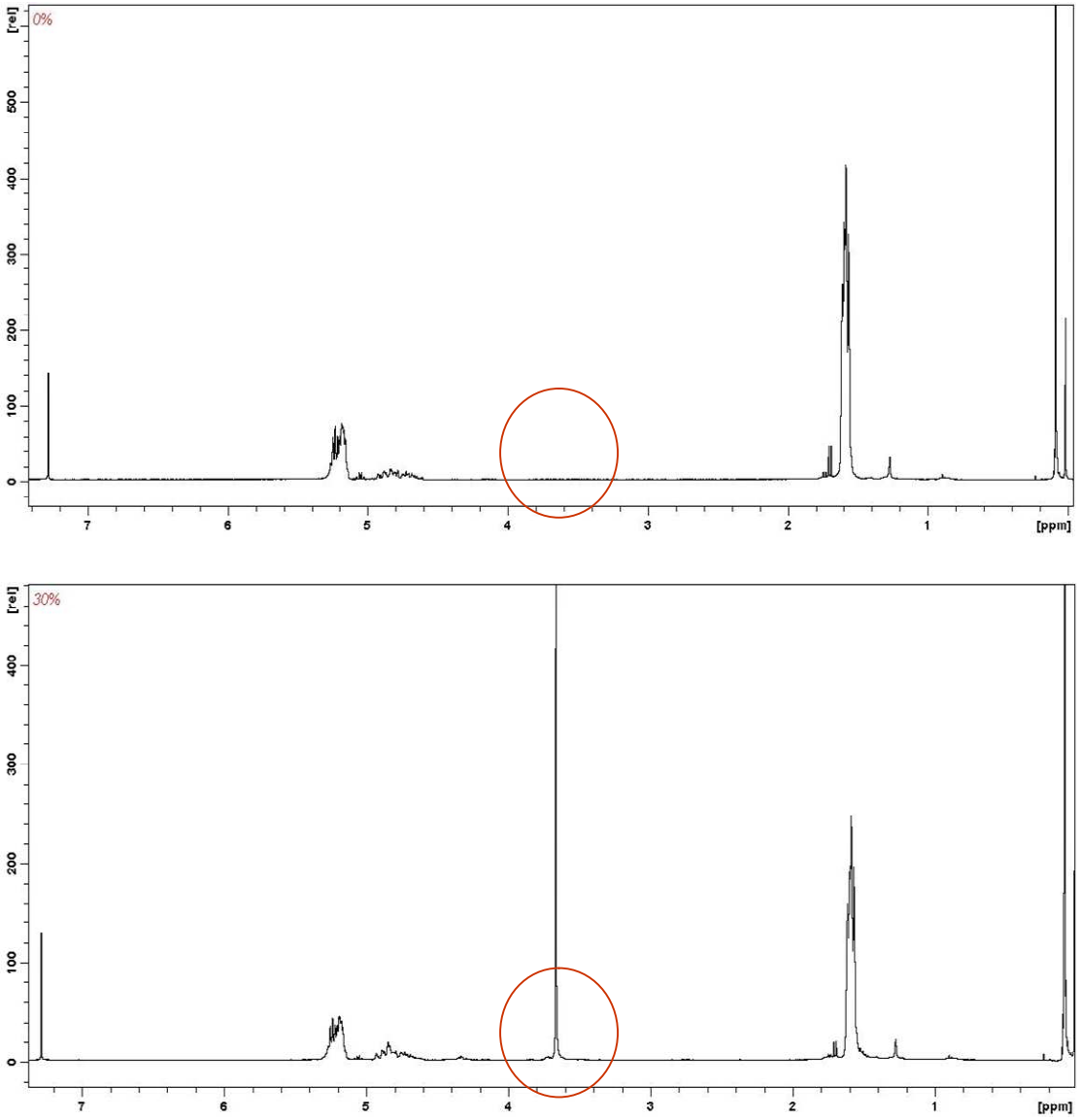


Figure 3.9: NMR Spectra for microspheres made from (A) PLGA blend; (B) PLGA + 30% Triblock blend. $^{1}H$ NMR analysis was used to determine if the triblock copolymer was entrapped within the microspheres. The presence of the $CH_2CH_2$ PEG peak at 3.65ppm in (B) as highlighted by the red circle, was used as an indication of retention of the triblock within the microspheres.

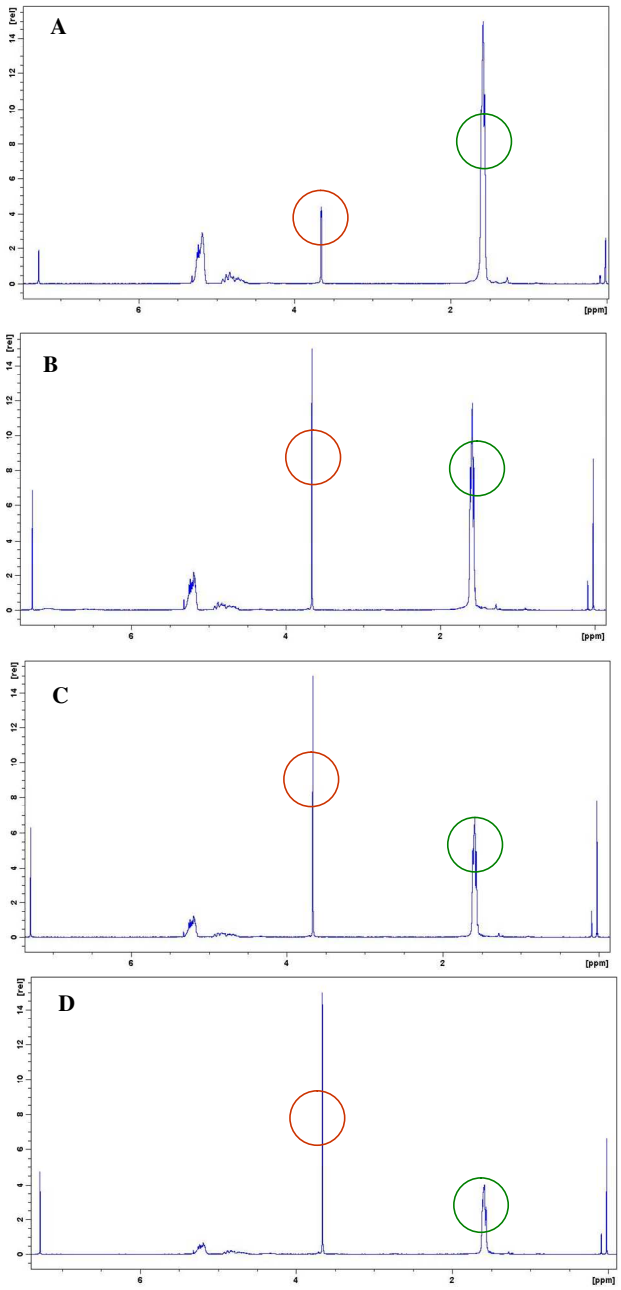


Figure 3.10: NMR Spectra for microspheres made from (A) PLGA + 10% Triblock blend; (B) PLGA + 20% Triblock blend; (C) PLGA + 30% Triblock blend; and (D) PLGA + 50% Triblock blend. $^{1}$H NMR analysis was used to investigate the effect of triblock composition on entrapment efficiency of the triblock within the microspheres. The ratio of the $CH_2CH_2$ PEG peak at 3.65ppm (highlighted by the red circles) and the $CH_3$ lactide peak at 1.60ppm (highlighted by the green circles), was used as an indication of the proportion of triblock relative to PLGA retained within the microspheres.

Fig 3.11 shows that the calculated values for the % triblock retained within the microspheres for microspheres made from PLGA / triblock blends containing 10%, 20%, 30% and 50% triblock was greater than 80% for all the blend mixtures. No significant difference in the % triblock retention was observed with blends containing various proportions of triblock within the blend.

### 3.4.5 Dynamic mechanical analysis of PLGA / triblock microspheres.

The effect of increasing triblock composition on the viscoelastic properties of microspheres was also investigated. Fig 3.12 illustrates the viscoelastic profile of the various blend formulations increasing from 0% (PLGA), to 50% triblock compositions. It was not possible to successfully fabricate microspheres from blends with 75% triblock composition. The temperature oscillation sweep curves showed that an increase in triblock concentration of the microspheres results in a similar earlier onset of glass to rubbery phase transition as observed by the characteristic shift to the left of the curve (Fig 3.5). Thus by increasing the triblock concentration (Table 3.2) a corresponding decrease in the glass transition temperature was also observed. Thereby suggesting that the microspheres showed similar thermoresponsive properties to the blends they were made from.

### 3.4.6 Mechanical testing of Scaffolds.

Compressive tests were performed to evaluate the effect of triblock on the mechanical properties of the scaffolds. Some typical stress-strain curves of the scaffolds fabricated from PLGA, PLGA + 10% triblock, PLGA + 30% triblock blends are shown in Fig. 3.13. Scaffolds fabricated from PLGA microspheres showed linear elastic deformation at small strains but fractured as the stress exceeded the

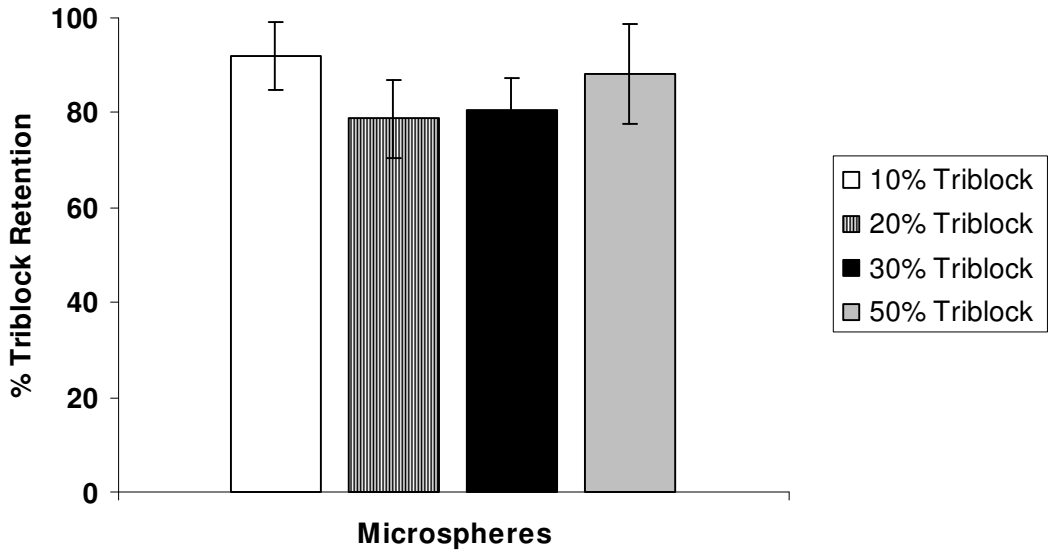


Figure 3.11: Retention of triblock within microspheres. $^{1}$H NMR analysis was used to investigate the effect of triblock composition on entrapment efficiency of the triblock within the microspheres. The % triblock retention was obtained by comparing the mole ratio of PEG: LA (PEG: Lactide) of triblock blend against that of the microspheres from the triblock blend. The PEG: LA mole ratio was obtained by comparing the ratio of normalised (to the number of H (4 and 3 respectively) within the monomer) integrated values for the signals specific to $CH_2CH_2$ (PEG) to that of $CH_3$ (lactide) monomers located at 3.65ppm and 1.60ppm respectively. No significant difference in % triblock retention was observed for varying triblock composition. Standard deviations of N = 4 experiments

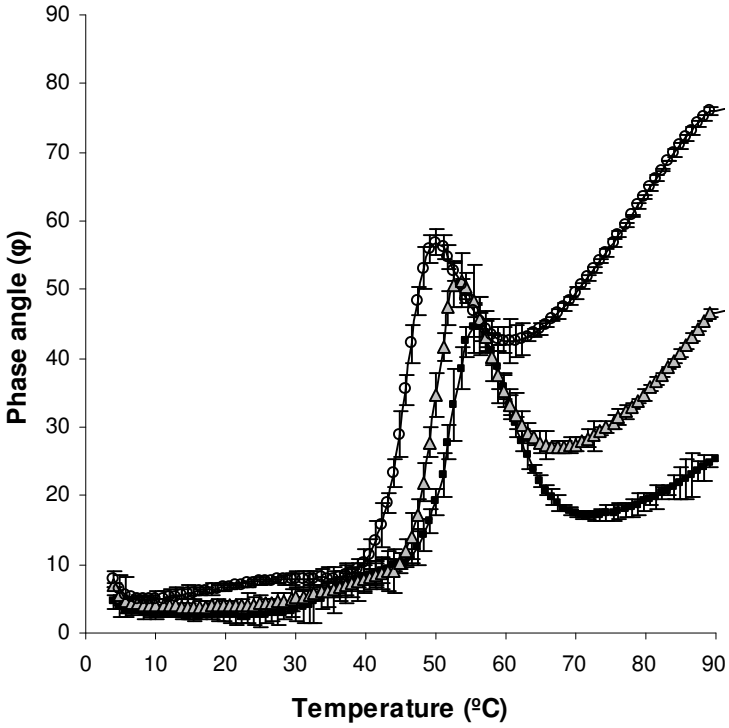


Figure 3.12: Rheological Profile of microspheres made from PLGA / Triblock Blends. The variation in phase angle (by which strain lags the applied stress) with temperature of microspheres made from PLGA + triblock blends was investigated by dynamic mechanical analysis using a Physica MCR 301 parallel plate rheometer. The glass transition temperature was set as the temperature corresponding to the peak phase angle value attained prior to descent. The glass transition temperature was significantly reduced with increasing triblock composition. PLGA (■ closed square), PLGA + 10% Triblock (▲ grey triangle), and PLGA + 30% Triblock (0 open circle). Values plotted on the charts are representative of four different independent experiments (i.e. N = 4).

| Material | Glass transition temperature ºC |
|---|---|
| PLGA | 59.7 ± 1.3 |
| 10% Triblock Blend | 54.1 ± 1.7 |
| 30% Triblock Blend | 36.1 ± 2.3 |
| 50% Triblock Blend | 32.0 ± 1.5 |
| PLGA Microspheres | 59.7 ± 1.3 |
| 10% Triblock Microspheres | 52.5 ± 1.9 |
| 30% Triblock Microspheres | 45.7 ± 1.4 |
| 50% Triblock Microspheres | 45.0 ± 1.5 |

Table 3.2: Table showing the effect of triblock composition within PLGA / triblock blends and corresponding microspheres on the glass transition temperatures (which is taken as the temperature corresponding to the maximum phase angle from the temperature oscillation sweep). N = 4.

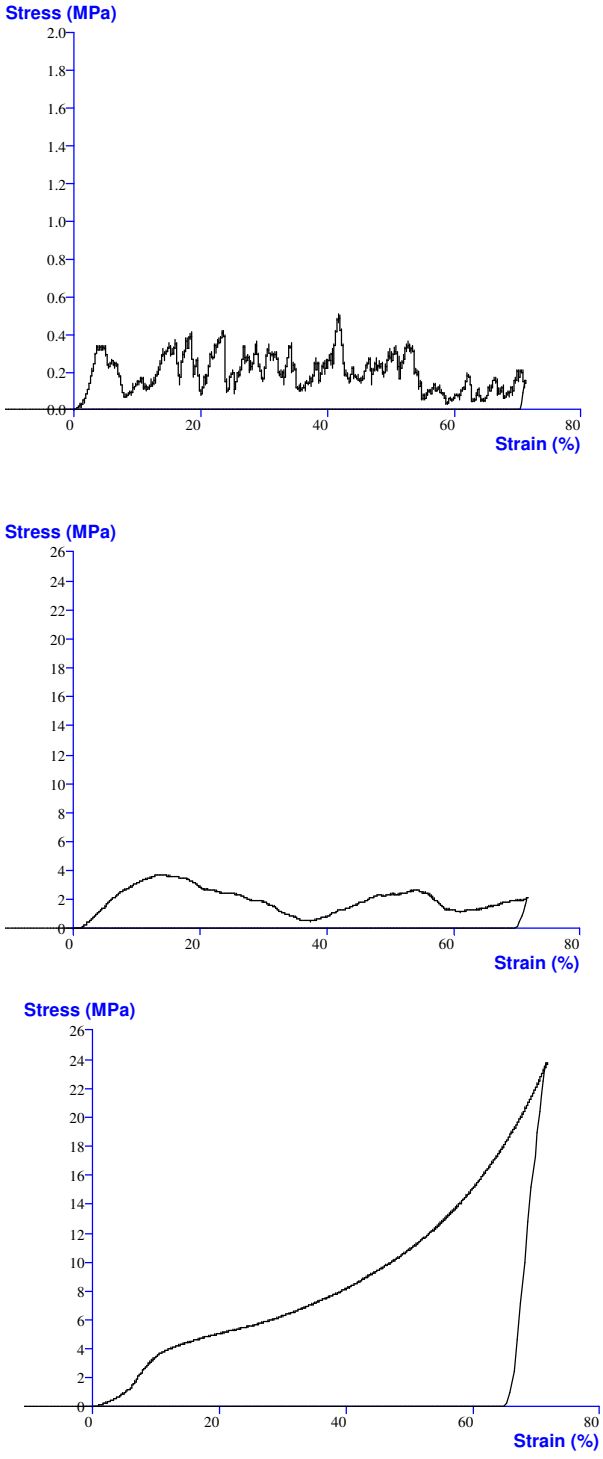


Figure 3.13: Typical stress strain curves for scaffolds made from PLGA / triblock microspheres containing A) 0%; B) 10% and C) 30% w/w triblock. Stress-strain curves were obtained by uniaxial compression testing of 5 x 10mm scaffolds up till a maximum of 70% strain.

compressive strength of the material indicating that the PLGA material showed brittle properties as the material was stressed beyond its compressive strength. However the addition of triblock resulted in a higher compressive strength value (Fig 3.14A) (3.87 ± 0.13MPa and 3.87 ± 0.47MPa vs. 0.23 ± 0.09MPa for PLGA / triblock containing 30%, 10% and 0% triblock (PLGA) respectively) and increased strain rate attained before the maximum compression stress value was attained (10.40 ± 1.00% and 13.79 ± 1.36% vs. 3.23 ± 0.48% respectively). No difference was observed in the compressive strength of scaffolds sintered at 60ºC from PLGA / triblock blends containing 10 and 30% triblock (Fig 3.15A), although the strain corresponding to the value for the maximum compressive stress differed (13.79 ± 1.36% vs. 10.40 ± 1.00% respectively).

The Young's Modulus of the scaffolds was calculated to give an indication of the flexibility and stiffness of the scaffolds. It was calculated as the ratio of the stress and strain over the linear range prior to the yield point of the material. Increasing proportion of triblock within the PLGA / triblock blends resulted in an increase in the Young's Modulus for scaffolds sintered at 60ºC made from microspheres of PLGA / triblock blends (Fig 3.14B) (53.6 ± 3.7MPa, and 39.2 ± 4.8MPa vs. 10 ± 3.3MPa for blends containing 30%, 10% and 0% triblock respectively).

The effect of temperature on the mechanical properties of the scaffold was also investigated by comparing the compressive strength and the Young's modulus of scaffolds made from blends containing 10% and 30% triblock, sintered at 45ºC and 60ºC respectively Fig 3.15B). Sintering microspheres at 60ºC resulted in scaffolds with significantly higher compressive strength (3.87 ± 0.47MPa vs. 0.23 ± 0.04MPa;

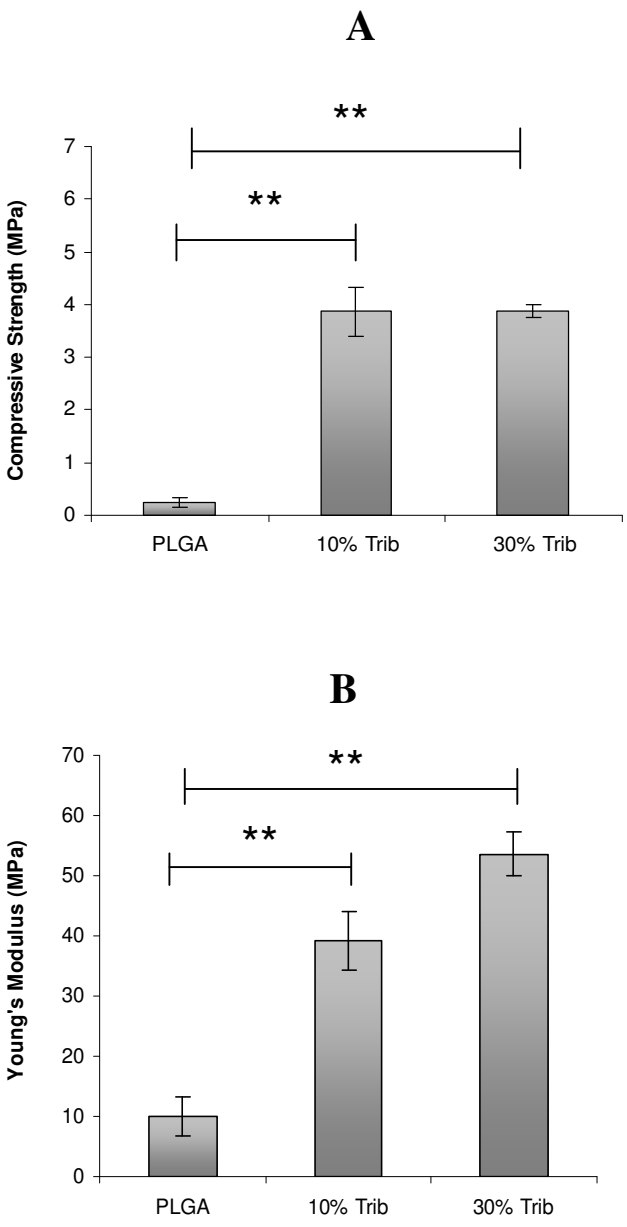


Figure 3.14: Compressive mechanical properties of scaffolds fabricated by sintering PLGA / PLGA-PEG-PLGA microspheres at 60ºC for three hours. A) Maximum compressive strength (corresponding to yield point); B) Young's modulus of scaffolds. Results expressed as mean ± STDEV, n = 4 (* indicates $p<0.05$, ** indicates $p<0.01$)

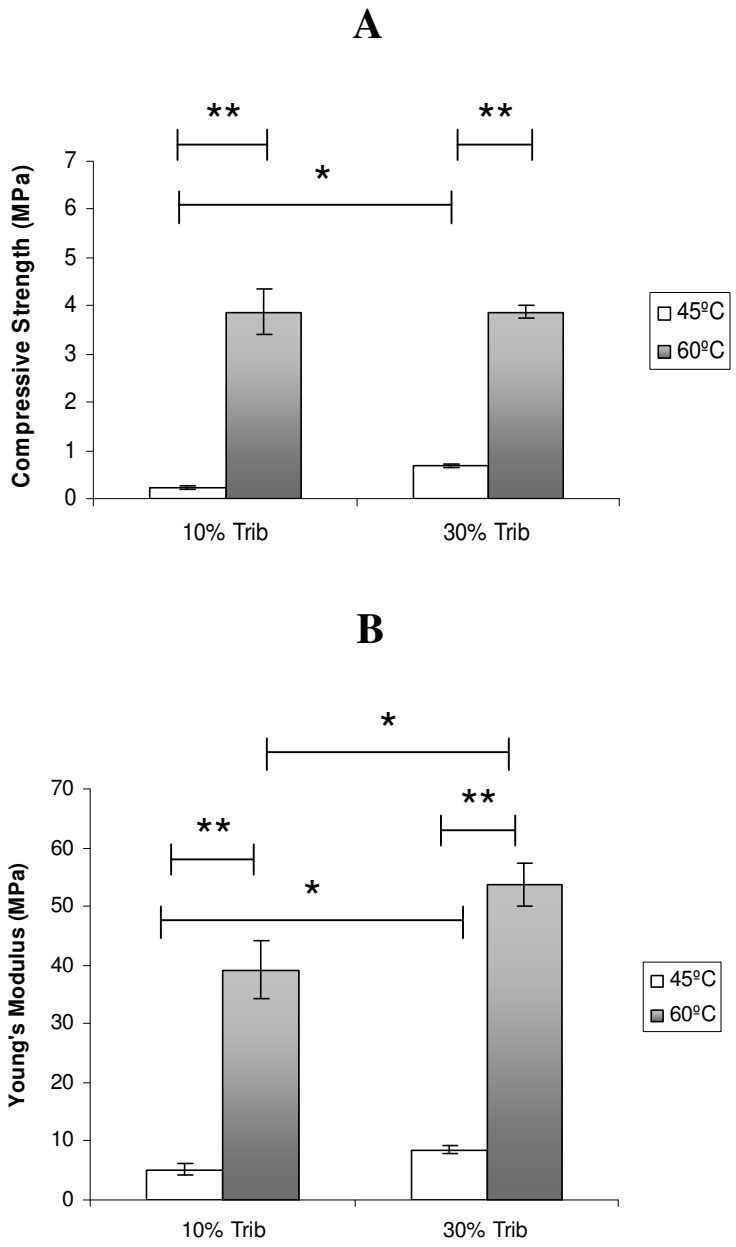


Figure 3.15: The effect of sintering temperature on the compressive mechanical properties of scaffolds. Scaffolds were fabricated by sintering PLGA / PLGA-PEG-PLGA microspheres at 45ºC or 60ºC for three hours. A) Maximum compressive strength (corresponding to yield point); B) Young's modulus of scaffolds. Results expressed as mean ± STDEV, n = 4 (* indicates $p<0.05$, ** indicates $p<0.01$)

and 3.87 ± 0.13MPa vs. 0.68 ± 0.04MPa) and Young's Modulus values (39.2 ± 4.8MPa vs. 5.1 ± 1.0MPa; and 53.6 ± 3.7MPa vs. 8.5 ± 0.7MPa) when compared to microspheres sintered at 45ºC for microspheres made from both blends of triblock.

## 3.5 Discussion.

The aim of this chapter was to develop a composite scaffold from PLGA and triblock based microspheres. The resultant composite scaffold will have the mechanical properties that are suitable for bone tissue engineering. This was achieved through the optimisation of properties of PLGA microspheres by blending with the triblock copolymer resulting in microspheres with reduced glass transition temperature. The reduced glass transition temperature of the microspheres will enable us to produce scaffolds with improved mechanical strength at reduced temperatures. This will result in the production of scaffolds with sufficient mechanical properties to fulfil the requirements for bone tissue engineering matrices, and for in situ injectable scaffold production. .

PLGA-PEG-PLGA triblock copolymer belongs to a class of triblock copolymers that are composed of A-blocks and B-blocks arranged as ABA or BAB type, where A is polyethylene glycol (PEG) and B is poly(dl-lactide-co-glycolide, PLGA). They are soluble in water at or below room temperature (Jeong et al., 1999). They've also been reported to possess reversible gelation properties and thermoresponsive properties (Cha et al., 1997; Jeong et al., 1997; Rathi et al., 2000; Rathi and Zentner, 1999; Qiao et al., 2005; Chen et al., 2005).

In addition, these formulations tend to spread into the tissue space to minimize tissue irritation. Thermosensitive polymers have met with increasing interest during the past two decades, particularly in the field of injectable delivery and controlled drug release (Eeckman et al., 2004). With these polymers, the aqueous solutions when administered gels at body temperature. These injectable formulations can be used as in situ scaffold fabrication, avoiding the need for use of prefabricated scaffolds (K|retlow et al., 2007).

Aqueous solutions of many commercially available block copolymers, such as Pluronics or poloxamers have been shown to undergo a temperature induced reversible sol gel transition with changes in temperature. Poloxamer hydrogels perhaps represent the most extensively studied systems since they are commercially available in a wide range of molecular weights and block ratios (Ruel-Gariepy and Leroux, 2004). However, despite the extensive use of these polymers within clinical settings as solubilising and thickening agents, their lack of biodegradability has limited their use as pharmaceutical and biomedical implants.

In this work, PLGA-PEG-PLGA triblock was blended with PLGA using our novel in house hot blending technique. NMR analysis was used to confirm the uniform distribution of the triblock within the PLGA blends. The presence of the $CH_2CH_2$ peak which is a fragment of the monomer – ethylene glycol ($CH_2CH_2$ OH) was used as an indication of the presence of the triblock. The intensity of the peak was used as an indication of the concentration of the triblock within the blend. The incremental increase in the $CH_2CH_2$ signal peak integrated value and PEG: LA mole ratio with increase in triblock composition, and decrease in LA: GA mole ratio suggested the

successful blending of the triblock within the PLGA, with good dispersion of the co-polymer. However the molecular mechanism behind the dispersion of the co-polymer within PLGA is not known. In experiments carried out by Dobry and Boyer-Kawenoki, it was observed that when two polymers are dissolved in an organic solvent, they spontaneously separate into two solution phases (Duclaux and Boyer-Kawenoki 1947). This spontaneous separation of the two polymers into two solution phases has been exploited in the developing of double walled 'polymer alloy' microspheres consisting of two different polymer layers. In experiments carried out by Cleek et al (1997). The spontaneous separation of the polymers was attributed to phase separation that occurs due to the polymers different solubility within the organic solvent.

By using the hot-blending method, a dry mixture of the two polymers (PLGA and triblock) ensuring a good dispersion of the triblock within the PLGA was created. In addition, the hot-blending will ensure that the polymer chains from both polymers are entangled together and possibly held together by van der Waals forces and molecular entanglement of these chains. This could possibly explain the high retention of the hydrophilic polymer triblock (> 80%) despite its exposure to the aqueous PVA solution during the microsphere fabrication process indicating that no phase separation occurred whilst the blend is dissolved in the dichloromethane.

Secondly, blending of PLGA with the triblock triblock copolymer resulted in blends with increased viscoelastic response. The increased viscoelastic response was observed as a shift to the left of the phase angle – temperature curve and storage and loss moduli – temperature curve with increasing triblock composition (Fig 3.5 and

3.6). The phase angle represents the phase difference between the stress and strain in an oscillatory test. It's a measure of the presence and extent of elastic behavior in a material. In general, the closer the phase angle is to zero, the greater the predominance of elastic properties and more solid like the material is. While the closer the phase angle is to 90º the closer the material displays Newtonian fluid like properties. In a temperature oscillation sweep, an increase in temperature results in a transition of the solid material from a glassy state to a rubbery state before finally forming a liquid due to the breaking of bonds that hold the chains together (Mezger, 2006). Fig 3.5 shows that an increase in triblock composition resulted in an earlier onset of the transition from a glassy solid like state to a more rubbery state as observed by the characteristic shift to the left of the curve with increasing triblock composition. Thus by increasing the triblock concentration (Table 3.2) a corresponding decrease in the glass transition temperature (the maximum phase angle peak value attained prior to descent) of the phase angle at which the at which the material changes from a glassy state to a more rubbery like state) is observed.

Whilst the loss moduli of PLGA / triblock blends followed the same trend of gradual increase to a peak value (around the temperature equivalent to the glass transition temperature) with increasing temperature and then reduction, the storage moduli differs in characteristics. The storage moduli of blends from PLGA and PLGA + 10% triblock followed the same trend as the loss moduli of increasing to a peak value before reducing, whilst blends containing 20% and 30% triblock did not show an initial increase but reduced with increasing temperature (Fig 3.6). The storage and loss moduli measures the stored energy and energy dissipated as heat respectively. They represent the modulus of the solid non-moving (in-phase chain) and the flowing

– mobile parts of the polymer chains (out of phase) (Suciati, 2006). The greater the storage modulus the greater the elastic properties of the material, and the more solid the material is. The loss modulus is a measure of the deformation energy used up by the polymer blend during the shear process. This energy is spent during the change that occurs due to increase in vibration and motion of the polymer chains as the thermal energy of the polymer chains increases with increase in temperature. The motion between the polymer chains of the superstructure causes frictional forces which is lost in the form of heat to the surrounding environment. Thus an increase in loss modulus gives an indication in increase in motion of the polymer chains. Thus the initial increase in storage modulus of the PLGA and PLGA + 10% triblock blends could attributed to the thermal energy absorbed by the blend as it works to disentangle the polymer chains of the polymer blend. This increase is not observed in blends containing 20% and 30% triblock possibly due to the increased amount of the gel like triblock reducing the requirement for disentanglement (Mezger, 2006).

By blending of the thermosensitive triblock with PLGA in different concentrations, we were able to produce blends of varying thermosensitive properties with reducing glass transition temperatures and increased viscoelastic response of the blends with increasing composition of the triblock. The increased viscoelastic response of the blends as indicated by the earlier onset of the glass transition phase, brings the possibility of utilising the material as an injectable micro particulate based scaffold. Hence at any given temperature, based on the triblock composition materials with varying degrees of thermoresponsiveness are obtainable. Thus at a set temperature scaffolds of different mechanical strength can be easily fabricated depending on the triblock composition.

The dynamic mechanical analysis also showed that by increasing the triblock composition, an increase in the thermoresponsiveness of the microspheres was observed. It was hypothesized that the thermoresponsiveness of the material will determine the mechanical strength of the resulting scaffold at a set temperature. As such, at a set temperature varying the triblock composition of the microspheres will result in scaffolds of varying mechanical strength. Based on this hypothesis, scaffolds were fabricated from PLGA, 10% and 30% triblock at 45ºC and 60 ºC and compressive mechanical tests were performed.

The process of microsphere fusion involves the inter-diffusion of polymer chains across the interface of the spheres at temperatures above the glass transition temperature of the polymer (Wool and O'Conner, 1981). As temperature increases during the sintering process, the increase in thermal energy results in an increase in vibrations of the polymer chains leading to the chains moving in a coordinated manner (Sperling, 1992; Painer and Coleman, 1997). The coordinated movements of the polymer chains is influenced amongst other parameters by the molecular weight of the polymer (Cho and Kardos, 1995), with the degree of polymer entanglement playing an important role in limiting polymer movement (de Gennes, 1971; Suciati, 2006). Low molecular weight polymer above its glass transition temperature has been shown to move in a snake like fashion termed reptation within a topological tube due to the presence of the confining surrounding polymers. The polymer chains within the microspheres at the surface diffuse across the interface and entangle with one another. When the scaffold matrix is cooled, the drop in temperature below the glass transition temperature results in the polymer chains no longer being mobile and as such the polymer structures are frozen in the state it was prior to cooling. Leading to the

entanglements formed at the interface of neighbouring microspheres solidifying to form bridges between microspheres.

As reported in section 3.4.6, scaffolds produced from PLGA microspheres differed from scaffolds produced from microspheres containing 10% and 30% triblock. The presence of triblock resulted in increased compression strength, stiffness and flexibility of the scaffolds. Fig 3.16 shows a schematic representation of compression testing of PLGA and PLGA + 30% triblock microsphere based scaffolds. The three segments observed in stress-strain curves obtained from uniaxial compression testing of scaffolds made from microspheres containing 30% triblock was similar to those obtained for open cell foam three dimensional cellular solids (Gibson, 2005). The segments of the stress-strain curve for a three dimensional cellular solid under compression tests are a linear elastic segment corresponding to cell edge bending; a stress plateau corresponding to progressive cell collapse by elastic buckling, plastic yielding or brittle crushing depending on the nature of the solid from which the material is made; and densification, corresponding to collapse of the cells throughout the material and subsequent loading of the cell edges and faces against one another (Gibson, 2005). On the other hand scaffolds made from PLGA microspheres only showed one segment – a short linear elastic segment followed by a fracture of the scaffold through brittle crushing. While scaffolds from PLGA + 30% triblock microspheres showed two segments (a linear elastic segment and a stress plateau segment), no densification was observed. These results shows that scaffolds made from PLGA + 30% triblock microspheres satisfies the mechanical properties required for tissue engineering applications such as bone tissue engineering, which requires scaffold of a compressive strength of 2 – 12MPa and Young's modulus of 50 –

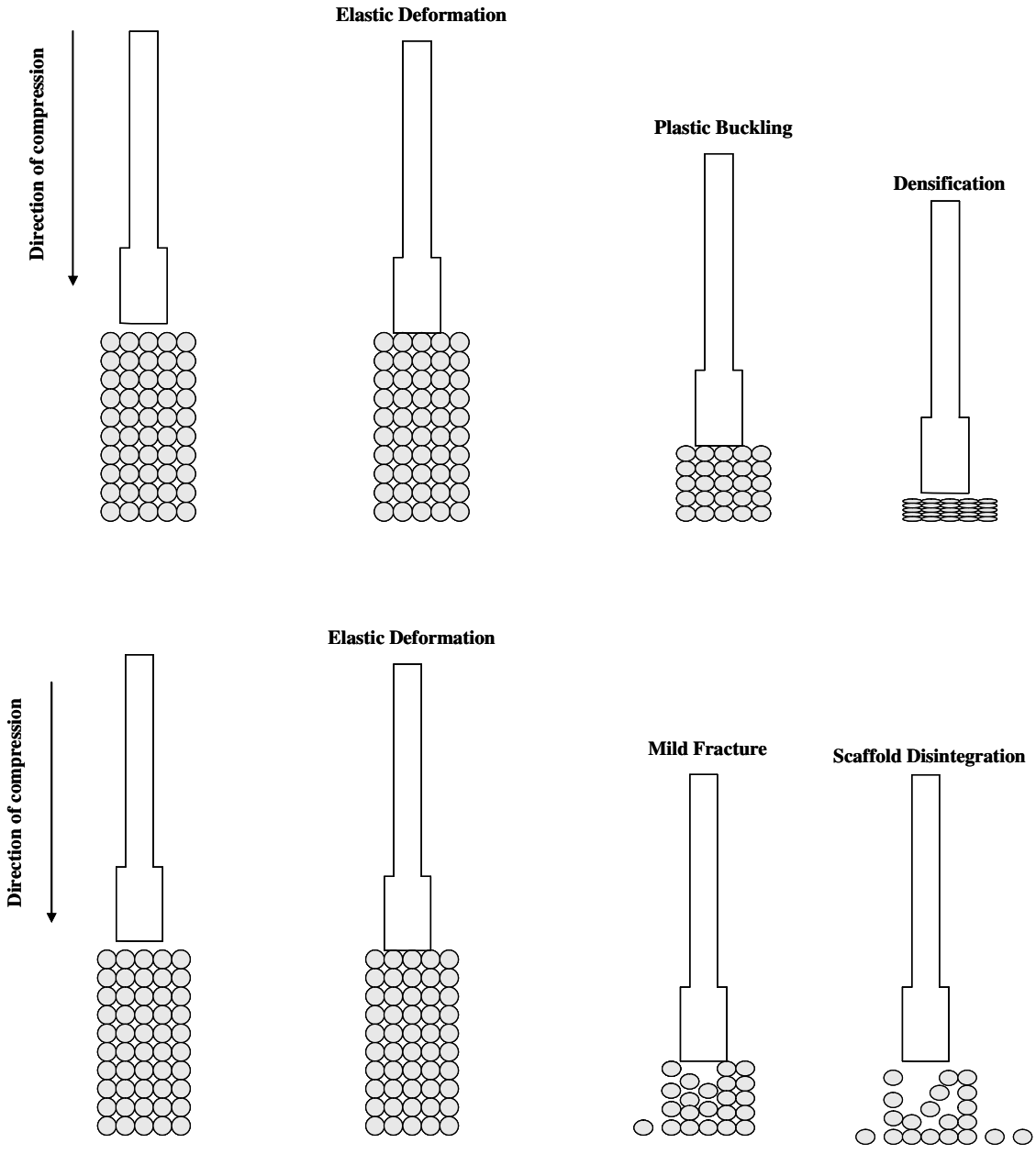


Figure 3.16: Schematic representation of series of events that occurs on uniaxial compression of scaffolds made from A) PLGA + 30% PLGA-PEG-PLGA and B) PLGA microspheres. Scaffolds were fabricated by sintering microspheres at 60ºC for three hours.

500MPa (Hench and Jones, 2005; Suciati et al., 2006). The open cell foam like structure enables the migration of cells for good tissue in-growth throughout the scaffolds (Kretlow et al., 2007). Low density trabecular bone was shown to have architecture resembling an open cell foam (Gibson, 2005). In studies carried out by van Rietbergen et al (1995); and Nazarian and Muller (2004), micro-computed tomography showed that bending is the dominant mode of linear elastic deformation in trabecular bone. In time lapsed micro-computed tomography imaging of trabecular bone loaded in uniaxial compression carried out, elastic buckling was indicated to be the primary wa of compression failure rather than brittle crushing (Nazarian and Muller (2004)).

Based on this approach of optimising the viscoelastic properties of the microspheres, e microspheres that could sinter to form scaffolds at physiological temperatures (37ºC) could be produced. Scaffolds formed from these microspheres can be loaded with drugs or chemical signals that can be used in directing cell growth, and the high porosity and interconnectivity of the scaffolds will provide it with added advantages over hydrogels for use as injectable materials.

Polymer blends has been used extensively in tissue engineering applications to provide composite scaffolds with improved mechanical strength, bioactivity, and release kinetics. Lee et al. (2008) showed that the addition of hydroxyapatite increased the mechanical (compression strength and elastic modulus), drug release and retarded the degradation of PLGA scaffolds. Kothapalli et al. (2005) prepared scaffolds comprising of PLA and nano-hydroxyapatite using a solvent-casting/ salt leaching technique, and found that the compression modulus and yield strength of the

scaffolds increased linearly as the nano-HA content was increased from 0 to 50% in the scaffolds. 'Injectabone' which is a novel biodegradable, microparticulate scaffold system which can be injected into bone defect sites is a system that consists of two types of microparticles – a PLGA/PEG composite that acts as an adhesive for second PLGA microparticles. The dynamics of the scaffold fabrication is based on the PEG acting as a plasticizer on the PLGA microspheres resulting in reduction in the glass transition temperature of the materials, as such the temperature of scaffold formation is tuned to that of physiological temperatures (Hamilton et al., 2006; Howard et al., 2008). The developed microspheres operate on a similar principle, but instead of having a two component system utilising PEG as a plasticizer, one component system that exploits the sol gel properties of triblock to reduce the glass transition temperature of the microspheres has been successfully developed.

.

## 3.6 Conclusion

From the studies presented in this chapters its been shown that blends of PLGA and triblock can be manufactured to form scaffolds with improved mechanical strengths sufficient to be used in tissue engineering applications such as bone tissue engineering.

PLGA / triblock blends of varying composition of triblock ranging from 0 to 75% were manufactured using our novel in house hot-blending technique. The blending of the 'gel like' triblock with PLGA resulted in blends with varying degrees of thermoresponsiveness and viscoelasticity. Increasing the composition of the triblock resulted in corresponding reduction in the glass transition temperature of the resulting blends.

The hydrophilic triblock was retained within the microspheres after microsphere fabrication from the PLGA / triblock blends as confirmed using $^{1}H$ NMR. Dynamic analysis tests on microspheres showed that microspheres with increasing triblock composition also showed a similar trend of increased thermoresponsiveness and reduced glass transition temperature, although to a lesser extent than was observed for the blends. The reduced decrease in reduction of glass transition temperature with increasing composition of triblock observed in the microspheres compared with that of the corresponding blend was attributed to the effect of the poly (vinyl alcohol).

Sintering the microspheres from the PLGA / triblock blends at a set temperature (60ºC) resulted in scaffolds with different mechanical properties. Scaffolds made from PLGA microspheres were relatively weak, brittle and in-flexible, whilst scaffolds made from microspheres containing 10% and 30% triblock showed good compressive strength and stiffness (Young's modulus). The scaffolds fabricated from microspheres containing 30% triblock showed the best mechanical properties and possessed mechanical properties similar to trabecular bone indicating its suitability for use as a scaffold for bone tissue engineering.

# CHAPTER 4

# Modulation of microsphere release kinetics

## 4.1. Introduction

The delivery of growth factors and small drug molecules alongside cells and scaffolds can be used to improve tissue regeneration especially in cells with low regenerative potential (Freiberg and Zhu, 2004). Biodegradable polymers such as poly lactic acid (PLA) and poly lactide-co-glycolide (PLGA) are currently used to present growth factors in a sustained release form. The main attractions of using biodegradable polymers include the ability to control the rate of degradation of polymer through modification of chemical structure of polymer and its breakdown to non-toxic degradation products which are easily cleared by the body. For example, PLGA breaks down into lactic and glycolic acid which are eliminated through the citric acid cycle (Chau et al., 2008).

The use of polymeric microspheres for controlled release applications has increased remarkably due to the increased ease at which drug / protein moieties can be loaded within microspheres without a loss in activity (Oldham et al., 2000). Protein and drug release from PLGA microspheres often exhibit a tri-phasic release pattern, consisting of a burst phase of rapid protein release (due to surface located protein), a lag phase of little or no release, followed by a steady continuous rate of release (Hou et al., 2004; Stammen et al., 2001). During the early stages of protein release (including the lag phase), protein release is governed by diffusion-controlled mechanism through a

network of water filled pores and channels In the latter phase, erosion of the polymer matrices is believed to control protein release from the core of microspheres (Hora et al., 1990; Berkland et al., 2007). The duration of the lag phase is normally dependent on several properties which influences the hydrophobicity of the polymer such as the polymer molecular weight and the LA:GA ratio, (with a positive correlation between GA content and hydrophillicity), other parameters such as microsphere size has also been shown to have an effect on the protein drug release kinetics.

Polymeric microspheres can be used for the sustained delivery of growth factors in vivo. However, the use of PLGA microspheres for growth factor delivery in tissue engineering applications is hampered by difficulties in obtaining a desirable controlled release pattern. This is due to the lag phase during which there is little or no protein release after the initial burst release (Biwa et al., 1985; Cohen et al., 1991). The presence of a lag phase can prove problematic for drug delivery and tissue engineering applications in which the growth factor is required to be presented in a defined concentration over an extended period for successful tissue growth. Thus an ideal scaffold for tissue engineering and drug delivery applications will have an initial burst release (which will provide a loading dose for a quick onset of action) followed by a constant release at a physiologically relevant dose over an extended period.

Several approaches are currently utilised in terms of obtaining controlled release over a sustained period. These approaches generally involves the use of low molecular weight PLGA polymers or PLGA polymers with high glycolic acid (GA) content both of which have a short degradation time (Makino et al., 2000), small microsphere particle size which results in an increase in surface area for hydrolytic degradation of

the microspheres (Bezemer et al., 2000), and the co-encapsulation of additives such as urea (Nam et al., 2000), PEG400 (Péan et al., 1999), sucrose (Lee et al., 2006), all of which reduce the polymer-protein interactions, and unfold the protein facilitating the diffusion of the protein through the polymer barrier. Other approaches used in improving polymeric release involve the use of thermosensitive and pH responsive polymers (Lee and Yoo, 2008). Despite the limited success of these approaches, prolonged attenuation of the profile of these microspheres to release a defined amount of drug / protein has not yet been achieved.

In this chapter we report a novel approach undertaken to control the release of proteins and drugs from PLGA microspheres through the blending with variable proportions of triblock co-polymer. By utilising composite blends of PLGA + triblock to fabricate protein / drug loaded scaffolds we were able to control the initial burst release, duration of lag phase and the total duration of sustained release of active moieties from the microspheres..

## 4.2 Chapter Aims.

The aim of this chapter was to first investigate potential factors that might affect the entrapment and release of drugs from microspheres, and secondly, to investigate ways of controlling the release kinetics of these compounds from microspheres. This was achieved by undertaking the following investigations:

(i) Investigate the effect of the following parameters on the encapsulation of proteins and drugs in PLGA microspheres:

(a) Effect of loading weight on the entrapment efficiency.

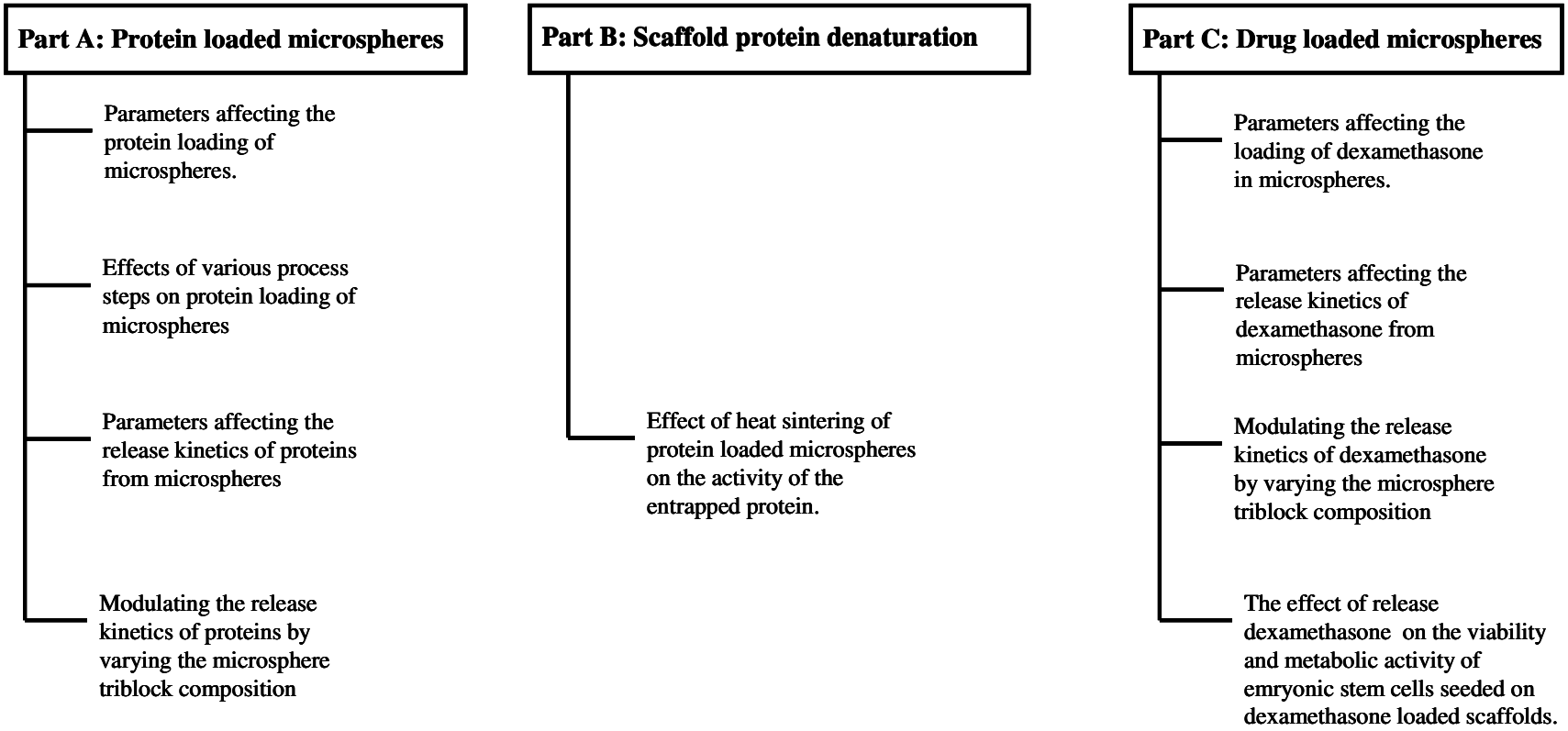


Figure 4.1: Flow chart showing experimental investigations undertaken in this chaper

(b) Prior micronisation of proteins prior to entrapment.

(c) Effect of different polymers on the entrapment efficiency of protein.

(d) The effect of various process steps (i.e. freeze drying etc.) on the entrapment efficiency.

(ii) Investigate the effect of the following parameters on the release of drugs and proteins from PLGA microspheres:

(a) Effect of different polymers on release of proteins.

(b) Effect of loading weight of drugs and proteins from PLGA microspheres.

(iii) Investigate the effect of a triblock co-polymer on the release kinetics of protein from PLGA based microspheres.

## 4.3. Materials and Methods

### 4.3.1. PLGA-PEG-PLGA Synthesis.

The triblock PLGA-PEG-PLGA co-polymer was synthesized via ring-opening polymerisation of D,L-lactide and glycolide onto PEG 1500 using the catalyst stannous octoate as described in Section 2.2.

### 4.3.2. Gel Permeation Chromatography (GPC).

The molecular weights and polydispersity indices of the synthesized triblock were determined by GPC (Section 2.2).

### 4.3.3. Nuclear Magnetic Resonance (NMR).

The molecular weight and the lactide: glycolide ratio of the synthesized PLGA-PEG-PLGA polymer was determined using 1H NMR (Section 2.2)

### 4.3.4. PLGA / triblock blend preparation

In order to investigate the effects of the triblock PLGA-PEG-PLGA on the release kinetics of PLGA 85:15 (M*w* 118kDa), 5%, 10%, 20%, and 30% w/w of triblock in PLGA blends was manufactured following the method described in Section 2.3.

## Part A: Protein encapsulation and release.

### 4.3.5. Fabrication of lysozyme loaded PLGA/ Triblock Microspheres

To investigate the effect of incorporating the triblock on the release kinetics of lysozyme from PLGA microspheres, 5% w/w lysozyme loaded microspheres were made from blends of 0% (PLGA), 5%, 10%, 20% and 30% w/w of triblock in PLGA using the S/O/W method (Section 2.6) with slight modifications.

### 4.3.6. Determining the protein loading of lysozyme within microspheres.

The lysozyme content of the microspheres was determined using the method described in Section 2.6.2. The activity of the entrapped protein was determined using the method described below (Section 4.3.7).

### 4.3.7. Assaying for active lysozyme.

Assaying for active lysozyme involved following the method described by Sohier et al. (2006) with slight modifications. The assay involves following the change in turbidity of a solution of *Micrococcus lysodeitikus* that occurs as lysozyme lyses the β1,4 glycosidic bond within the cell wall of the bacteria. In brief, 150µl of the lysozyme solution was placed in a 96 well plate, to which 100µl of a 2.3mg/ml solution of *Micrococcus lysodeitikus* (Sigma Aldrich, Dorset UK) in distilled water

was added. The change in turbidity over a 1min period was determined, by following the decrease in absorbance values obtained at 450nm using KC4 plate reader (Labtech, Ringmer UK). The change in absorbance values was then correlated to values obtained from the standard concentration curve (0.5 - 20μg/ml) to determine the amount of active protein.

### 4.3.8. The effect of micronisation on protein entrapment efficiency.

To investigate the effect of micronising protein before dispersion in the polymer solution during protein entrapment, myoglobin and lysozyme loaded microspheres were made with and without the micronisation step as outlined in section 2.6. The protein content of the microspheres was then determined using the micro BCA method described in section .2.6.4.1.

### 4.3.9. Comparing the effect of loading weight on protein entrapment efficiency.

To investigate the effect of loading weight on protein entrapment efficiency, l0mg, 30mg and 50 mg of lysozyme, myoglobin, trypsin, ribonuclease and Horse radish peroxidase (HRP) were independently micronised using PEG 6000 following the method described in section 2.6.1. The resulting protein/PEG lyophilisate was then dispersed in a solution of polymer in DCM (containing 30% w/w PEG 400 and 70% w/w PLGA) and fabricated into microspheres using the method described in Section 2.6.1. The total dry weight of the polymer and protein used was 1.0g to give a theoretical loaded weight of 1%, 3% and 5% respectively. The actual loading weight of the microspheres was determined using the method for determining protein content within microspheres described in Section 2.6.2.

### 4.3.10. Investigating the effect of process parameters on protein entrapment within microspheres.

To investigate the effect of process parameters on the entrapment of the protein within the microspheres, the amount of protein remaining after each process stage was determined as a percentage of the expected amount. The effect of the freeze-drying process on the protein activity, and the amount of protein leached out during microsphere fabrication was determined. In brief, 30mg of lysozyme was micronized following the process described in Section 2.6.1. After freeze drying for 48 hours, the amount of active lysozyme was determined by assaying for active lysozyme (section 2.6.4.2) and expressed as a percentage of the amount of lysozyme initially freeze dried (30mg). The amount of lysozyme that leached during microsphere hardening was determined using micro BCA for the amount of lysozyme present in the hardening bath after harvesting of the microspheres. Lysozyme standards prepared by dissolving lysozyme in a solution of DCM in 0.3% PVA in distilled water (1ml of DCM in 25ml of PVA solution) to simulate the hardening bath solution were used for this particular assay.

### 4.3.11. Comparing the effect of different polymers on protein entrapment efficiency.

To investigate the effect of different polymers on protein entrapment efficiency, lysozyme loaded microspheres containing a theoretical loading weight of 30mg of lysozyme per gram of polymer were fabricated using poly (lactic acid) ($P_{DL}LA$), polycaprolactone (PCL), and poly (lactide-*co*-glycolide) (PLGA) with LA:GA ratios of 85:15; 75:25; 65:35 and 50:50 following the method described in Section 2.6.1. The actual loading weight of lysozyme within the microspheres was determined using

the method for determining protein content within microspheres described in Section 2.6.2.

### 4.3.12. Comparing the effect of different polymers on release kinetics of trypsin.

To investigate the effect of different polymers on protein release kinetics, trypsin was used as a model protein. Trypsin loaded microspheres containing a theoretical loading weight of 20mg of trypsin per gram of polymer were fabricated using poly(lactic acid) ($P_{DL}LA$), polycaprolactone (PCL), and poly(lactide-*co*-glycolide) (PLGA) with LA:GA ratios of 85:15; 75:25; 65:35 and 50:50 following the method described in section 2.6.3. The actual loading weight of trypsin within the microspheres was determined using the method for determining protein content within microspheres described in section 2.6.3.

Release kinetics of trypisn from the different polymers was investigated by incubating trypsin loaded microspheres in PBS. Briefly, 100mg of trypsin loaded microspheres were incubated in glass scintillation vials containing 2ml of PBS (pH 7.4) at 37ºC and agitated on a plate shaker at 25rpm. The amount and activity of the released protein over a seven day period were measured using the micro BCA protocol described in Section 2.6.4.1.

### 4.3.13. Stability of Lysozyme in Solution.

The stability of lysosyme in a solution of phosphate buffered saline (PBS) at 5°C, 37°C and 60°C was followed over a period of 30 days, by making a series of solutions at a concentration of 50μg/ml, placing them in glass scintillation vials and incubating at the above temperatures. At predetermined intervals, glass vials were removed and

the lysozyme samples assayed for active protein by following the change in turbidity of *Micrococcus lysodeitickus* as described in Section 2.6.4.2.

### 4.3.14. Investigating the possible adsorption of Lysozyme unto Microspheres.

To investigate the possible adsorption of lysozyme in solution unto microspheres, 50mg of PLGA microspheres (with no protein loaded within) were weighed into glass scintillation vials. 2ml of a 50μg/ml solution of lysozyme was added to the glass vials containing the microspheres and stored in an incubator at 37ºC. At various time intervals over a 30-day period, glass vials were removed and the microparticles filtered from the protein solution. This protein solution was assayed for active protein by following the change in turbidity of *Micrococcus lysodeitickus* as described in section 2.6.4.2.

### 4.3.15. Controlled Release of lysozyme from Microspheres

Controlled release of lysozyme from microspheres was determined using the experimental set up described in Section 2.6.3. On completion of the set up (See Fig 2.4), the Harvard PHD 2000 pump was set to deliver a continuous infusion of phosphate buffer saline (PBS) at pH 7.4 at a rate of 2.0μl/min. The set-up was allowed to run and the eluent was collected at fixed periods to assay for protein content. The protein content in the eluent was determined by assaying for active protein using the method described in section 2.6.4.2.

### 4.3.16. Comparing the effect of loading weight on protein release kinetics

Lysozyme loaded microspheres with protein content of 1%, 2% and 2.5% w/w were fabricated using the method described in section 2.6. The protein release kinetics was then investigated using the method described in section 2.6.3.

### 4.3.17. Effect of triblock on release kinetics of PLGA microspheres.

To investigate the effect of the triblock co-polymer on the release kinetics of lysozyme microspheres, 60 day controlled release experiments of lysozyme from microspheres into PBS were performed. The controlled release experiment was performed following the method described in section 2.6.3 using 20mg of lysozyme loaded microspheres of PLGA/triblock blends containing 0%, 5%, 10%, 20% and 30% w/w of triblock. The activity of released lysozyme was quantified using the micro BCA method as described above (Section 2.6.4.1). All samples were prepared and analyzed in triplicates.

### 4.3.18. Structural integrity of lysozyme

The primary structure of lysozyme released over a 28 day period during controlled release experiments was investigated using SDS-PAGE gel electrophoresis. All gels were run under reducing conditions. The eluent from controlled release experiments of the lysozyme loaded microspheres made from PLGA and PLGA/including 30% w/w triblock blend) were separately pooled over a 28 day period for each polymer. MicroBCA was used to quantify the total amount of lysozyme present in the controlled release pool from each polymer. The concentration of the resulting lysozyme solutions was equilibrated and its structural integrity determined by gel electrophoresis. Gel electrophoresis was performed following the gel manufacturer's protocols for reducing gel electrophoresis using a 10 well NuPage10% Bris-Tris-HCl gel (NP0301, Invitrogen, Paisley, UK) with MES running buffer. To 2µl of lysozyme solution (1mg/ml), 2.5µl of NuPAGE® LDS Sample Buffer (4X) and 4.5µl of deionized water was added. 1µl of NuPAGE® Reducing Agent (10X) was added to the resulting solution. This solution was mixed together, and heated at 70°C for 10

minutes in a fan assisted oven to denature the lysozyme protein. While the solution was in the oven, the gel was prepared as follows. The gel was removed from the pouch, rinsed with distilled water and the tape peeled from the bottom of the cassette. The comb was then gently removed from the cassette, and the sample wells rinsed with the MES running Buffer. The gel was then loaded into Mini-Cell and locked into place. The upper buffer chamber was filled with 200ml of MES running buffer containing 500µl of the NuPAGE® antioxidant. 10µl of the denatured lysozyme solutions being analysed were then loaded into wells 2-10 (1 well per denatured lysozyme solution) of the gel, while 5µl of the Prestained See Blue Plus 2 molecular weight ladder was added to the first well. 600ml of the MES running buffer was then added to lower buffer chamber. Gel electrophoresis was then run for 35mins at 200V and an expected start current of 110-125 mA using a PowerEase 500 Pre-Cast gel system (EI8675UK, Invitrogen, Paisley, UK). Prestained See Blue Plus 2 molecular weight ladder was used to estimate the molecular mass of each protein sample. The gels were stained with Commasie Blue (Invitrogen, Paisley, UK) and then photographed and dried. The apparent molecular mass of the stained bands from the eluent samples was compared to that of the standards.

## Part B: Scaffold Protein Denaturation

### 4.3.19. Scaffold fabrication from microspheres.

Scaffolds were fabricated from the microspheres by placing into a mould and heating above their glass transition temperature (Tg) for a short duration. Approximately 70mg of microspheres were loaded into 10” by 5” (length x breath) wells of a Teflon

mould. Microparticles were then heat sintered at 60°C for 3 hours, and allowed to cool down to room temperature before removal of scaffolds from the mould.

### 4.3.20. The effect of heat sintering of microspheres on entrapped protein

This experiment was conducted to investigate if the heat sintering of microspheres during fabrication of scaffolds resulted in the denaturation of protein entrapped within the microspheres. In brief, approximately 70mg of ribonuclease A loaded microspheres were loaded into the Teflon mould (Section 4.3.19) and heat sintered for 2, 4, 6 and 24 hours in a preheated oven preset to 60°C respectively. The protein content of the fabricated microspheres was then determined following the micro BCA method described in section 2.6.4.1. This was then compared to ribonuclease A loaded microspheres not exposed to the heat sintering process.

For controls, a series of 100μg/ml ribonuclease A solutions were made and placed in glass scintillation vials. These vials were than placed in a preheated oven at 60°C, and incubated for 2, 4, 6 and 24 hours. The protein content of the solutions after heat incubation was then determined using the micro-BCA assay (Section 2.6.4.1) and compared to a series of 100μg/ml ribonuclease A solutions not exposed to the heat incubation.

## Part C: Drug encapsulation and release.

### 4.3.21. Fabrication of Dexamethasone loaded PLGA/ Triblock Microspheres

To investigate the effect of incorporating the triblock on the release kinetics of dexamethasone (Dex) loaded microspheres, 5% (w/w) Dex loaded microspheres were made from PLGA, 10% w/w, and 30% w/w PLGA/ triblock blends using the S/O/W

method described in section 2.6. The encapsulation efficiency of dexamethasone within the microspheres was determined by dissolving 20mg of sieved microspheres (100 - 300µm) microspheres in acetonitrile (Fisher, Loughborough UK) and quantified by HPLC-UV (246nm) using a Phenomenex C18 column (4.6 x 150mm) on an Agilent 1090 HPLC machine. The mobile phase was 58:42 2mM acetate buffer (pH 4.8) and acetonitrile respectively.

### 4.3.22. Controlled release of dexamethasone from PLGA/triblock microspheres.

To investigate the effect of triblock on the release kinetics of Dex loaded microspheres, controlled release experiments of dexamethasone from microspheres into PBS were performed. The controlled release experiment was performed following the method described by Aubert-Poussell et al. using 20mg of dexamethasone loaded microspheres of PLGA and PLGA/triblock blends (Section 4.3.21). The amount of Dex released was quantified using HPLC as described in section 4.3.21.

### 4.3.23. The effect of dexamethasone concentration on viability of murine embryonic stem cells.

The effect of dexamethasone concentration on the viability of murine embryonic stem cells (mES) was investigated to ascertain the concentration at which dexamethasone becomes toxic to the cells. The series of experiments used to determine this are described below.

#### 4.3.23.i. Culture of murine Embryonic stem cells (mESC) on the scaffolds

Embryoid bodies from mESC were formed as detailed in Section 2.8.3. The mES cells obtained by trypsinising of 5 day old embryoid bodies into single cells were then

suspended at a concentration of 20 x $10^7$ cells/ml and 50µl (1 x $10^6$ cells) were seeded onto each scaffold following the methods described in Section 2.8.3. The cell seeded scaffolds were then cultured for 28 days in 3ml of the differentiation media. The differentiation media consisted of DMEM supplemented with 15% (v/v) of fetal calf serum (FCS), 2mM L-glutamine, 1% (v/v) antibiotic solution (consisting of 10,000 units/ml of penicillin and 100mg/ml of streptomycin sulphate), 10mM β-glycerophosphate and 50µg/ml ascorbic acid. To investigate the effects of dex concentration on mES cells, differentiation media containing between 0nm to 10µm dex concentration was used. Three cell seeded scaffolds were used for each dex concentration differentiation media. Culture media was changed twice a week.

#### 4.3.23.ii. Cell viability studies.

After 28 days of continuous culture in differentiation media, cell seeded scaffolds were rinsed in PBS and the viability of cells investigated using alamar blue and alkaline phosphatase assays following the methods described in Section 2.9.1 and 2.9.3 respectively. The amount of DNA on each scaffold was determined using the methods described in Section 2.9.3. Alamar blue and alkaline values were normalised to the amount of DNA as determined using Hoescht assay (section 2.9.2).

### 4.3.24. The effect of scaffold released dexamethasone on mES viability.

Scaffolds fabricated from 5% w/w dexamethasone loaded microspheres (made from PLGA + 30% w/w triblock blend) were pre-washed for 0, 3, 7 and 14 days respectively by incubating in PBS solutions. After prewashing of scaffolds, mES cells were seeded on the pre-washed scaffolds following the methods described above

(Section 4.3.23.i). The cell seeded scaffolds were then cultured for 28 days in 3ml of the differentiation media. Culture media was changed twice a week.

After 28 days of continuous culture in differentiation media, Dex loaded cell seeded scaffolds were rinsed in PBS and the viability of cells investigated using alamar blue and alkaline phosphatase assays following the methods described in Section 2.9.1 and 2.9.3 respectively. The amount of DNA on each scaffold was determined using the methods described in Section 2.9.3. Alamar blue and alkaline values were normalised to the amount of DNA. The degree of differentiation of the mES cells was determined qualitatively through alizarin red staining of constructs using the methods described in Section 2.11.1.

### 4.3.25. The effect of mixing microspheres of blends of different triblock composition on dexamethasone release kinetics.

To investigate the effect of mixing dexamethasone-loaded microspheres made from 10% triblock and 30% w/w triblock blends on the release kinetics, controlled release experiments of dexamethasone from microspheres into PBS were performed. The controlled release experiment was performed as described in section 4.3.22 using mixtures of 5.0% w/w Dex loaded microspheres made from 10% and 30% triblock in the following proportions, 0/100; 25/75; 50/50; 75/25 and 100/0 (10% / 30% w/w triblock. HPLC-UV as described in section 4.3.22 was used to determine the amount of dexamethasone released.

### 4.3.26. PLGA + Triblock Microspheres Incubation.

$^{1}$H NMR analysis was used to investigate the effect of incubation in PBS at 37ºC on microsphere triblock content over a 28 day period. Microspheres made from PLGA

blends containing 10% w/w and 30% w/w triblock were incubated PBS solution with mild agitation at 37ºC for 0, 7, 14 and 28 days. The % triblock retention in microspheres was obtained by comparing the mole ratio of PEG: LA (PEG: Lactide) of triblock blend against that of the resulting microsphere. The PEG: LA mole ratio was obtained by comparing the ratio of normalised (to the number of H (4 and 3 respectively) within the monomer) integrated values for the signals specific to $CH_2CH_2$ (PEG) to that of $CH_3$ (lactide) monomers located at 3.65ppm and 1.60ppm respectively.

### 4.3.27. Statistical analysis.

All experiments were performed in triplicates with the results expressed as means ± standard deviations. Unpaired, two-tailed t-tests were performed at each time point for the controlled release experiments. The threshold for statistical significance was set at $p<0.05$. For the controlled release experiments, a Higuchi's plot and corresponding linear regression was investigated.

## 4.4. Results.

### 4.4.1. Particle Size Analysis.

Characterization of the lysozyme loaded microspheres made from PLGA showed a particle size ranging from 45µm to 300µm (Fig 4.2) with the average size of particles being 223µm.

### 4.4.2. Effect of process parameters on protein entrapment.

To investigate the effect of micronisation on the protein entrapment efficiency, lysozyme was loaded into microspheres with and without the micronisation step (see

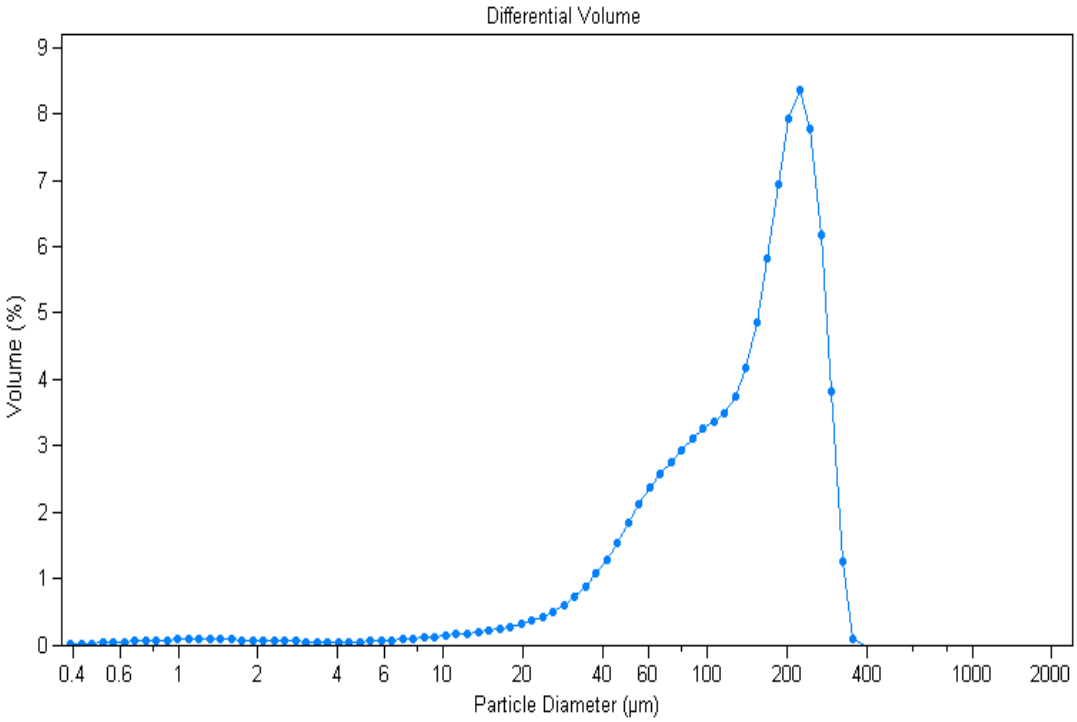


Figure 4.2: Chart showing microsphere size distribution as determined using LS Coulter 230, on optical mode

section 4.3.5). Fig 4.5 shows the entrapment efficiency of the microspheres formed from both processes. Micronising lysozyme prior to encapsulating into microspheres showed an entrapment efficiency of 59.9 ± 1.1%, compared to 14.6 ± 0.5% for lysozyme encapsulation without the micronisation step. This whole experiment was repeated using myoglobin, with similar results observed with (65.4 ± 1.3%) and without (16.8 ± 0.4%) the micronisation step respectively.

Other parameters investigated in the microsphere fabrication process, were (a) the effect of freeze drying process on the lysozyme concentration, and (b) investigating the amount of protein that leached out of the microspheres during the hardening process. These parameters were selected as they have previously been shown to be areas of protein loss from microspheres (Luan et al., 2006). The variation of these parameters with varying loading weight of protein within microspheres was also investigated.

The results showed that the freeze drying process in the presence of PEG 6000 resulted in no loss in amount of lysozyme for all the different loading weights investigated (104.1 ± 2.2%; 104.7± 1.8%; 97.6 ± 1.6%; 96.4 ± 0.5%; for 1%; 3%; 5% and 10% w/w lysozyme loaded microspheres respectively). However the proportion of protein that leached out during the microsphere hardening step increased with increasing loading weight (7.7 ± 2.4%; 32.2 ± 6.6%; 40.3 ± 5.3%; 47.3 ± 5.6%; for 1%; 3%; 5% and 10% w/w lysozyme loaded microspheres respectively) (Fig. 4.6.).

### 4.4.3. Effect of loading weight on the entrapment efficiency of proteins.

The effect of loading weight on the entrapment efficiency of different proteins was investigated. Lysozyme, ribonuclease, trypsin, myoglobin and horse radish peroxidise

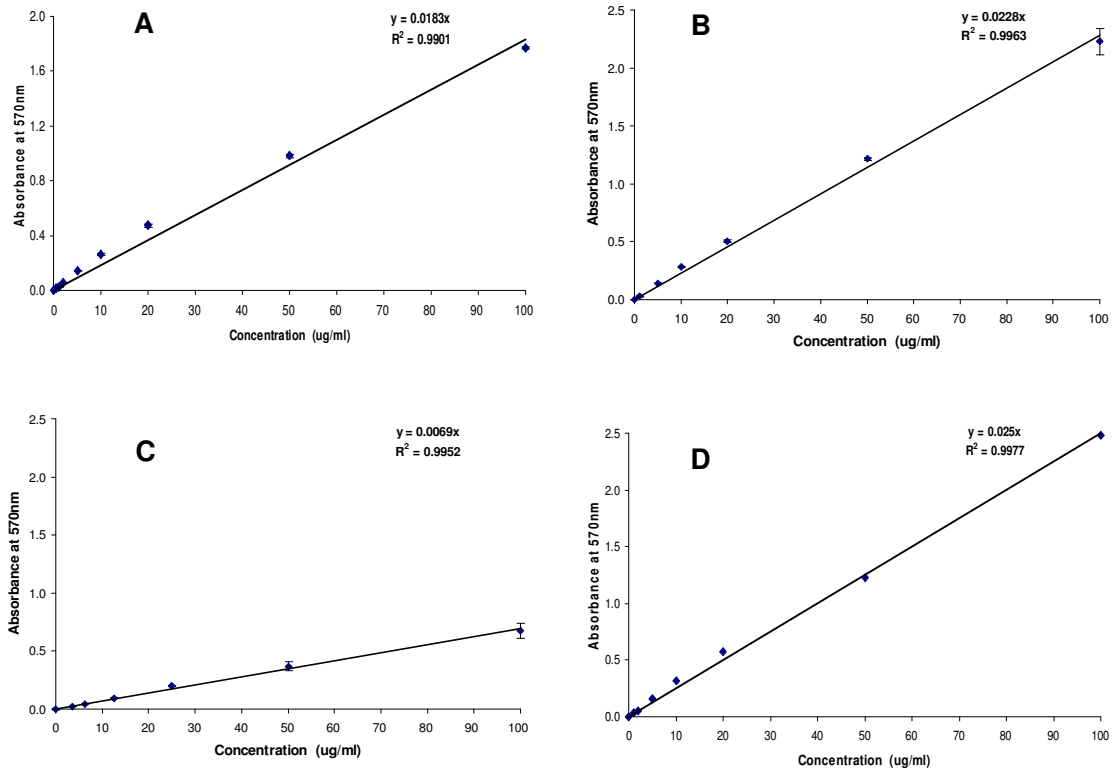


Figure 4.3: Chart showing a typical micro BCA standard curve. Absorbance values of various concentrations of PBS solutions (A) ribonuclease A, (B) trypsin, (C) myoglobin and (D) lysozyme (2µg/ml - 100µg/ml) was determined and plotted against the corresponding concentration. Values plotted on the chart are average values obtained from three different independent experiments (i.e. N = 3 ± Standard deviation). These standard curves were used for the quantification of protein in all experiments involving protein loaded microspheres.

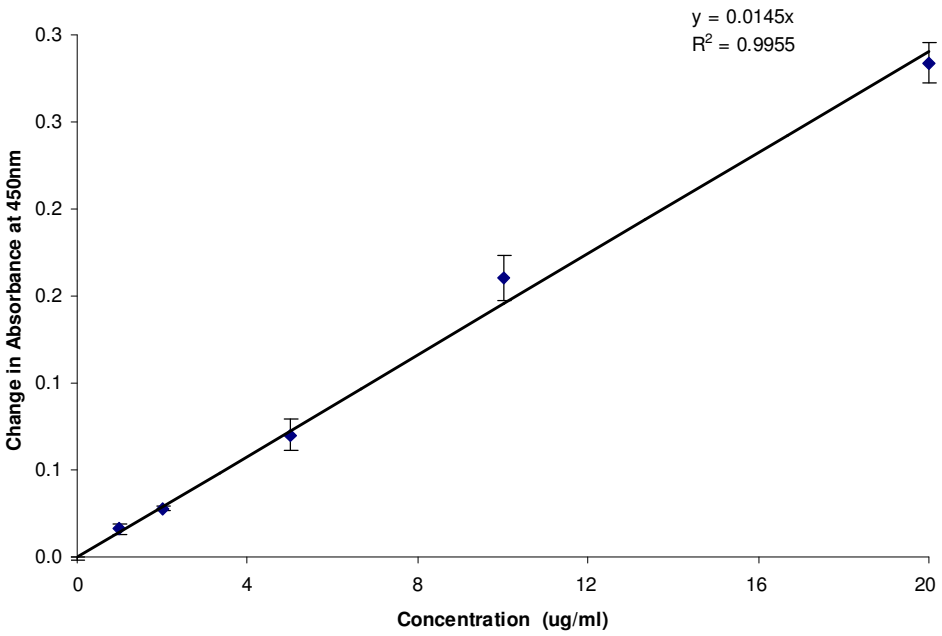


Figure 4.4: Chart showing a typical lysozyme activity standard curve. The change in absorbance of various concentrations of PBS solutions lysozyme (0.5µg/ml - 20µg/ml) was determined and plotted against the corresponding concentration. Values plotted on the chart are average values obtained from three different independent experiments (i.e. N = 3 ± Standard deviation). These standard curves were used in experiments for determination of the entrapment efficiency and controlled release studies of lysozyme loaded microspheres,

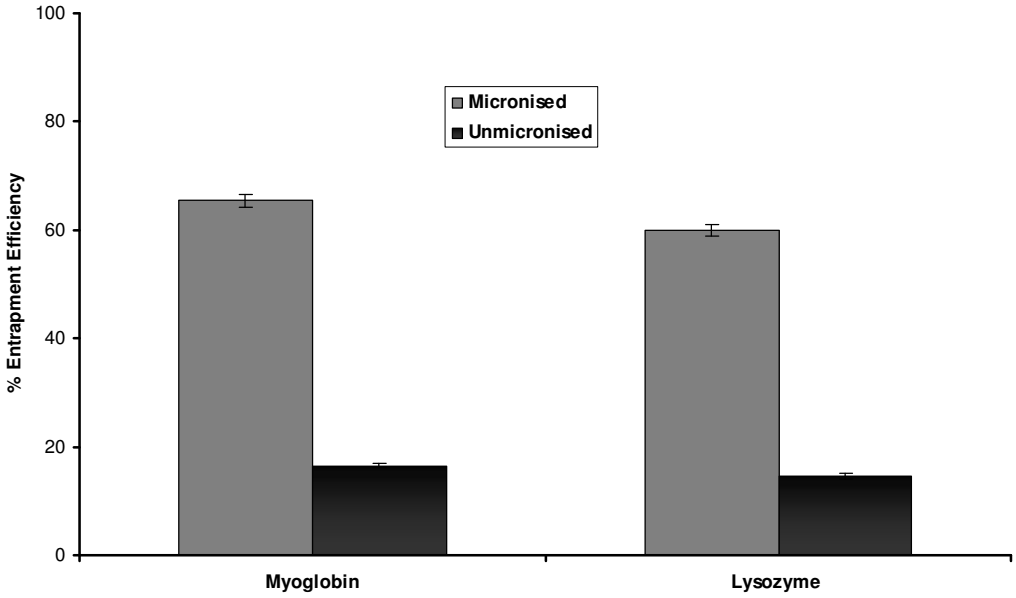


Figure 4.5: Chart showing the effect of micronisation of protein on the entrapment efficiency using single emulsion method. Micronised protein loaded microspheres involved a micronisation step prior to microsphere fabrication. The micronisation step involved the lyophilization of a solution of the protein in PEG. Values plotted on the chart are average values obtained from three different independent experiments (i.e. N = 3 ± Standard deviation).

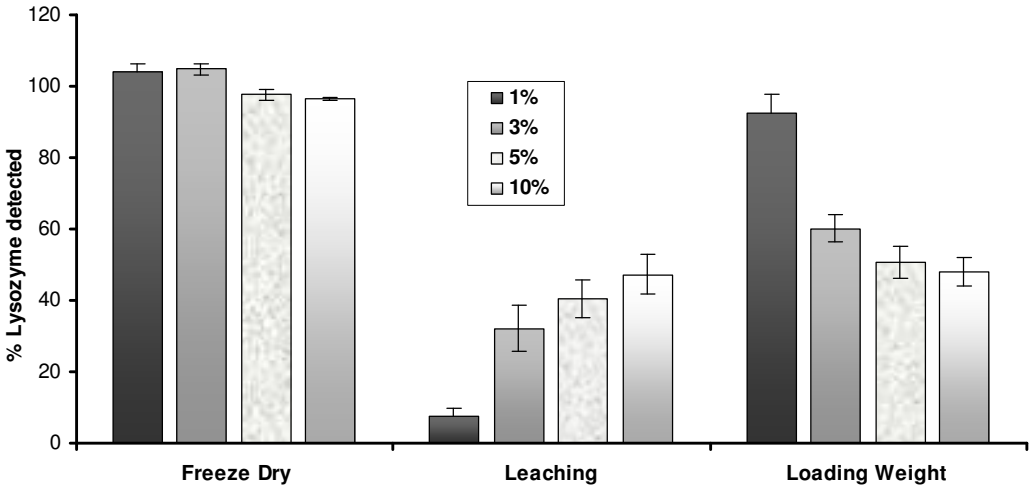


Figure 4.6: Chart showing the amount of lysozyme detected during each stage of the microsphere fabrication process. The amount of lysozyme at each step was quantified using micro-BCA protein quantification kit. Values plotted on the chart are average values obtained from three different independent experiments (i.e. N = 3 ± Standard deviation).

(HRP) were chosen as model proteins due to their variation in molecular weights and isoelectric points. Molecular weights and isoelectric points for the proteins are as follows: 14.3 kD and pI 10.7 for lysozyme (Stadelman and Cotterill, 1990); 12.7 kD and pI 7.8 for ribonuclease (Rothen, 1940); 23.8 kD and pI 10.5 for trypsin (Cunningham, 1954); 17.5 kD and pI 7.0 for myoglobin (Murakami, 1998); 40 kD and pI 7.2 for HRP (Maehly, 1955). The entrapment efficiency of the proteins was observed to decrease with increasing loading weight for all the proteins (Fig 4.7).

### 4.4.4. Effect of polymer on the entrapment efficiency and release kinetics of proteins.

The effect of polymer on the entrapment efficiency and release kinetics of trypsin was investigated. Poly(caprolactone), Poly (lactide) and PLGA polymers with LA:GA ratios of 50:50; 65:35; 75:25; and 85:15 were used for the study. The molecular weight of the polymers ranged from 63 kD to 68 kD. The entrapment efficiency of trypsin overall increased with increasing LA:GA ratio with the maximum entrapment efficiency observed in PLGA (75:25) (73.6 ± 3.4%). The difference in entrapment efficiency observed for trypsin entrapped within microspheres made from PLGA (85:15), PLGA (75:25), and $P_{DL}LA$, was statistically insignificant (69.1 ± 2.8%; 73.6 ± 3.4%; 70.8 ± 2.8% respectively) (Fig. 4.8). Entrapment efficiency of trypsin in PCL was statistically lower when compared to that of $P_{DL}LA$ (61.4 ± 3.9% vs. 69.1± 2.8).

The release kinetics of the trypsin loaded microspheres was observed over a 7 day period. The initial burst release (release on the first day) was highest for poly(caprolactone) (PCL) (17.9 ± 0.3%), and was marginally more than that of PLGA (50:50) and PLGA (65:35) (17.1 ± 0.4% and 15.8 ± 0.6% respectively). However, the

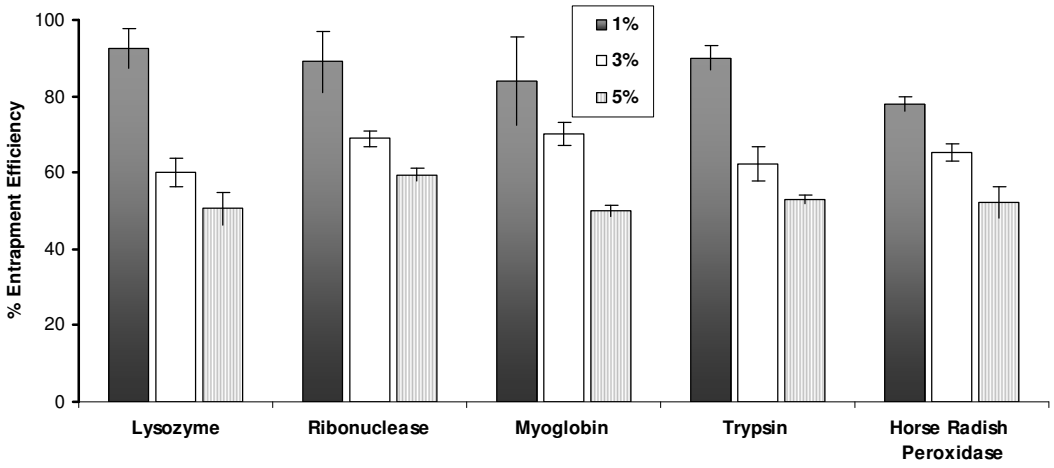


Figure 4.7: Chart showing the effect of loading weight on the entrapment efficiency of the proteins in PLGA microspheres. 10mg, 30mg, 50mg, and 100mg of protein was loaded into PLGA microspheres to yield 1%, 3%, 5%, and 10% w/w protein loaded microspheres. The amount of protein remaining in the microspheres was determined by dissolving the microspheres in ethyl acetate, extracting the protein into PBS and quantifying. using micro-BCA protein quantification kit. Entrapment efficiency values were obtained by expressing the protein retained within the microspheres as a percentage of the amount of protein loaded. Values plotted on the chart are average values obtained from three different independent experiments (i.e. N = 3 ± Standard deviation).

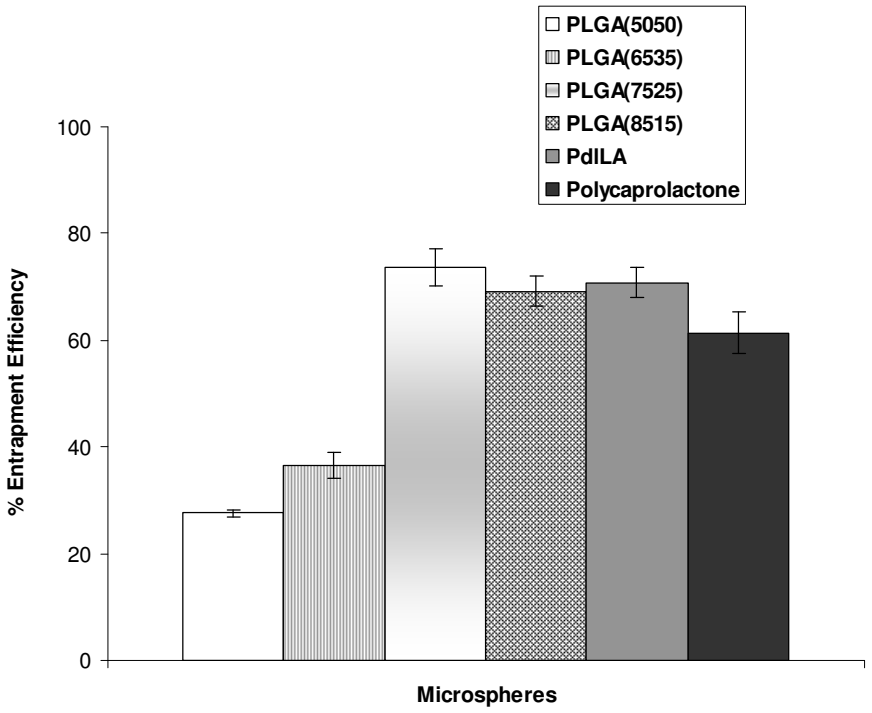


Figure 4.8: Chart showing the entrapment efficiency of trypsin in various polymers. For each polymer, 10mg of protein was loaded into 1g of polymer using a single emulsion method. The amount of protein remaining in the microspheres was determined by dissolving the microspheres in ethyl acetate and extracting the protein into PBS. The amount of the protein in the PBS was quantified using micro-BCA protein quantification kit. Entrapment efficiency values were obtained by expressing the protein retained within the microspheres as a percentage of the amount of protein loaded. Values plotted on the chart are average values obtained from three different independent experiments (i.e. N = 3 ± Standard deviation).

initial burst release of trypsin from microspheres made from PLGA (75:25), PLGA (85:15); and $P_{DL}LA$ was significantly less than that of PCL (3.4 ± 0.2%, 3.6 ± 0.1% and 2.3 ± 0.1% vs. 17.9 ± 0.3% respectively) (Fig 4.9). The rate of release of trypsin after the initial burst release was observed to be faster for microspheres made from PCL, PLGA (50:50) and PLGA (65:35), than those made from PLGA (75:25), PLGA (85:15); and $P_{DL}LA$ (Fig 4.9).

### 4.4.5. Effect of loading weight on the release kinetics of lysozyme.

Prior to the commencement of the controlled release experiment, a series of experiments was conducted to investigate the stability of lysozyme in the PBS used for the controlled release experiments, and its rate of adsorption onto the PLGA (85:15) microspheres present within a solution of lysozyme. The results obtained (Figs 4.10 and 4.11) show that lysozyme was stable in PBS buffer at 37°C, with no significant adsorption of lysozyme unto the PLGA microspheres over a 30-day period (84.3 ± 1.4 vs. 78.3 ± 8.2% of active lysozyme detected for solutions of lysozyme incubated at 37ºC with and without microspheres respectively).

The effect of loading weight on protein release kinetics was investigated using the flow through method (Aubert Poussell 2002) as described in section 4.3.16. The results are summarised in Fig 4.12. For the three different loading weights, the release profile was characterized by a marked initial protein release within the first 24h (13.0 ± 2.2% for 1.0%; 13.1 ± 3.3% for 2.0%; and 15.7 ± 5.2% for the 2.5% loading weight). This was followed by a phase of little or no release for the next 17 days. Another phase of rapid release was observed between days 21 and 28 in which

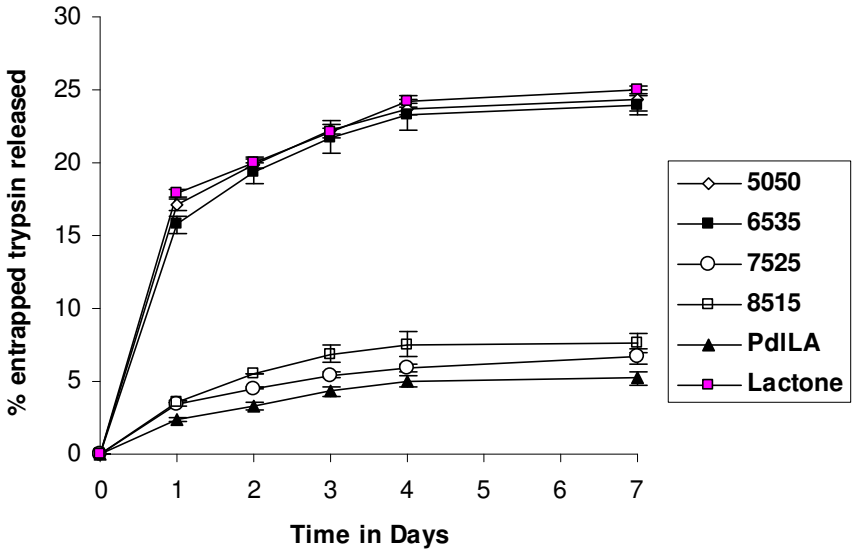


Figure 4.9: Chart showing the release of trypsin from various polymers. For each polymer, 100mg of protein loaded microspheres was incubated in 2ml of PBS at 37$^{o}$C. The supernatant was harvested at various time points and the amount of protein released was quantified using micro-BCA protein quantification kit. Values plotted on the chart are average values obtained from three different independent experiments (i.e. N = 3 ± Standard deviation).

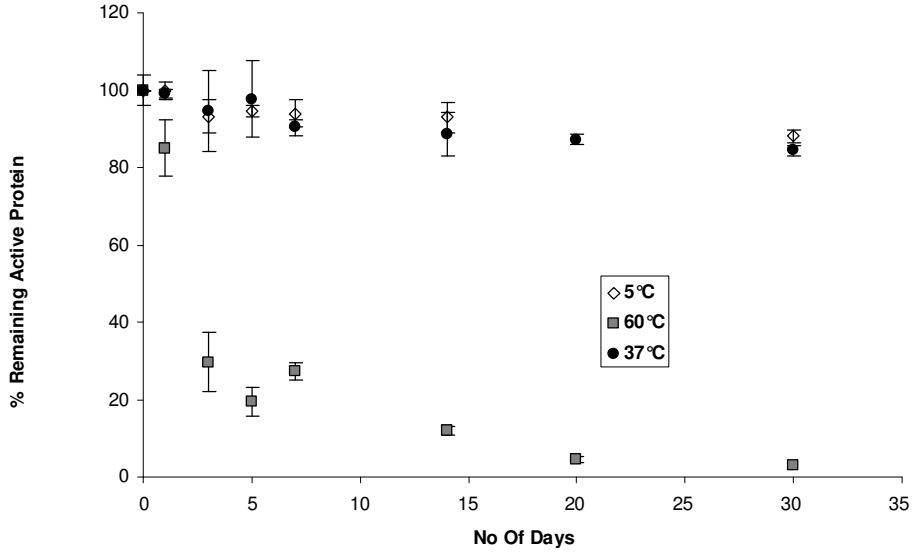


Figure 4.10: Chart showing the effect of temperature on lysozyme activity. Vials containing lysozyme solution with concentration of 100µg/ml were exposed to 5ºC, 37ºC and 60ºC. At various time points, 3 vials for each temperature were removed and the activity of the lysozyme solution was determined using a lysozyme activity assay. Values plotted on the chart are average values obtained from three different independent experiments (i.e. N = 3 ± Standard deviation).

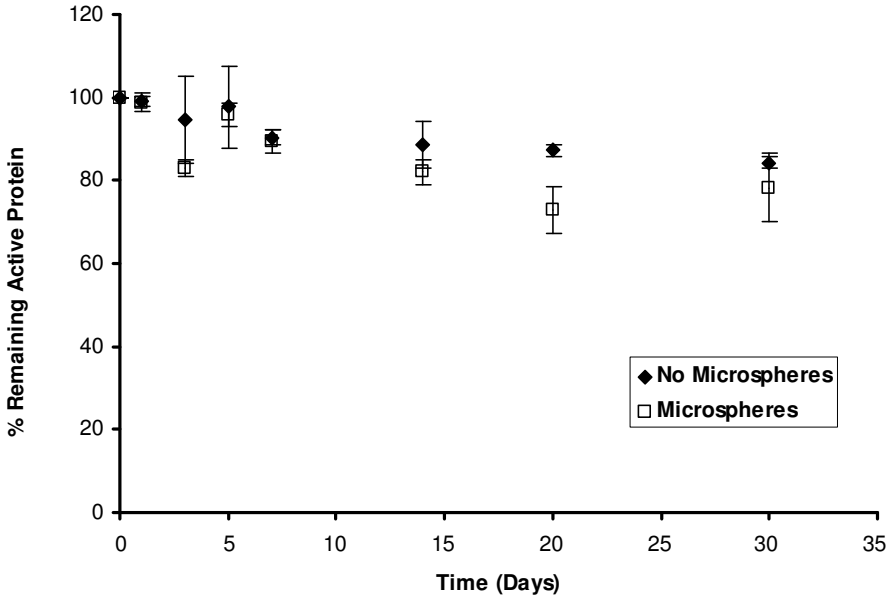


Figure 4.11: Chart showing the effect of incubating lysozyme solution in the presence of microspheres on the amount of protein remaining in solution. Vials containing 2ml of lysozyme solution with concentration of 100µg/ml was incubated in the presence or absence of 50mg. At various time points, 3 vials each were removed and the activity of the lysozyme solution determined using lysozyme activity assay. Values plotted on the chart are average values obtained from three different independent experiments (i.e. N = 3 ± Standard deviation).

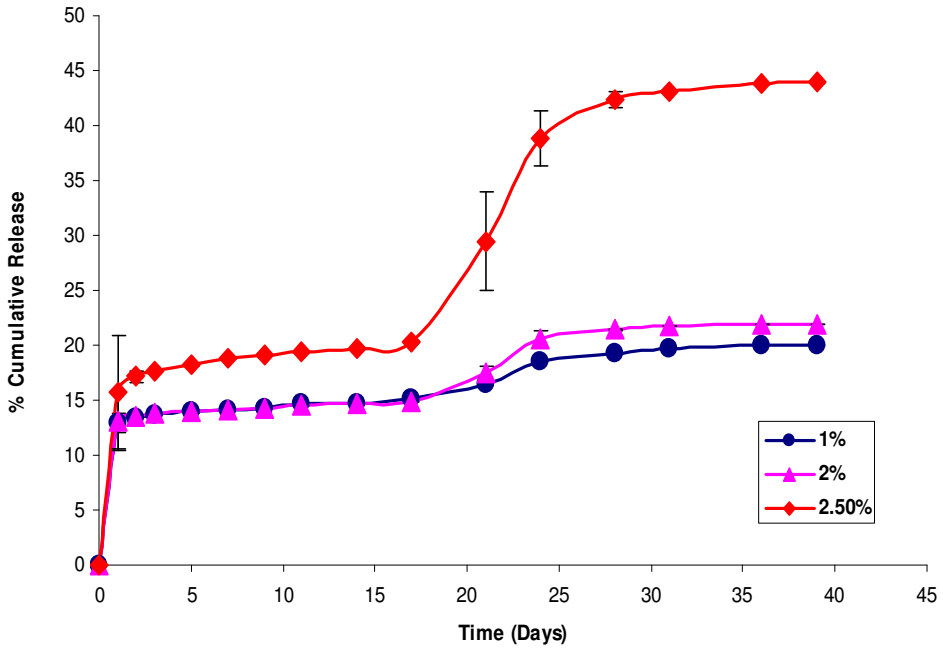


Figure 4.12: Chart showing the effect of loading weight on the release kinetics of lysozyme. 1%, 2% and 2.5% w/w lysozyme loaded microspheres made from PLGA. For each loading weight the release kinetics of lysozyme from 20mg of lysozyme loaded microspheres was investigated using the flow chamber at 37ºC. The supernatant was harvested at various time points and the amount of protein released was quantified using a micro-BCA protein quantification kit. Values plotted on the chart are average values obtained from three different independent experiments (i.e. N = 3 ± Standard deviation).

a further 4.2 ± 3.2 %, 6.5 ± 4.2% and 22 ± 15.2% of lysozyme was released from the 1.0%, 2.0% and 2.5% loading weight microspheres respectively.

However, the microspheres exhibited an incomplete release with only 21.94 ± 4.73% and 19.95 ± 3.96% of the total lysozyme released after 40 days for the 1.0% and 2.0% loading weights respectively. While the amount of lysozyme released from microspheres of the 2.5% protein loading weight was about 43.91 ± 7.73%. After 40 days, the remaining microspheres were analyzed for the protein content remaining within the microparticles. Protein content measurements indicated that 84.3 ± 2.2%, 69 ± 3.2% and 64.3 ± 1.25% of active lysozyme remained within the 1%, 2% and 2.5% loaded microspheres respectively.

### 4.4.6. Effect of heat sintering microspheres on protein stability.

Ribonuclease A was chosen to study the effect of heat sintering on protein stability due to its instability at the temperature (60°C) used for scaffold manufacture (Stelea et al., 2001). The degradation rates of ribonuclease A entrapped in dry microspheres was then compared to the degradation rate of ribonuclease A in solution as a control. The results obtained are summarised in Fig 4.13. There was no significant difference in the degradation rates of protein when in microspheres or when in solution (5.46 ± 1.80 vs. 5.52 ± 1.27; 13.57 ± 2.49 vs. 13.74 ± 2.21; 17.77 ± 2.59 vs. 17.86 ± 1.92; and 17.96 ± 2.04 vs. 18.04 ± 1.52 for microspheres and solutions after 2, 4, 6 and 24 hours heat incubation respectively), indicating that the polymer (PLGA) does not confer any form of protection on the encapsulated ribonuclease A.

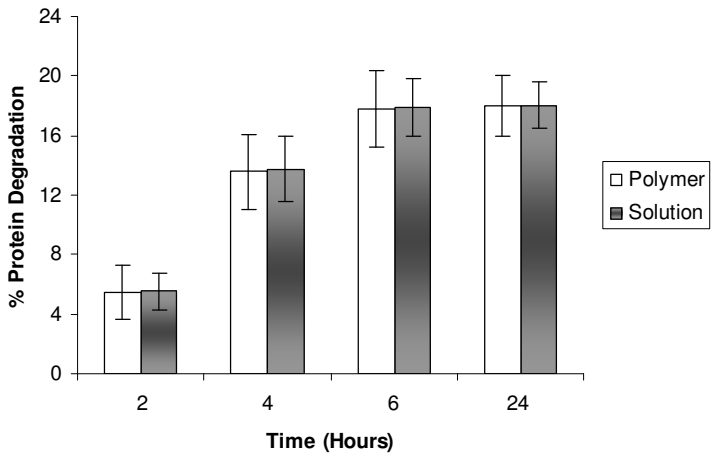


Figure 4.13: Chart showing the effect of heating ribonuclease A (in solution and entrapped in microspheres) for various time durations on the degradation of the protein. Ribonuclease A (5% w/w) loaded PLGA microspheres were fabricated and amount of protein entrapped was determined. Ribonuclease loaded microspheres (70mg) and 100µg/ml ribonuclease solution were heated at 60ºC for various time durations. Amount of non-degraded protein remaining in microspheres was quantified using a micro-BCA protein quantification kit. Percentage protein degradation was determined by expressing the difference in values obtained before and after heating microspheres or solution (at 60ºC) as a percentage. Values plotted on the chart are average values obtained from three different independent experiments carried out (i.e. N = 3 ± Standard deviation).

### 4.4.7. Effect of triblock composition on entrapment efficiency and release kinetics of lysozyme from PLGA microspheres.

The triblock PLGA-PEG-PLGA synthesized was observed to have a molecular weight of 8,900 by GPC using polystyrene standards and 6,800 (2650 – 1500 – 2650) by NMR. The triblock was utilised in making triblock / PLGA blends, which was used subsequently to fabricate microspheres. Fabrication of lysozyme loaded microspheres using the single emulsion method resulted in entrapment efficiencies greater than 50%, for a protein loading weight of 5% (w/w). Varying the amount of the triblock polymer within the PLGA/triblock polymer blend did not have any significant effect on the entrapment efficiency of the lysozyme within the microspheres (see Table 4.1 for values).

However, the 60-day controlled release experiments in PBS at 37°C showed a positive correlation between the rate of lysozyme release and triblock content within microspheres. Increasing the amount of triblock within the blends resulted in an observed increase in the initial burst release of lysozyme (Table 4.1). Initial burst release from PLGA microspheres was 4.83 ± 0.85 %; while burst release of 5.12 ± 0.28%; 9.39 ± 1.33; 20.76 ± 6.17% and 40.09 ± 9.31% were observed for triblock compositions of 5%, 10%, 20% and 30% (*w/w*) within the PLGA/triblock blend respectively.

The release profile also showed that by increasing the content of the hydrophilic triblock present within the microspheres, there was an increase in the rate of release of lysozyme from the microspheres. A reduction in the duration of the lag phase with an increase in triblock composition was also observed. A linear release profile of

| Polymer Blend | Entrapment Efficiency | % Initial Burst Release | Sustained Release Duration (Days) | Protein Activity after 28 days cumulative release) |
|---|---|---|---|---|
| PLGA | 52.01 ± 1.58 | 4.83 ± 0.85 | > 60 | 84.09 ± 5.58 |
| 5% Triblock | 59.00 ± 0.86 | 5.12 ± 0.28 | 60 | 93.09 ± 8.75 |
| 10% Triblock | 60.34 ± 2.86 | 9.39 ± 1.33 | 49 | 88.22 ± 3.35 |
| 20% Triblock | 59.46 ± 1.55 | 20.76 ± 6.17 | 30 | 88.96 ± 6.82 |
| 30% triblock | 55.55 ± 1.23 | 40.09 ± 9.35 | 20 | 86.09 ± 9.37 |

Table 4.1: Table showing the entrapment efficiency, burst release, duration of sustained release and activity of cumulative lysozyme release after 28 days. Data were obtained from experiments conducted using 5% lysozyme loaded (theoretical amount) microspheres. Values indicated in the table are average values obtained from three different independent experiments (i.e. N = 3 ± Standard deviation).

lysozyme approaching zero order kinetics (with no lag phase) was observed from microspheres with triblock composition of 30% (Fig 4.14). In addition to reduction in the lag phase with varying triblock composition, the duration of sustained release of the protein also varied from about 60 days (5% triblock) to 14 days (30% triblock). The lysozyme released from the microspheres up to day 28 was observed to be active and structurally intact as indicated by the activity assay and SDS-PAGE gel electrophoresis (Table 4.1) and Fig 4.15

### 4.4.8. Effect of triblock composition on dexamethasone entrapment and release kinetics.

The effect of varying the triblock composition on the release kinetics of dexamethasone was investigated by manufacturing 5.0% (*w/w*) protein loaded microspheres from 0%, and 10% and 30% w/w triblock in PLGA referred to as PLGA, 10% and 30% triblock. SEM imaging showed no apparent morphological differences between the microspheres made from the different polymer blends (Fig. 4.16). Entrapment efficiencies greater than 75% were obtained with no significant difference between 0%, 10% and 30% triblock microspheres (see Table 4.2 for values). However, the incorporation of the triblock was observed to increase the initial burst release (Table 4.2) and significantly accelerate the release of dexamethasone post the burst release phase (Fig 4.18). Dexamethasone loaded microspheres made from PLGA was observed to show a long lag phase with little or no Dex released after the initial burst release (2nd day onwards) until the end of the controlled release experiment (day 90). Dex loaded microspheres made from 10% triblock showed a lag phase period (although with significantly more dexamethasone released in this phase than that of the lag phase of PLGA (5.92 ± 1.01% vs. 1.64 ± 0.16% respectively))

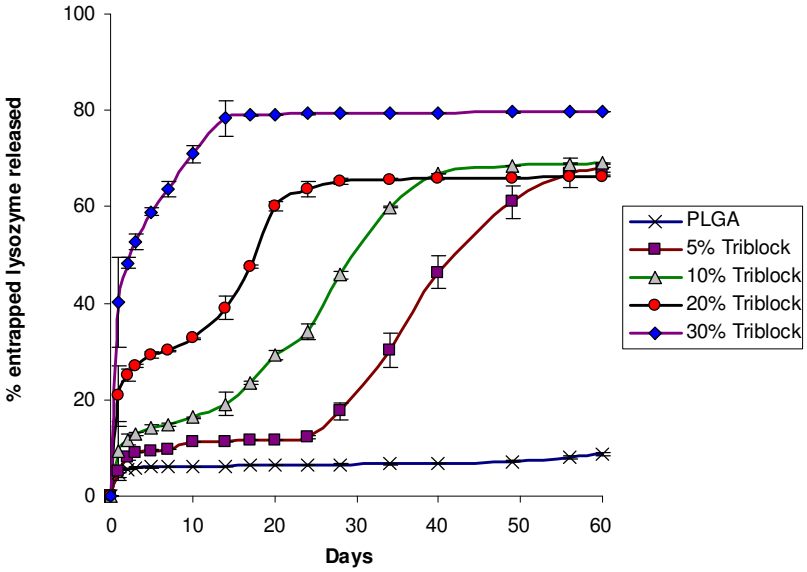


Figure 4.14: Chart showing the effect of triblock co-polymer on the release kinetics of lysozyme. Lysozyme loaded (5% w/w) microspheres made from PLGA; and PLGA containing 5% w/w; 10-% w/w; 20% w/w and 30% w/w triblock blends. For each blend, the release kinetics of lysozyme from 20mg of lysozyme loaded microspheres was investigated using the flow chamber at 37ºC. The supernatant was harvested at various time points and the amount of protein released quantified using a micro-BCA protein quantification kit. Values plotted on the chart are average values obtained from three different independent experiments (i.e. N = 3 ± Standard deviation).

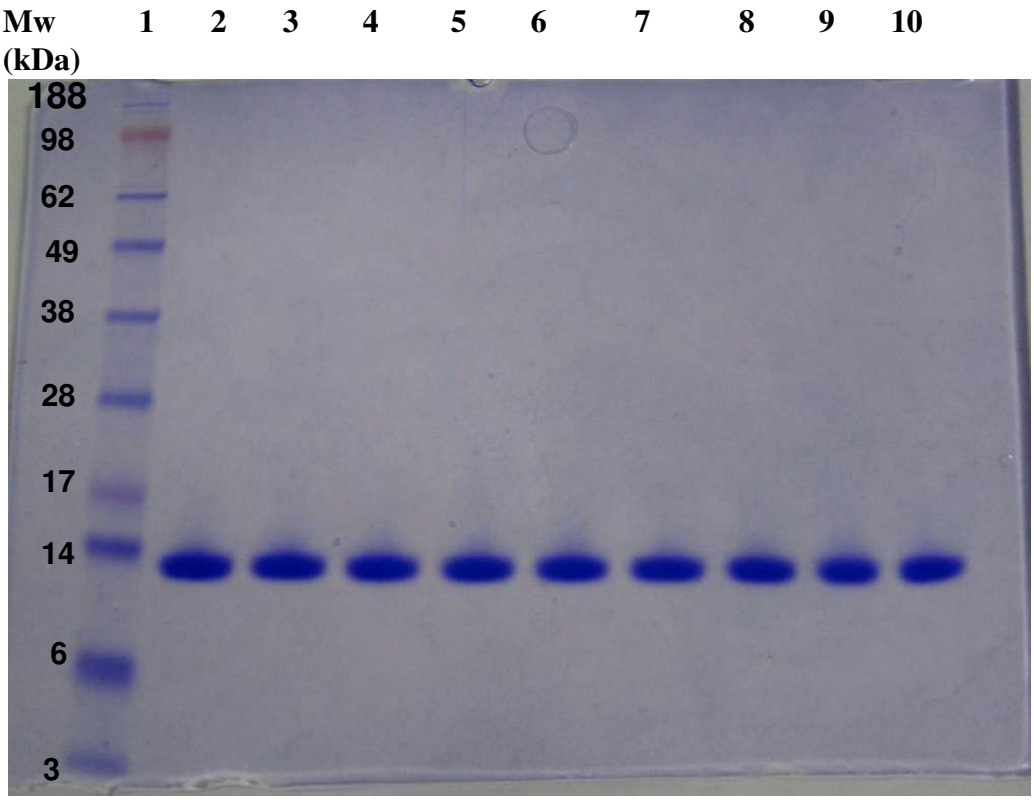


Figure 4.15: SDS Page gel images of lysozyme released after a total of 28 days from (A) PLGA: Lanes 2 - 4 and (B) PLGA + 30% w/w Triblock microspheres: Lanes 5 – 7. (C) Native lysozyme dissolved in PBS: Lanes 8 - 10. Lane 1 indicates molecular weight markers obtained using seeblue plus 2 standards.

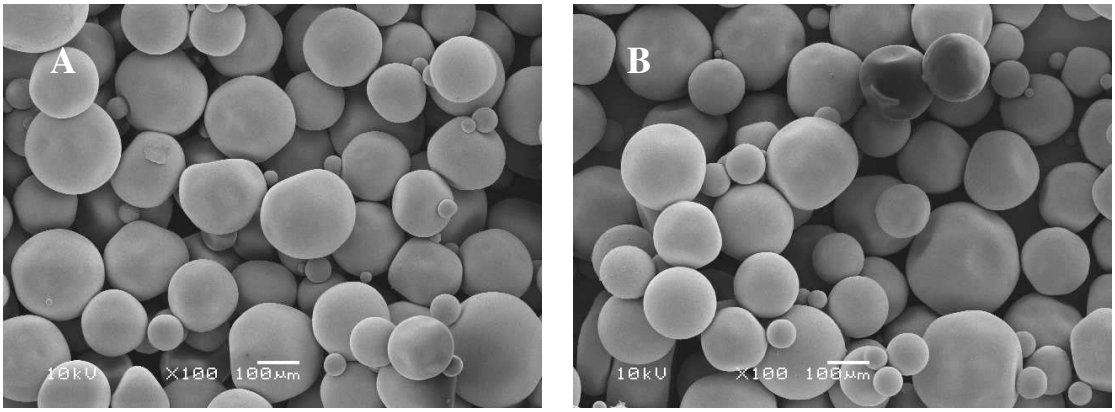


Figure 4.16: SEM images of lysozyme loaded microspheres. 5% lysozyme loaded microspheres fabricated from A) PLGA blends; B) PLGA containing 30% triblock w/w. SEM images were obtained by imaging gold coated microspheres using a JEOL JSM-6060LV scanning Microscope operated at an ionizing radiation of 10 kV. Scale bar is 100µm.

| Polymer Blend | Entrapment Efficiency | % Initial Burst Release | Duration of Sustained Release (Days) |
|---|---|---|---|
| PLGA | 74.76 ± 7.31 | 1.44 ± 0.18 | > 90 |
| 10% Triblock | 73.48 ± 2.97 | 2.31 ± 0.91 | 86 |
| 30% triblock | 74.51 ± 4.67 | 5.30 ± 1.28 | 40 |

Table 4.2: Table showing the entrapment efficiency, burst release, and duration of sustained release of dexamethasone from dexamethasone loaded microspheres. Data were obtained from experiments conducted using 5% dexamethasone loaded (theoretical amount) microspheres. Values indicated in the table are average values obtained from three different independent experiments (i.e. N = 3 ± Standard deviation).

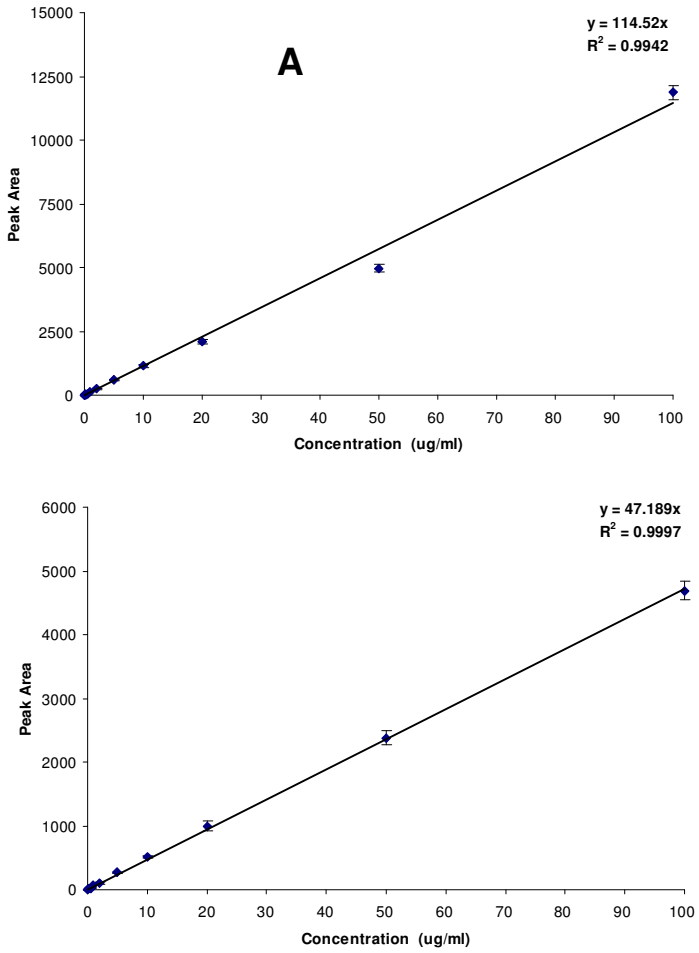


Figure 4.17: Chart showing a typical dexamethasone standard curve. The peak area of various concentrations of (A) PBS and (B) acetonitrile solutions of dexamethasone (0.2µg/ml - 100µg/ml) was determined by HPLC-UV and plotted against the corresponding concentration. Values plotted on the chart are average values obtained from three different independent experiments (i.e. N = 3 ± Standard deviation). These standard curves were used in experiments for determination of the release kinetics and entrapment efficiency of dexamethasone loaded microspheres respectiively

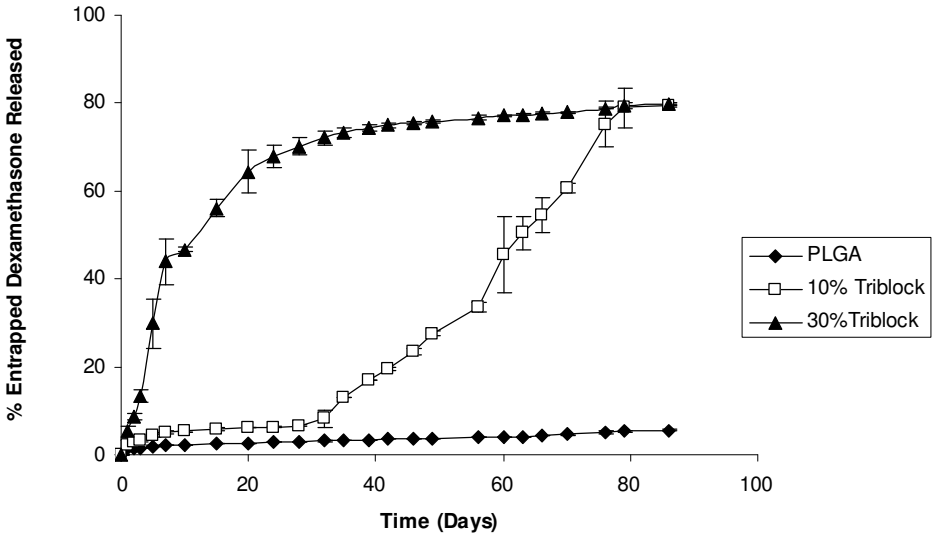


Figure 4.18: Chart showing the effect of triblock co-polymer on the release kinetics of dexamethasone. Dexamethasone loaded (5% w/w) microspheres made from PLGA; and lends of PLGA containing 10% w/w and 30% w/w of triblock. For each blend, the release kinetics of dexamethasone from 20mg of dexamethasone loaded microspheres was investigated using the flow chamber at 37ºC. The eluent was harvested at various time points and the amount of dexamethasone released was quantified using HPLC-UV. Values plotted on the chart are average values obtained from three different independent experiments (i.e. N = 3 ± Standard deviation).

extending from the 2nd day until the 32nd day, after which rapid release of dexamethasone occurred until day 90 of the controlled experiments. However microspheres made from 30% triblock showed a zero order kinetic release profile from day 2 onwards until day 32 in which complete release of entrapped dexamethasone had occurred.

Release kinetics of microspheres are the kinetic models that best reflect the release mechanisms of protein or drugs from microspheres (Wu et al., 2002). Hence zero-order release equation (Eq. 4.1), and Higuchi equation ( Eq. 4.2) were applied to process the controlled release data to find the equation with the best fit The best fit equation indicates the kinetic model representing the mechanism of release (Moore and James, 1996).

Equation 4.1 $Q=k_1t$

Equation 4.2 $Q=k_2(t)^{0.5}$

Where $Q$ is the release percentage at time $t$. The $k_1$ and $k_2$ are the rate constant of zero-order, and Higuchi order model, respectively.

By fitting the controlled release data of lysozyme from the triblock blends to the Higuchi and zero order release models, the mechanism governing the release kinetic profile was obtained. Higuchi model describes the release of the drug from polymer matrices through diffusion due to pore formation. The model proposes that after the initial release of the drug from the polymer surface, a progressively thicker drug depleted area around the polymer surface forms. This leads to a decrease in the initial rate of drug release, as the remaining drug must diffuse through the progressively thickened drug depleted polymer membrane (Higuchi 1981). While the zero order

release model describes polymer matrices where drug release is independent of its concentration, and proposes that polymer erosion plays the dominant role in drug release from polymer matrices (Najib and Suleiman, 1985). The release kinetics of lysozyme and dexamethasone released from PLGA and blends containing 30% w/w triblock can be best fitted to the Higuchi's model, whilst that of microspheres made from the other blends containing 5 - 20% w/w of triblock can be best fitted to a zero order kinetic model (Fig. 4.19 and Table 4.3).

### 4.4.9. Effect of released dexamethasone on osteogenic induction of murine embryonic stem cells.

Scaffolds were fabricated from 5.0% w/w dexamethasone loaded microspheres from PLGA, 10% and 30% triblock by sintering 100mg microspheres in a Teflon mould at 60ºC for 3hours. These scaffolds were used to investigate its effect on induction of osteogenesis in murine embryonic stem cells. Dexamethasone loaded scaffolds from PLGA, 10% and 30% triblock were fabricated and washed in PBS for 0, 3, 7 & 14 days prior to use in the experiment. mES cells were seeded on the scaffolds and cultured on the scaffold for 28 days, prior to analysis. An increase in the duration of the washout period of the dexamethasone loaded scaffolds (for 10% and 30% triblock) resulted in an increase in cell viability and apparent cell differentiation, as indicated by the increase in Alamar blue values and alkaline phosphatase activity respectively (Fig 4.20). In addition, an increase in calcium deposits, as indicated by alizarin red staining for bone mineralization, with an increase in the duration of the washout period of dexamethasone loaded scaffolds (made from 30% triblock) was detected (Fig 4.21).

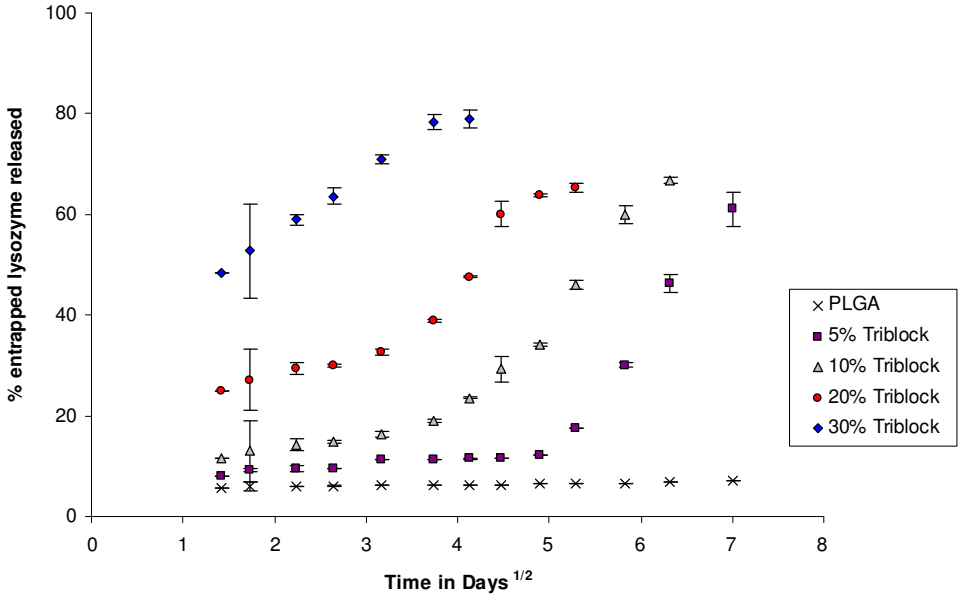


Figure 4.19: Higuchi's plot showing the effect of triblock co-polymer on the release kinetics of lysozyme. 5.0% lysozyme loaded microspheres made from PLGA; and PLGA containing 5% w/w; 10-% w/w; 20% w/w and 30% w/w triblock blends. Higuchi's plot was obtained by plotting cumulative release against square root of time in days Values plotted on the chart are average values obtained from three different independent experiments (i.e. N = 3 ± Standard deviation).

| **Polymer Blend** | **Lag Phase (R2)** | | **Release Phase (R2)** | | **Overall (R2)** | |
|---|---|---|---|---|---|---|
| | Zero - order | Higuchi | Zero - order | Higuchi | Zero - order | Higuchi |
| PLGA | 0.8552 | 0.9202 | - | - | 0.9512 | 0.9526 |
| 5% Triblock | 0.8632 | 0.924 | 0.9804 | 0.9873 | 0.8025 | 0.6527 |
| 10% Triblock | 0.9581 | 0.982 | 0.9797 | 0.953 | 0.9456 | 0.8464 |
| 20% Triblock | 0.9553 | 0.9553 | 0.9554 | 0.9299 | 0.9543 | 0.9052 |
| 30% Triblock | - | - | 0.9851 | 0.9993 | 0.985 | 0.989 |

Table 4.3: Table showing the R2 linear regression values of Higuchi's plot and Zero-order model for lysozyme released from PLGA + triblock blend microspheres during the period of sustained release. Lag phase was chosen as period over which less than 1% w/w of entrapped lysozyme was released over a 3 day period. Release phase is period of sustained release after the initial burst phase in which over 1% w/w of entrapped protein is released over a 3 day period. Overall is total duration of protein release including both lag and release phases. No lag phase was observed for blends containing 30% w/w triblock, whilst no period of sustained release was observed after the initial burst phase during the 60 day sampling period. Hence no R2 values were recorded for these blends. Values indicated in the table are average values obtained from three different independent experiments (i.e. N = 3 ± Standard deviation).

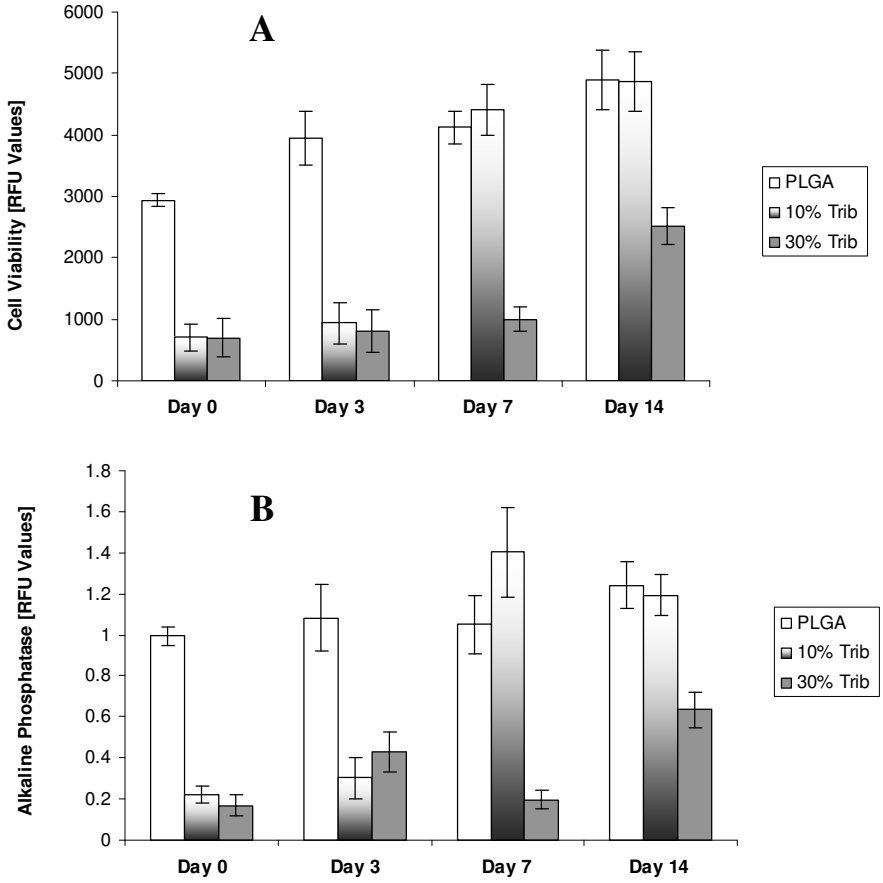


Figure 4.20: Chart showing the effect of dexamethasone released from dexamethasone loaded scaffolds containing different triblock compositions on the viability of murine embryonic stem (mES) cells seeded on PLGA scaffolds. A) Cellular metabolic activity measurement; B) Measure of alkaline phosphatase enzyme activity. Scaffolds were fabricated by sintering dexamethasone loaded microspheres at 60ºC in a teflon mould. mES cells were seeded onto the scaffolds and seeded scaffolds were cultured for 28 days in media supplemented with 50µg/ml ascorbate and 10mM β-glycerophosphate. Alkaline phosphatase enzyme activity was measured by incubating scaffolds in solution containing 1.0 mg/ml p-Nitrophenyl phosphate (pNPP) in 0.2 M Tris buffer for 20 minutes. The supernatant was harvested and absorbance read at 405nm. Cellular metabolic activity as indirect measure of cell viaility of cells seeded on the scaffolds was determined using alamar blue

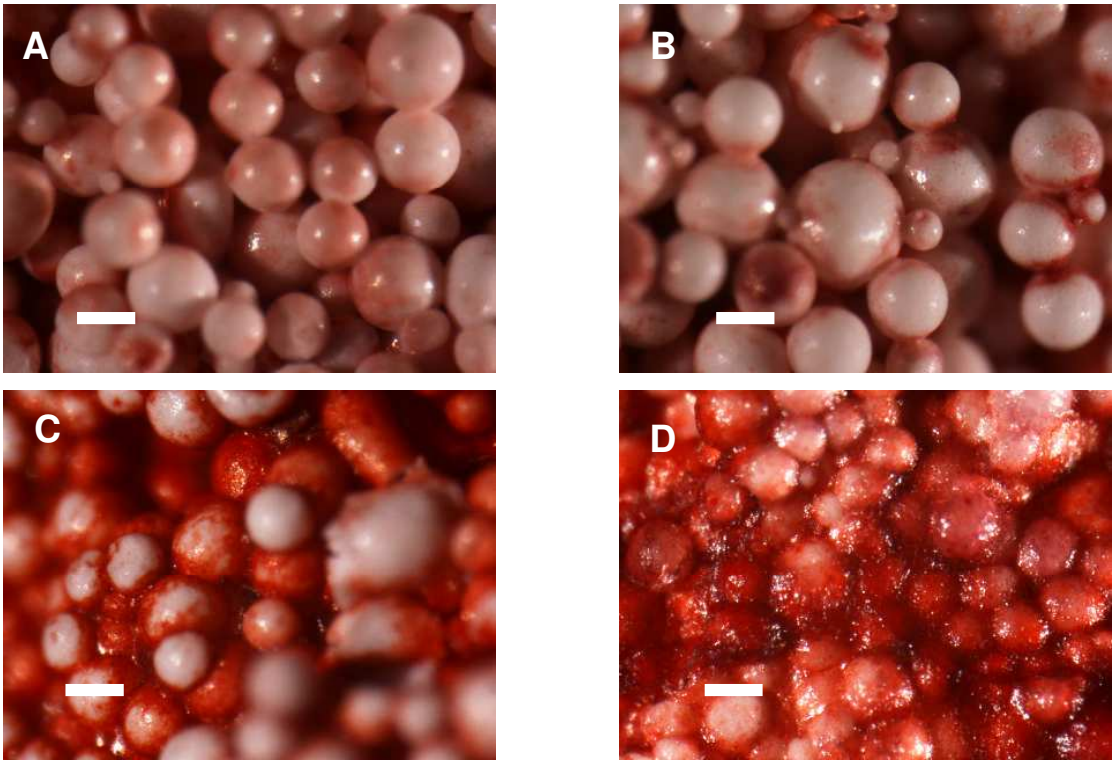


Figure 4.21: Micrographs showing regions of calcium deposits on mES seeded dexamethasone loaded scaffolds. Prior to mES cell seeding, scaffolds were pre-washed by incubating in PBS for (A) O; (B) 3; (C) 7 and (D) 14 days. Seeded scaffolds were cultured for 28 days, after which they were stained for calcium deposits by incubating paraformaldehyde fixed scaffolds in 2% w/v Alizarin red solution for 15 mins. Scale bar is 200µm.

The results in Fig 4.20 can be explained by observing the theoretical amount of dexamethasone the cells on the scaffolds will be exposed to assuming the release kinetics of the scaffolds are similar to that of the microspheres (Fig 4.17) based on the controlled release experiments. As can be observed in Fig 4.22, the theoretical maximum amount of dexamethasone the cells seeded on scaffolds from 10 and 30% triblock with washout periods of 0,3, 7 & 14 days respectively were exposed to was higher than the toxic limit of dexamethasone (>1µM with an upper limit of 10µM) (Fig 4.23) for murine embryonic stem cells. While cells seeded on PLGA scaffolds would be theoretically exposed to a dexamethasone concentration range necessary for osteogenesis induction. Thus indicating that the amount of dexamethasone released for the 10% and 30% triblock at the earlier washout periods exceeded the toxic level of dexamethasone and as such killed the cells, while at later washout periods (7, & 14) the remaining viable cells were inducted along osteogenic pathways.

### 4.4.10. Effect of loading weight of dexamethasone on entrapment efficiency and release kinetics.

The effect of loading weight on the entrapment efficiency and release kinetics was investigated. PLGA and 30% triblock were used for the entrapment efficiency and release kinetics studies respectively. Fig 4.24 shows that by increasing the loading weight of dexamethasone, the entrapment efficiency is increased for both PLGA (Fig 4.24A) and 30% triblock based microspheres (Fig 4.24B). This could possibly be due to the hydrophobicity of dexamethasone limiting the amount of drug that leaches out during microsphere fabrication. Controlled release experiments showed no difference in the release kinetics when varying the loading weight of the dexamethasone within the microspheres (Fig 4.25).

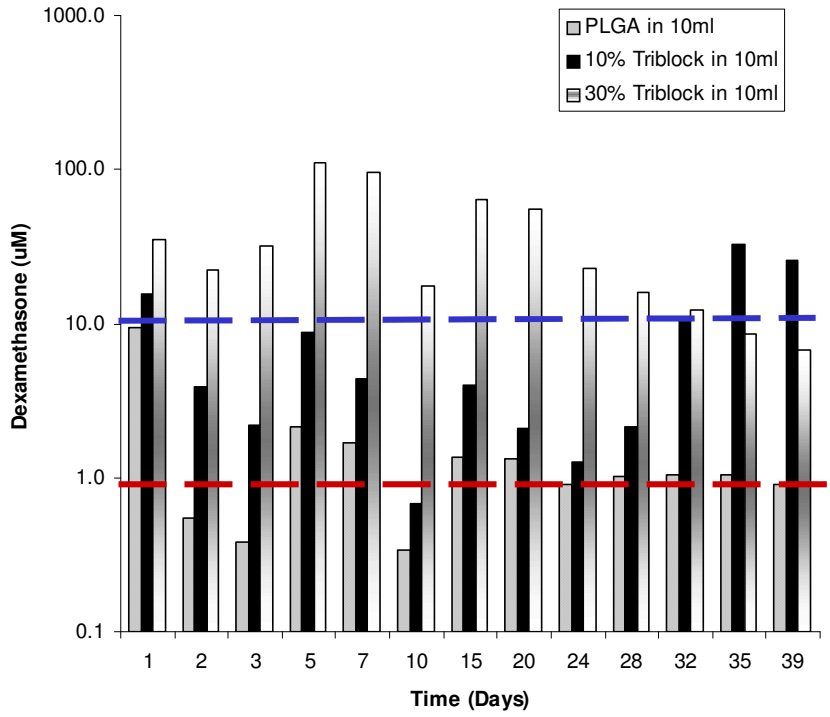


Figure 4.22: Chart showing the theoretical concentration (based on extrapolated microsphere release kinetics results) mES cultured on Dex loaded scaffolds are exposed to. Red broken lines represents the concentration of dexamethasone below which osteogenic differentiation of mES cells was successfully induced, and represents the lower limit of dexamethasone concentration for which becomes toxic to mES cells. Blue dotted line represents the dexamethasone concentration above which becomes toxic to cells.

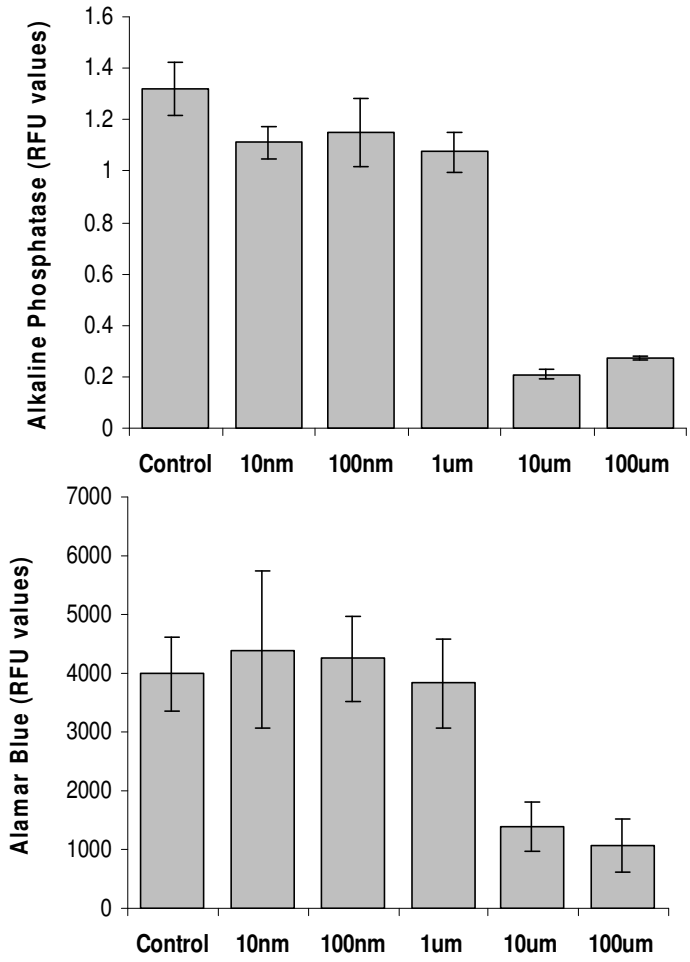


Figure 4.23: Chart showing the effect of dexamethasone concentration on the viability of murine embryonic stem (mES) cells seeded on PLGA scaffolds. A) Measure of alkaline phosphatase enzyme activity; B) Cell metabolic activity measurement. PLGA scaffolds were fabricated by sintering PLGA microspheres at 60ºC in a teflon mould. mES cells were seeded onto the scaffolds and seeded scaffolds were cultured for 28 days in media supplemented with 50µg/ml ascorbate and 10mM β-glycerophosphate and varying concentrations of dexamethasone ranging from 0 (control) to 100µM. Alkaline phosphatase enzyme activity was measured by incubating scaffolds in solution containing 1.0 mg/ml p-Nitrophenyl phosphate (pNPP) in 0.2 M Tris buffer for 20 minutes. The supernatant was harvested and absorbance read at 405nm. Cell viability of cells seeded on the scaffolds was determined using alamar blue

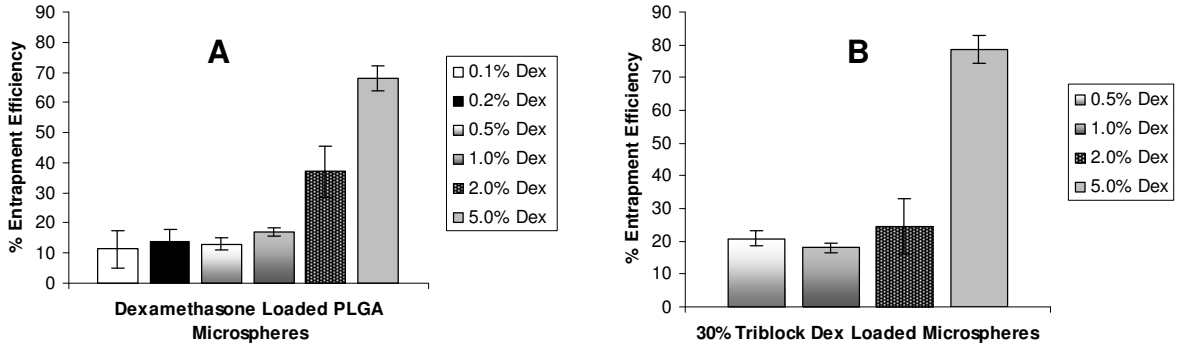


Fig 4.24: Chart showing the effect of loading weight on the entrapment efficiency of dexamethasone. (A) Dex loaded PLGA microspheres; and (B) Dex loaded 30% Triblock microspheres. For (A) 1mg, 2mg, and (A) & (B) 5mg, 10mg, 20mg, and 50mg of dexamethasone was loaded into microspheres to yield 0.1%, 0.2%, 0.5%, 1%, 2%, and 5% w/w dexamethasone loaded microspheres. The amount of dexamethasone remaining in the microspheres was determined by dissolving the microspheres in acetonitrile, and quantified by assaying using HPLC-UV. Entrapment efficiency values were obtained by expressing the dexamethasone retained within the microspheres as a percentage of the initial amount of dexamethasone loaded. Values plotted on the chart are average values obtained from three different independent experiments carried out (i.e. N = 3 ± Standard deviation).

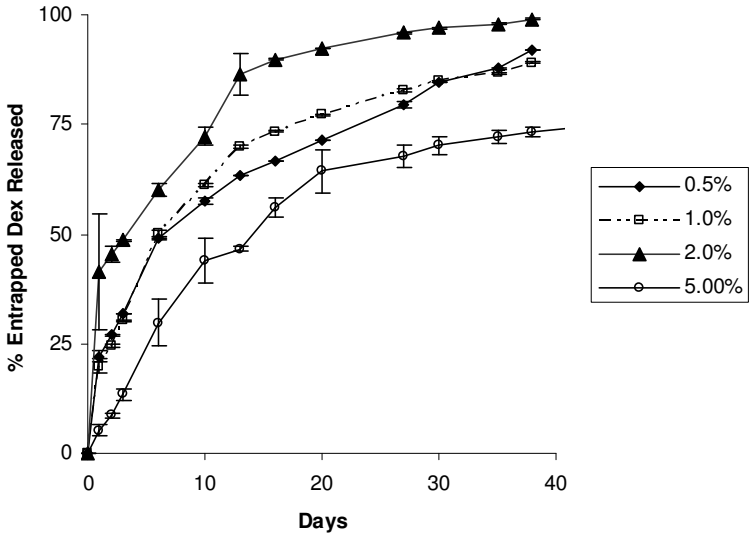


Figure 4.25: Chart showing the effect of loading weight on the release kinetics of dexamethasone. 5mg, 10mg, 20mg, and 50mg of dexamethasone was loaded into microspheres made from PLGA containing 30% w/w triblock blends to form 0.5%; 1.0%; 2.0% and 5.0% w/w dexamethasone loaded microspheres. For each loading weight, the release kinetics of dexamethasone from 20mg of dexamethasone loaded microspheres was investigated using the flow chamber at 37ºC. The eluent was harvested at various time points and the amount of dexamethasone released was quantified using HPLC-UV. Values plotted on the chart are average values obtained from three different independent experiments (i.e. N = 3 ± Standard deviation).

### 4.4.11. The effect of mixing microspheres of blends of different triblock composition on dexamethasone release kinetics.

The effect of mixing dexamethasone-loaded microspheres made from 10% triblock and 30% triblock blends on the release kinetics was investigated. Controlled release experiments of dexamethasone from microspheres into PBS were performed, using mixtures of 5.0% dex loaded microspheres made from 10% and 30% triblock in the following proportions, 0/100; 25/75; 50/50; 75/25 and 100/0 (10% / 30% triblock). Fig 4.26 shows that a positive correlation exists with increasing amount of 30% triblock microspheres and release rate of dexamethasone. Although the 25/75 mixture seems to be an anomaly with an initial high release rate in the first 12 days occurring and then levelling out later on. The results from the controlled release experiment suggest that both the 30% and 10% triblock microspheres released their contents independently

### 4.4.12. PLGA + Triblock Microspheres Incubation.

A series of triblock microsphere degradation experiments were undertaken to determine the mechanism driving the increased rate of release of dexamethasone and lysozyme from the microspheres. 10% triblock and 30% w/w triblock microspheres were incubated in PBS for 28 days, and the amount of triblock remaining after the experiment as a percentage of the amount initially present before start of experiment was determined using $^{1}H$ NMR analysis. These experiments were undertaken to determine if the improved release kinetics of dexamethasone and lysozyme from the loaded triblock microspheres were as a result of increased rate of bulk polymer degradation or increased formation of aqueous channels in microspheres due to selective dissolution of the hydrophilic triblock co-polymer. The results showed that

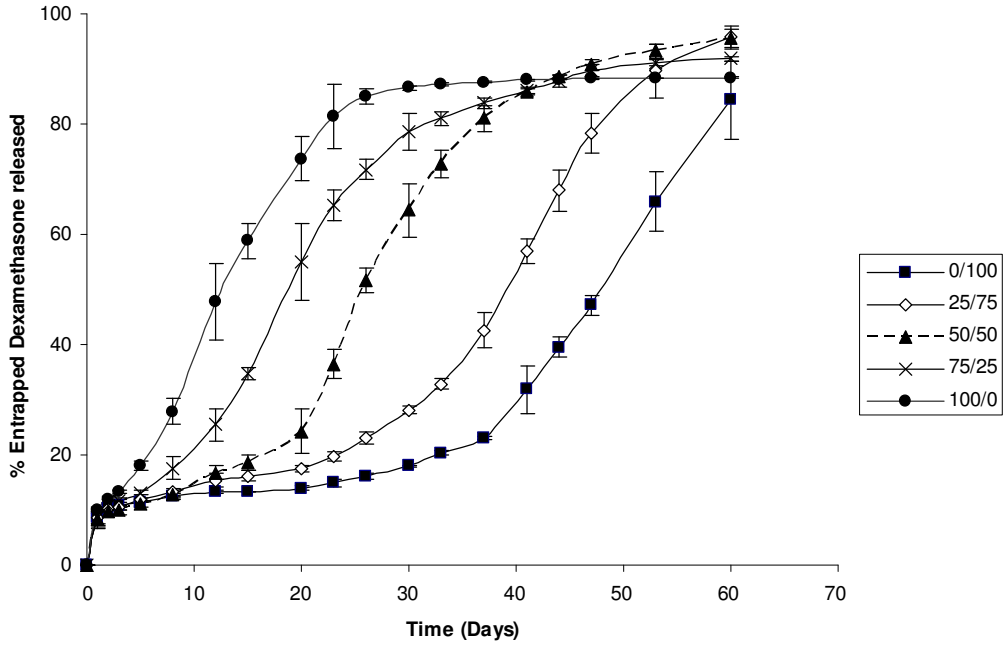


Figure 4.26: Chart showing the effect of mixing 10% and 30%w/w triblock dexamethasone loaded microspheres on the release kinetics of dexamethasone. 5.0% dexamethasone loaded microspheres made from PLGA containing 10-% w/w; and 30% w/w triblock blends was mixed together in various proportions (0/100; 25/75; 50/50; 75/25; and 100/0). For each blend, the release kinetics of dexamethasone from 20mg of dexamethasone loaded microspheres was investigated over a 60 day period using the flow chamber at 37ºC. The eluent was harvested at various time points and the amount of dexamethasone released was quantified using HPLC-UV. Values plotted on the chart are average values obtained from three different independent experiments (i.e. N = 3 ± Standard deviation).

there was a significant decrease in amount of triblock remaining in microspheres after 28 days of incubation in PBS for both 10% triblock (65.08 ± 0.77% vs. 98.41 ± 0.14%) and 30% triblock microspheres (55.80 ± 2.01% vs. 87.29 ± 2.78%) when compared against microspheres prior to incubation in PBS. However, no significant difference in the amount of triblock remaining in microspheres was observed with 10% triblock (98.41 ± 0.14%vs. 98.41 ± 0.77% and 98.41 ± 0.66%) and 30% triblock (87.29 ± 2.78% vs. 82.87 ± 1.41% and 86.19 ± 4.42%) microspheres before and after 7 and 14 days of PBS incubation (Fig 4.27).

## 4.5. Discussion

The aim of this chapter was three fold: (a) to investigate the parameters that affect the entrapment and release of proteins and drugs from biodegradable polymeric microspheres; (b) improve the release kinetics of proteins and drugs from PLGA microspheres through the incorporation of the triblock co-polymer; and (c) determine the mechanism by which the triblock facilitates the release of proteins and drug molecules from microspheres. In addition to these aims the effects of heat sintering on the activity of entrapped proteins was also investigated to provide more information on the temperature at which we can sinter protein loaded scaffolds. It was anticipated that the successful achievement of these aims and understanding of these effects will enable us develop growth loaded microsphere based scaffolds for tissue engineering applications. The successful entrapment of protein within polymeric microspheres has been shown to be determined by the method of microsphere fabrication (Suciati, 2006; Castellanos et al 2002); loading weight (Mundgari et al 2007); and the presence of excipients such as poly (ethylene glycol), sucrose and glycerol (Gu et al., 2007).

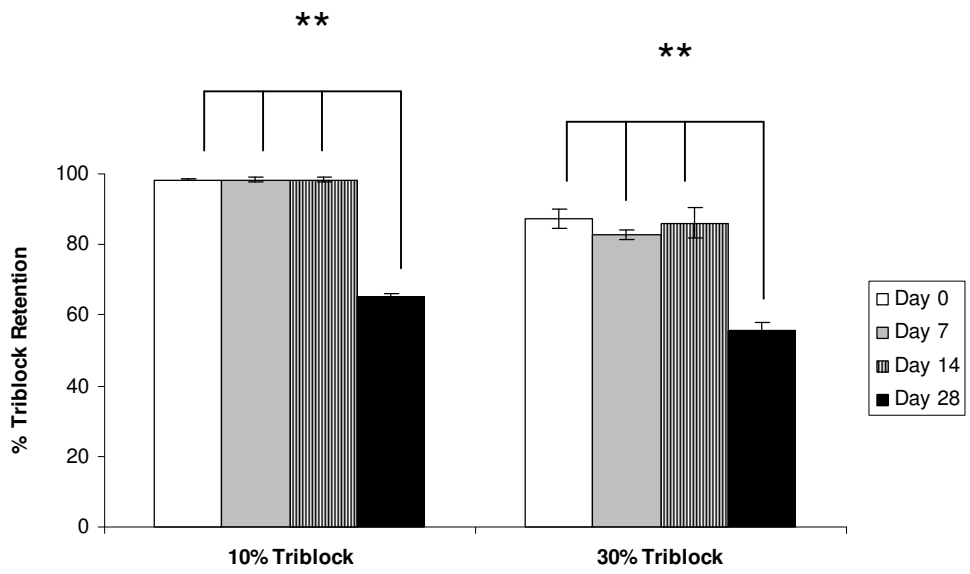


Figure 4.27: Chart showing the effect of microsphere incubation in PBS on microsphere triblock content.1H NMR analysis was used to investigate the effect of microsphere incubation in PBS on microsphere triblock content. Microspheres made from PLGA blends containing 10% w/w and 30% w/w triblock were incubated in PBS solution with mild agitation at 37ºC for 0, 7, 14 and 28 days. The % triblock retention was obtained by comparing the mole ratio of PEG: LA (PEG: Lactide) of triblock blend against that of the microspheres from the triblock blend. The PEG: LA mole ratio was obtained by comparing the ratio of normalised (to the number of H (4 and 3 respectively) within the monomer) integrated values for the signals specific to CH2CH2 (PEG) to that of CH3 (lactide) monomers located at 3.65ppm and 1.60ppm respectively. No significant difference in % triblock retention was observed for varying triblock composition, but a significant decrease in triblock remaining in microspheres after 28 days of microsphere incubation in PBS was observed. Values plotted on the chart are average values obtained from three different independent experiments carried out (i.e. N = 3 ± Standard deviation).

The double emulsion method is the most common technique used to encapsulate proteins within microspheres. The double emulsion method involves dissolving the MOI into water, followed by the dispersion of this in an organic solution containing the polymer – leading to the formation of the primary W/O emulsion. The final O/W emulsion is formed by dispersion of the primary emulsion in an aqueous medium containing stabilizers such as poly (vinyl alcohol) (PVA) or poly (ethylene glycol) (PEG), under continuous mechanical agitation. However despite the wide use of this technique, the shear force used in making the primary emulsion results in protein aggregation at the water oil interface. This occurs due to unfolding of the protein molecules leading to protein aggregation (by exposure and interaction of hydrophobic groups) and inactivation (by exposure of buried reactive groups) (Putney and Burke 1998). This leads to reduced activity of the protein.

The solid-in-oil-in-water (s/o/w) technique was developed as an alternative to the double emulsion technique because through the avoidance of the primary water/oil emulsion step there is a reduced risk of protein inactivation at the water oil interface (Castellanos et al, 2001; Castellanos et al 2001; King and Patrick 2000; Morita et al, 2000). This procedure involves the suspension of protein (in its solid form) in the organic solvent of choice to form a solid-in-oil suspension. Proteins in solid form have been shown to have a drastically reduced conformational mobility (Griebenow et al., 2001). As a result, large structural changes are prohibited because the proteins are kinetically trapped in their native conformation (Griebenow and Klibanov 1996; Griebenow et al, 1999; Griebenow et al., 2001).

Despite the improved entrapment efficiency of proteins obtained with the S/O/W emulsion method, 100% entrapment efficiency has still not yet been achieved. Two reasons have so far been implicated for this. Firstly, protein aggregation and inactivation upon S/O/W encapsulation also occurs during the organic solvent/water emulsion step (Castellanos and Griebenow 2003; Castellanous et al 2005; Castellanous et al 2003). At the organic solvent / water interface, the conformational mobility of the protein molecule will increase due to the contact with water (Griebenow and Klibanov 1996). This change in conformation could result in the denaturation and aggregation of the protein (Castellanos and Griebenow, 2003) causing a loss of their therapeutic effect and possible promotion of immune reactions that can cause anaphylactic shock (Wischke and Schwendeman, 2008).

Secondly, another contribution to the decreased entrapment efficiency is the possible rehydration of protein molecules due to the diffusion of water into organic solvent droplets during the microsphere hardening step. It is believed that the rehydrated protein would leach out of the organic droplets, down the concentration gradient, through aqueous channels into the aqueous hardening bath. The aqueous channels in the organic droplets could be formed due to the ingress of the aqueous water from the hardening bath into the hardening organic droplet (Castellanous and Grienenow 2003). The first part of this chapter was aimed at investigating the parameters influencing the entrapment of proteins and drugs within PLGA microspheres fabricated using S/O/W technique.

The first parameter investigated was the effect of micronisation on the entrapment efficiency of the protein. Micronisation of proteins prior to entrapment within

microspheres has been shown to be important for achieving high entrapment efficiencies (Putney and Burke 1998; Morita et al., 2000). Based on this, it was hypothesized that one of the reasons for decreased entrapment efficiency of the protein during S/O/W fabrication, could be that during the emulsion formation step, the solid protein (due to the particle size) could be concentrated at the water-oil interface during homogenization (or vortexing). By reducing the size of the solid protein particles, the protein could be better dispersed within the oil droplets leading to greater entrapment.

The results showed that micronising proteins co-lyophilised with PEG led to an increase in entrapment efficiency. The micronisation process has been shown to be an important step in the formation of protein loaded microspheres (Morita et al., 2001). Co-lyophilisation of proteins with PEG has been shown to result in the formation of spherical micro-domains with micronized protein particles within a continuous phase of PEG (Morita et al., 2001). The differences in the entrapment efficiencies between the micronized and the unmicronised protein can be attributed to the following reasons. Firstly, the increased surface area of the protein following micronisation could lead to an increased interaction of the protein with the polymer and improved dispersion in the organic polymer solution. The improved dispersion within the organic polymer solution reduces the leaching out of the protein into the aqueous water bath during microsphere fabrication. Secondly, co-lyophilising the protein with PEG has been previously demonstrated to improve the stability of proteins by preventing direct contact of the protein with hydrophobic interfaces during microsphere preparation (Castellanous et al 2002; 2003). Several studies have also shown that the addition of water soluble additives such as sugars, PEG and polyols

have positive effects on protein protection by increasing the Gibbs free energy of unfolding proteins when added into the polymer formulation. The unfolding of protein has been shown to be a key step for protein aggregation and inactivation (Lam et al, 2001; van der Weert et al, 2000; Gu et al 2007). In addition, the presence of PEG has recently been shown to reduce the migration of proteins to the water-oil interface and out of the droplets during the microsphere hardening step (Malzert-Freon et al, 2008).

The second parameter investigated was the effect of loading weight of different proteins and drugs on the entrapment efficiency. In this study, the protein:PEG ratio was kept as a constant as the microspheres fabricated were intended for use in a further experiment (the effect of loading weight on release kinetics). The increase in loading weight resulted in a decrease in the entrapment efficiency of the proteins within microspheres. These results are in agreement with the results obtained from many studies reported in the literature (Yang et al 2001; Sun et al, 2003; Kang and Singh 2001; Gu et al., 2007). The reduction in entrapment efficiency with increasing loading weight of protein has been attributed to this higher protein loading leading to a higher concentration gradient between the organic phase and the external water phase (Gu et al., 2007). Another explanation for this observed effect is that by increasing the amount of protein within the organic phase there is an increase in the hydrophobic contacts between the protein and the polymer leading to an increased rate of protein unfolding and aggregation (Crotts and Park 1997; Gaspar et al., 1999). These denatured protein and aggregates are not successfully entrapped within the microspheres. Further experiments undertaken to investigate the most likely steps where protein loss occurs indicated that the increased concentration gradient between either the organic phase and the external water phase or the organic droplets and water

phase of the hardening bath during the microsphere hardening process contributes the most to the reduced entrapment efficiency.

Based on the indication that the interaction of proteins with polymers had an effect on the entrapment efficiency (Crotts and Park 1997; Gaspar et al., 1999), the effect of different polymers and PLGA compositions on the entrapment efficiency of trypsin was investigated. Increasing the LA:GA ratio of PLGA polymers from 50:50 to 75:25 resulted in a significant increase in the entrapment efficiency of trypsin. However no significant increase (or decrease) in entrapment efficiency was observed on increasing the LA:GA ratio from 75:25 to 100:0. On the other hand encapsulating the protein in poly(caprolactone) instead of PLGA resulted in an decrease in the entrapment efficiency of the protein. These results seemed to suggest an optimum level of 'hydrophobicity' is necessary for good protein entrapment. Polymers below this level of hydrophobicity might not form a sufficient barrier to prevent leaching of the protein out of the forming microspheres. On the other hand, above this level of hydrophobicity, the hydrophobic interactions between the polymer and the protein might be deleterious to the stability of the entrapped protein Although these results were obtained using trypsin as a model protein, the trends should be applicable to other proteins albeit with different optimum levels of hydrophobicity.

Loading weight seemed to have a reverse effect on the entrapment efficiency of dexamethasone within PLGA microspheres (compared to proteins). The high entrapment efficiency of dexamethasone obtained (at the 5% w/w loading weight) could be explained by the partitioning of the dexamethasone molecule into the oil phase (Huang et al., 2006). These results are similar to results obtained by Mundgari

and co-workers, in which increasing the loading of doxycycline into PLGA microspheres from 30 to 60% led to an increase in entrapment efficiency from 15.3 ± 0.3 to 17.6 ± 0.4% (Mundgari et al 2007). This partitioning effect, coupled with the decreased solubility of dexamethasone in water (which is 100ug/ml although in the presence of 0.3% PVA, the solubility might be significantly increased; Giunchedi et al., 1998; Merck Index, 2006; Wischke and Schwendeman 2008), could reduce the diffusion of dexamethasone along the concentration gradient from the microspheres into the hardening bath during the microsphere hardening step, leading to a higher entrapment efficiency. On the other hand, reducing entrapment efficiency with reducing loading weight could be attributed to the increased proportion of the dexamethasone that has leached out into the hardening bath. This is based on the assumption that the diffusion of the dexamethasone along the concentration gradient is limited by the rate at which the hardening bath reaches its saturation point. Thus, the proportion of dexamethasone leaching out of the microspheres will increase as the loading weight decreases.

The second part of this chapter was to investigate the factors influencing the release kinetics of proteins and drugs from microspheres, again the effects of loading weight and polymer type was investigated.

The controlled release experiment indicated that loading weight has an effect on both the initial burst release and overall release rate. The release kinetics of the 1.0% and 2.0% w/w lysozyme loaded microspheres showed a similar pattern. However a significant increase in both the burst release and release rate was observed on increasing the lysozyme loading weight from 2.0% to 2.5% w/w. The exact rationale

behind this is not yet known. It has been shown that increasing the loading weight of proteins and water-soluble drugs above a critical loading weight results in a non-linear increase in both the initial burst release and release rate of the proteins (Luan et al., 2006 and Ravivarapu et al., 2000b).

The microspheres exhibited an incomplete release with only approximately 20% of the total lysozyme released after 40 days for the 1.0 and 2.0% w/w loading weights. While the amount of lysozyme released from microspheres of the 2.5% protein loading weight was about 42%. After 40 days, the remaining microspheres were analyzed for the unreleased protein content. Protein content measurements indicated that 84.3 ± 2.2%, 69 ± 3.2% and 64.3 ± 1.25% of active lysozyme remained within the 1%, 2% and 2.5% loaded microspheres respectively. This incomplete release has been frequently observed with proteins (Kim & Park 1999). Interactions between PLGA and encapsulated proteins have been indicated as possible causes of incomplete protein release in in-vitro controlled release experiments (Weert et al., 2000). Park et al., 1998 attributed the incomplete release of proteins from microspheres to non-covalent aggregation and surface adsorption of lysozyme within the microspheres. However the insignificant adsorption of lysozyme onto the PLGA microspheres observed in the adsorption studies presented here (section 4.4.5) contradicts the findings of Park and co-workers.

Electrostatic interactions of the polymer with the protein, has also been shown to play an important role in protein release from PLGA microspheres. Blanco and Alonso (1998) compared the release rate of bovine serum albumin (BSA) from microspheres consisting of PLGA with uncapped (i.e. free carboxylic groups) and capped

carboxylic end groups. They observed a significantly slower release rate from the microspheres with uncapped carboxylic end groups. Park et al showed that electrostatic interactions between lysozyme and the free carboxylic end groups mainly controlled the initial release of lysozyme from uncapped PLGA microspheres. Non-covalent and hydrophobic protein polymer contacts were responsible for the overall incomplete protein release observed (Park et al., 1998; Weert et al., 2000).

Proteins are generally inactivated during release from fast degrading polymer microspheres due to the very acidic environment within the microspheres (Sandrap and Moes, 1996; Fu et al., 2000). However, the release induced inactivation of the lysozyme was limited as indicated by the retention of activity and structural integrity as indicated by the SDS Page. The use of slow degrading PLGA microspheres (with high molecular weight PLGA; 145kD) and the presence of microchannels due to the quick released triblock co-polymer (Jiang and Schwendeman, 2001) could prevent acid built-up within the microspheres thereby preserving the protein structure.

The successful incorporation and release of proteins from microspheres fabricated from biodegradable polymers such as PLGA and PLA has been widely investigated for production of sustained release formulations for protein administration (Rocha et al., 2008; Goraltchonk et al., 2006; and Kim et al., 2004). However, despite achieving success in utilizing microspheres as a sustained delivery device of active protein, challenges still exist in developing microspheres with an ideal (zero-order) controlled release profile. The release profile of active protein from PLGA microspheres has been shown to follow a tri-phasic pattern: an initial burst release; lag phase and a phase of continuous release (Porjazoska et al., 2004; and Zolnik et al., 2007). The

duration of the lag phase, where there is little or no release, is dependent on both the rate of diffusion of the protein through the intact polymer (PLGA) and the rate of polymer bulk degradation (Kim et al., 2004). An approach taken in this study to meet this challenge involved blending of a hydrophilic polymer with the PLGA blend in order to improve the rate of polymer degradation and diffusion of protein through the polymer barrier. It was hypothesised that the presence of a hydrophilic polymer within the PLGA microsphere would result in increased hydration of the polymer, accelerate the rate of degradation and possibly reduce the tortuousness of the protein diffusion pathway through the formation of aqueous channels. All of which would contribute to a reduction in the duration of the lag phase and an acceleration of rate of protein release.

By modifying the hydrophilic properties of PLGA through blending with various compositions of triblock, microspheres with attenuable release properties were developed. Entrapment of lysozyme and dexamethasone within the microspheres made from blends of PLGA and triblock resulted in entrapment efficiencies of >50% for both the dexamethasone and active protein with no observable degradation or denaturation of the protein as determined by the SDS PAGE. These high entrapment efficiencies observed and maintenance of the structural integrity is in line with results obtained by Morita and co-workers. (Morita et al., 2001).

Following the encapsulation of drugs and proteins and investigation of parameters affecting the release kinetics, the effect of triblock on the controlled release of dexamethasone (a model hydrophobic drug) and lysozyme (a model protein) from microspheres was investigated. The initial burst release of lysozyme and

dexamethasone increased with increasing triblock concentration. A high initial burst release of proteins generally results from the diffusion of the proteins at the surface of the microspheres which are adsorbed during the microsphere hardening step (Pean et al., 1999). In this study, the high increasing initial burst release could be attributed to the protein entrapped within the hydrophilic triblock polymer portion of the microspheres or due to the triblock polymer dissolving in the release medium leaving aqueous channels through which the release medium penetrates the microspheres quickly to release the protein/drug. Another explanation, could be the increasing rate of hydration of the microspheres with increasing triblock composition (Jiang and Scwendeman, 2001; Kim and Park, 2004).

Controlled release experiments conducted using various PLGA/triblock blends showed that increasing the proportion of triblock within the blends resulted in a reduction in duration of the lag phase. The release profile of lysozyme from microspheres made from PLGA (Mw 118kDa (85:15)) indicated little initial burst release (4.8 ± 0.9%) with little further release over the next 60 days (3.8± 0.3%). This can be attributed to the poor hydrophilic and degradation properties of the PLGA polymer. Its high molecular weight and lactide content corresponds to a reduced likelihood for surface hydration, polymer bulk degradation and ultimately poor protein release kinetics. By incorporating the hydrophilic triblock copolymer PLGA-PEG-PLGA within the microspheres, an increase in the initial burst release and reduction in the lag phase and duration of release was observed.

In addition to acceleration of initial drug release and the reduction in lag phase duration, the presence of the triblock co-polymer in the microspheres resulted in a

change of the overall release kinetics. Using linear regression of data plotted in the Higuchi's plot and the zero-order kinetic models indicating diffusion mediated and polymer degradation mediated release respectively, the values suggest that with the incorporation of triblock, the release of lysozyme from the microspheres is due to an increase in both the rate of protein diffusion and rate of polymer degradation. The increase in the diffusion rate of proteins and degradation of polymers with increased triblock composition could be explained by the selective dissolution of the triblock out of the microspheres (Fig. 4.23) leaving channels for further ingress of controlled release medium into the microspheres. These results are similar to that observed by Morita et al. (Morita et al., 2001) in which the zero order release profiles were obtained when the ampiphilic polymers PEG and pluronic were individually co-dissolved with PLGA / PLA to form bovine serum albumin (BSA) loaded microspheres.

Another contributory factor possibly influencing the release kinetics of lysozyme and dexamethasone from microspheres made from the triblock blend is the presence of micelles containing entrapped lysozyme and dexamethasone formed by the triblock polymer chains that leached out from the microspheres. Although the presence of micelles within the PBS environment the microspheres were incubated in was not determined, amphiphilic triblock copolymers with hydrophobic end-groups and hydrophilic midblocks have been shown to self-assemble into micellar systems with the hydrophobic end chains packing themselves into a condensed core surrounded by a swollen hydrophobic corona, when placed in an aqueous environment (Semenov et al., 1995; Liu et al., 1999; Jeong et al., 2000). As the polymer concentration of the solution increases the hydrophobic end moieties associate with the neighbouring

micelles to form a network of cross-linked micelles or large aggregates. In work carried out by Agrawal and co workers, micellar solutions of PLA–PEO–PLA was demonstrated to yield a zero order continuous release kinetic profile for the hydrophobic drugs sulindac and tetracaine. The rate of drug release was also shown to be significantly modified by slight changes in the composition of the triblock copolymer (Agrawal et al., 2006).

The effect of dexamethasone released from scaffolds made from PLGA, 10% w/w, 30% w/w triblock microspheres on murine embryonic stem cells was investigated and compared. Dexamethasone within the concentration range of 39ng/ml - 3900ng/ml (0.1μM - 10μM) has been shown to be potent inductor of differentiation in stem cells (Michalopoulos et al., 2003; Takagi et al., 2007; and Buttery et al., 2001), and in the presence of ascorbic acid and β-glycerophosphate is able to induce bone formation (Buttery et al, 2001, Bielby et al., 2004; and Randle et al., 2007). However concentrations of dexamethasone above this range were observed to be toxic to stem cells (Fig 4.19). Murine embryonic stem cells cultured on scaffolds made from PLGA alone microspheres were viable and showed evidence of differentiation along the osteogenic pathway as evidenced by alizarin red staining. However embryonic stem cells cultivated on dexamethasone loaded scaffolds fabricated from blends containing 10% w/w and 30% w/w did not show similar viability and differentiation as evidenced by the alizarin red staining and reduced alamar blue values. A possible theory for this effect is that the toxicity of the high concentration of dexamethasone released from the 10% and 30% w/w scaffolds on the cells could have resulted in the reduced viability of the cells on these scaffolds. To investigate this theory, dexamethasone loaded scaffolds made from PLGA, 10% and 30% w/w triblock were prewashed in

PBS for 0, 3, 7 and 14 days prior to stem cell seeding and cultivation. It was hypothesized that increasing the duration of prewashing would result in the initial burst release of high levels of dex would be removed resulting in the reduction in the amount of dexamethasone remaining within the scaffold. Increasing the duration of prewashing resulted in an increase in cell viability and subsequent differentiation as observed by increased Alamar blue, alkaline phosphatase values and mineralized calcium deposits as indicated by alizarin red staining respectively

The last factor investigated was the effect of heat sintering microspheres on protein integrity within microspheres. Heat sintering of microspheres within a mould at temperatures above their glass transition temperature (Tg) results in the formation of scaffolds (Bodemeir et al., 2001). Sintering increases the flexibility of the polymer chains of the microspheres leading to fusion of neighbouring microspheres to yield a porous polymeric scaffold. These polymeric scaffolds have been utilised in the design of tissue-engineered constructs in delivering several growth factors for the correction of a wide range of medical conditions. The polymer has been shown to stabilise the biological activity of encapsulated growth factor, and provide sustained delivery over an extended period. However, the temperature at which sintering was conducted at is higher than the normal physiological temperatures. This can result in the denaturing of the proteins that are entrapped within the microspheres. Hence a series of experiments were undertaken to investigate if the PLGA polymer used in manufacturing the microspheres is able to protect the encapsulated protein from temperature related degradation.

The results obtained here indicated that the polymer did not confer any protection on the protein during sintering. These results suggested that heating the protein loaded microspheres at temperatures in excess of the melting point of the protein could result in the denaturing of the protein. As a result, a trade off between the transition temperature of the polymer and the melting point of the entrapped protein is needed.

## 4.6. Conclusion

From the studies presented in this chapter, it has been shown that loading weight, protein micronisation and type of polymer materials are important factors that influence the entrapment efficiency of proteins and drugs in PLGA microspheres. During microsphere protein encapsulation, leaching of protein from the microspheres during the hardening step was identified as the main cause of protein loss. The amount and proportion of protein loss was observed to be dependent on the initial loading weight of the protein.

Other studies investigating the factors influencing release kinetics of proteins and drugs from microspheres indicated that increasing the loading weight of proteins above a critical point (2% for lysozyme) increased the rate of release from PLGA microspheres. The effect of increasing the loading weight of dexamethasone on its release kinetics and varying polymers used on the release kinetics of trypsin were inconclusive.

A novel approach of controlling the release kinetics of drug molecules and proteins from PLGA molecules through the incorporation of varying proportions of the

triblock co-polymer PLGA-PEG-PLGA co-polymer was also reported in this chapter. PLGA / triblock blends of varying composition of triblock ranging from 0 to 30% were manufactured. The initial burst release, duration of sustained release, rate of release, and duration of lag phase of both lysozyme and dexamethasone loaded microspheres fabricated from these blends were dependent on the composition of triblock in the blends.

Finally, the results obtained from studies involving dexamethasone from loaded microspheres and embryonic stem cells indicates that these microspheres can be used as delivery devices for various clinical and tissue engineering applications.

# CHAPTER 5

# Scaffold Induced Differentiation

## 5.1. Introduction.

Scaffolds have been utilised as delivery devices for single growth factor delivery, which has been shown to induce differentiation of stem cells. However natural tissue regeneration is a much more complex process than the delivery of a single growth factor to the responsive cells. Rather it often involves the interplay between several environmental signals including the attraction of cells to the site of tissue repair and coordinated presentation of a multitude of growth factors to these responsive cells.

Scaffolds to date have not been extensively researched for the delivery of multiple growth factors with distinct kinetics, a likely requirement to drive tissue development to completion (Richardson, T. P. et al., 2001). In this report the development of a bilayered scaffold system for the formation of osteochondral plugs consisting of a bone and cartilage layer is outlined. Murine embryonic stem cells (mES) were seeded on bilayered scaffolds fabricated from BMP-4 and TGF-β3 loaded microspheres, with each layer of the scaffold consisting of one of the growth factor loaded microspheres. The induction of chondrogenesis and osteogenesis in the seeded mES was investigated for evidence of bone and cartilage tissue formation.

The pluripotency of embryonic stem cells potentially offers an infinite source of cell supply for tissue engineering applications. Seeding stem cells on growth factor loaded scaffolds offers the potential of promoting regeneration and repair of a wide variety of tissues through their directed differentiation into the required tissue cells. The approach of exploiting embryonic stem cells in creating biphasic tissue constructs is a novel approach and if successful can be extended to the engineering of tissues at interfaces, tissues where growth factor gradients are required to direct cell movement or growth (e.g. nerve repair), and provide the foundations for engineering fully functional organs (Suciati, T. et al., 2006).

The design of bilayered scaffold systems which could incorporate different growth factors or different cells has shown immense applications in treatment of conditions such as osteochondral defects (Holland, T. A. et al., 2005; Elisseeff, J. et al., 2005). This multi-layered approach allows the co-culturing of distinct cell types within 3D systems without the risk of growth factors or other extracellular matrix molecules produced by the encapsulated cells to influence the proliferation or differentiation of the other cells. Previous work carried out by Suciati et al has shown the successful localisation of C2C12 cell differentiation to the BMP2 loaded regions of bilayered scaffolds (Suciati, T. et al., 2006).

## 5.2 Chapter Aims.

The aim of this chapter was to develop a biphasic tissue construct consisting of a bone and cartilage layer. This was achieved by undertaking the following procedures.

(i) Bone tissue formation through the induction of osteogenesis in murine embryonic stem cells seeded on dexamethasone and ascorbate-2- phosphate releasing scaffolds.

(ii) Cartilage tissue formation through the induction of chondrogenesis in murine embryonic stem cells seeded on transforming growth factor beta-3 releasing scaffolds.

(iii) Formation of bilayered scaffold consisting of two growth factor regions with growth factor release localised to each region.

## 5.3. Methods

### 5.3.1. Drug loading and controlled release.

Ascorbate 2 phosphate (asc) and dexamethasone (dex) were encapsulated into microspheres made from blends of 30% w/w triblock + PLGA blends using the w/o/w and s/o/w method respectively. The release kinetics of these drugs from a scaffold containing these microspheres was then investigated.

#### 5.3.1.1. Ascorbate-2-phosphate and dexamethasone microsphere fabrication.

Asc loaded microspheres were fabricated using a w/o/w double emulsion method. In brief 100mg of asc was dissolved in 400µl of distilled water. The resulting asc solution was then added to 5ml of DCM solution containing 1g polymer using VM20 vortex mixer for 1min, at scale 7. 4ml of 0.3% polyvinyl alcohol (PVA) solution (Sigma Aldrich, Dorset UK) was added to protein / polymer mixture and emulsified using the vortex mixer for 20s at scale 3. The resulting emulsion was then poured into 100ml 0.3% PVA stirring at 300rpm with a magnetic stirrer. This was allowed to stir till the microspheres hardened (approximately three hours), after which the microspheres were harvested through vacuum filtration and allowed to dry in a freeze dryer.

1% dex loaded microspheres were made using the S/O/W method as described by Morita *et al*., (2001) with slight modifications. In brief, 10mg of dex (Sigma Aldrich) was dispersed in 4ml of dichloromethane (DCM) (Fisher) solution of 1g polymer using VM20 vortex mixer (1min, scale 5). Microsphere was then fabricated following the method detailed in section 4.3.21. (Fabrication of dexamethasone loaded microspheres).

The encapsulation efficiency of asc within the microspheres was determined by dissolving 20mg of sieved microspheres (100 - 300µm) microspheres in DCM (Fisher). This was followed by a series of washes with PBS to extract the Asc from the DCM. Quantity of Asc in the aqueous phase was determined by HPLC- UV (257nm) using a novopak column (4.6 x 150mm) on an Agilent 1090 machine. The mobile phase was 95:5 50mM $KH_2PO_4$ (containing 0.0475% *n* - octylamine as the ion pairing agent) buffer (pH 2.2) and acetonitrile at a flow rate of 1ml/min.

The encapsulation efficiency of dex loaded microspheres was determined following the method detailed in detailed in section 4.3.21.

#### 5.3.1.2. Scaffold fabrication

Scaffolds were fabricated following the method detailed in section 2.7. (Scaffold fabrication) by using a mixture of nine portions of 10% asc loaded and one portion of 1% dex loaded microspheres respectively.

#### 5.3.1.3. Controlled release

Asc / dex scaffolds fabricated from section 5.3.1.2 were incubated in 2ml of distilled water. At regular intervals over a 28 day period, the supernatant was removed and

replaced with fresh distilled water. The supernatant was then assayed for asc and dex using HPLC. Assaying for dex using HPLC was undertaken following the HPLC protocol described in section 4.3.21 (Fabrication of dexamethasone loaded microspheres). Whilst assaying for asc was undertaken following the HPLC protocol detailed in section 5.3.1.1.

### 5.3.2. Drug induced osteogenesis

The effect of asc and dex released from scaffolds on the induction of osteogenesis in murine embryonic stem cells (mES) seeded on scaffolds were investigated following the methods detailed below.

#### 5.3.2.1. Embryonic stem cell culturing

mES cells were cultured and expanded following the methods described in section 2.8.2.

#### 5.3.2.2. Embryoid body formation.

Embryoid bodies were made from mES cells by culturing 2 x $10^6$ cells on a 70mm diameter petri dish in DMEM supplemented with 10% (v/v) FCS, 1% (w/v) antibiotic solution (consisting of 10,000 units/ml of penicillin and 100mg/ml of streptomycin sulphate) (Invitrogen), 2mM L-glutamine and 500μM β-mercaptoethanol (β-Mercap), for five days. The media was changed after three days, by transferring the media with embryoid bodies from the petri dish into 50ml falcon tubes using a 25ml pipette. The embryoid bodies were allowed to settle to the bottom of the falcon tube, the supernatant media was then gently aspirated and replaced with fresh media. The

embryoid bodies were then gently re-suspended in the fresh media and then transferred into new petri dishes.

#### 5.3.2.3. Scaffold cell seeding.

mES embryoid bodies cultured following the methods detailed in section 2.8.3 were trypsinised into single cell suspensions and seeded onto asc / dex microsphere based scaffolds produced following the method detailed in section 5.3.1.2. Cells were subsequently seeded onto the scaffolds following the method detailed in section 2.8.3.

#### 5.3.2.4. Cell Differentiation.

Cell seeded scaffolds obtained from the section above (section 5.3.2.3.) were cultured for 35 days in differentiation media. The differentiation media consisted of DMEM supplemented with 15% (*v/v*) of fetal calf serum (FCS), 2mM L-glutamine, 1% (v/*v*) antibiotic solution (consisting of 10,000 units/ml of penicillin and 100mg/ml of streptomycin sulphate), and 10mM β-glycerophosphate. Control scaffolds consisting of blank (non loaded microspheres based) scaffolds were cultured in differentiation media further supplemented with 1µM dex and 50µg/ml asc to form positive controls. Whilst negative controls were control scaffolds cultured in differentiation media. Culture media was changed at regular intervals, by matching the rate of change with the rate of change of supernatant in the controlled release section (section 5.3.1.3).

#### 5.3.2.5. Histochemical and immunocytochemical staining.

The cell scaffold constructs cultured in differentiation media in section 5.3.2.4 was investigated for evidence of osteogenesis through alizarin red staining and osteocalcin immunostaining.

Alizarin red staining for calcium deposits were performed on cell seeded scaffolds after 35 days of culturing. The staining was done on asc/dex scaffolds, negative and positive control scaffolds following the method detailed in section 2.11.1. Immunostaining for osteocalcin localisation in asc / dex scaffold after 25 day culture in the differentiation media was performed following the protocol for single antigen immunostaining outlined in section 2.11.4 (single and immunostaining). Primary antibody used was polyclonal mouse osteocalcin antibody raised in goats, whilst the secondary antibody was FITC conjugated anti goat antibody raised in rabbits.

#### 5.3.2.6. Osteocalcin assay.

The amount of osteocalcin present in the media after 28 days of culture of asc / dex and control scaffolds in the differentiation media was quantified following the method described in section 2.9.4.

### 5.3.3. Drug induced Chondrogenesis.

The effect of TGF-β3 released from scaffolds on the induction of chondrogenesis in murine embryonic stem cells (mES) seeded on scaffolds were investigated following the methods detailed below.

#### 5.3.3.1. TGF-β3 microsphere fabrication.

TGF- β3 loaded microspheres were made using the S/O/W method as described by Morita *et al*., with slight modifications. In brief, 20µg of TGF- β3 (Peprotech, UK) was micronised by dissolving in 1ml of distilled water containing 60mg of PEG 6000 (BDH Chemicals, Poole UK) followed by freeze-drying for 48 hours – this constitutes the micronisation step. The resulting TGF- β3 / PEG lyophilisate was then dispersed

in 1ml of dichloromethane (DCM) (Fisher Scientific, Loughborough UK) by vortexing at scale 4 for 30seconds using a VM20 vortex mixer (Chiltern Scientific, Bucks UK) to form a suspension. The resulting protein suspension was then added to 3ml of DCM solution containing 1g polymer using VM20 vortex mixer for 1min, at scale 3. 4ml of 0.3% polyvinyl alcohol (PVA) solution (Sigma Aldrich, Dorset UK) was added to protein / polymer mixture and emulsified using the vortex mixer for one minute at scale 5. The resulting emulsion was then poured into 100ml 0.3% PVA stirring at 300rpm with a magnetic stirrer. This was allowed to stir till the microspheres hardened (approximately three hours), after which the microspheres were harvested through vacuum filtration and allowed to dry in a freeze dryer.

The encapsulation efficiency of TGF-β3 within the microspheres was determined by dissolving 20mg of sieved microspheres (100 - 300µm) microspheres in 1ml ethyl acetate (Fisher, Loughborough UK). This was followed by a series of washes with PBS to extract the TGF-β3 from the ethyl acetate, following the method described in section 2.6.2 (Encapsulation efficiency of protein loaded microspheres). Quantity of TGF-β3 extracted into the PBS was determined by ELISA using a TGF-β3 ELISA kit and following the manufacturers instructions.

#### 5.3.3.2. Controlled release

100mg of pre-sieved TGF-β3 loaded microspheres (100 - 300µm) was loaded into a teflon mould and heat sintered to form TGF- β3 scaffolds by following the method described in section 2.7. The resulting scaffolds were incubated in 2ml of PBS pH 7.4, in an incubator set at 37ºC, 5% $CO_2$. At regular intervals the supernatant (PBS) was extracted and replaced with fresh PBS. The amount of TGF- β3 in the extracted

supernatant was determined by ELISA using the TGF-β3 ELISA kit and following the manufacturers instructions.

#### 5.3.3.3. Scaffold cell seeding and culture.

Trypsinised mES embryoid body cells were produced and seeded on TGF-β3 scaffolds by following the methods detailed in sections 2.8.3. The cell seeded scaffolds were then cultured in differentiation media for 28 days. The differentiation media consisted of DMEM supplemented with 15% (*v/v*) of fetal calf serum (FCS), 2mM L-glutamine, 1% (v/*v*) antibiotic solution (consisting of 10,000 units/ml of penicillin and 100mg/ml of streptomycin sulphate), 50µg/ml ascorbate 2 phosphate, 1% (v/v) non essential amino acids, 100µm sodium pyruvate and 100µg/ml L-Proline.

Trypsinised mES embryoid body cells were also seeded on non loaded scaffolds and cultured in differentiation media to form control scaffolds. Negative and positive control scaffolds were cultured in differentiation media, and differentiation media further supplemented with 10ng/ml of TGF-β3 respectively.

#### 5.3.3.4. Alcian blue staining.

Prior to alcian blue staining, scaffolds were fixed with 4% paraformaldehyde, and stored in PBS solution at 4ºC until when required. For alcian blue staining, fixed scaffolds were incubated at room temperature in 0.5% (*w/v*) alcian blue solution for 20 minutes. The scaffolds were then rinsed in distilled water to wash off background staining, blot dried and then washed twice with 1% acetic acid solution for 5 minutes.

The scaffold was then allowed to dry overnight in the fume hood before viewing for stained region.

#### 5.3.3.5. Biochemical analysis.

The degree of chondrogenesis induced in mES cells seeded on TGF-β3 loaded and control scaffolds was quantified by measuring the amount of glycosaminoglycans (GAG) and collagen deposited on the scaffolds by the cells. The amount of GAG and collagen deposited on the scaffolds were quantified by following the methods detailed in sections 2.9.5 and section 2.9.6 respectively.

### 5.3.4. Biphasic scaffold formation.

A series of bilayered scaffolds consisting of two separate regions of BMP2 and TGF-β3 loaded microspheres, dex + asc and non loaded microspheres, BMP2 and non loaded microspheres respectively were fabricated. Their effects on inducing localised differentiation of mES cells along osteogenic and chondrogenic pathways was investigated following the methods described below.

#### 5.3.4.1. Protein loaded microsphere fabrication.

BMP2 and TGF-β3 loaded microspheres were fabricated for use in bilayered scaffold formation. TGF- β3 loaded microspheres were fabricated using the methods described in section 5.3.3.1. BMP2 loaded microspheres were also fabricated following the same methods detailed in section 5.3.3.1.

#### 5.3.4.2. Proof of concept fabrication.

In order to investigate if protein released from bilayered scaffolds are localised to the areas immediately surrounding the corresponding protein loaded region, bilayered scaffold consisting of two separate regions of red and green food dye loaded

microspheres were fabricated and incubated in PBS using the set up shown in Fig 2.5. The set up in Fig 2.5 separates the PBS into two separate regions - with each PBS region immediately surrounding a section of the bilayered scaffold. Release of the dyes from the scaffolds over a seven day period was investigated. It was hypothesized that as the green dye is released from the green dye loaded region, the PBS solution will turn green. Presence of the green solution was thus taken as indication of the distribution of the released green dye. Images of the set-up were taken after 1, 3, 5 and 7 days using a finepix digital camera (Sainsbury's, Nottingham, UK) and visualised for presence of the green solution.

Green dye loaded and red dye loaded microspheres were fabricated by dispersing 100µl of green and red food dye solutions (Sainsbury's, Nottingham, UK) in 4ml of DCM containing 1g of dissolved polymer (triblock – PLGA blend) by vortexing at scale 3 for 1 min using a VM20 vortex mixer. 4ml of 0.3% polyvinyl alcohol (PVA) solution (Sigma Aldrich, Dorset UK) was added to the mixture and emulsified using the vortex mixer for one minute at scale 5. The resulting emulsion was then poured into 100ml 0.3% PVA stirring at 300rpm with a magnetic stirrer. This was allowed to stir till the microspheres hardened (approximately three hours), after which the microspheres were harvested through vacuum filtration and allowed to dry in a freeze dryer.

#### 5.3.4.3. Controlled release.

Bilayered scaffolds consisting of separate regions of TGF-β3 and BMP2 loaded microspheres were incubated in PBS pH 7.4 at 37ºC, 5% CO2 using the set-up in Fig 2.5, over a 28 day period. At regular intervals the top and bottom layers of PBS

supernatant was extracted separately and replaced with fresh PBS. The amount of TGF--β3 and BMP2 in both the top and bottom extracted PBS layers was then determined by ELISA using the TGF- β3 duoset and human BMP4 quantikine ELISA kits (both obtained from R&D Systems, Abingdon, UK). ELISA tests for TGF-β3 and BMP2 were performed following the manufacturers instructions.

#### 5.3.4.4. Bilayered scaffold cell seeding and culture.

Trypsinised mES embryoid body cells were produced and seeded on bilayered scaffolds A, B and C, by following the methods detailed in section 2.8. The cell seeded scaffolds were then cultured in differentiation media for 35 days. The differentiation media for bilayered scaffold A consisted of DMEM supplemented with 15% (*v/v*) of fetal calf serum (FCS), 2mM L-glutamine, 1% (v/*v*) antibiotic solution (consisting of 10,000 units/ml of penicillin and 100mg/ml of streptomycin sulphate), 50µg/ml ascorbate 2 phosphate, 1% (v/v) non essential amino acids, 100µm sodium pyruvate and 100µg/ml L-Proline. Differentiation media for bilayered scaffold C consisted of DMEM supplemented with 15% (*v/v*) of fetal calf serum (FCS), 2mM L-glutamine, 1% (v/*v*) antibiotic solution (consisting of 10,000 units/ml of penicillin and 100mg/ml of streptomycin sulphate), and 10mM β-glycerophosphate. Whilst the differentiation media for bilayered scaffold B, consisted of the differentiation media used for bilayered scaffold C supplemented with 50µg/ml ascorbate-2-phosphate.

#### 5.3.4.5. SEM imaging of embryoid bodies.

5 day old embroid bodies were rinsed with PBS and fixed in 2.5% glutaraldehyde (Sigma Aldrich, Dorset UK) diluted in 0.1M PBS solution for 1 h. After rinsing, samples were further treated in 1% osmium tetroxide (Sigma Aldrich, Dorset UK) for

1 h. Samples were dehydrated in graded ethanol dilutions and allowed to dry overnight in the fume cupboard The sample was then sputter coated with gold for 3 min using a Balzer Union SCD 030 sputter coater. The surface morphology of the coated sample (embroid body) was examined and image obtained by SEM using a JSM-6060 imaging system (JEOL ltd. Herts, UK) with an ionising radiation of 12kV.

#### 5.3.4.6. Immunohistochemistry and histochemical staining.

After 28 days of continuous culture of cell seeded bilayered scaffolds in the differentiation media, the cell scaffold constructs were investigated for evidence of osteogenesis and chondrogenesis through double antigen immunocytochemical and several histochemical staining procedures. The bilayered scaffolds investigated were TGF-β3 / BMP4; BMP4 + dex / plain; and asc + dex / plain loaded scaffolds, hitherto referred to as A, B and C bilayered scaffolds.

#### 5.3.4.6.i. Alizarin red staining.

Alizarin red staining for calcium deposits were performed on B and C bilayered cell seeded scaffolds after 35 days of culture in their respective differentiation media. The staining was done on these scaffolds, and their respective negative and positive control scaffolds following the method detailed in section 2.11.1.

#### 5.3.4.6.ii. Alcian blue / Sirius red staining

Alcian blue / Sirius red staining of bilayered scaffold A, was used to ascertain the presence of proteoglycans and collagen fibrils on the cell seeded scaffolds, after 28 days of continuous culture in the differentiation media. The staining was done following the method outlined in section 2.11.3.

#### 5.3.4.6.iii. Masson trichrome staining.

Masson's trichrome staining of cell seeded bilayered scaffold A after 28 days of culturing in differentiation media, was used to differentiate between collagenous tissue associated with cartilage and smooth muscle tissue from bone or other tissue types by following the method outlined in section 2.11.2.

#### 5.3.4.6.iv. Immunocytochemistry.

Double antigen immunocytochemical staining for osteocalcin and collagen II was undertaken to determine the localisation of bone and cartilage tissue on bilayered scaffolds A after 25 day culture in the differentiation media. Immunocytochemical staining was performed following the protocol for double antigen immunostaining outlined in section 2.11.4.

## 5.4. Results

### 5.4.1. Drug loading and controlled release.

#### 5.4.1.1. Entrapment efficiency

The entrapment efficiency of ascorbate-2-phosphate (asc) and dexamethasone (dex) was investigated. The entrapment efficiency of asc in microspheres made from PLGA blends containing 30% w/w of triblock was determined as 28.53 ± 1.42%. The effect of triblock composition on the entrapment efficiency of asc in microspheres was also investigated. The results in Fig 5.1 show that the entrapment efficiency of asc decreases when the triblock composition of the polymer blend is increased from 0 to 10%, and 10% to 30% (53.48 ± 5.30% vs. 44.65 ± 1.71%; and 44.65 ± 1.71% vs.

28.53 ± 1.42% respectively). Whilst the entrapment efficiency of dex in 1% dex loaded microspheres, was determined to be 18.16 ± 3.22%.

#### 5.4.1.2. Controlled release

The release kinetics of asc and dex from a scaffold made from both asc and dex loaded microspheres (section 5.3.1.3 controlled release) was investigated. The results are summarised in Fig 5.2. After an initial burst release of 50.03 ± 2.73%, a linear release profile of dex approaching zero order kinetics (with no lag phase) was observed for the release of dex from the asc + dex combination scaffold. Whilst the release of asc from the combination scaffold was characterised by an initial burst release of 68.3 ± 2.35%, followed by a lag phase period with only a further 3.8% released during the duration of the experiment.

To investigate if the release kinetics of asc and dex were affected by the presence of each other, scaffolds consisting of only asc and dex loaded microspheres were fabricated. The release kinetics of the drugs (asc and dex) from their respective scaffolds was investigated. An increase in the initial burst release (17.34 ± 3.89% vs. 50.03 ± 2.73%) and release rate of dex was observed when the release profile of dex from the asc + dex combination scaffolds was compared to the release profile of dex from dex loaded scaffolds (Fig 5.4). A decrease in the initial burst release (68.3 ± 2.35%, vs. 79.3 ± 5.48%) was observed when the release of asc from the combination scaffolds was compared to the release of asc from asc loaded scaffolds

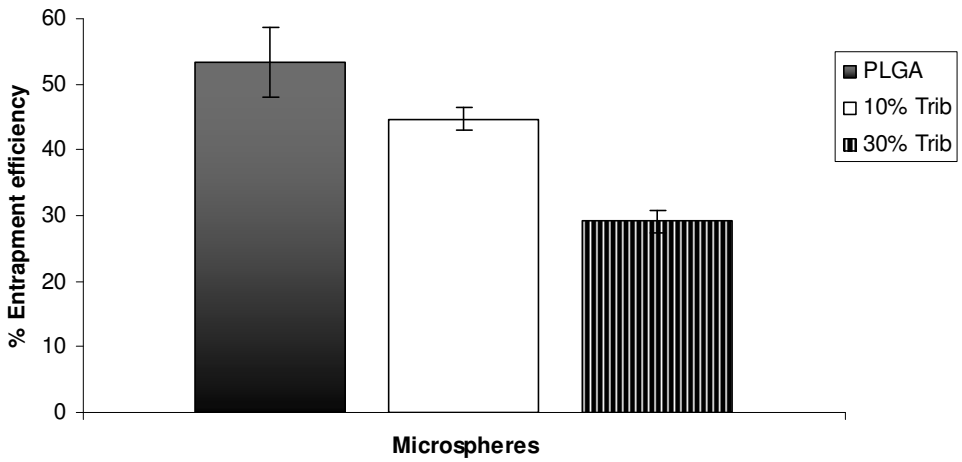


Figure 5.1 Chart showing the effect of triblock on the encapsulation efficiency of ascorbate -2-phosphate. Asc was loaded into microspheres using the double emulsion method. Values plotted on the chart are average values obtained from three different independent experiments carried out (i.e. N = 3 ± Standard deviation).

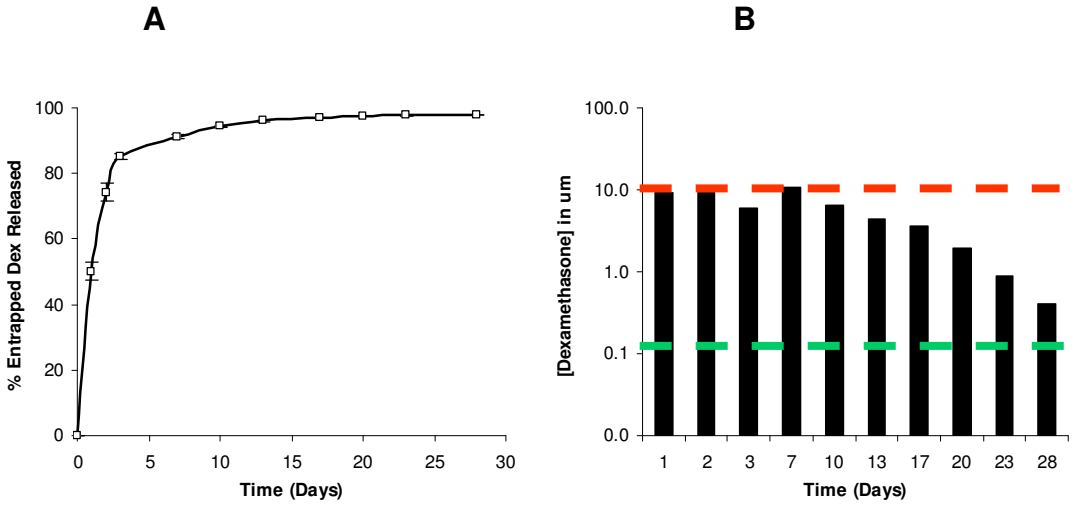


Figure 5.2: Chart showing the release of dexamethasone from various 30% w/w triblock / PLGA microsphere based scaffold. 100mg of dex loaded microspheres was incubated in 2ml of PBS at 37ºC. The supernatant was harvested at various time points and the amount of dexamethasone released was quantified using HPLC-UV. Values plotted on the chart are average values obtained from three different independent experiments carried out (i.e. N = 3 ± Standard deviation). A) 0.1% Dex loaded scaffold controlled Release; B) Theoretical Dex concentration mES are exposed to is within the range necessary for induction of osteogenesis. Green and Red dashed line – lower limit at 0.1µM and upper limit at 0.1µM respectively.

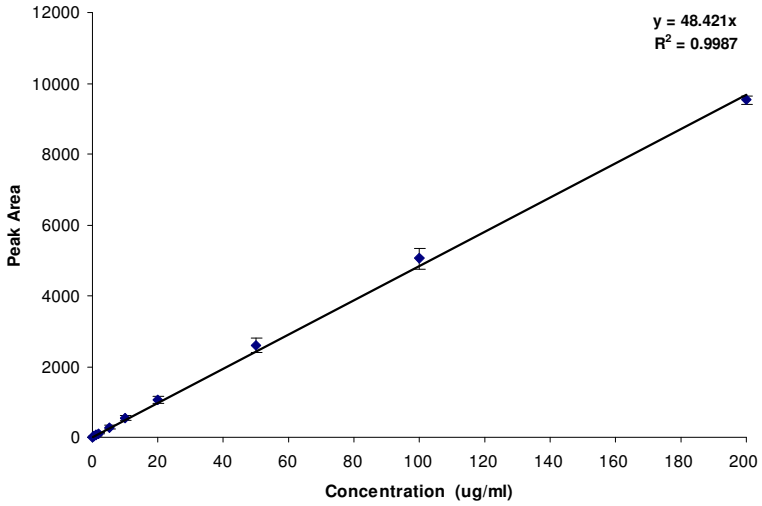


Figure 5.3: Chart showing a typical ascorbate phosphate standard curve. The peak area of various concentrations of PBS solutions ascorbate phosphate (0.2µg/ml - 200µg/ml) was determined by HPLC-UV and plotted against the corresponding concentration. Values plotted on the chart are average values obtained from three different independent experiments (i.e. N = 3 ± Standard deviation). These standard curves were used in experiments for determining the entrapment efficiency and release kinetics of the ascorbate phosphate loaded microspheres

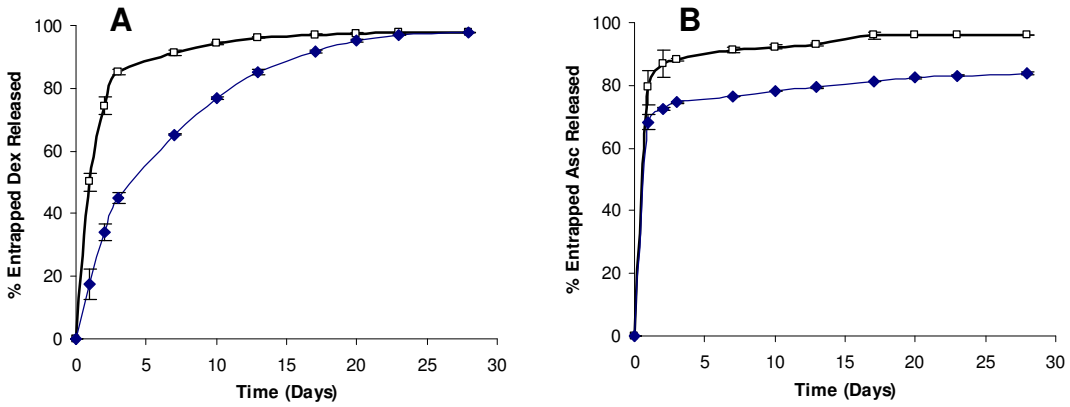


Figure 5.4: Chart showing the effects of dexamethasone (dex) and ascorbate-2-phosphate (asc) release on each other. Asc + dex loaded scaffold was made by sintering 10% asc and 1% dex loaded microspheres in 9:1 ratio. Asc and dex loaded scaffolds were made by sintering the respective microspheres with non-loaded scaffold in a 9:1 and 1: 9 ratio for asc loaded and dex loaded scaffold respectively. Values plotted on the chart are average values obtained from three different independent experiments carried out (i.e. N = 3 ± Standard deviation). A) Chart showing the release of dex from dex loaded scaffold (blue diamonds) and asc + dex loaded scaffolds (open squares); B) Chart showing the release of asc from asc loaded scaffold (open circles) and asc + dex loaded scaffolds (red squares);

### 5.4.2. Drug induced osteogenesis

#### 5.4.2.1. Cell imaging.

Images of mES cells, SNL cells, and embryoid bodies were obtained by SEM and microscope to provide details of the morphology of the cells (Fig 5.5).

#### 5.4.2.2. Alizarin red staining.

Alizarin red staining of cell seeded scaffolds after culturing in differentiation media was carried out to investigate the effects of asc and dex released from the scaffolds on the induction of osteogenesis in mES cells. After alizarin red staining, a patchy distribution of red stained calcium deposits was observed on asc + dex combination scaffolds and positive control scaffolds. There were no observable red stained calcium deposits in the negative controls (Fig 5.6).

#### 5.4.2.3. Osteocalcin assay.

The degree of osteogenesis induced in the cell seeded scaffolds after culturing in the differentiation media, was investigated by quantifying the amount of osteocalcin secreted by the cells into the media (standard curve shown in Fig 5.7)). The amount of osteocalcin detected in the media of non loaded scaffolds were 48.06 ± 4.72ng and 2.00 ± 1.28ng for positive and negative control scaffolds respectively, and 13.22 ± 1.44ng for the asc + dex drug loaded scaffolds (Fig 5.8)

#### 5.4.2.4. Immunocytochemical staining.

Immunocytochemical staining of asc + dex loaded and non-loaded scaffolds for osteocalcin was undertaken to determine the presence and localisation of bone nodules within the scaffold. Fig 5.9 shows the presence of osteocalcin containing

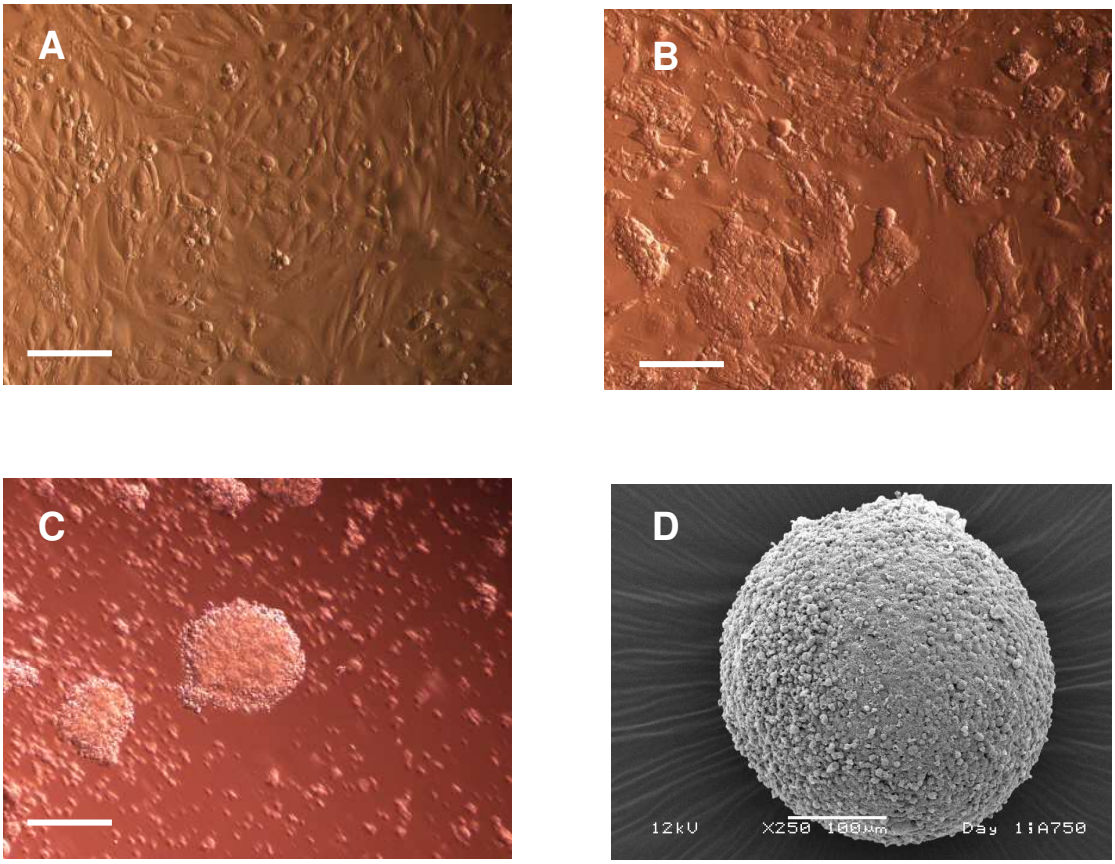


Figure 5.5: Micrographs showing images of SNL mouse fibroblasts and murine embryonic stem cells (A) Image of mitotically inactivated murine SNL fibroblasts cultured on T75 flask (10X magnification) (B) Image of murine ES cell colonies cultured on SNL feeder layer (10X magnification) (C) Image of embryoid bodies formed after two days of continuous culture of murine ES cells in LIF deficient culture media (10X magnification). (D) SEM image of embryoid body formed after five days of continuous culture of murine ES cells in LIF deficient culture media (100X magnification). Scale bar is 100µm

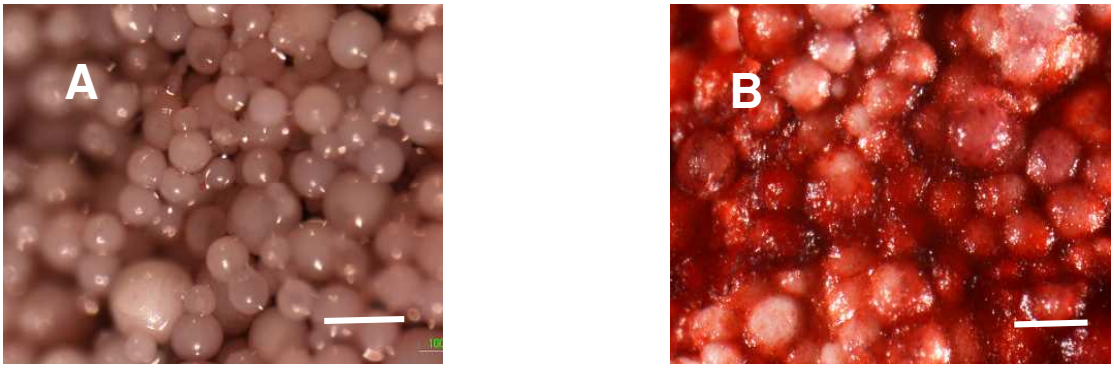


Figure 5.6: Micrographs showing regions of calcium deposits on mES seeded asc + dex loaded scaffolds and non loaded scaffolds. (A) Control scaffolds; (B) Asc + dex loaded scaffold. Seeded scaffolds were cultured for 28 days in differentiation media, after which they were stained for calcium deposits using Alizarin red. Scale bar is 500µm

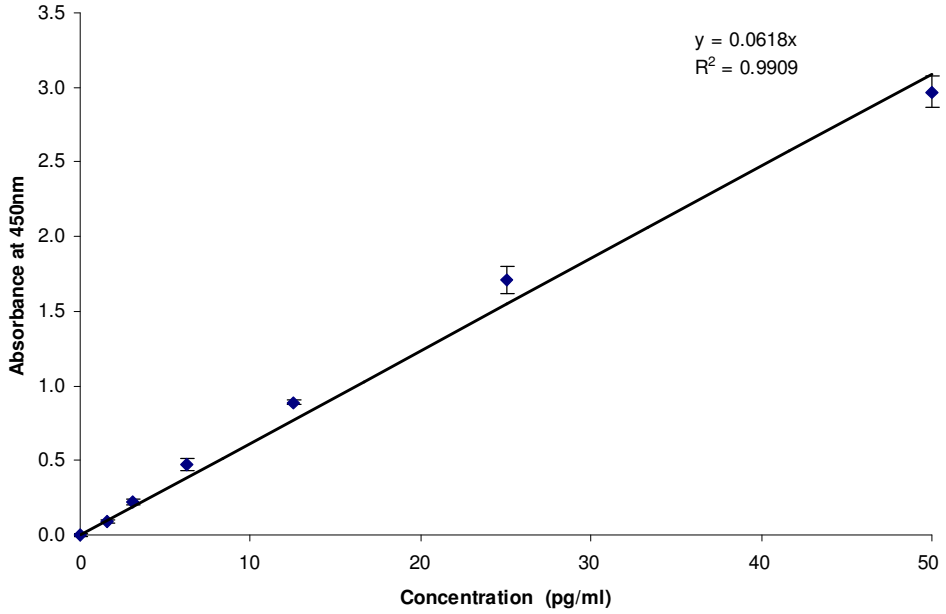


Figure 5.7: Chart showing an osteocalcin ELISA standard curves. Absorbance values of various concentrations of PBS solutions of osteocalcin (1.56ng/ml – 50ng/ml) was determined and plotted against the corresponding concentration. Values plotted on the chart are average values obtained from three different independent experiments (i.e. N = 3 ± Standard deviation).

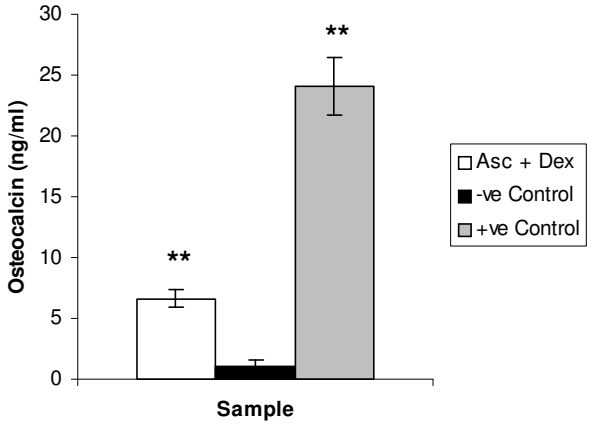


Figure 5.8: Osteocalcin levels present in media following 28 days of culture were measured to indicate differentiation of mES cells into osteoblasts. Those cultured on Dex + Asc loaded scaffolds, and on nonloaded scaffolds with exogenous addition of Dex + Asc (positive control) secreted significantly higher levels of osteocalcin when compared to mES cells cultured on non loaded scaffolds without exogenous addition of these supplements (negative control). Results are mean ± standard deviation (n = 3; **p<0:01).

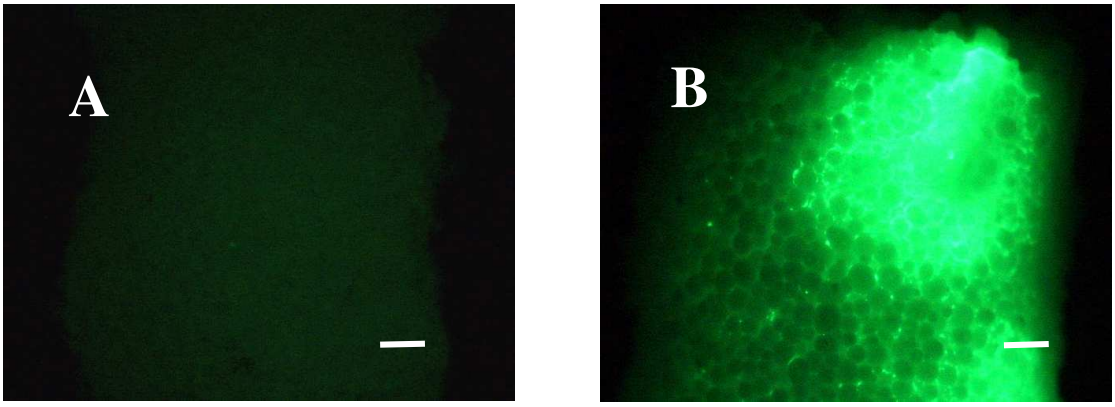


Figure 5.9: Micrographs showing osteocalcin rich regions of bone nodules on mES seeded asc + dex loaded scaffolds and non loaded scaffolds. (A) Control scaffolds; (B) Asc + dex loaded scaffold. Seeded scaffolds were cultured for 28 days in differentiation media, after which they were stained immunocytochemically for osteocalcin using goat polyclonal osteocalcin antibody. Scale bar is 500µm

bone nodules in the asc + dex combination scaffold. No bone nodules were observable in non-loaded control scaffolds.

### 5.4.3. Drug induced chondrogenesis.

The induction of chondrogenesis in mES cells seeded on scaffolds through the controlled release of TGF-β3 was investigated. Scaffolds made from TGF-β3 loaded microspheres were fabricated and seeded with mES cells. The amount of proteoglycans and collagen deposited on the scaffold after 35 days of culture was determined as an indication of chondrogenesis.

#### 5.4.3.1. Entrapment efficiency and controlled release

The entrapment efficiency of TGF-β3 in TGF-β3 loaded microspheres was determined using an ELISA kit (standard curve – Fig 5.10) to be 28.75 ± 5.33%. The effect of scaffold fabrication on the entrapment efficiency of the microspheres was also investigated to determine if the heat sintering had a deleterious effect on TGF-β3. The retention activity of TGF-β3 after scaffold fabrication was 85.72 ± 6.33% compared to before scaffold fabrication. The retention activity was calculated using the equation below:

$$\frac{\textbf{Entrapment efficiency of 100mg microspheres}}{\textbf{Entrapment efficiency of 100mg scaffold}} \times \frac{100}{1} = \textbf{Retention activity.}$$

The release kinetics of TGF-β3 from scaffolds was also investigated. The initial burst release was observed to be 23.25 ± 3.55%, with complete release (97.22 ± 8.55%) and a linear release profile observed in over a 30 day period (Fig 5.11).

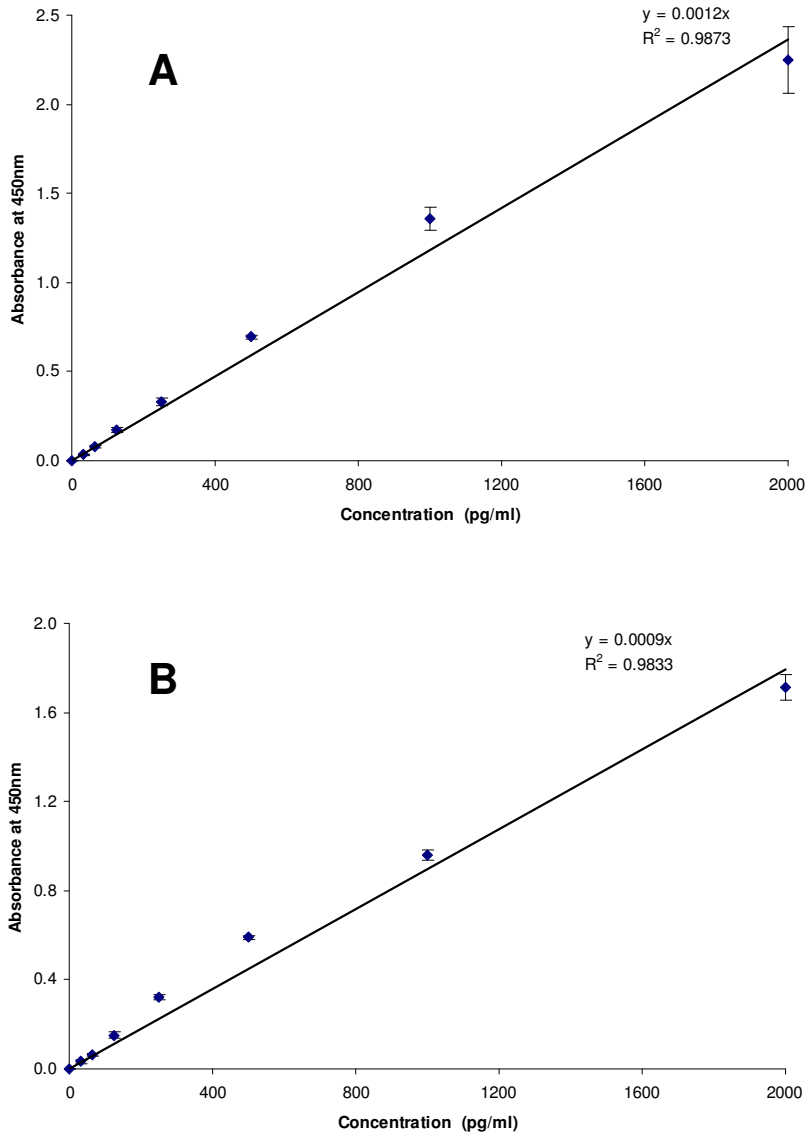


Figure 5.10: Chart showing the ELISA standard curves for (A) BMP-4 and (B) TGF-β3 Absorbance values of various concentrations of PBS solutions of BMP-4 and TGF-β3 (2pg/ml – 2000pg/ml) was determined and plotted against the corresponding concentration. Values plotted on the chart are average values obtained from three different independent experiments (i.e. N = 3 ± Standard deviation). These standard curves were used in experiments for determination of the entrapment efficiency and controlled release studies involving BMP-4 and TGF-β3 loaded microspheres and scaffolds respectively.

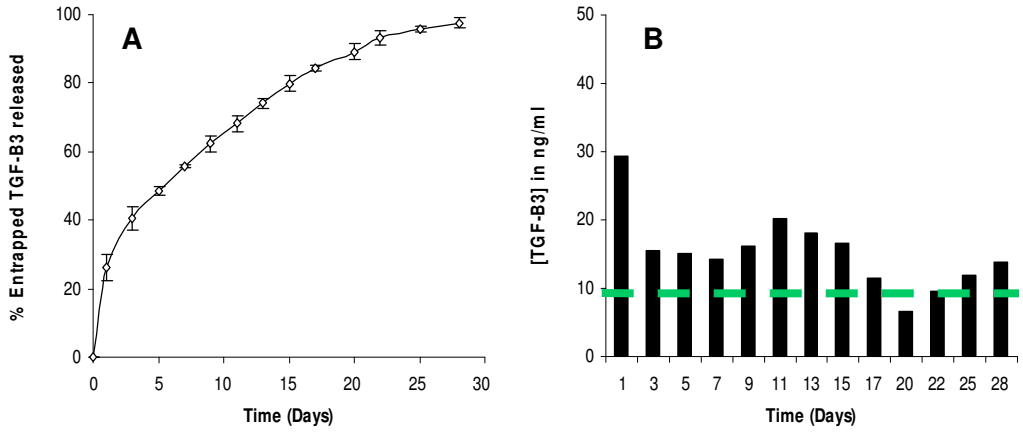


Figure 5.11: Chart showing the release of TGF-β3 from various 30% w/w triblock / PLGA microsphere based scaffold. 100mg of TGF-β3 loaded microspheres was incubated in 2ml of PBS at 37ºC. The supernatant was harvested at various time points and the amount of TGF-β3 released was quantified using ELISA. Values plotted on the chart are average values obtained from three different independent experiments carried out (i.e. N = 3 ± Standard deviation). A) TGF-β3 loaded scaffold controlled Release; B) Theoretical TGF-β3 concentration mES are exposed to is above the range necessary for induction of chondrogenesis. Green dashed line – limit at 10ng/ml for chondrogenesis.

### 5.4.3.2. Alcian blue staining.

Alcian blue staining of cell seeded scaffolds after culturing in differentiation media was carried out to investigate the effects of TGF-β3 released from the scaffolds on the induction of chondrogenesis in mES cells. After alcian blue staining, a patchy distribution of blue proteoglycan deposits was observed on TGF-β3 loaded scaffolds. There were no observable blue stained deposits in the negative controls (Fig 5.12).

### 5.4.3.2. Biochemical analysis.

The degree of chondrogenesis induced in the TGF-β3 loaded cell seeded scaffolds after culturing in the differentiation media, was investigated by quantifying the amount of glycosaminoglycans (GAG) and collagen deposited on the scaffolds. The amount of GAG and collagen scaffold deposited on the TGF-β3 loaded scaffolds per100mg scaffold was 4.55 ± 0.49µg and 10.55 ± 2.22µg respectively. Whilst the amount of GAG and collagen (Fig 5.13) deposited control scaffolds were 1.35 ± 0.55µg and 2.44 ± 1.10µg for negative control scaffolds, and 5.32 ± 1.32µg and 17.32 ± 3.11µg positive control scaffolds respectively.

### 5.4.4. Biphasic scaffold

Biphasic scaffolds consisting of two separate regions of non-loaded microspheres and BMP4 loaded microspheres; non-loaded microspheres and asc and dex loaded microspheres; and TGF-β3 loaded microspheres and BMP4 loaded microspheres were fabricated. Their effects on inducing zonal differentiation of mES cells along different pathways were investigated.

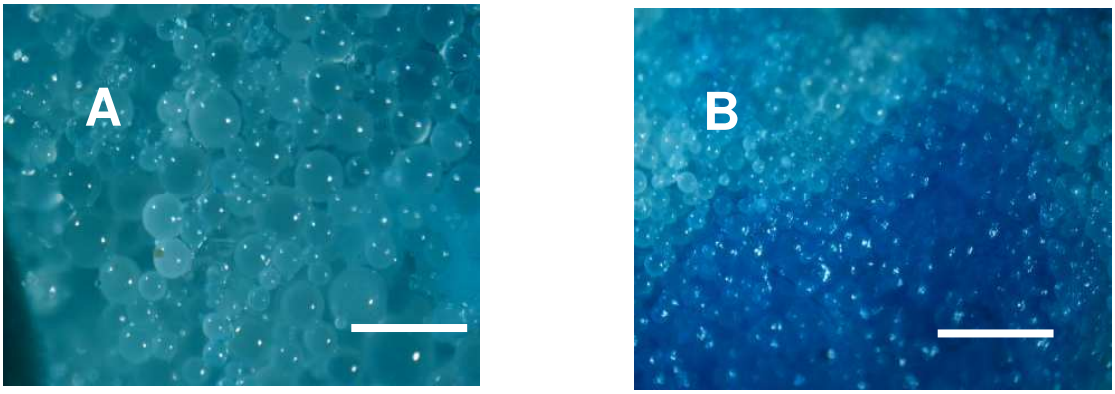


Figure 5.12: Micrographs showing regions of calcium deposits on mES seeded TGF-β3 loaded scaffolds and non loaded scaffolds. (A) Control scaffolds; (B) TGF-β3 loaded scaffold. Seeded scaffolds were cultured for 28 days in differentiation media, after which they were stained for presence of glycisaminoglycan deposits (blue) using Alcian blue. Scale bar is 500µm

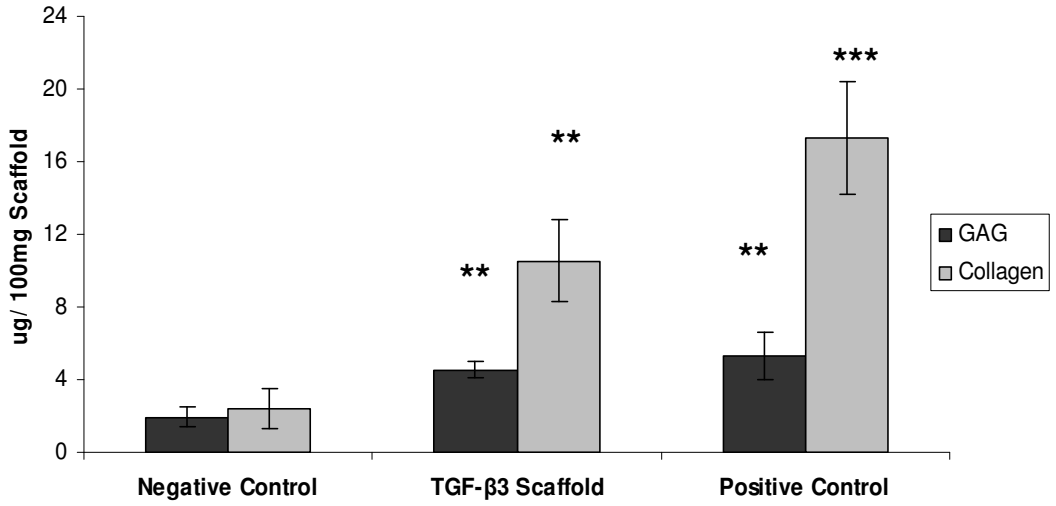


Figure 5.13: Glycosaminoglycan (GAG) and Collagen deposition on scaffold were measured as an indication of mES cells differentiation into chondrocyte respectively. mES cells cultured on, TGF-β3 loaded scaffolds, and on non-loaded scaffolds with exogenous addition of TGF-β3 (positive control scaffolds) showed significant increase in GAG production and collagen deposition. Results are mean ± standard deviation (n = 3; **p<0:01, ***p<0:001).

#### 5.4.4.1. Proof of concept.

In order to investigate the feasibility of localising the release of drug or protein molecules from one region of the bilayered scaffolds to the other region of the scaffold, a bilayered scaffold consisting of two separate regions of red and green food dye loaded microspheres was fabricated. Fig 5.14 shows a series of photographs taken to track the release of the green food dye from the green dye loaded region of the scaffold. The green dye was observed to be localised to the fluid section surrounding the green dye loaded region of the scaffold for 3 days (Figs 5.14C &G). After 5 days, evidence of diffusion of the green food dye from the green dyed loaded region to the fluid surrounding the other region was observed (Figs 5.14D &H).

#### 5.4.4.2. Entrapment efficiency

The entrapment efficiency of BMP4 and TGF-β3 in BMP4 and TGF-β3 loaded microspheres was observed to be 25.52 ± 4.13% and 28.75 ± 5.33% respectively. Whilst the retention activity after scaffold fabrication (as determined in section 5.4.3.1), was 88.75 ± 9.33% and 85.72 ± 6.33% respectively.

#### 5.4.4.3. Controlled release.

The release kinetics of TGF-β3 from scaffolds was investigated and the results reported in section 5.4.3.1 (entrapment efficiency and controlled release) and Fig 5.11. The release kinetics of BMP4 from scaffolds was also investigated (Fig 5.15). The initial burst release was observed to be 20.21 ± 4.25%, with complete release (94.22 ± 3.55%) and a linear release profile observed in over a 30 day period.

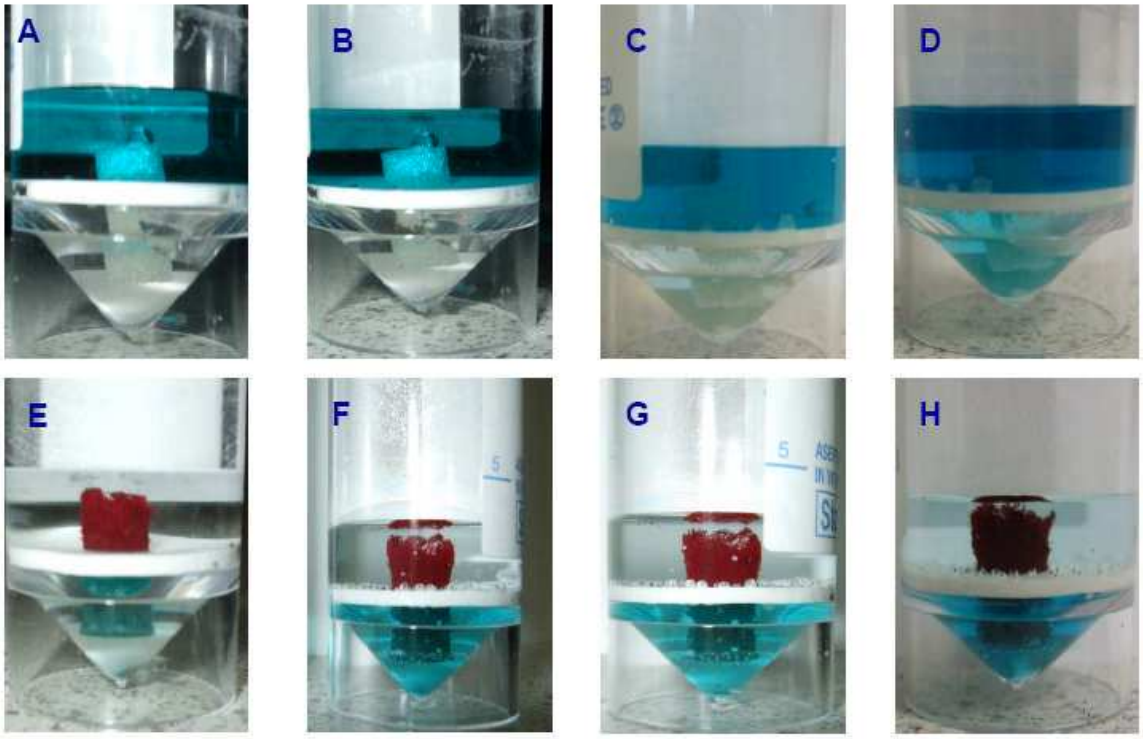


Figure 5.14: Images tracking the localisation of dye release.. A) & E) Day 0; B) & F) Day 1; C) & G) Day 3; D) & H) Day 5. Images A) – D) Tracking the diffusion of coloured solution (placed in top layer) through plain scaffolds. E) – H) Tracking diffusion of coloured dye released from bilayered scaffold made from coloured microspheres (green and red). Green dye was released from the green dye loaded microspheres. Red dye was not released from the red loaded microspheres section of the scaffold during the duration of the study, due to its hydrophobicity.

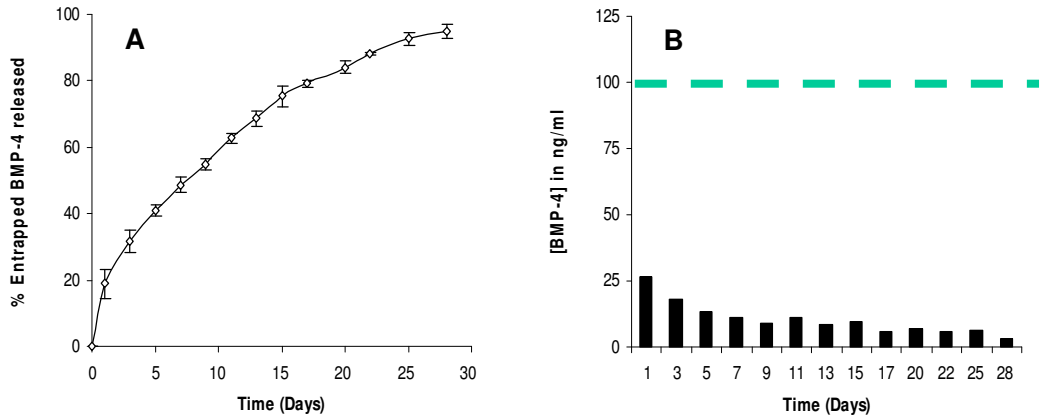


Figure 5.15: Chart showing the release of BMP4 from various 30% w/w triblock / PLGA microsphere based scaffold. 100mg of BMP4 loaded microspheres was incubated in 2ml of PBS at 37ºC. The supernatant was harvested at various time points and the amount of BMP4 released was quantified using ELISA. Values plotted on the chart are average values obtained from three different independent experiments carried out (i.e. N = 3 ± Standard deviation). A) Chart showing BMP4 loaded scaffold controlled release profile; B) Theoretical BMP4 concentration mES are exposed to is lower than the values of 100ng/ml known to be necessary for induction of osteogenesis. Green dashed line – limit at 100ng/ml for osteogenesis.

The release kinetics of BMP4 and TGF-β3 from the BMP4 and TGF-β3 loaded bilayered scaffolds was investigated. The amount of BMP4 and TGF-β3 present in the PBS surrounding both BMP4 and TGF-β3 regions of the scaffold was determined and are recorded in Fig 5.16. The bilayered scaffold consisted of a top layer of BMP loaded microspheres and a bottom layer of TGF-β3 loaded microspheres. Throughout the duration of the controlled release experiment, it was observed that between 64% - 83% and 65% to 72% of the total BMP4 and TGF-β3 released was localised to the top and bottom layers respectively.

**5.4.4.4. Histochemical staining.**

A series of histochemical stains were undertaken to determine the successful localised differentiation of mES stem cells to the drug loaded region of the bilayered section. Alizarin red staining was used to show the localisation of osteogenic differentiation to the drug or protein loaded region of the scaffold (Figs 5.17A – H). Alcian blue / sirius red and masson trichrome staining was used to differentiate between the tissues deposited on the different regions of the TGF-β3 + BMP4 bilayered scaffold (Figs 5.18A – H).

Localised red stains of calcium deposit was observed in the asc + dex region of the alizarin red stained non-loaded / asc + dex and non-loaded / BMP4 + dex bilayered scaffolds (Figs. 5.14A-H). A patchy distribution of blue and red stained proteoglycan and collagen tissues respectively was observed on TGF-β3 / BMP4 bilayered scaffolds after alcian blue /sirius red staining (Figs 5.18A-D). Preferential localisation of these stained areas to either the TGF-β3 or BMP4 regions of the bilayered scaffold was not observed. Masson trichrome staining of the TGF-β3 / BMP4 bilayered

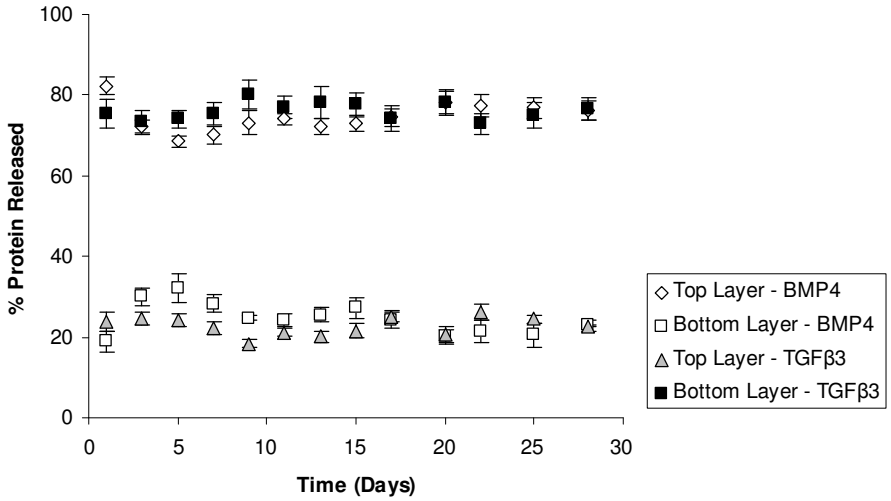


Figure 5.16: Release of BMP-4 and TGF B3 from bilayered scaffold was investigated using a set up shown in figure 2.6. The top and bottom layers was assayed for the presence of both proteins using ELISA.

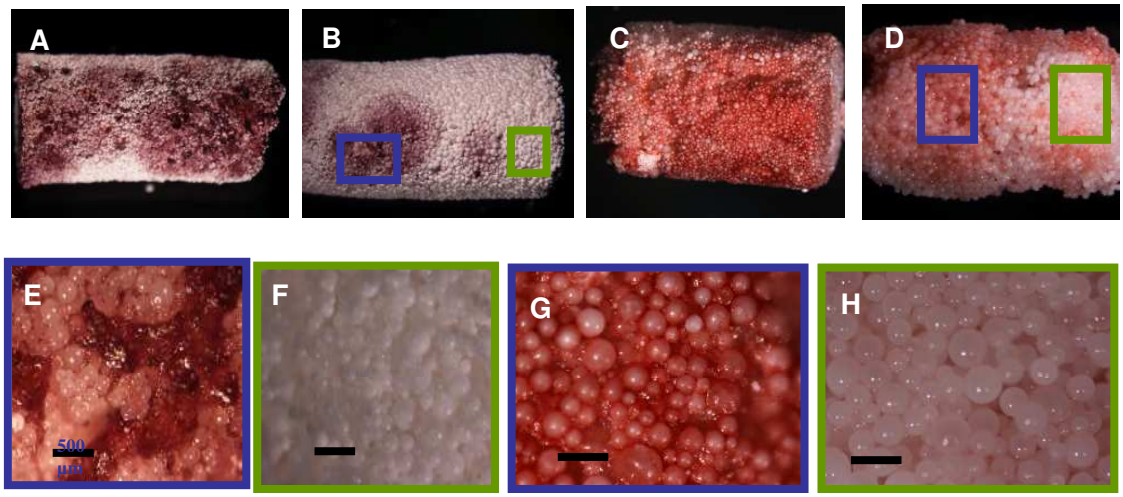


Figure 5.17: Micrographs showing the presence of calcium deposits on alizarin red stained scaffolds A) , B) , E) , & F) Dex loaded scaffold; C) , D) , G) , & H) BMP4 loaded scaffolds. B) & D) half loaded scaffolds. E) & F) and G) & H) magnified images of highlighted regions from images B) and D) respectively. Scale bar is 500µm. Half loaded scaffolds are scaffolds in which dex or BMP4 are loaded in only half of the scaffolds. Cell seeded scaffolds were cultured for 28 days in differentiation media, after which they were stained for collagen and gag deposits using alcian blue / sirius red staining and stained for collagenous tissue using masson trichrome staining.

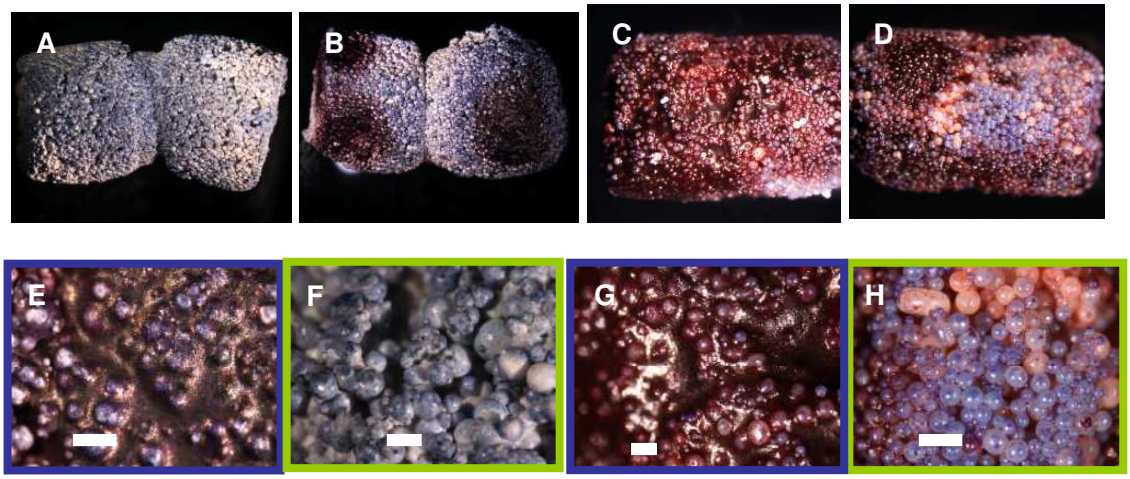


Figure 5.18: Micrographs showing the alcian blue/ sirius red and masson trichrome stained TGF-β3 / BMP4 loaded bilayered scaffolds. A) , B) , E) , & F) Alcian blue/sirius red stained bilayered scaffolds; C) , D) , G) , & H) masson trichrome stained bilayered scaffolds. A) & C) non loaded control scaffolds, B) & G) TGF-β3 / BMP4 loaded bilayered scaffold. E) & F) and G) & H) magnified images of highlighted regions from images B) and D) respectively. Scale bar is 500µm. Bilayered loaded scaffolds are scaffolds in which TGF-β3 and BMP4 are loaded in each half of the scaffolds. Cell seeded scaffolds were cultured for 28 days in differentiation media, after which they were stained for collagen and gag deposits using alcian blue / sirius red staining and stained for collagenous tissue using masson trichrome staining.

scaffolds showed a limited localisation of the blue cartilaginous tissue to the TGF-β3 region of the bilayered scaffold. However variable results were obtained following the masson trichrome staining of the TGF-β3 / BMP 4 bilayered scaffold, with stained cartilaginous tissue not always localised to the TGF-β3 region.

#### 5.4.4.5. Immunocytochemical staining.

Immunocytochemical staining of TGF-β3 and BMP4 loaded bilayered and non-loaded scaffolds for osteocalcin and collagen was undertaken to determine the presence and localisation of bone nodules and cartilage within the scaffold. Fig 5.19 shows the presence of osteocalcin (green) primarily within the BMP4 region of the bilayered scaffold, and collagen II (red) to the TGF-β3 region of the bilayered scaffold. The middle region of the bilayered scaffold showed the presence of both osteocalcin and collagen II (yellow).

## 5.5. Discussion.

In addition to the utilization of scaffolds and microspheres as cell delivery and support devices in aiding *in vivo* tissue repair, microspheres and scaffolds have been used extensively for the delivery of growth factors and drug molecules (Simmons, C. A. et al., 2004; Green, D. W. et al., 2006; Jin, Q. et al, 2008; Shi, S. et al., 2009). Several studies have demonstrated successful tissue regeneration with the delivery of a single growth factor from polymeric carriers (Lutolf, M. P. et al., 2003; Chen, F. et al., 2006 and Patel, Z. S. et al., 2008), at protein concentrations matching physiological levels. The incorporation of these molecules into scaffolds have been shown to further promote stem cell recruitment from basal tissue into the scaffold (Schantz, J. et al., 2007), encourage cell differentiation (Park, H. et al., 2007), enhance scaffold tissue

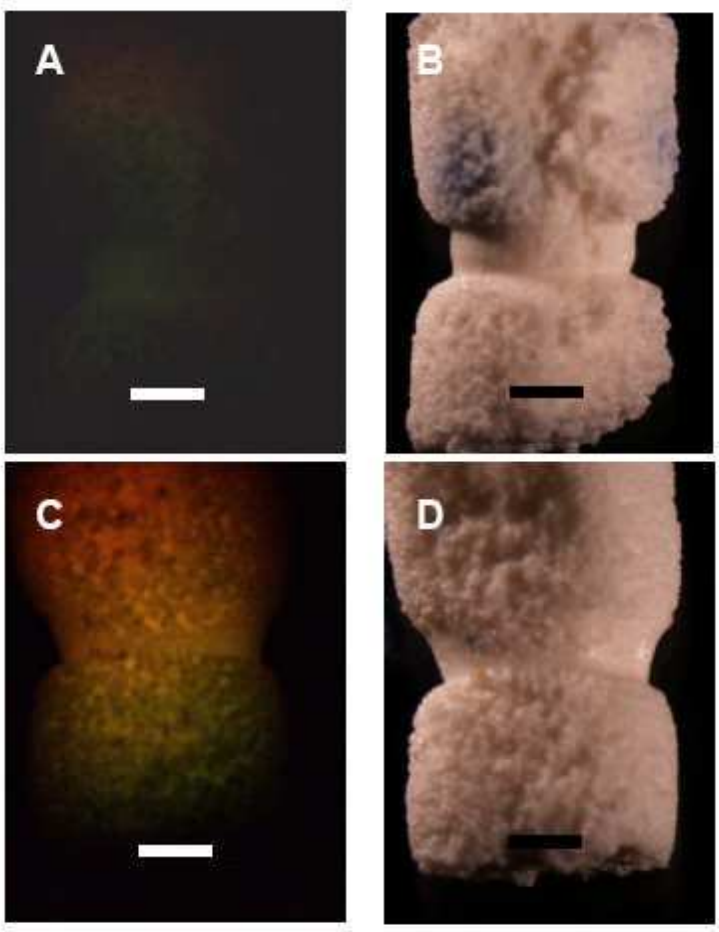


Figure 5.19: Double immunofluorescence staining for osteocalcin (green) and collagen II (red) of bilayered scaffold. Bilayered scaffolds were incubated in a mixture of osteocalcin (raised in goat) and collagen II (raised in rabbit) primary antibodies for 24 hours followed by incubating in a mixture of antigoat and antirabbit secondary antibodies for 2 hours. A) Fluorescent and B) bright field images of control scaffolds; C) Fluorescent and D) Bright field Images of growth factor loaded bilayered scaffolds. Scale bar is 2mm. Images were obtained by combining TRITC and FITC images of the scaffold using image calculator of the image J software.

integration (Shi, S. et al., 2009), and improve overall tissue growth and regeneration (Chen, R. R. et al., 2007; Kimura, Y. et al., 2008).

Differentiation from progenitor cells indicates a commitment to lineage specification and is the first step in tissue morphogenesis and repair. The data presented in this chapter represents an original demonstration of the promotion of osteogenic differentiation of mES cells by the controlled release of ascorbate and dexamethasone from microsphere based scaffolds for up to 21–28 days. The advantage of controlled release of growth factors and drug molecules, as opposed to addition in culture medium, is that controlled release enables continuous exposure of cells to the growth factor, and has the potential to avoid rapid denaturation and, if in an in vivo model, rapid diffusion.

In the work reported in this study, drug and protein loaded microsphere based scaffolds have successfully been fabricated, and utilised for the differentiation of murine embryonic stem cells along the osteogenic and chondrogenic pathways. Ascorbate -2-phosphate and dexamethasone were chosen as model drugs for this study due to their implications in induction of osteogenesis in human and murine embryonic stem cells (Buttery, L. D. K. et al., 2008; Bourne, S. et al, 2004; Pittenger, M. F. 2008) and the presence of a well characterised assay protocol for their detection and quantification (Kim, H. et al., 2003; Galeska, I. et al., 2005). Along side β-glycerophosphate they are regular requirements for osteogenesis induction in embryonic and mesenchymal stem cells. Asc is required for use in the synthesis of collagen (a major component of bone) and cell proliferation (Chan, D. et al., 1990; Choi, K.; et al., 2008). Dex is a synthetic member of the glucocorticoid class of

steroid hormones. Although the mechanism and signaling involved in dex-induced osteogenesis is not fully understood, its ability to induce osteoblast differentiation from stem cells has been reported extensively. It is believed that it plays an active role in promoting the differentiation of stem cells (Chang, J. et al., 2007; Li, X. et al., 2005; Phillips, J. E. 2006). β-glycerophosphate is an organic phosphate added to induce mineralization of the collagen matrix through calcium phosphate deposition (Garimella R. 2006). Tissue mineralization is a necessary precursor to bone tissue formation. Bone tissue is characterized by bone nodules which occur through secretion of ECM and osteocalcin which plays a key role in the deposition of calcium phosphate crystals within this matrix by osteoblasts (Cao, T. et al.; 2005).

Dex, asc, TGF-β3 and BMP4 were entrapped into microspheres made from PLGA blends containing 30% *w/w* triblock. mES cell seeded scaffolds were fabricated from these loaded microspheres, cultured in differentiation media for induction of osteogenesis and chondrogenesis The entrapment efficiency of asc and dex were quite low (<30%), and could be explained by leaching of the small molecular moieties into the solution during the microsphere fabrication. Whilst the poor entrapment efficiency of the growth factors TGF-β3 and BMP4 could be explained by the deleterious effect of the organic phase, protein aggregation and leaching. However the quantities retained within the microspheres were significantly above the amount required for induction of osteogenesis and chondrogenesis.

Having successfully incorporated dex and asc into the microspheres and fabrication of scaffolds from these microspheres, an underlying question needed to be answered, before embarking on the differentiation studies. Would the scaffold provide a

sustained release of the molecules at concentrations required for osteogenesis? In answering this question, controlled release experiments were designed to measure the amount of dex and asc released from the scaffold over a 30 day period. The thirty day period was taken, based on the extensive reports in the literature indicating this as the duration of time required for osteogenesis to occur in the presence of the relevant promoters (Tu, Q. et al., 2006; Buttery, L. D. K. et al., 2001; Bourne, S. et al., 2004; Sun, X. et al., 2008). In studies carried out by Jaiswal et al, for successful induction of osteogenesis in mesenchymal stem cells, constant concentrations exceeding 10ng/ml and 16µg/ml of dex and asc were required (Jaiswal, N. et al., 1997). Based on these findings it was hypothesized that aiming for concentrations exceeding these values will increase the probability of osteogenic induction. Although these studies were performed using embryonic stem cells, which are progenitors to mesenchymal stem cells and less committed to osteogenesis, several studies reported in the literature have indicated that osteogenesis can be achieved from embryonic stem cells using similar concentrations (Buttery, L. D. K. et al., 2001; Bourne, S. et al., 2004).

The controlled release studies undertaken for the asc + dex loaded scaffolds, showed a zero-order release profile post initial burst release for the release of dexamethasone, whilst asc release was characterized by a high initial burst phase with very little further release. The presence of asc in the scaffold was observed to increase both the initial burst and rate of release of dex from the scaffold. The high initial burst release and lag phase associated with asc from the scaffolds can be explained by the localization of entrapped asc closer to the surface of the microspheres due to its hydrophilic nature (Kim, H. et al., 2003). The reason for the lag phase release of the asc from the scaffold is not yet known. The higher initial burst release and accelerated

rate of release dex from the asc + dex loaded scaffolds compared against plain loaded dex scaffolds can be explained by the increased rate of hydration of the scaffold due to the hydrophilic nature of asc.

Based on knowledge of the amount of dex and asc released from the scaffolds, for a given volume of media the concentration of dex and asc seeded mES cells are exposed to during culturing could be determined, if the interval of media change matches the sampling interval for the controlled release. These results indicate that the concentrations of dex the cells were exposed to during the differentiation were within the concentration required for osteogenesis. After the initial burst (first three days) subsequent concentrations of asc was below the minimum concentration required for osteogenesis.

Increased osteocalcin production and mineralized bone nodules are the hallmark of the presence of mature osteoblasts (Bronckers, A. L. et al., 1987; Cao, T. et al., 2005; Al-Salleeh, F. et al., 2008). The patchy distribution of alizarin red stained calcium deposits indicated the successful induction of osteogenesis. Immunocytochemical staining for osteocalcin and osteocalcin assay showed an increased synthesis of osteocalcin. Osteocalcin is a vitamin K dependent protein and together with calcium forms the bone matrix. Increased production is an indication of committal of progenitor pathways and has been shown to increased synthesis from the $12^{th}$ day (Cao, T. et al., 2005). The reduced osteocalcin values (when compared to the values obtained for positive controls) could be explained by the reduced amount of asc in the media from the $2^{nd}$ day onwards as indicated by the controlled release experiments.

The amount of asc required for osteogenesis was shown to be at a concentration of 16µg/ml (Jaiswal, N. et al., 1997).

Despite the low concentrations of asc achieved during the majority of the culture period, a measurable degree of osteogenesis was still detectable, although to a lesser degree than that achieved for scaffolds incubated with a continuous exogenous supply of dex and asc. The low concentration of asc the mES cells were exposed to could possibly explain the reduced degree of osteogenesis observed in the asc + dex loaded scaffold. Two theories could possibly explain the surprise detectable osteogenesis observed in the asc + dex loaded scaffolds despite the low concentrations of asc released. The first theory is that the high amount of asc released during the initial burst phase was sufficient in inducing the collagen synthesis normally associated with asc functions. The second theory is that whilst the concentration of asc was low, the concentration of asc at the surface of the scaffold is not known and might exceed the minimal asc concentration required for osteogenesis. The results obtained suggest that rather than one of the theories being the dominant factor in promoting the osteogenesis, a complex interplay of both theories might seem more plausible. The high concentrations of asc achieved during the first three days of culturing due to the high initial burst release initiates a cascade of actions that leads to collagen formation. The little amount of asc further released was possibly sufficient to sustain a low amount of collagen synthesis.

Similarly to dex release from asc + dex loaded scaffolds, controlled release of TGF-β3 from the TGF-β3 loaded scaffolds, showed a zero-order release profile post initial burst release. Again utilizing a similar approach to that used for asc + dex scaffolds,

the concentrations of TGF-β3 mES cells are exposed to could be determined. The concentration of TGF-β3 was observed to be above the minimal amount of 10ng/ml concentration shown to be required for chondrogenesis (Moioli, E. K. and Mao, J. J. 2006; Huang, A. H. et al., 2008). Alcian blue staining for presence of proteoglycans in the matrix and assays for collagen and glycosaminoglycans confirmed the presence of chondrocytes and neo-cartilage formation. Proteoglycans and collagen are matrix proteins that make up the hyaline cartilage, and are important in providing the osmotic resistance and tensile strength necessary for cartilage to carry out its functions in resisting compressive loads (Knudson, C. B. and Knudson, W. 2001; Asanbaeva, A. et al., 2008). TGF-β3 has also been shown to inhibit bone osteogenesis, promote collagen synthesis and chondrogenesis in stem cells and progenitor stem cells (Huang, A. H. et al., 2008; and Moioli, E. K. et al., 2007).

One challenge of tissue engineering is to manufacture scaffolds that will support multi tissue repair (Holland, T. A. et al., 2005; Richardson, T. et al., 2005). The approach undertaken in this report in meeting this challenge was by building on the apparent success achieved in making a cell seeded biphasic scaffold that can be used in inducing differentiation of the cells along the chondrogenic and osteogenic pathways. The next approach was to investigate the possibility of building on the use of the loaded scaffolds as a delivery device for inducing osteogenesis and chondrogenesis in mES scaffold, by developing multi-layered tissue constructs. It was hypothesized that by fabricating a bilayered scaffold consisting of two separate regions of osteogenic and chondrogenic growth factor loaded microspheres it will be possible to develop a tissue construct consisting of bone and cartilage. Although the approach of developing multi-layered scaffold for multi-tissue constructs has been applied for osteochondral

(Holland, T. A. et al., 2005), bone (Patel, Z. S. et al., 2008) and vascular tissue engineering (Rophael, J. A. et al., 2007) has been previously reported, the concept of utilizing a purely microsphere based scaffold segmented across various regions is a novel one. It builds on work reported by Suciati et al, showing the successful localization of protein release and cell differentiation to the loaded regions (Suciati, T. et al., 2006).

A major difficulty envisaged was how to localise the release of the osteogenic promoting growth factor to one end and the chondrogenic promoting growth factor to another end. A novel set-up involving a silicon washer was designed. The set up involved using an  using an impermeable washer, with inner and outer diameter set to match the outer diameter of the scaffold and inner diameter of the universal tube respectively, to separate the two growth factor loaded regions from each other and limit the diffusion of the released proteins across the regions. The effectiveness of the set-up was initially investigated for localisation of protein by undertaking proof of concept studies. Proof of concept studies was undertaken by incubating a coloured bilayered scaffold in PBS and observing the change in colour of the PBS solution as the released dye diffuses through the solution. The bilayered scaffold consisted of green dye loaded microsphere region and a red dye or plain loaded microsphere region. Only the green dye was expected to be released over the duration of observation due to its hydrophilic properties and the hydrophobic properties of the red dye. The red dye was used mainly for visualization of the scaffold. The results obtained showed that it took about 5 days for a visually detectable amount of dye from one side of the washer to diffuse to the other side. Although the proportion of dye diffused to the other side of the washer, wasn't quantified, the results obtained by

visual comparisons were indicative that utilisation of this set-up was promising. Further controlled release studies of TGF-β3 and BMP4 loaded scaffolds using this set-up showed that about 70% of the protein released from one section of the washer was localised to that section of the scaffold. It was believed that the approximately 30% of protein present in the other section possibly diffused through the pores of the scaffold from one layer of the scaffold to the other.

Bilayered scaffolds consisting of one region of TGF-β3 loaded microspheres, and the other region of BMP4 + dex loaded regions was used to investigate possible formation of osteochondral plugs consisting of bone cartilage biphasic constructs. BMP4 is a growth factor belonging to the bone morphogenic protein group and is a potent promoter of osteogenesis in mesenchymal stem cells (Kawaguchi, J. et al., 2005; Chen, X. et al., 2004). BMP4 and dex was used instead of dex and asc due to the implication of TGF-β3 in inhibition of osteogenesis, and requirement of dex and asc (howbeit at different concentrations) for chondrogenesis.

Analysis of the bilayered scaffolds for GAG and collagen production, presence of organised collagen fibrils, and mineralized bone nodules showed promising results for the chondrogenic and osteogenic differentiation of the stem cells. However zonation of the tissues to the relevant growth factor regions was inconclusive as indicated by the masson trichrome and double antigen immunocytochemical staining. Further improvement of biphasic tissue zonation could be obtained through the use of an impermeable layer or a layer of smaller microspheres in between the two growth factor region to limit the diffusion of the proteins from one region to another.

## 5.6. Conclusion

From the studies presented in this chapter, dexamethasone and ascorbate -2 – phosphate has been successfully encapsulated into polymeric microspheres and utilised to form scaffolds. These scaffolds were utilised in inducing the differentiation of murine embryonic stem cells into osteoblasts through the release of the encapsulated drug molecules. TGF-β3 growth factor was also encapsulated into the polymeric microspheres and utilised to form scaffolds for the induction of differentiation of murine embryonic stem cells into chondrocytes through the release of the encapsulated growth factor molecule.

Bilayered scaffolds consisting of a layer of TGF-β3 loaded microspheres and another layer of BMP4 and dexamethasone loaded microspheres were fabricated and utilised in the formation of biphasic tissue constructs consisting of bone and cartilage, through the differentiation of seeded embryonic stem cells into osteoblasts and chondrocytes. Exploration of these scaffolds for the development of biphasic tissue constructs showed promising but inconclusive results.

# Chapter 6

## 6.1. Conclusion

Scaffolds have been utilised as devices for the delivery of growth factors and as a support for the proliferation and differentiation of cells in various tissue engineering applications (Hou et al., 2004). However the utilisation of scaffolds for the co-delivery of multiple growth factors and drug molecules for the induction of differentiation of stem cells has not been extensively demonstrated. The delivery of multiple growth factors alongside stem cells are important facets needed for the successful regeneration of heterogeneous cellular tissues such as brain and liver, organs and repair across tissue interfaces such as osteoarthritis (Holland et al., 2005).

Despite numerous publications on the development and use of *in situ* scaffolds for tissue engineering and drug delivery applications existing (Kretlow et al., 2007), most of these scaffolds have been hydrogels (Stabenfeldt et al., 2006; Ohya and Matsuda 2005; Crompton et al., 2007) and thermogelling polymer systems involving poloxamers and PNIPAAm (Na et al., 2006; Yasuda et al., 2006; Cortiella et al., 2006). These systems have shown limitations for bone tissue engineering applications, due to the resulting poor mechanical properties of the scaffolds (Temenoff and Mikos 2000). Current injectable materials that have been explored for bone tissue engineering revolve around the use of ceramics, however the slow resorbable rates, and low tensile strength properties of the resulting scaffolds (Miyamoto et al, 1997;

Constanz et al., 1995) have necessitated the focus on polymers, due to the ability to tailor the mechanical properties and degradation rates (Anseth et al., 1999). Majority of the polymers that have been used have involved materials requiring initiator and crosslinker systems for *in situ* crosslinking (Holland et al., 2003; Temenoff et al., 2003; Holland et al., 2005). The approach reported in chapter this thesis has involved exploiting the thermosensitive properties of the triblock PLGA-PEG-PLGA to reduce the glass transition temperature of PLGA for the development of injectable scaffolds.

The novel triblock-PLGA blend formulation developed in chapter three showed a reduction in the glass transition temperature when compared against the unblended PLGA. These findings can be exploited in the design of *in situ* scaffold through the delivery of microspheres into the body in a slurry form. The resulting increase in temperature (from room to body temperature) will result in the microspheres sintering to form scaffolds. Successful development of *in situ* forming scaffolds will have immense clinical and commercial impact through the reduction in cost, trauma, and morbidity associated with invasive surgery encountered with the use of patient specific pre-fabricated scaffolds. *In situ* scaffolds incorporating stem cells can also be formed by pre-mixing the microsphere slurry with the cell suspensions before delivery to the desired site. Even though the glass transition temperature of the microspheres obtained from the triblock-PLGA formulation was above the 37ºC (required for *in vivo* sintering of the scaffold), preliminary unpublished data of work carried out by Lloyd Hamilton (unpublished thesis, University of Nottingham, UK) indicated that wet sintering (in the presence of water) of microspheres into scaffolds required lower temperatures (upto a 5ºC reduction) than corresponding dry sintering. It was hypothesized that water acted as a plasticizer for the scaffold. In additional

work carried out by Suciati and co-workers heat sintering of $P_{DL}LA$ microspheres, with water content ranging from 2.1% to 5.3% to form scaffolds, resulted in an increase of compressive strength of resulting scaffolds from 3MPa to 12MPa (Suciati et al., 2006). Previous work carried out by Passerini and Craig, showed a negative correlation between the residual water content of PLA, and PLGA (50:50 and 75:25) microspheres, and the glass transition temperature as measured by differential scanning calorimetry (DSC). This correlation was observed to be in agreement with a Gordon-Taylor relationship, implying a perfect distribution of the water within the microspheres (Passerini and Craig, 2001). These findings corroborates our results and lends support to the hypothesis that wet sintering of microspheres (possibly through pre-mixing of microspheres with cell suspension) at physiological temperatures made from the novel triblock-PLGA formulation will yield scaffolds of sufficient strength for bone tissue engineering applications.

In chapter four, protein and drug loaded microspheres with zero-order release kinetic profile, tuneable initial burst release and duration of sustained release was successfully fabricated. Although the development of microspheres showing a zero – order release profile has been previously demonstrated (Lee et al., 2006; Makino et al., 2000; Lee and Yoo 2008). These approaches have involved the utilisation of low molecular weight polymers (Makino et al., 2000), or through the co-encapsulation of additives such as urea (Nam et al., 2000), PEG400 (Péan et al., 1999), sucrose (Lee et al., 2006). However these techniques cannot be applied to microspheres made from high molecular weight polymers, and the co-encapsulation of additives alongside growth factors could have deleterious effects on their overall activity. The utilisation of the triblock polymer for optimization of the release kinetics of the PLGA

microspheres, to produce microspheres with zero-order release kinetic profile is a novel approach that successfully combines the hydrophilic properties of the triblock with the mechanical properties of the high molecular PLGA. As a result these microspheres can be exploited as delivery devices for tissue engineering and other clinical applications, and provides the option of controlling the loading dose and duration of continuous release of the entrapped moiety. Combination of the findings from chapter 3 and 4 provides the technology for developing drug or protein eluting *in situ* forming scaffolds.

In chapter five, growth factor loaded microsphere based scaffolds was used to induce the differentiation of stem cells along different lineages. Dexamethasone and ascorbic loaded microsphere based scaffolds were utilised in induction of osteogenesis in the embryonic stem cells seeded on the scaffolds, as evidenced by the presence of osteoblast-like cells showing detectable levels of osteocalcin and calcium deposition. TGF-β3 loaded microsphere based scaffolds were utilised in induction of chondrogenesis in the embryonic stem cells seeded on the scaffolds, as evidenced by the presence of chondrocyte-like cells showing detectable levels of collagen and proteoglycan deposition. While the differentiation of mesenchymal stem cells into osteoblasts-like cells through the controlled release of dexamethasone and ascorbic acid from polymeric scaffolds has been demonstrated (Kim et al., 2003), this is the first time this approach has been demonstrated utilising dexamethasone and ascorbate loaded microspheres. It is also the first time embryonic stem cells have been shown to differentiate into osteoblast-like cells by utilising dexamethasone loaded microspheres.

Chapter five also reports the development of bilayered scaffolds for use in treatment of osteochondral defects. Bilayered scaffold has been successfully developed for tissue engineering of nerves (Carone and Hasenwinkel 2006), skin (Wang et al., 2006) and osteochondral defects (Keeney and Pandit, 2009). Current approaches for development of bilayered scaffolds for osteochondral defects have involved the production of heterogeneous bilayered scaffolds either by assembling of two separated layers (Gao *et al*., 2001; Chen *et al*., 2006b) or the production of integrated bilayered scaffolds (Hung *et al*., 2003; Holland *et al*., 2005). In the review by Mano and Reiz, the rationale behind the strategy of utilising heterogeneous bilayered scaffolds was due to the ability to incorporate two different cell types within their favoured environment consisting of different chemical surroundings, mechanical features and pore morphology. This environment enables the successful development and growth of the two different tissues, by satisfying the different biological requirements (Mano and Reiz 2007). However poor integration of the two tissues at the interface region and the need for large number of primary cells are current limitations for this approach (O'Shea and Miao 2008). In addition the expansion of primary cells may also result in a degradation of their functionality, e.g. the expansion of articular chondrocytes can lead to the expression of fibrocartilage (Lipman *et al*., 1983).

In experiments carried out by Gao and co workers. the potential of using a single cell source - bone marrow–derived progenitor cells (MPCs), in osteochondral tissue engineering by using a calcium phosphate bone layer and a hyaluronan sponge cartilage layer was demonstrated (Gao et al., 2001, 2002). In the first study, fibrin sealant was used to combine two single cell source–seeded scaffolds together. *In vivo*

studies in a rat using these scaffolds produced inappropriate fibrocartilage tissue in the cartilage layer (Gao et al., 2001). In the second study, the group used an injectable calcium phosphate cell-free scaffold together with a MPC cell seeded hyaluronan matrix. This bilayered structure was implanted by press fit before ceramic hardening in a rabbit model with 4- and 12-week revisions. The hyaluronan and calcium phosphate sections of the bilayered scaffolds was able to support the differentiation of MPC cells into the cartilage and bone respectively, with good bioactivity observed in the bone layer, and zonal arrangements within the cartilage region (Gao et al., 2002).

Li and co-workers developed a minimum common osteochondrocytic differentiation medium (MCDM) consisting of dexamethasone and ascorbic acid, which was successfully used to induce chondrogenic and osteogenic differentiation in bone marrow stromal stem cells (BMSCs). Further supplementation of the MCDM with TGF-β3 and osteogenic protein-1 (OSP-1) resulted in the induction of BMSCs into osteogenic and chondrogenic lineages respectively. Chondrogenic and osteogenic induction of the BMSCs occurred in both two-dimensional and three-dimensional culture systems, as evidenced by the increased expression of glycosaminoglycans and type II collagen (for TGF-β3 supplemented medium) and detectable expression of osteopontin and osteocalcin (for OSP-1 supplemented medium). These chondrogenic and osteogenic differentiation markers were significantly enhanced in the three-dimensional cultures compared to the two-dimensional monolayer cultures (Li et al., 2009).

By building on the work carried out by Gao and co- workers, showing the successful differentiation of MPC cells on a heterogeneous bilayered scaffolds, and Li and co-

workers, in the development of a common osteochondrocytic differentiation, bilayered scaffold consisting of two different regions of growth factor loaded microspheres and their ability in inducing differentiation of osteogenesis and chondrogenesis in seeded murine embryonic stem cells were investigated. The growth factors used for fabrication of the bilayered scaffolds were TGF-β3 and BMP-4. BMP-4 and TGF-β3 loaded microspheres were formed from 30% triblock/PLGA blend formed and characterised in chapters' four and five. The bilayered scaffold was shown to release the growth factors independently in a controlled release manner with zero order release kinetics over a 4 week period. The bilayered scaffold was exploited for use in development of biphasic tissue construct through the actions of localised release of growth factors on murine embryonic stem cells.

In conclusion, this thesis details the development of free-flowing microspheres made from triblock/PLGA blends, and can be exploited for the development of growth factor loaded *in situ* forming scaffolds that can be applied for the regeneration of tissues across tissue interfaces (e.g. include osteochondral defects) and developing of multiple tissues, through the development of bilayered scaffolds.

## 6.2. Future Work

The scaffolds developed in this thesis were fabricated by dry sintering following the methodology indicated by Borden and co-workers (Borden et al., 2004). However the development of in situ scaffolds will require the sintering of scaffolds in the presence of physiological fluids. Hence future experimental objectives worth investigating would be investigating the effect of wet sintering (using distilled water, PBS, and culture media) on the mechanical properties of scaffolds and sintering temperature

required for scaffold fabrication. The results obtained from these studies will be more indicative of the suitability of the use of the triblock-PLGA formulation for developing microspheres for injectable scaffolds.

Evidence of bone-cartilage tissue formation from growth factor loaded bilayered scaffold was based on data obtained from immunocytochemical staining, histochemical staining and quantification of proteins associated with these tissues such as osteocalcin and GAG. The limitations of following this approach are that most of these tissue specific marker proteins are not present in detectable quantities even in mature tissue (Garnero et al., 2000). Characterisation of the tissue constructs obtained from the bilayered scaffold using amplificatory molecular techniques such as western blotting and RT-PCR for detecting small amounts of tissue specific proteins and RNA will provide more conclusive data supporting the presence or absence of the various tissue types.

The growth factors investigated for formation of biphasic tissue constructs were TGF-β3 and BMP4, both of which are members of the transforming growth factor superfamily (Miyazawa et al., 2002). Their structure and actions on stem cells have been shown to be quite similar (Pucéat, 2006). Also the chondrogenic and osteogenic differentiation pathway of stem cells are similar and closely related, with calcification of chondrocytes shown to result in bone formation (Jukes et al., 2008). These highlighted details could provide an explanation for the complete tissue zonation of bone and cartilage not being observed. The use of proteins belonging to different growth factor superfamilies and that induce stem cell differentiation along different pathways and precursors, such as basic fibroblast growth factor (bFGF) and BMP4 to

develop muscle and bone tissue; or BMP4 and VEGF to develop bone and blood vessel rich tissues, will provide more information on the use of these bilayered scaffold for biphasic tissue development.

Further experiments that can be investigated include undertaking *in vivo* studies using animal models to explore the possibility of the cell seeded bilayered scaffold promoting tissue repair and regeneration in osteochondral defects; or utilising bilayered scaffold consisting of other growth factors such as glial growth factors -2 (GGF) and basic fibroblast growth factors (bFGF) for the differentiation of stem cells into glial and neurones in the formation of hierarchical organs such as the brain.

# REFERENCES

Al-Salleeh, F.; Beatty, M. W.; Reinhardt, R. A.; Petro, T. M.; Crouch, L. "Human osteogenic protein-1 induces osteogenic differentiation of adipose-derived stem cells harvested from mice". Archives of Oral Biology (2008), 53: 928-936

Asanbaeva, A.; Masuda, K.; Thonar, E.J.-M.A.; Klisch, S.M.; and Sah, R.L. "Cartilage growth and remodeling: modulation of balance between proteoglycan and collagen network in vitro with β-aminopropionitrile" Osteoarthritis and cartilage 16: (2008) 1 -11.

Aubert-Pouëssel, A. et al. "A novel in vitro delivery system for assessing the biological integrity of protein upon release from PLGA microspheres". Pharm Res. 19 (2002) 1046 – 1051

Babensee, J. E., L. V. McIntire, et al. "Growth Factor Delivery for Tissue Engineering." Pharm. Res. 17 (2000) 497 - 504.

Bellows C., Aubin J., Heersche J., Antosz N. (1986) Mineralized bone nodules formed in vitro from enzymatically released rat calvaria cell populations. Calcif Tissue Int 38:143–54.

Berkland, C., Kim, K., and Pack, D. W. "Fabrication of PLG microspheres with precisely controlled and monodisperse size distributions". J. Control. Release 73 (2001) 59 – 74.

Berkland, C. et al. "Precise control of PLG microsphere size provides enhanced control of drug release rate". J. Control Release 82 (2002) 137 – 147.

Berkland, C. et al., "Macromolecule release from monodisperse PLG microspheres: Control of release rates and investigation of release mechanism". Journal Pharm Sci 96 (2007): 1176 -1191.

Bezemer, J. M. et al. "Microspheres for protein delivery prepared from amphiphilic multiblock copolymers 2. Modulation of release rate". J. Control Release. 67 (2000) 249 – 260.

Bezemer, J. M. et al. "Zero-order release of lysozyme from poly9ethylene glycol)/ poly(butylenes terphthalate) matrices". Journal of Controlled Release. 64 (2000) 179 – 192.

Bielby, R. et al.,. “In Vitro Differentiation and In Vivo Mineralization of Osteogenic Cells Derived from Human Embryonic Stem Cells” Tissue Eng 10: (2004) 1518 – 1525.

Biwa R., Siegel R.A., Marasa B., Karel M., and Langer R. An explanation for the controlled release of macromolecules from polymers. Journal of Controlled Release 1(1985): 259–267

Blanco, M.D., Alonso, M.J. (1997) Development and characterisation of protein-loaded poly(lactide-co-glycolide) nanospheres, Eur. J. Pharm. Biopharm. 43 (1997) 287– 294.

Blanco, D., and Alonso, M. J. “Protein encapsulation and release from poly(lactide-co-glycolide) microspheres: effect of the protein and polymer properties and of the co-encapsulation of surfactants. Eur. J. Pharm. Biopharm. 45 (1998) 285-294.

Blanco-Prieto, M. J. et al.“Importance of single or blended polymer types for controlled in vitro release and plasma levels of a somatostatin analogue entrapped in PLA/PLGA microspheres”. J. Control. Release. 96 (2004) 437 – 448.

Bodmeier, R. and McGinty, J.W. “The preparation and evaluation of drug-containing poly(D,L-lactide) microspheres formed by the solvent evaporation method”. Pharm. Res 4 (1987) 465 – 471.

Bodemeier, R. and Chen, H. “Preparation of biodegradable poly(lactide) microparticles using a spray drying technique. J. Pharm. Pharmacol. 40 (1988) 754 – 757.

Borden, M. et al. “Tissue engineered microsphere-based matrices for bone repair: design and evaluation.” Biomaterials 23 (2002) 551 – 559.

Bourne, S.; Polak, J. M.; Hughes, S. P. F.; Buttery, L. D. K. “Osteogenic Differentiation of Mouse Embryonic Stem Cells: Differential Gene Expression Analysis by cDNA Microarray and Purification of Osteoblasts by Cadherin-11 Magnetically Activated Cell Sorting”. Tissue Engineering 10: 796 – 806.

Bronckers, A.L.; Gay, S.; Finkelman, R.D.; Butler, W.T.. “Developmental appearance of Gla proteins (osteocalcin) and alkaline phosphatase in tooth germs and bones of the rat”. Bone Miner. 2(1987): 361–373.

Burdick, J.A. Mason, M.N.. Hinman, A.D Thorne K. and Anseth, K.S., Delivery of osteoinductive growth factors from degradable PEG hydrogels influences osteoblast differentiation and mineralization. J. Control. Release 83(2002): 53–63.

Burgess, D. J. et al., “Assuring quality and performance of sustained and controlled release parenterals: workshop report”. AAPS PharmSci 4 (2002) E7.

Buttery, L. D. K.; Bourne, S.; Xynos, J. D.; Wood, H.; Hughes, F. J.; Hughes, S. P. F.; Episkopou, V.; Polak, J. M. (2001) “Differentiation of Osteoblasts and in Vitro Bone Formation from Murine Embryonic Stem Cells”.

Cao, T.; Heng, B. C.; Ye, C. P.; Liu, H.; Toh, W. S.; Robson, P.; Li, P.; Hong, Y. H.; Stanton, L. W. "Osteogenic differentiation within intact human embryoid bodies result in a marked increase in osteocalcin secretion after 12 days of in vitro culture, and formation of morphologically distinct nodule-like structures". Tissue and Cell 37(2005) 325–334

Carino, P. G. et al. "Bioadhesive polymers for increased intestinal uptake". In: Mathiowitz, E., Chickering, D. E., and Lehr, C. M. "Bioadhesive drug delivery systems – Fundamentals, Novel Approaches and Development" Marcel Dekker Eds. (1999) 459 – 475.

Castellanos I.J. et al.,. "Encapsulation-induced aggregation and loss in activity of g-chymotrypsin and their prevention. J Control Release 81(2002):307–319.

Castellanos IJ, Griebenow K.. Improvement a-chymotrypsin stability upon encapsulation in PLGA microspheres by solvent replacement. Pharm Res 20(2003):1873–1880.

Castellanos I.J. et al.,. "Effect of the covalent modification with polyethylene glycol on a-chymotrypsin stability upon encapsulation in poly(lactic-co-glycolic) microspheres. J Pharm Sci 94(2005):1–14.

Castellanos I.J. et al., Poly(ethylene glycol) as stabilizer and emulsifying agent: a novel stabilization approach preventing aggregation and inactivation of proteins upon encapsulation in bioerodible polyester microspheres. J Control Rel 88(2003):135–145.

Castellanos, I.J. et al., "Encapsulation of bovine serum albumin in poly(lactide-co -glycolide) microspheres by the solid-in-oil-in-water technique. J. Pharm. Pharmacol.53(2001), 167 - 178.

Castellanos, I.J., et al., "Prevention of structural perturbations and aggregation upon encapsulation of bovine serum albumin into poly(lactide- co -glycolide) microspheres using the solid-in-oil-inwater technique". J. Pharm. Pharmacol. 53(2001), 1099 - 1107.

Castellanos, I.J. et al .,. "Encapsulation induced aggregation and loss in activity of gamma-chymotrypsin and their prevention. J. Control Rel. 81(2002), 307–319.

Castellanos, I.J. et al.,. "Poly(ethylene glycol) as stabilizer and emulsifying agent: a novel stabilization approach preventing aggregation and inactivation of proteins upon encapsulation in bioerodible polyester microspheres, J. Control. Release 88(2003): 135–145.

Chan, D.; Lamande, S. R.; Cole, W. G.; and Bateman, F. F. "Regulation of procollagen synthesis and processing during ascorbate-induced extracellular matrix accumulation in vitro". Biochem J. 269(1990): 175–181.

Chang, J.; Li. C.; Wu, S.; Yeh, C.; Chen, C.; Fu, C.; Wanga, G.; Ho, M.

"Effects of anti-inflammatory drugs on proliferation, cytotoxicity and osteogenesis in bone marrow mesenchymal stem cells". Biochemical Pharmacology 74 (2007): 1371 – 1382.

Chau, D. Y. S.; Agashi, K., and Shakesheff, K. M. S. "Microsparticles as Tissue Engineering Scaffolds: Manufacture, Modification and Manipulation" Mater Tech Sci. In Press

Chen, R. R.; Silva, E. A.; Yuen, W. W.; Mooney, D. J. "Spatio–temporal VEGF and PDGF Delivery Patterns Blood Vessel Formation and Maturation" Pharmaceutical Research 24(2007): 258 – 264.

Chen, X.; Fisher, L. W.; Robey, P. G.; and Young, M. F. "The small leucine-rich proteoglycan biglycan modulates BMP-4-induced osteoblast differentiation". FASEB J. 18(2004), 948–958

Chen S., Pieper R., Webster D. C., and Singh J. Triblock copolymers: synthesis, characterization, and delivery of a model protein International Journal of Pharmaceutics. 288(2005): 207–218.

Chen, F; Zhao, Y.; Wu, H; Deng, Z; Wang, Q et al. (2006) Enhancement of periodontal tissue regeneration by locally controlled delivery of insulin-like growth factor-I from dextran–co-gelatin microspheres.

Chickering, D., Jacob, J. and Mathiowitz, E. "Poly(fumaric-co-sebacic) microspheres as oral drug delivery systems". Biotechnol. Bioeng. 52 (1996) 96 – 101.

Choi, K.; Seo, Y; Yoon, H.; Song, K.; Kwon, S.; Lee, H.; and Park, J. "Effect of Ascorbic Acid on Bone Marrow-Derived Mesenchymal Stem Cell Proliferation and Differentiation". Journal of Bioscience and Bioengineering. 105(2008): 586-594.

Cleek, R. L. et al. "Microparticles of Poly(D,L-lactic-co-glycolic acid)/poly(ethylene glycol) blends". J. Control. Release 48 (1997) 259 - 268.

Cohen S., Yoshioka T., Lucarelli M., Hwang L.H., and Langer R. Controlled delivery systems for protein based on poly (lactic/glycolic acid) microspheres. Pharmaceutical. Research. 8(1991): 713–720

Cooke, M. N., J. P. Fisher, et al. "Use of Stelithography to Manufacture Critical-Sized 3D Biodegradable Scaffolds for Bone Ingrowth." J. Biomed. Mater. Res. Part B: Applied Biomaterials 64B (2002) 65 - 69.

Cortesi, R. et al. "Gelatin microspheres as a new approach for the controlled delivery of synthetic oligonucleotides and PCR generated DNA fragments". Int. J. Pharm. 105 (1994) 181 – 186.

Cosgrove B. D, Griffith L. G. Lauffenburger, D. A. "Fusing tissue engineering and systems biology toward fulfilling their promise. Cellular and Molecular Bioengineering 1(2008):33-41.

Crotts, G. and Park, T.G. “Preparation of porous and non-porous biodegradable polymeric hollow microspheres”. J. Control Release 35 (1995) 91 –105.

Crotts, G. Park, T.G. (1997) “Stability and release of bovine serum albumin encapsulated within poly(d,l-lactide-co-glycolide) microparticles, J. Control. Release 44: 123– 134.

Cunningham, L. W., Jr., (1954) “Reactivation of diethyl p-nitrophenyl phosphate-inhibited alpha-chymotrypsin by hydroxylamine”. J. Biol. Chem., 207, 443 – 458.

Davis, K. A. “Photoinitiated crosslinked degradable copolymer networks for tissue engineering applications”. Biomaterials 24 (2003) 2485 – 2495

Drury, J. L. and Mooney, D. J. "Hydrogels for tissue engineering: scaffold design variables and applications." Biomaterials 24 (2003) 4337 - 4351.

D’Souza, S. S. and DeLuca, P. P. “Methods to Assess in vitro drug release from injectable polymeric particulate systems”. Pharm. Res. 23 (2006) 460 – 474.

Edlund, U., and Albertsson, A. C. “Morphology engineering of a novel poly(L-lactide)/poly(1,5-dioxepane-2-one) microsphere system for controlled drug delivery. J. Polym. Sci.: Part A: Pol. Chem. 38 (2000) 786 – 796.

Engler, A.; Sen, S.; Sweeney, H.; and Discher, D. (2006) “Matrix Elasticity Directs Stem Cell Lineage Specification” Cell 126: 677-689

Elisseeff. J. “Injectable cartilage tissue engineering”. Expert Opinion on Biological Therapy 4 (2004) 1849 -1859.

Ernis, D., and Yuksel, A. “Preparation of spray-dried microspheres of indomethacin and examination of the effects of coating on dissolution rates”. J. Microencapsul. 16 (1999) 315 – 324.

Ereshefsky, L.; Mannaert, E. “Pharmacokinetic Profile and Clinical Efficacy of Long-Acting Risperidone: Potential Benefits of Combining an Atypical Antipsychotic and a New Delivery System.” Drugs in R & D. 6(3):129-137, 2005.

Freiberg, S., and Zhu, X. X. “Polymer microspheres for controlled drug release”. Int. J. Pharm. 282 (2004) 1 – 18.

Gaspar, M.M., Blanco, D., Cruz, M.E.M and Alonso, M.J. (1998) Formulation of -asparaginase-loaded poly(lactide-co-glycolide) nanoparticles: influence of polymer properties on enzyme loading activity and in vitro release. J. Control. Release 52 (1998), pp. 53–62.

Galeska, I.; Kim, T.; Patil, S. D.; Bhardwaj, U.; Chatttopadhyay, D.; Papadimitrakopoulos, F.; Burgess, D. J. (2005) “Controlled Release of

Dexamethasone from PLGA Microspheres Embedded Within Polyacid-Containing PVA Hydrogels". AAPS Journal 7: E231 – E240.

Ghaderi, R., Struesson, C. and Carlfors, J. "Effect of preparative parameters on the characteristics of poly(D,L-lactide-coglycolide) microspheres made by the double emulsion method". Int. J. Pharm. 141 (1996). 205 – 216.

Gido, C. et al. " Conventional versus novel conditions for the in vitro dissolution testing of a parenteral slow release formulations: application to doxepin parenteral dosage forms". Pharmazie 48 (1993) 764 – 769.

Giunchedi, P., Alpar, H.O., Conte, U., 1998. PDLLA microspheres containing steroids: spray drying, o/w and w/o/w emulsification as preparation methods. J. Microencapsul. 15, 185–195.

Goraltchouk A. et al. "Incorporation of protein-eluting microspheres into biodegradable nerve guidance channels for controlled release." J. Control Release 110 (2006) 400 – 407.

Green, D. W.; Mann, S,; and Oreffo, R. O. C. (2006) "Mineralized polysaccharide capsules as biomimetic microenvironments for cell, gene and growth factor delivery in tissue engineering". Soft Matter 2: 732 – 737.

Griebenow K, Klibanov AM. (1996). "On protein denaturation in aqueous-organic but not in pure organic solvents". J Am Chem Soc 118:11695– 11700.

Griebenow K, et al., (1999) "Improved enzyme activity and enantioselectivity in organic solvents by methyl-b-cyclodextrin. J Am Chem Soc 121:8157–8163

Griebenow, K. et al., (2001) "Nativelike enzyme properties are important for optimum activity in neat organic solvents" J Am Chem Soc. 123: 5380-1.

Griffith, L. G. and Naughton G. (2002) "Tissue Engineering--Current Challenges and Expanding Opportunities" Science 295:1009 -1014.

Griffith L.G. and Swartz M.A. (2006). Capturing complex 3D tissue physiology in vitro. Nature Rev. Mol. Cell Biol. 7:211-224.

Gu, H. et al., (2007) "Controlled release of recombinant human nerve growth factor (rhNGF) from poly[(lactic acid)-co-(glycolic acid)] microspheres for the treatment of neurodegenerative disorders". Polym Int 56:1272–1280.

Hendriks. J,; Riesle, J.; and van Blitterswijk C. A. (2007). "Co-culture in cartilage tissue engineering". Journal of tissue engineering and regenerative medicine 1:170-8

Herrero-Vanrell, R. and Refojo, M. F. "Biodegradable microspheres for vitreoretinal drug delivery". Adv. Drug. Del. Rev. 52 (2001) 5 –16.

Higuchi, T., (1963). “Mechanism of sustained-action medication: Theoretical analysis of rate of release of solid drug dispersed in solid matrices”. J. Pharm. Sci. 52: 1145–1149.

Hiraoka Y., Yamashiro H., Yasuda K., Kimura Y., Inamoto T., and Tabata Y. (2006) In situ regeneration of adipose tissue in rat fat pad by combining a collagen scaffold with gelatin microspheres containing basic fibroblast growth factor, Tissue Engineering. 12: 1475–1487

Hora M.S., Rana R.K., Nunberg J.H., Tice T.R., Gilley R.M., and Hudson M.E. (1990) Release of human serum albumin from poly (lactide co-glycolide) microspheres. Pharmaceutical Research 7: 1190–1194

Houtmacher, D. M. et al. "Scaffold-based tissue engineering: rationale for computer-aided design and solid free-form fabrication systems." TRENDS in Biotechnology 22 (2004) 354 - 362.

Hou, Q. DeBank, P. A. and Shakesheff, K. M. “Injectable scaffolds for tissue regeneration”. J. Mater. Chem. 14 (2004) 1915 – 1923

Huang, A. H.; Motlekar, N. A.; Stein, A.; Diamond, S. L.; Shore, E. M.; and Mauck, R. L. (2008) “High-Throughput Screening for Modulators of Mesenchymal Stem Cell Chondrogenesis”. Annals of Biomedical Engineering 36: 1909 – 1921.

Huang, Y. Y., Chung, T. W., and Tzeng, T. W. “A method using biodegradable polylactides/polyethylene glycol for drug release with reduced initial burst”. Int. J. Pharm. 182 (1999) 93 –100.

Huang, J. et al., (2006) “A delivery strategy for rotenone microspheres in an animal model of Parkinson's disease”. Biomaterials 27: 937-946.

Hubbell, J.A. (1995) Biomaterials in tissue engineering. Biotechnology (NY), 13(6), 565-576

Inanc, B.; Elcin, A. E.; and Elcin, Y. M. (2006) “Osteogenic Induction of Human Periodontal Ligament Fibroblasts Under Two- and Three-Dimensional Culture Conditions” Tissue Engineering. 12: 257-266

Jaiswal, N.; Haynesworth, S. E.; Caplan, A. I.; and Bruder, S. P. (1997) “Osteogenic Differentiation of Purified, Culture-Expanded Human mesenchymal Stem Cells In Vitro” Journal of Cellular Biochemistry 64:295–312

Jeyanthi, R. et al. “Effect of solvent removal technique on the matrix characteristics of polylactide/glycolide microspheres for peptide delivery”. J. Control. Release 38 (1996) 235 – 244.

Jiang, W., Schwendeman, S.P., 2001. Stabilization and controlled release of bovine serum albumin encapsulated in poly(d,l-lactide) and poly(ethylene glycol) microsphere blends. Pharm. Res. 18, 878–885.

Johnson, O. L. et al. “The stabilization and encapsulation of human growth hormone into biodegradable microspheres”. Pharm Res. 14 (1997) 730 – 735.

Jones, C. D., and Lyon, L. A. “Synthesis and characterization of multiresponsive core-shell microgels”. Macromolecules 33 (2000) 8301 – 8306.

Kang F and Singh J, AAPS PharmSciTech 2:30 (2001).

Kawaguchi, J.; Mee, P. J.; and Smith, A.G. (2005) “Osteogenic and chondrogenic differentiation of embryonic stem cells in response to specific growth factors”. Bone 36:758 –769.

Khetani, SR, and Bhatia, SN (2008): Microscale culture of human liver cells for drug development. Nature Biotechnology, 26: 120-126.

Kim, H. et al., (2005) “Development of New Reverse Micellar Microencapsulation Technique to Load Water-Soluble Drug into PLGA Microspheres”. Arch Pharm Res 28: 370-375

Kim, J. et al., “Stability of bovin serum albumin complexed with PEG-poly(l-histidine) diblock copolymer in PLGA microspheres. J. Control. Rel. 109. (2005) 86 – 100.

Kim, H.; Kim, H. W.; and Suh, H. (2003). “Sustained release of ascorbate-2-phosphate and dexamethasone from porous PLGA scaffolds for bone tissue engineering using mesenchymal stem cells”. Biomaterials 24: 4671–4679.

Kim, H. K. and Park, T. G. “Comparative study on sustained release of human growth hormone from semi-crystalline poly(L -lactic acid) and amorphous poly(D ,L -lactic-co-glycolic acid) microspheres: morphological effect on protein release.” J. Control Release 98 (2004) 115 – 125.

Kim, H.K., Park, T.G., 1999. Microencapsulation of human growth hormone within biodegradable polyester microspheres :protein aggregation, stability and incomplete release mechanism. Biotechnol. Bioeng. 65, 659 - 667.

Kimura, Y.; Hukogo, A.; Takomoto, T.; Tabata, Y.; Kurosawa, H. (2008) “Regeneration of Anterior Cruciate Ligament by Biodegradable Scaffold Combined with Local Controlled Release of Basic Fibroblast Growth Factor and Collagen Wrapping” Tissue Eng C: Methods 14: 47 – 57.

King, T. W., Patrick, C. W. (2000) Development and in vitro characterization of vascular endothelial growth factor (VEGF)-loaded poly(dl-lactic-co-glycolic acid)}poly(ethylene glycol) microspheres using a solid encapsulation}single emulsion}solvent extraction technique. J. Biomed. Mater. Res. 51: 383±390.

Knothe, M.L. ; Shvartsman, S.; and Friedman, A (2008) “Cell and Tissue Engineering—Taking Cues from Nature's Engineering Paradigm for Developing, Growing, and Repairing Tissues” Tissue Engineering Part A. 14: 1459-1460.

Knudson, C. B. and Knudson, W. (2001) “Cartilage proteoglycans”. CELL & DEVELOPMENTAL BIOLOGY 12: 69–78

Koay, E. J.; Hoben, G. M.; Athanasiou, K. A. (2007) “Tissue Engineering with Chondrogenically-differentiated Human Embryonic Stem Cells” Stem Cells 25:2183–2190.

Kostanki. J., and DeLuca, P. P. “A novel in vitro release technique for peptide containing biodegradable microspheres”. AAPS PharmSciTech 1 (2000) article 4.

Kretlow, J. D., Klouda, L., and Mikos, A. G. “Injectable matrices and scaffolds for drug delivery in tissue engineering”Adv. Drug. Del Rev 59 (2007) 263 – 273.

Lam, X. M. et al., (2001). “Encapsulation and stabilization of nerve growth factor into poly(lactic-co-glycolic) acid microspheres”. J. Pharm. Sci. 90: 1356–1365.

Langer, R and Vacanti, J. P. (1993) Tissue Engineering. Science 260: 920 – 926.

LeCorre, P. et al. “Preparation and characterization of bupivacaine-loded polylactide and polylactide-co-glycolide microspheres”. Int. J. Pharm. 107 (1994) 41 – 49.

Lee, T. H., Wang. J., and Wang, C. H. “Double walled microspheres for sustained release of highly water soluble drug characterization and irradiation studies”. J. Control Release. 83 (2002) 437 – 452.

Lee et al., “Stabilisation of protein encapsulated in poly(lactide-co-glycolide) microspheres by novel viscous S/W/O/W method.” Int. J. Pharm. (2006).

Lee, J. I. and Yoo, H. S. (2008) “Biodegradable microspheres containing poly(-caprolactone)–Pluronic block copolymers for temperature-responsive release of proteins”. Coll Surf B: Bio 61: 81 – 87.

Li, X.; Jin, Li.; Cui, Q.; Wang, G.; and Balian, G. (2005) “Steroid effects on osteogenesis through mesenchymal cell gene expression”. Osteoporos Int 16: 101–108.

Lim, F. and Moss, R. D. “Microencapsulation of living cells and tissues”. J. Pharm. Sci. 70 (1981) 351 – 354.

Liu, X. and Ma, P. X. "Polymeric Scaffolds for Bone Tissue Engineering." Annals of Biomedical Engineering. 32 (2004) 447 - 486.

Lorenzo-Lamosa, et al. “Design for micro encapsulated chitosan microspheres for colonic drug delivery”. J. Control Release 52 (1998) 109 – 118.

Luan, X. et al., “Key parameters affecting the initial release (burst) and encapsulation efficiency of peptide containing poly(lactide-co-glycolide) microparticles”. Int. J. Pharm. 324 (2006) 168 – 175.

Lutolf, M. P. and Hubbell, J. A. "Synthetic biomaterials as instructive extracellular microenvironments for morphogenesis in tissue engineering." Nature Biotechnology 23 (2005) 47 - 55.

Lynn, D., Amiji, M., and Langer, R. “pH responsive polymer microspheres: rapid release of encapsulated material within the range of intracellular pH”. Angev. Chem. Int. Ed. 40 (2001) 1707 – 1710.

Maehly, A. (1955) “Plant Peroxidase, Methods in Enzymology” Vol. 2,S. Colowick and N. Kaplan, Academic Press, NY, 807.

Makino et al. “Pulsatile drug release from poly(lactide-co-glycolide) microspheres: how does the composition of polymer matrixes affect the time interval between the initial burst and pulsatile release of drugs?”. Colloid Surf. B.: Biointerfaces 19 (2000) 173 – 179.

Malzert-Fre´on, A. et al., (2008) “Interactions between poly(ethylene glycol) and protein in dichloromethane/water emulsions: A study of interfacial properties”. Eur Journal Pharm Biopharm 69: 835–843.

Marra, K. G. et al. "In vitro analysis of biodegradable polymer blend/hydroxyapatite composites for tissue engineering." J. Biomed.Mater.Res. 47(1999) 324 -355.

Mathiowitz, E. and Langer, R. “Polyanhydride microspheres as drug carriers 1. Hot melt microencapsulation”. J. Control. Rel. 5 (1987). 13 – 22.

Meinel, L. et al. “ Stabilizing insulin-like growth factor-1 in poly(D,L-lactide-co-glycolide) microspheres”. J. Control. Release 70 (2001) 193 – 202.

Merck Index, 2006, 14th Edition. Merck Publishing, Rahway.

Metger, T. “The Rheology Handbook” William Andrews Publishing 2nd Ed. (2006).

Mi, F. L. et al “Chitin/PLGA blend microspheresas a biodegradable drud delivery system: phase-separation”. Biomaterials 23 (2002) 3257 – 3267.

Michalopoulos, G.K. et al., (2003). “HGF-, EGF-, and dexamethasone-induced gene expression patterns during formation of tissue in hepatic organoid cultures”. Gene Expr. 11, 55–75.

Mikos, A. G. et al. "Preparation and characterization of Poly(L -Lactic acid) foams." Polymer 35 (1994) 1068 - 1077.

Miyata T, Devuyst O, Kurokawa K et al. (2002) "Toward better dialysis compatibility: Advances in the biochemistry and pathophysiology of the peritoneal membranes". Kidney Int. **61**: 375–86

Moioli, E. K. and Mao, J. J. (2006). “Chondrogenesis of Mesenchymal Stem Cells by Controlled Delivery of Transforming Growth Factor-3” Proceedings of the 28th IEEE EMBS Annual International Conference 2647 -2650.

Moioli, E. K.; Hong, L.; and Mao, J. J. (2007) “Inhibition of osteogenic differentiation of human mesenchymal stem cells” Wound repair and regeneration 15: 413 – 421.

Morita, T. et al. "Protein encapsulation into biodegradable microspheres by a novel S/ O/ W emulsion method using poly(ethylene glycol) as a protein micronization adjuvant." J. Control. Release 69 (2000) 435 - 444.

Morita, T. et al.. "Applicability of various amphiphilic polymers to the modification of protein release kinetics from biodegradable reservoir-type microspheres." Eur. J. Pharm. Biopharm. 51(2001) 45 - 53.

Mundargi, R. C. et al., (2007) “Development and evaluation of novel biodegradable microspheres based on poly(d,l-lactide-co-glycolide) and poly(ε-caprolactone) for controlled delivery of doxycycline in the treatment of human periodontal pocket: In vitro and in vivo studies” Journal Control Rel 119: 59 -68.

Murakami, K. et al., (1998) “Identification of minor proteins of human colostrum and mature milk by two-dimensional electrophoresis”. Electrophoresis 19: 2521 -2527.

Nakahara T., Nakamura T., Kobayashi E., Inoue M., Shigeno K., Tabata Y., Eto K., and Shimizu Y. (2003) Novel approach to regeneration of periodontal tissues based on in situ tissue engineering: effects of controlled release of basic fibroblast growth factor from a sandwich membrane, Tissue Engineering. 9: 153–162

Nam, Y. S. et al. “Lysozyme microencapsulation within biodegradable PLGA microspheres: urea effect on protein release and stability”. Biotech. Bioeng. 70 (2000) 270 – 277.

Odom, D. T.; Dowell, R. D.; Jacobsen, E. S. et al (2007) “Tissue-specific transcriptional regulation has diverged significantly between human and mouse” Nature Genetics 39, 730 - 732

Ohya, S. and Matsuda, T. “Poly (N-isopropylacrylamide) (PNIPAM)- grafted gelatine as thermoresponsive three-dimensional artificial extracellular matrix: molecular and formulation parameters vs. cell proliferation potential. J. Biomater. Sci. Polym. Ed. 16 (2005) 809 -827.

Okada, H. et al. “Drug delivery using biodegradable microspheres”. J. Control. Release 28 (1994) 121 – 129.

Okada, H. and Toguchi, H. “Biodegradable microspheres in drug delivery” Crit. Rev. Ther. Drug Carrier Syst. 12 (1995) 1 – 99.

Oldham, J. B. et al. “Biological Activity of rhBMP-2 Released From PLGA Microspheres” J. Biomech. Eng. 122 (2000) 289 – 292.

Park, T. G. “Degradation of poly(D,L-lactic acid) microspheres effect of molecular weight”. J. Control Release 30 (1994) 161 – 173.

Park, T. G. “Degradation of poly(D,L-lactic acid) microspheres effect of copolymer composition”. Biomaterials 16 (1995) 1123 – 1130.

Park, T.G., Lee H.Y., and Nam, Y.S. (1998) A new preparation method for protein loaded poly( -lactic-co-glycolic acid) microspheres and protein release mechanism study. J. Control. Release 55. 181–191.

Park, H.; Temenoff, J.; Tabata, Y.; Caplin, A. I.; Mikos, A. G. (2007) “Injectable biodegradable hydrogel composites for rabbit marrow mesenchymal stem cell and growth factor delivery for cartilage tissue engineering”. Biomaterials 28: 3217 – 3227.

Pachence, J.M.; and Kohn, J. (1997) “Biodegradable polymers for tissue engineering”. In: R.P. Lanza, R. Langer and W.L. Chick, Editors, Principles of tissue engineering, R.G. Landes Co., Austin, Texas, USA (1997), pp. 273–293.

Patel, Z. S. et al., (2008) “Dual delivery of an angiogenic and an osteogenic growth factor for bone regeneration in a critical size defect model”. Bone 43: 931 -940.

Péan, J. M. et al. “Why does PEG 400 Co-encapsulation improve NGF stability and release from PLGA biodegradable microspheres?”. Pharm. Res. 16 (1999). 1294 – 1299.

Pe´rez, C., Griebenow, K.,. Improved activity and stability of lysozyme at the water/methylene chloride interface:enzyme unfolding and aggregation and its prevention by polyols. J. Pharm. Pharmacol. 53 (2001)1217- 1226.

Phillips, J. E.; Gersbach, C. A.; Wojtowicz, A. M.; García, A. J. (2006) “Glucocorticoid-induced osteogenesis is negatively regulated by Runx2/Cbfa1 serine phosphorylation”. Journal of Cell Science 119: 581 – 591.

Piirma, I. “Colloids” In: Mark , H. F. et al. “Encyclopedia of polymer science and engineering”. 2nd Ed. (1985) John Wiley & Sons. New York 125 – 130.

Pittenger, M. F. (2008) “Mesenchymal Stem Cells from Adult Bone Marrow” Methods in Molecular Biology 449: 27 – 44.

Porjazoska, A. et al “Poly(lactide-co-glycolide) microparticles as systems for controlled release of proteins – Preparation and characterization” Acta Pharm. 54 (2004) 215–229

Pratoomsoot, C., Tanioka, H., et al. “A Thermoreversible hydrogel as a biosynthetic bandage for corneal wound repair” Biomaterials 29 (2008) 272 – 281

Putney, S. D. “Encapsulation of proteins for improved delivery”. Curr. Opin. Chem. Biol. 2 (1998) 548 – 552.

Putney, S. D. and Burke, P. A. (1998) “Improving protein therapeutics with sustained-release formulations”. Nat Biotech. 16: 153 -157.

Randle, W. L. et al., (2007). “Integrated 3-Dimensional Expansion and Osteogenic Differentiation of Murine Embryonic Stem Cells” Tissue Eng 13: 2957 – 2970.

Rangarajan, A.; Hong, S. J.; Gifford, A.; Weinberg, R. A. (2004) “Species- and cell type-specific requirements for cellular transformation” Cancer Cell 6: 171 – 183

Ravivarapu, H. B., Lee. H., and DeLuca, P.P. “Enhancing initial release of peptide from poly(D, L- lactide-co-glycolide) (PLGA) microspheres by addition of a porosigen and increasing drug load”. Pharm. Dev. Technol. 5. (2000b) 287 – 296.

Richardson, T. P.; Peters, M. C.; Ennett, A. B.; and Mooney, D. J. (2001) “Polymeric system for dual growth factor delivery” Nature Biotechnology

Rocha, F. G. et al. “The effect of sustained delivery of vascular endothelial growth factor on angiogenesis in tissue-engineered intestine” Biomaterials 29 (2008) 2884 – 2890.

Rophael, J. A.; Craft, R. O.; Palmer, J. A.; Hussey, A. J.; Thomas, G. P. L.; Morrison, W. A.; Penington, A. J. and Mitchell, G. M. (2007) “Angiogenic Growth Factor Synergism in a Murine Tissue Engineering Model of Angiogenesis and Adipogenesis”. Am J Pathol. 171: 2048–2057.

Rose F., Oreffo R (2002). Bone tissue engineering: hope vs. hype. Biochem Biophys Res Commun. 292: 1–7.

Rothen, A., J. (1940). “Molecular weight and electrophoresis of. crystalline ribonuclease”. Gen. Physiol., 24, 203 – 211.

Sah H. (1997). “ A new strategy to determine the actual protein content of poly(lactide-co-glycolide) microspheres. J. Pharm. Sci. 86 (1997) 1315 – 1318.

Sah, H. “Protein instability towards organic solvent/water emulsification: implications for protein microencapsulation into microspheres”. PDA J. Pharm. Sci. Technol. 53 (1999), pp. 3–10

Schantz, J., Chim, H., Whiteman, M. (2007) “Cell Guidance in Tissue Engineering: SDF-1 Mediates Site-Directed Homing of Mesenchymal Stem Cells within Three-Dimensional Polycaprolactone Scaffolds”. Tissue Engineering 2615 – 2624.

Shi, S. et al., (2009) “RhBMP-2 Microspheres-Loaded Chitosan/Collagen Scaffold Enhanced Osseointegration: An Experiment in Dog”. Journal of Biomaterials Appl 23: 331 -346.

Siepman, J., et al. “Effect of the size of biodegradable microparticles on drug release: experiment and theory”. J. Control Release. 96 (2004) 123 – 134.

Simmons, C. A.; Alsberg, E.A.; Hsiong, S.; Kim, W. J.; Mooney, D. (2004). “Dual growth factor delivery and controlled scaffold degradation enhance in vivo bone formation by transplanted bone marrow stromal cells”. Bone 35: 562 – 569.

Sinha, V. R., and Trehan, A. “Biodegradable microspheres for protein delivery”. J. Control. Rel. 90 (2003) 261 – 280.

Sivaraman A, Leach JK, Townsend S, Iida T, et al. (2005). A microscale in vitro physiological model of the liver: Predictive screens for drug metabolism and enzyme induction. Curr Drug Metab 6(6): 569-591.

Sohier, J. et al. “Dual release of proteins from porous polymeric scaffolds” J. Control. Release 111 (2006) 95 – 106

Sokolsky-Papkov, M. et al. “Polymer carriers for drug delivery in tissue engineering” Advanced Drug Delivery Reviews 59 (2007) 187–206.

Sparnacci, K. et al “ Core-shell microspheres by dispersion polymerisation as drug delivery systems”. Macromol. Chem. Phys 203 (2002) 1364 – 1369.

Stachowiak, A.N and Irvine D.J, (2007) “Inverse opal hydrogel-collagen composite scaffolds microenvironment for immune cell migration” Current Opinion in Immunology 19 463-469.

Stadelman, W. J., Cotterill, O. J. (1990). Egg science and technology, 3rd edition, p. 112. Food Products Press, NY.

Stammen, J. A. Williams, S. . Ku, D. N, and Guldberg, R. E. “Mechanical properties of a novel PVA hydrogel in shear and unconfined compression” Biomaterials 8 (2001) 799 – 806.

Suciati, T. (2006) “Zonal release of proteins from Tissue Engineering Scaffolds”. Univ Nott Thesis.

Suggs, L. J. et al. “In vitro cytotoxicity and in vivo biocompatibility of poly(propylene fumarate –co-ethylene glycol) hydrogels “ . J. Biomed. Mater. Res. 46 (1999) 22 -32.

Sun, X.; Gan, Y.; Tang, T.; Zhang, X.; and Dai, K. (2008) “In Vitro Proliferation and Differentiation of Human Mesenchymal Stem Cells Cultured in Autologous Plasma Derived from Bone Marrow” Tissue Engineering Part A. 14: 391-400

Sun SW, Jeong YI, Jung SW and Kim SH, J Microencapsul 20:479 (2003).

Swainston. H. T. Plosker, G. L; Keam, S. J. “Extended-Release Intramuscular Naltrexone. Adis Drug Profile” Drugs. 66(13):1741-1751, 2006.

Tabata, Y. (2004). "Tissue regeneration based on tissue engineering technology." Congenital Anomalies 44: 111 - 124.

Tabata Y., Ikada Y., Morimoto K., Katsumata H., Yabuta T., Iwanaga K., and Kakemi M. (1999) Surfactant-free preparation of biodegradable hydrogel microspheres for protein release, Journal of Bioactive and Compatible Polymers 14: 371–384

Takagi, M. et al., (2007). "High inoculation cell density could accelerate the differentiation of human bone marrow mesenchymal stem cells to chondrocyte cells". Journal Biosci & Bioeng 103: 98 -100.

Temenoff , J. S. et al. "In vitro cytotoxicity of redox radical initiators for cross-linking of oligo(poly(ethylene glycol) fumarate) macromers. Biomaterials 4 (2003) 1605 – 1613.

Tsang, V. L. and Bhatia, S. N. "Three-dimensional tissue fabrication" Adv. Drug Del. Rev. 56 (2004) 1635 - 1647.

Tu, Q.; Valverde, P.; and Chen, J. (2006) "Osterix enhances proliferation and osteogenic potential of bone marrow stromal cells". Biochemical and Biophysical Research Communications 341:1257–1265.

van de Weert, M. et al., (2000). "The effect of a water/organic solvent interface on the structural stability of lysozyme, J. Control. Release 68: 351–359.

Vargo-Gogola T and Rosen JM, (2007) "Modeling breast cancer: one size does not fit all." Nature Reviews Cancer 7: 659-72.

Vasir, J. P., Tambwekar, K., and Garg, S. "Bioadhesive microspheres as a controlled drug delivery system". Int. J. Pharm. 255 (2003) 13 – 32.

Wang, J., Wang, B. M., and Schwendeman, S. P. "Mechanistic evaluation of the glucose-induced reduction in initial burst release of octreolide acetate from poly(lactide-co-glycolide) microspheres". Biomaterials 25 (2004) 1919 – 1927.

Weert, M.; Hennink, W. E. and Jiskoot, W. "Protein Instability in Poly(lactic-co-Glycolic Acid) Microparticles". Pharm. Res. 17 (2000) 1159 – 1167.

Whitaker, M. J. et al. "Growth factor release from tissue engineering scaffolds." J. Pharm. Pharmacol. 53 (2001) 1427 - 1437.

Whittlesey, K. J. and Shea, L. D. "Delivery systems for small molecule drugs, proteins, and DNA; the neuroscience/biomaterial interface." Exp. Neur. 190 (2004) 1 –16.

Wischke, C. Schwendeman, S. P. (2008) "Principles of encapsulating hydrophobic drugs in PLA/PLGA microparticles" Int Journal Pharm in press.

Woo, B. H. et al. “In vitro characterisation and in vivo testosterone suppression of 6-month release poly(D,L-lactide) leuprolide microspheres”. Pharm. Res. 19 (2002) 546 – 550.

Yang, Y; Chung, T. and Ng, N. P. “Morphology, drug distribution, and in vitro release profiles of biodegradable polymeric microspheres containing protein fabricated by double-emulsion solvent extraction/evaporation method”. Biomaterials 22 (2001) 231 – 241.

Yeong, W. et al. "Rapid prototyping in tissue engineering: challenges and potential." TRENDS in Biotechnology 22 (2004). 643 - 652.

Young, T. J. et al. “Encapsulation of lysozyme in a bioedegradable polymer by precipitation with a vapor-over-liquid antisolvent”. J. Pharm. Sci 88 (1999) 640 – 650.

Zentner G.M., Rathi R., Shih C., McRea J.C. et al. (2001) Biodegradable block copolymers for delivery of proteins and water-insoluble drugs. Journal of Controlled Release 72: 203-215

Zhu, G. and Schwendeman, S. P. “ Stabilization of proteins encapsulated in cylindrical poly(lactide-co-glycolide) implants: Mechanism of stabilization by basic additives”. Pharm. Res. 17 (2000) 351 – 357.

Zolnik, B. S., and Burgess D. J. “Effect of acidic pH on PLGA microsphere degradation and release.” J. Control Release 122 (2007) 338 – 344.